Final Report — NASA CR — 165525

Assessment of Crash Fire Hazard of LH_2 — Fueled Aircraft

by G.D. Brewer
G. Wittlin
E.F. Versaw
R. Parmley
R. Cima
E.G. Walther

LOCKHEED-CALIFORNIA COMPANY
BURBANK, CALIFORNIA

SUPPORTED BY
[illegible] AND SPACE CO. INC.
[illegible] INSTITUTE — UNIV. OF NEVADA

[illegible] NAS3-[illegible]
[illegible] 1981

NASA

[illegible]

Final Report — NASA CR — 165525

Assessment of Crash Fire Hazard of LH_2 — Fueled Aircraft

by G.D. Brewer
G. Wittlin
E. F. Versaw
R. Parmley
R. Cima
E. G. Walther

LOCKHEED-CALIFORNIA COMPANY
BURBANK, CALIFORNIA

SUPPORTED BY
LOCKHEED MISSILES AND SPACE CO. INC.
AND THE JOHN MUIR INSTITUTE – UNIV. OF NEVADA

CONTRACT NAS3-2483
DECEMBER, 1981

NASA

LEWIS RESEARCH CENTER
CLEVELAND, OHIO

FOREWORD

This is the final report of a study made under Contract NAS 3-2483 for NASA - Lewis Research Center, Cleveland, Ohio. Mr. Harold Schmidt at Lewis Research Center was technical monitor for the study. The report presents results of work performed during the 14 month period, August 1980 through September 1981.

The Lockheed-California Company was the prime contractor to NASA and the work was performed in the Commercial Advanced Design Division at Burbank, California. Important segments of the work which required special expertise were subcontracted to the Thermal Sciences Laboratory at Lockheed Missiles and Space Company, Inc., Palo Alto, California, and to the Visibility Research Center of the John Muir Institute, University of Nevada, Las Vegas, Nevada. The following individuals were principal contributors.

Lockheed-California Company

G. Daniel Brewer - Study Manager
Edward F. Versaw - Fuel Systems
Gil Wittlin - Crash Dynamics

Lockheed Missiles and Space Co., Inc.

Richard Parmley - Coordinator
Richard Cima - Near Field Analysis and Heat Transfer

John Muir Institute

Dr. Eric G. Walther - Atmospheric Dispersion
Dr. John Sanders
Dr. Dennis Weber
Dr. Michael D. Williams

TABLE OF CONTENTS

TABLE OF CONTENTS (Continued)

LIST OF FIGURES

LIST OF TABLES

LIST OF TABLES (Continued)

ASSESSMENT OF CRASH FIRE HAZARD OF LH_2 FUELED AIRCRAFT

G.D. Brewer, G. Wittlin, E.F. Versaw
R. Parmley*, R. Cinn*, E.G. Walther†

SUMMARY

Liquid hydrogen (LH_2) is a primary candidate fuel for future transport aircraft. Studies performed for NASA have shown its advantages in almost every category of comparison. Accordingly, when the international air transport industry is forced to turn to an alternative for conventional petroleum-base Jet A for reasons of either price or availability, or both, LH_2 is expected to be a leading contender.

In the meantime, there is much technology development which should proceed in order that, when the time for a decision is at hand, the decision regarding the choice of fuel for the industry can be made on a credible basis, giving full consideration to all the factors which are important. One of the factors about which there is a serious lack of credible data is safety. How safe is liquid hydrogen compared to other fuels? What special precautions should be taken in design to accommodate it properly? In event of a crash in which passengers and crew survive the impact, would they be exposed to more or less hazard from fire or explosion if LH_2 is the fuel, rather than other fuels? - how about surrounding areas? What studies and experiments should be performed to resolve such issues?

The subject study was performed to determine answers to these questions. Four scenarios describing situations involving fuel spills which can and do arise in commercial transport aircraft were studied to determine the hazard to airplane passengers and surroundings posed by LH_2 if it is employed as the aircraft fuel. The findings were then compared with results derived for liquid methane (LCH_4), aviation grade kerosine (Jet A), and wide-cut gasoline (JP-4).

*Lockheed Missile and Space Company, Inc.
†John Muir Institute

In summary, on the basis of the analysis performed, LH_2 was found to be a safer fuel than any of the other candidates. The passengers on board, and people and property in the immediate surroundings, would both be exposed to less hazard if a crashed aircraft were fueled with LH_2.

This results from three fundamental considerations: the LH_2 tanks are less apt to suffer damage resulting in spilled fuel; if spilled, LH_2 vaporizes, becomes buoyant, and dissipates into the atmosphere so rapidly it minimizes the hazard; finally, if the vapor cloud is ignited, the size and duration of a fire from spilled LH_2 are both significantly less than with any other fuel.

LH_2 tanks are considered less apt to be damaged because

1) being mounted in the fuselage, LH_2 tanks expose a far smaller dimension to frontal impact, compared with conventional fuel which is stored in the wing and occupies nearly the entire span.

2) they are designed to withstand a significantly higher pressure than the rest of the fuselage and are therefore less apt to be the point of failure in a survivable crash.

In the event a tank is ruptured and there is a large spill of fuel, LH_2 does not spread as far as other fuels, it evaporates in much shorter time, becomes buoyant almost immediately, and finally, rises and dissipates into the atmosphere so rapidly that very little hazard is presented to surroundings outside the immediate area of the crash. For example, the following results were calculated for a survivable crash situation involving spillage of nearly half the fuel load of aircraft designed to carry 400 passengers 10,190 km (5500 n.mi.):

				Vapor Cloud				
				Start to Rise		Dissipated		
Fuel	Quantity Spilled	Liquid Spread Radius	Time to Vaporize	Time	Distance	Time	Distance	Height
	(kg)	(m)	(s)	(s)	(m)	(s)	(m)	(m)
LH_2	12,600	35	32	12	1.0	146	411	575
LCH_4	34,398	61	117	1,560	624	1,624	713	72
JP-4	42,210	143	785	Does not rise		11,736	6,816	0
Jet A	42,210	331	*	*			*	

*The vapor pressure of Jet A is not high enough at standard atmospheric conditions to form a combustible mixture with the atmosphere.

Finally, in event the spilled fuel is ignited, the duration of the LH_2 fire would be so brief it would not heat the fuselage to the point of collapse, as would be the case with the other fuels, so the passengers would be safe if they stay in their seats until the fuel-fed fire is burned out. For example, in the aircraft crash situation just cited, the resulting fire will burn itself out in about 22 seconds in the case of LH_2, versus approximately 43 seconds for LCH_4, more than 10 minutes for JP-4, and even longer for Jet A.

The subject study represents a preliminary investigation. The findings look very favorable for hydrogen. However, it must be recognized that there are many other cases and circumstances to be analyzed, the tools for analysis need to be improved, and experimental testing must be performed to establish a basis for validation of the computer model results before complete and final conclusions can be reached.

SYMBOLS AND UNITS

a = constant

A_e = area of puff through which air is entrained (m^2)

A_ℓ = area of liquid pool (m^2)

b = constant

C_{pa} = specific heat capacity of air at constant pressure (cal/gK)

C_{pf} = specific heat capacity of gaseous fuel at constant pressure (cal/gK)

C_{pp} = specific heat capacity of puff at constant pressure (cal/gK)

d_s = length parameter defining surface roughness (m)

e = vapor pressure of water (mb)

e_{sp} = saturation water vapor pressure in the puff (mb)

E = evaporation rate of liquid fuel (m/s)

f = Fanning friction factor for open channel flow

Fr = Froude number of the liquid flow

g = acceleration of gravity (m/s^2)

H_e = enthalpy of air entrained during one time increment (cal)

H_p = enthalpy of puff at start of a time increment (cal)

h_{fg} = latent heat of vaporization (kW sec/kg)

L_x = length of puff in downwind direction (m)

L_y = crosswind (cross runway) width of puff (m)

L_w = latent heat of water vapor condensation (cal/kg)

L'_w = latent heat of fusion of liquid water (cal/kg)

$\dot{m}_E$ = maximum rate of vaporization from the liquid spread (kg/sec)

m_e = mass of air entrained during one time increment (g)

$\dot{m}'_E$ = maximum mass rate of vaporization per unit spill length (kg/sec·M)

m_f = mass of fuel in puff (g)

m_p = mass of puff at start of time increment (g)

m_w = mass of water entrained during one time increment (g)

$\dot{m}_A$ = mass flowrate of air (kg/sec)

$\dot{m}_F$ = mass flowrate of fuel vapor (kg/sec)

M = molecular weight of fuel vapor or air

M_a = molecular weight of air (g/mole)

M_f = molecular weight of fuel (g/mole)

M_p = molecular weight of puff mixture (g/mole)

M_w = molecular weight of water (g/mole)

n = Mannings roughness coefficient

P = atmospheric pressure (dynes cm^{-2})

p = exponent of height ratio in wind speed profile (-)

Q_o = total volume of the liquid spilled (m^3)

$\dot{Q}_o$ = volume rate of the liquid spill (m^3/s)

Q'_o = volume of liquid spill per unit of spill centerline length (m^3/m)

q''_C = convective heat flux from flames (kW/m^2)

q''_F = incident radiation heat flux from flames (kW/m^2)

q''_R = absorbed radiation heat flux from flames (kW/m^2)

q'' = heat rate per unit area to the solid surface (kW/m^2)

r = puff radius (m)

r_m = maximum radius of the spread from the center (m)

R* = universal gas constant (erg/mole K)

Re = Reynolds number of the flow

t = time elapsed since start of vaporization from liquid (seconds)

t_m = time to maximum axial spread (s)

Δt = time increment (s)

T_a = temperature of air (K)

T_F = flame temperature (K)

T_p = puff temperature at start of time increment (K)

T'_p = intermediate puff temperature after balancing sensible heat transfer (K)

T''_p = intermediate puff temperature after condensing water vapor (K)

T'''_p = intermediate puff temperature after freezing water droplets (K)

T''''_p = intermediate puff temperature after any melting of ice crystals and re-evaporation of water droplets (K)

u = wind speed (m/s)

u_p = horizontal downwind speed of puff (m/s)

u_e = entrainment speed (m/s)

u_1 = first term of entrainment speed (m/s)

u_2 = second term of entrainment speed (m/s)

V_A = aircraft velocity along spill line (m/s)

$\dot{V}_A$ = volumetric flowrate of air at atmospheric temperature and pressure (m^3/s)

V = mean horizontal velocity of the liquid flow (m/s)

V = volume of puff (m^3)

V' = volume of puff at end of time increment (m^3)

$\dot{V}F$ = volumetric flowrate of fuel at atmospheric temperature and pressure (m^3/s)

V_o = initial puff volume (m^3)

V_e = volume of air entrained during one time interval (m^3)

V_E = rate of fall of still liquid surface (m/s)

w = vertical puff speed (m/s)

x = axial distance from the center of the spill line (m)

x_m = maximum half axial spread, from spill centerline (m)

x_p = downwind distance of puff from origin (m)

Δx = change in downwind displacement (m)

y_{min} = minimum combustible mole fraction of fuel in the air

z = height of puff above ground (m)

z_o = reference height for wind speed profile (m)

z_p = height of puff above ground (m)

Δz_p = puff thickness in vertical direction (m)

Γ = lapse rate of temperature in the atmosphere (K/m)

δ = liquid flow depth (m)

ϵ_F = effective flame emissivity

ρ_a = density of air at height of puff (g/m^3)

ρ_g = density of gaseous fuel at 1 atmosphere pressure and boiling point (g/m^3)

ρ_ℓ = density of liquid fuel (g/m^3)

ρ_Γ = density of puff (g/m^3)

λ = wave velocity (m/s)

μ_L = liquid viscosity (kg/s m)

SECTION 1

INTRODUCTION

This is the final report of a study performed for NASA-Lewis Research Center to assess the hazard posed by liquid hydrogen when used as fuel in commercial transport aircraft. In addition to liquid hydrogen (LH_2), the hazards presented by three other fuels were also calculated for comparison. The other fuels were liquid methane (LCH_4), Jet A (aviation grade kerosine currently used in commercial transport aircraft), and JP-4 (the widecut gasoline used as jet fuel by the Air Force).

Four specific scenarios or descriptions of incidents leading to spilled fuel were specified by NASA to serve as a basis for the safety analysis. The incidents ranged from a very small leak such as might result from a crack in a faulty weld on a fuel line or tank, to a catastrophic crash which would cause simultaneous rupture of all the fuel tanks on board the aircraft.

The study was initiated because LH_2 is a candidate fuel to be used when Jet A, produced from crude oil, is no longer available to the world transport fleets on an economically acceptable basis. Previous studies conducted for NASA have shown numerous advantages which can be gained by using LH_2[1,2,3,4]. These include

- Global availability. It can be made from a renewable resource, water, using any source of energy which might be locally available. Fossil resources are not required.
- Pollution. Its major product of combustion is water vapor. It emits none of the noxious effluents of carbon-containing fuels save a minimum amount of NO_x.
- Noise. Because they are lighter and therefore can use smaller engines, LH_2-fueled aircraft would be about half as objectionable to airport neighbors.

- Energy. Coal is an example of an energy resource which can be used to produce any of the alternate fuels. Fewer tons of coal would be required to produce the fuel used by aircraft to fly their design missions if LH_2 is the fuel.

- Direct Operating Cost. LH_2-fueled aircraft can be competitive in DOC using current fuel production technology[27]. With advanced processes, LH_2 can be produced from coal and water at costs which offer significant advantage.

The relative safety of LH_2 has been subject to question. The present study is an important step toward establishing a sound basis for judgement on this matter. In addition to providing a preliminary answer to the question of how LH_2 compares with the other fuels in terms of crash safety, it also provides suggestions for additional analyses and experiments which are considered necessary for final resolution of the problem.

SECTION 2

TECHNICAL APPROACH

2.1 Study Team Organization and Work Plan

The study team consisted of representatives from three companies selected to provide expertise in the diverse technology areas needed to perform this study effectively and efficiently.

The Lockheed-California Company was the prime contractor to NASA and managed the study. LCC also reviewed transport aircraft accident data from various sources to derive a basis for establishing what would constitute credible damage associated with each of the crash scenarios specified by NASA. These damage assessments were then considered in conjunction with aircraft designed for each of the subject fuels to specify typical fuel spill rates and quantities for each scenario.

Under subcontract to LCC the Thermal Sciences Laboratory of Lockheed Missiles and Space Company, Inc. (LMSC) was responsible for analyzing the hazard resulting from spill of the liquid fuels. A computer model was created by Mr. Richard Cima to characterize the spreading and vaporization of volatile liquid spilled in both a radial and an axial pattern. The latter represented the spill situation where, for example, an aircraft strikes an obstacle during a landing shortly after touchdown and spills fuel during deceleration to a stop. A radial spill pattern would be produced when impact with an obstacle stops the aircraft immediately.

The geometry and mixing characteristics of the cloud of vaporized fuel as it disperses into the atmosphere were modeled by Dr. Eric Walther and co-workers at John Muir Institute. The geometry of the cloud, the profile of the flammable mixture within it, and the path followed by the dispersing cloud under various atmospheric conditions were needed to provide information about

the extent and duration of the exposure to hazard of the aircraft passengers and the area surrounding the crash scene. For example, the time-history of the geometry and location of the flammable mixture within the dispersing cloud provided information about the potential size of fire which might result if the cloud were ignited at various times.

Another type of hazard which was explored by LMSC related to the problem of how to handle a small leak of fuel into an internal cavity in the airplane. There is the possibility that if such a leak occurs, an explosive mixture could develop and a detonation result. The problem was resolved by determining, for various size leaks, the quantity of air flow required to assure that a flammable mixture could not develop in the compartment as a whole. A flammable mixture will always exist locally at the leak source of course.

Finally, hazard to passengers inside the aircraft cabin was evaluated for the case where the outside of the fuselage is exposed to flames from burning fuel spilled as a result of one of the survivable crash scenarios.

2.2 Study Guidelines

The objectives of the study were:

- To assess the hazards associated with non-normal and crash landings, failed takeoffs, and ground accidents involving turbine-powered aircraft fueled with liquid hydrogen (LH_2).
- To compare LH_2-fueled aircraft with similar designs fueled with liquid methane, Jet A, and JP-4, on the basis of:
  - Post-crash fuel system damage
  - Potential deflagration and detonation hazard
  - Survivability potential for persons in and adjacent to the damaged aircraft
- To formulate a program of research and testing found to be needed to fill technological gaps.

The hazards associated with LH_2 were to be evaluated and compared with those from liquid methane (LCH_4), Jet A, and JP-4 in connection with the following accident scenarios:

1. A non-normal landing or ground accident which results in fuel system insulation damage and/or fuel system damage permitting liquid hydrogen to vent, escape, leak or run out of a punctured tank or broken line.

2. A survivable crash landing or failed takeoff where damage to fuel tankage or lines results in massive release of liquid hydrogen after the aircraft has come to rest.

3. A survivable crash landing or failed takeoff where damage to fuel tankage or lines results in massive release of liquid hydrogen upon impact and during aircraft deceleration.

4. A nonsurvivable or catastrophic crash resulting in the maximum rate of energy release in the form of a conflagration and/or explosion.

SECTION 3

INPUT DATA

In this section, data required as input to perform the crash hazard analyses of each of the four fuels in the situations specified by NASA are presented. In turn, subsections present data on pertinent properties of each of the fuels; results are described of previous experiments with LH_2 and LCH_4 which were performed to assess some of their safety-related characteristics; typical designs of transport aircraft for each of the fuels are described which were used as a basis for establishing damage likely to result from the specified crashes; results of study of aircraft accident records are reported; and finally, the damage selected as representative of that likely to occur to the specified aircraft in the subject crash scenarios is described, along with resulting fuel spill rates and quantities. These fuel spill data are used in work described in subsequent sections in evaluation of the consequences of the spills.

3.1 Fuel Characteristics

A number of properties of the four fuels considered during this study are presented in table 1. The properties selected for presentation include some which are of general interest in comparing fuels for the aircraft application; most are properties which were involved in the analysis of hazards associated with spills resulting from the kind of aircraft crashes postulated for this study.

As noted on the table, the properties of the cryogenic fuels, LH_2 and LCH_4, were taken from reference 5, a recent compilation by the Center for Chemical Engineering at the National Bureau of Standards in Boulder, Colorado. The data for Jet A and JP-4 were primarily derived from the respective specifications for the two fuels, references 6 and 7, except as noted in the table.

TABLE 1. - SELECTED PROPERTIES OF FUELS

	Hydrogen [6]	Methane [6]	Jet A [6]	JP-4 [7]
Nominal Composition	H_2	CH_4	$CH_{1.93}$	$CH_{1.93}$
Molecular Weight	2.016	16.04	~166[8]	~132[8]
Heat of Combustion (low), k J/g	120	50.0	42.8	42.8
Liquid Density, g/cm^3 at 283 K	0.071*	0.423*	~0.811	~0.774
Boiling Point, K (at 1 Atmosphere)	20.27	112	440 to 539	333 to 519
Freezing Point, K	14.4	91	233	215
Specific Heat*, J/g K	9.69	3.50	1.98[9]	2.04[9]
Heat of Vaporization, J/g (at 1 Atmosphere)	446	510	360[9]	344[9]
Vapor Pressure, kPa	–	–	–	18
Diffusion Vel. in NTP Air, cm/s	≤2.00	≤0.51	<0.17	<0.17
Buoyant Vel. in NTP Air, m/s	1.2 to 9	0.8 to 6	Non Buoyant	Non Buoyant
Flammability Limits in Air, Vol. %	4.0 to 75.0	5.3 to 15.0	0.6 to 4.7[9]	0.8 to 5.8[9]
Vaporization Rate W/O Burning, cm/min (From Liquid Pool)	2.5 to 5.0	0.05 to 0.5	N/A	0.005 to 0.02
Min. Ignition Energy in Air, mJ	0.02	0.29	0.25[10]	0.25[10]
Autoignition Temp., K	858	813	>500	>500
Rate of Liquid Lowering of Burning Pool, cm/min	3 to 6.6	0.3 to 1.2	0.17[5]	0.20[5]
Burning Vel. in NTP Air, cm/s	265 to 325	37 to 45	18[10]	381[10]
Flame Temp in Air (Stoichiometric), K	2318	2148	2200[10]	2200[10]
Thermal Energy Radiated to Surroundings %	17 to 25	23 to 33	30 to 42	30 to 42
Detonability Limits in Air, Vol. %	18.3 to 59.0	6.3 to 13.5	N/A	1.1 to 3.3

*At Normal Boiling Point
NTP = Normal Temperature and Pressure

3.2 Previous Safety Experiments

There is a surprisingly meager history of well-organized, scientifically executed safety experiments conducted with either LH_2 or LCH_4 to establish the nature and extent of hazards associated with large instantaneous spills, or long duration spills of sizable quantities.

A search was made for experimental evidence to be used for validation of the analytical models created for use in the subject study. In the limited time available, the following four sources were found to provide the most useful information:

- Testing performed by the Advanced Development Projects Organization at Lockheed-California Company in 1956-57[11].

This very early work at Lockheed's "Skunk Works" included a series of tests to determine the detonability of LH_2. Although the tests involved only small quantities of LH_2, they were informative in establishing that LH_2 would not detonate, even when solid oxygen was immersed in the liquid hydrogen, unless a strong explosive charge was used as an initiator.

In the series of experiments LH_2 contained in a thermos bottle was subjected to heavy impact 61 times. Ignition never occurred as a result of the impact alone. When a squib or a hot wire was employed to ignite the hydrogen vapor following smashing of the thermos bottle by a heavy weight, very little overpressure was measured, indicating deflagration without detonation. Detonation occurred in two tests, both in cases where oxygen was deliberately mixed with the LH_2.

- Spill tests performed by Arthur D. Little, Inc. for the Air Force in 1958[12].

This test program was designed to simulate a set of conditions which might be encountered in storage or transport of large quantities of LH_2, with the objective of establishing a basis for realistic quantity-distance relationships and safe-handling procedures. The tests included spills of several quantities of LH_2 ranging in size from 5 liters to 5000 gallons to study the magnitude of the hazards involved. Spill tests of some hydrocarbon fuels were also made for comparison purposes. Once again it was demonstrated that hydrogen

will not ignite from impact, either from bullets being fired through the container or from the container being smashed, and that, unless confined on at least three sides, it will not detonate when ignited.

The comparison tests with hydrocarbon fuels demonstrated the difference in burning characteristics. Spills of 32 gallons of each of the fuels produced the following results:

Fuel	Duration of Fire
LH_2	27 seconds
Propane	4 minutes
Gasoline	≈5 minutes
JP-4	≈7 minutes

Radiation measurements of the hydrogen flame indicated a maximum emissivity of 0.085, compared with a value of about 1.0 for the hydrocarbon fuels.

Following are conclusions taken from reference 12 which are considered pertinent to the subject study:

1. Detonation effects of a large-scale spill - There was no evidence to substantiate the premise that the mixture of hydrogen and air formed by the sudden release of liquid hydrogen will detonate when ignited by a spark.

    a. In no spill did the resulting vapor cloud detonate.

    b. In all tests (in which an ignition source was provided), the pressure effects of the resulting fireball were negligible except where there was semi-confinement of the gases.

    c. Transition from deflagration to detonation requires a significant pressure buildup.

    d. Detonation of a perfect stoichiometric mixture of hydrogen and air took place only when initiated by a strong detonator.

    e. It is probable that a perfect mixture of hydrogen and air will not occur.

2. Deflagration effects of large-scale liquid-hydrogen release - The hazards associated with fire occurring after the release of liquid hydrogen vary according to the limits and duration of the flames.

   a. Deflagration effects are considerably less if ignition occurs immediately upon liquid release. Initial fireball size increases greatly with delayed ignition.

   b. In all large spills of hydrogen, the duration of the fireball would be so brief that metal structures would suffer no significant damage; however, combustible materials would probably be ignited and personnel within the fireball would be severely burned.

   c. After dissipation of the initial fireball, flames would be confined to a region directly over the diked area, but could extend 150 ft into the air.

3. Hydrogen hazards as compared to those of hydrocarbons - The hazards associated with the handling and storage of liquid hydrogen are less than those encountered with petroleum fuels.

   a. Liquid hydrogen evaporates much more rapidly. (When a flame was present, a pool of hydrogen vaporized in 1/20 to 1/50 the time required to evaporate a gasoline or propane pool of equal depth.)

   b. The flame from combustion of liquid hydrogen radiates less than 1/10 the energy per unit flame area emitted by the hydrocarbon fuels (emissivity of the hydrogen <0.1; emissivity of a hydrocarbon ≈ 1).

   c. The high evaporation rate and low heat transfer from flame to liquid pool make the probability of boil-over (i.e., the superheating of a large mass of liquid until a sudden flashing to vapor by a sizable portion of the mass occurs) improbable with liquid hydrogen.

4. Effects of storage-tank rupture - In cases where rupture of a storage tank is caused by a pressure buildup in excess of the capacity of the pressure-relieving device, a fire may be caused by the tearing of the metal at the time of rupture.

- Spill tests of LH_2 performed by NASA at White Sands Test Facility, New Mexico, during 1980[13].

These consisted of seven spills, six approximately 5.7 m^3 (1500 gallons) of LH_2, the seventh was about 2.7 m^3. No ignition was planned and none occurred. The objectives were to determine the time required for evaporation of the LH_2 and to study the path of the gaseous hydrogen as it dissipated in the

atmosphere. Preliminary data, supplemented by movie and still photographs showing the movement of the cloud of water vapor formed as the gaseous hydrogen dissipated, provided a basis for validating the mathematical model of such an event developed for the subject study.

- Spill tests of liquid natural gas (LNG) conducted by Lawrence Livermore National Laboratory for Department of Energy at China Lake[14].

Lawrence Livermore National Laboratory (LLNL) is conducting an extensive series of spill tests with LNG under contract to the Department of Energy (DOE). The purpose of the work is to determine experimentally how LNG dissipates in the atmosphere, and then to represent the occurrence with a mathematical model. The objective is to provide DOE with the capability of predicting the hazard to surrounding areas in the event large quantities of LNG are spilled. Since natural gas is generally at least 85 percent methane the results of LLNL's test program were of interest in determining the validity of the atmospheric dispersion computer model created by John Muir Institute for the subject program.

Two series of LNG spills have been conducted by LLNL at China Lake, California; an initial series used 5 m^3 in each spill, a later series involved nine spills of approximately 28 m^3 (roughly 7400 gal.) each. The tendency of the visible cloud associated with vaporized LNG to remain nonbuoyant for extended periods compared to the relatively rapid rise of the cloud resulting from a LH_2 spill as observed in the NASA experiments provided confirmation of data calculated by the subject atmospheric dispersion model.

These four experimental programs were helpful in providing information which was of use in carrying out the evaluations in this study. However, it is obvious much more experimental testing should be done to provide authentication of the analytical conclusions presented herein. Section 7 of this report suggests a number of examples.

3.3 Aircraft Design Characteristics

During previous studies for NASA[4], Lockheed established preferred designs of aircraft fueled with LH_2, LCH_4, and Jet A, respectively, for a series

of missions. Aircraft designed for one of those missions were selected to serve as a basis for the crash fire hazard comparison of the present study. The mission selected was to carry 400 passengers, plus appropriate cargo, a design range of 10,190 km (5500 n.mi.), at a nominal cruise speed of Mach 0.85.

Some characteristics of the aircraft designed for each of the specified fuels to accomplish this mission are shown in table 2. Because of the similarity of the heating values and physical properties of Jet A and JP-4 it was assumed, for purposes of this study, that the characteristics listed for the Jet A-fueled aircraft also represent the JP-4 design.

TABLE 2. - CHARACTERISTICS OF LH_2, LCH_4, JET A, AND JP-4 FUELED SUBSONIC TRANSPORTS

(400 Passenger, 10,190 km (5500 n.mi.), Mach 0.85)

			Liquid Hydrogen		Liquid Methane		Jet A and JP-4	
Gross Weight	kg	(lb)	168,740	(372,000)	225,680	(497,300)	232,060	(511,600)
Total Fuel Weight	kg	(lb)	25,600	(56,460)	69,040	(152,200)	84,780	(186,900)
Block Fuel Weight	kg	(lb)	21,620	(47,670)	58,980	(130,030)	72,350	(159,500)
Operating Empty Weight	kg	(lb)	103,300	(227,750)	116,170	(256,120)	107,360	(236,700)
Wing Area	m^2	(ft^2)	296.7	(3,195)	385.0	(4,144)	380.2	(4,093)
Span	m	(ft)	51.8	(170.0)	58.9	(193.1)	58.5	(192.0)
Fuselage Length	m	(ft)	65.7	(215.6)	61.4	(201.3)	60.0	(197.0)
Fuselage Diameter	m	(ft)	6.63	(21.75)	6.10	(20.0)	5.84	(19.17)
Thrust Per Engine	N	(lb)	136,000	(30,350)	177,030	(39,800)	185,030	(41,600)
Specific Fuel Consumption (Cruise)	kg/hr / N	lb/hr / lb	0.0206	0.202	0.0504	0.494	0.0615	0.603
L/D (Cruise)	--	--	17.4		19.21		19.13	
Takeoff Field Length	m	ft	2440	8006	2430	7973	2431	7976
Approach Speed	m/sec	kts	71.0	138	66.5	129	65.3	127

Data from Reference 4

The geometry and general arrangement of the three aircraft designs are illustrated in figures 1, 2, and 3. It will be noted that the tanks for the cryogenically-fueled aircraft are located within the fuselage, one just aft of the flight station and one just forward of the empennage. An extensive design study was made for both the LH_2 and the LCH_4-fueled aircraft to determine if other tankage arrangements might offer advantage. It was found that for both fuels the fore and aft internal fuselage arrangement provided the best arrangement; i.e., lowest direct operating cost for a practical design. Accordingly, the tankage arrangements shown in figures 1 and 2 were adopted for the LH_2 and LCH_4 aircraft designs, respectively.

The noncryogenic fuels, viz., Jet A and JP-4, are conventionally carried as shown in figure 3; i.e., with the fuel contained within the wing structural box.

3.3.1 Fuel system arrangements

3.3.1.1 Conventional fuel system. - Figure 4 is an illustration of a fuel system arrangement for a conventionally-fueled modern transport aircraft. Insofar as possible all fuel system plumbing is carried within the wing structural box in the same volume in which the fuel is contained. Thus, in event of a leak in the plumbing no fuel is lost. Also, burying the plumbing within the tank eliminates concern about damage to that part of the fuel plumbing system in event of a crash. The portions of the plumbing system inside the wing box can be damaged only if the tank itself is penetrated, an event of much more serious consequence. The only portions of the fuel plumbing system which are vulnerable to primary damage leading to large fuel spills in event of a survivable crash are those lines and components external to the tanks. For example, the line leading from the tank to an engine will be sheared off if the engine pod is torn from the wing.

In a four-engine aircraft the auxiliary power unit (APU) is usually mounted in the tail section. Accordingly, a fuel line must run from the wing tank aft through the fuselage, back to where the APU is located. Under normal

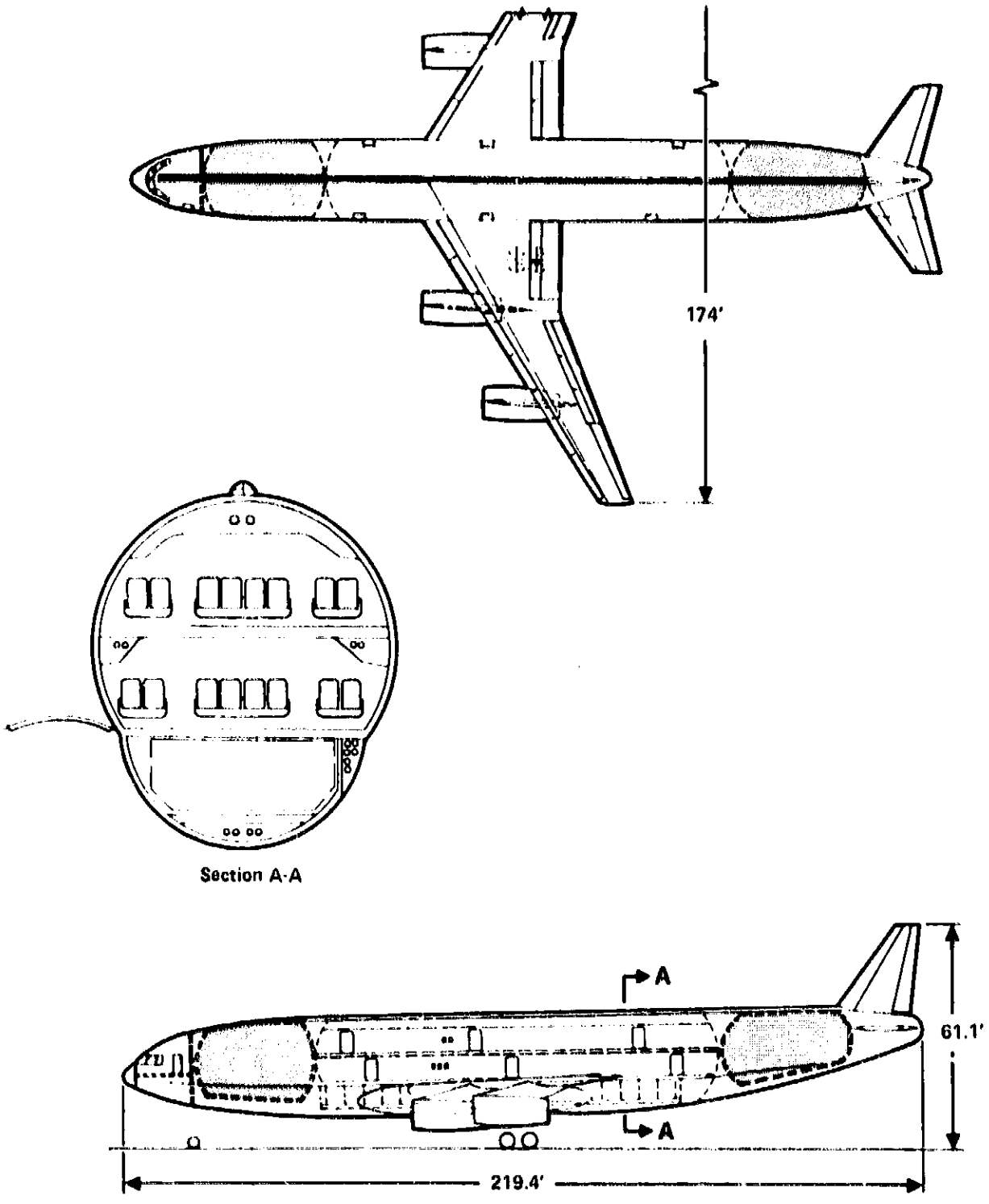

Figure 1. - LH_2 - fueled transport.

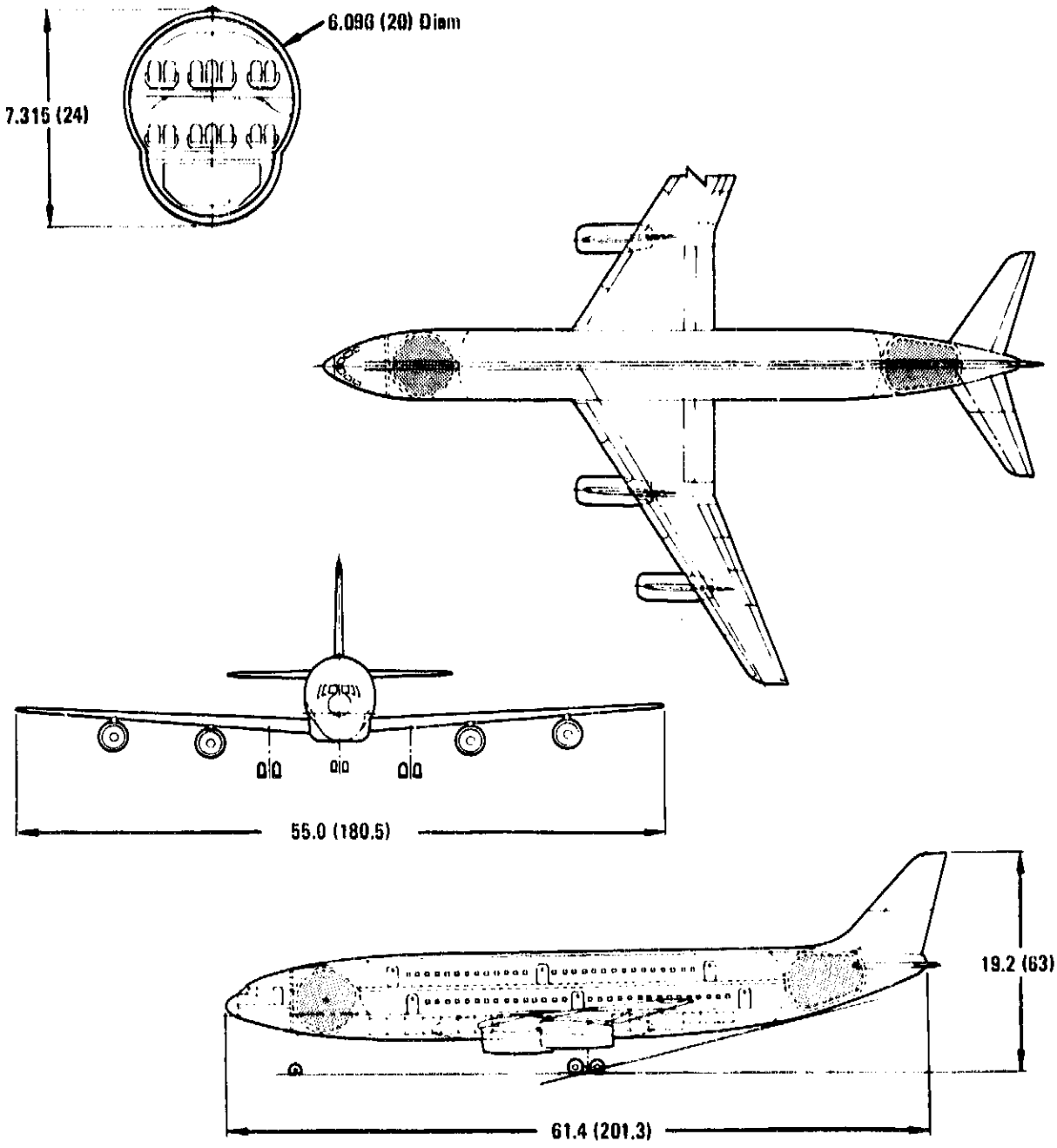

Figure 2. - Methane-fueled transport.

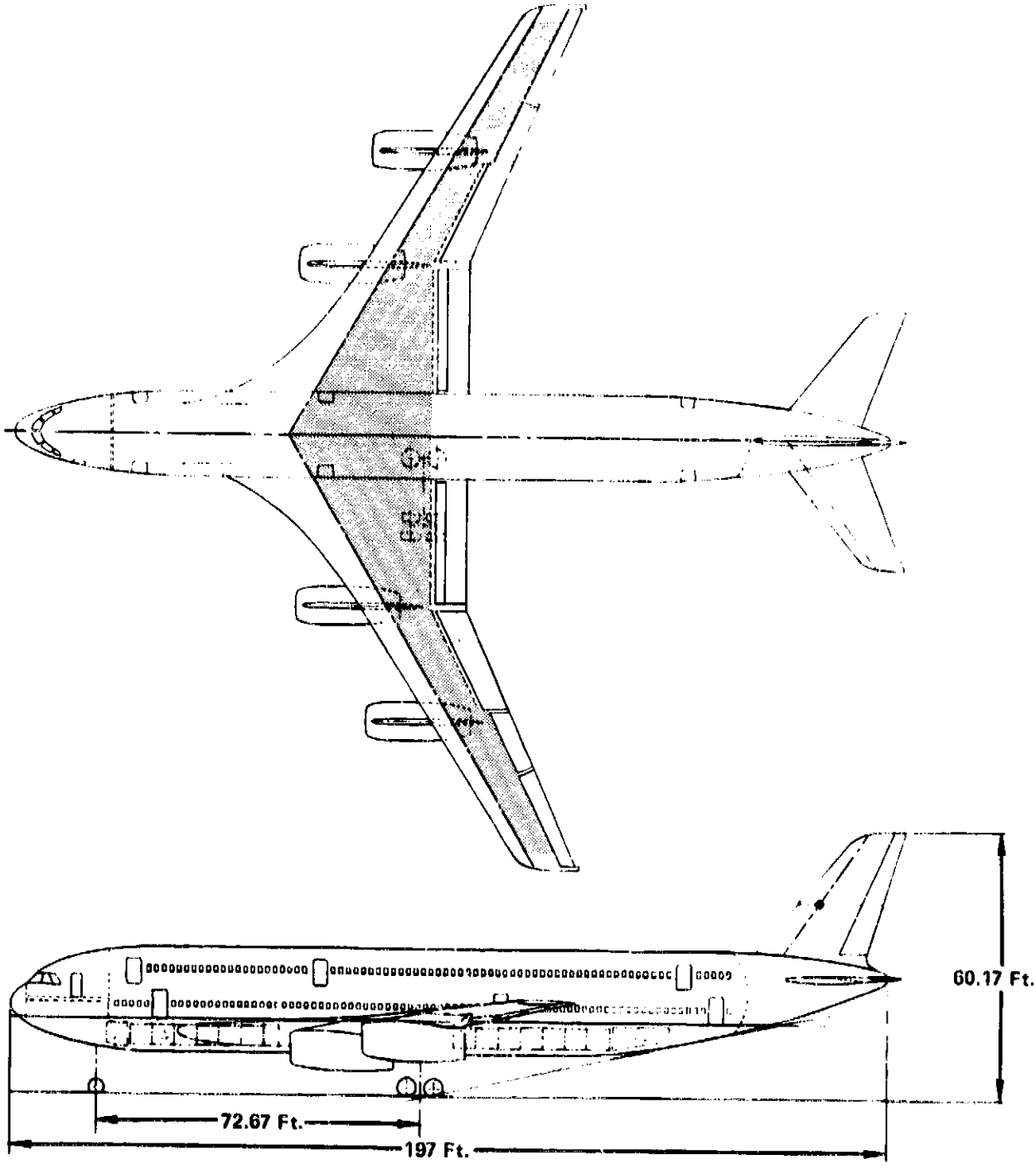

Figure 3. - Jet A - fueled transport.

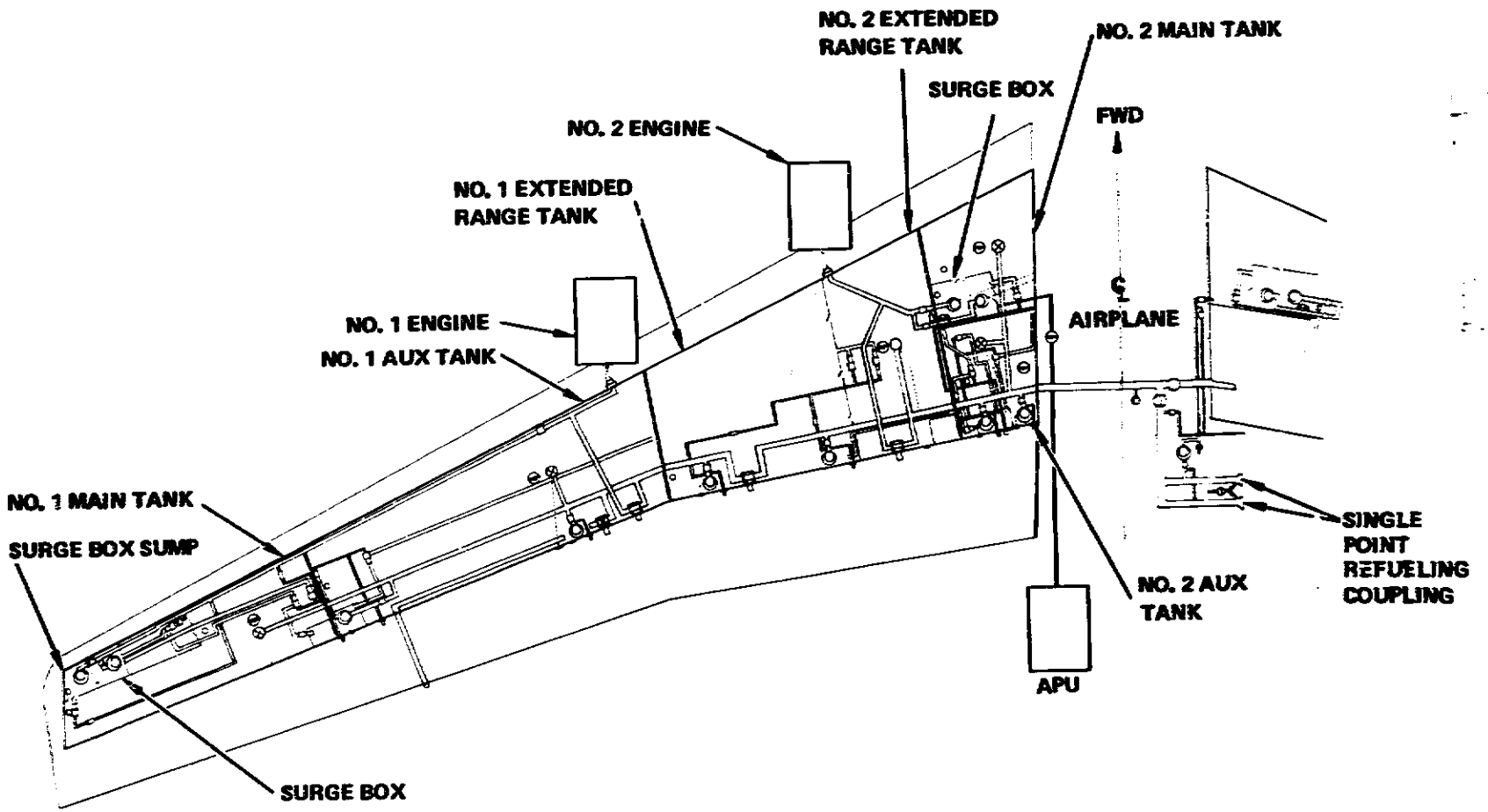

Figure 4. - Fuel system arrangement for conventionally fueled transport aircraft.

circumstances this fuel line can be located well within the fuselage structure and thus be virtually invulnerable to serious damage, except in cases where the fuselage is physically torn apart. For example, in the three-engine Lockheed L-1011 aircraft, the fuel line which runs aft to the No. 2 engine and to the APU, is located just below the cabin floor and very close to the vertical centerline. There is about eight feet of structure below the fuel line to the aircraft skin which effectively protects the fuel plumbing in the event the airplane makes a wheels-up landing.

In addition to being located in the fuselage where the line is physically protected, since 1967 fuel lines in commercial transport aircraft have been required by Federal Aircraft Regulation to provide "a reasonable degree of deformation and stretching without leakage" to accommodate limited amounts of fuselage separation. Again as an example, Lockheed policy is to make the fuselage-mounted fuel lines capable of stretching to 50 percent of their original length. Thus, it would require a crash severe enough to separate sections of the fuselage by several feet in order for the No. 2 engine/APU fuel feed line in the L-1011 to pull apart and spill fuel. The accident data analyzed and reported in section 3.4 shows the probability of this happening in a survivable crash is fairly small.

3.3.1.2 Cryogenic fuel system. - The general arrangement of a fuel system for a cryogenically-fueled airplane is depicted in figure 1. With fuel tanks located fore and aft in the fuselage it is apparent fuel lines must run between the tanks and also out to the engines mounted in the wings. In this case, as contrasted with the conventionally-fueled aircraft, even though the lines running to the engines are located in the wing structural box for maximum protection against damage, they will be the source of fuel leakage resulting from any impact that severs or massively punctures the wing.

The comparison of fuel spillage which might result from wing damage in a cryogenically fueled airplane versus one fueled conventionally is a matter of quantity and fuel spill rate. With Jet A or JP-4 fuel, both of which are stored in the wing, a puncture of the wing box will result in spill of all the fuel in that tank at a rate which is a function of the size of the hole.

With LH_2 or LCH_4, the worst that will happen in event of wing damage is that an engine feed line will be severed. The amount of fuel spilled as a result will be contingent on whether the boost pumps and the fuel shut-off valve are turned off or not. The rate of spillage will almost certainly be far less than in the case of the conventional fuels.

Fuel lines for cryogenic fuels will be insulated to minimize heat leak. Without adequate insulation, the fuel would vaporize on its way to the engine fuel pump, ultimately causing the pump to cavitate, thereby starving the engine. Accordingly, the lines will typically be designed as shown in figure 5. The line carrying fuel to each engine will be approximately 2.54 cm (1.0 inch) in diameter for the size aircraft adopted as a basis for this study. It will be encased in a closed-cell, rigid plastic foam about 3.81 cm (1.5 inch) thick. In turn, the foam insulation is contained within a thin aluminum tube 10.16 cm (4 inch) in diameter which serves the dual function of mechanically protecting the foam and preventing air from cryopumping in event of local failure of the foam. Bellows will be provided at intervals to accommodate thermal expansion and contraction, plus mechanical vibration and flexing. Wherever these fuel lines pass through pressurized areas they are contained in a shroud which is provided with positive air flow. Hydrogen (or methane) detectors will be located at the discharge to sense leaks.

For a more complete description of a representative cryogenic fuel system see reference 3. There are many more elements to a complete system which are required to perform the various functions needed on board an aircraft. These include pressurization, venting, fueling, defueling, crossfeed, etc. However, for purposes of assessing the crash fire hazard, the engine fuel supply system just described, represents the principal challenge. Crash damage to the other systems, with the exception of crossfeed, will not result in significant fuel spillage.

The crossfeed system involves the fuel lines which traverse the fuselage connecting the tanks so that there are multiple routes by which any engine can be fed fuel from any tank. They are located in the fuselage just below the cabin lower floor as shown in the right side of section AA in figure 1. These lines are subject to damage in event of a crash in which the fuselage

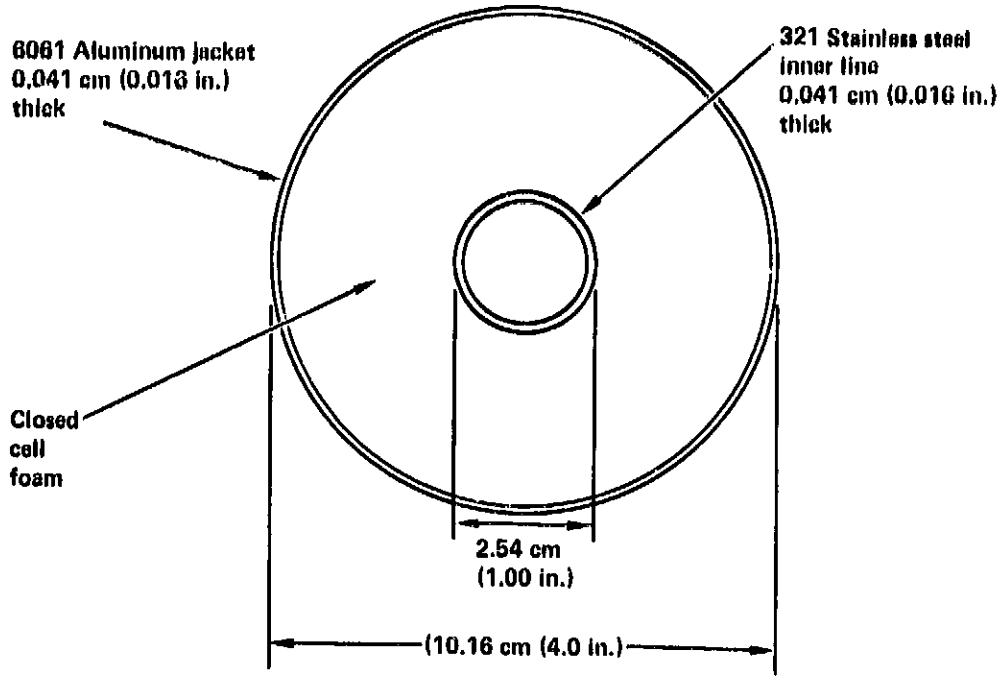

Figure 5. - LH2 fuel line cross section.

is broken. They are the same size as the engine fuel feed lines in the wings and their severance will result in the same fuel spillage potential.

3.3.1.3 Cryogenic tankage. - Tanks for cryogenic fuel are designed to entirely different specifications than their counterparts for conventional fuels. Both LH_2 and LCH_4 are tanked as saturated liquids at a nominal pressure of 145 kPa (21 psi). The tanks are pressurized with their own vapor product, and so they contain no air or oxygen. Consequently, there is no fire or explosion hazard within the tanks. Conventional fuel tanks, on the other hand, are vented to the atmosphere to minimize differential pressure on the structure, so there is continually a mix of fuel vapor and air above the surface of the liquid fuel which may be susceptible to ignition. The cryogenic fuels therefore are inherently safer in this regard in event of a crash.

Tank pressure in the case of the cryogenic fuels is controlled by venting to relieve excess pressure when heat buildup is too great, and by intentionally

vaporizing liquid fuel when tank pressure drops below a specified limit. The cryogenic tanks are designed to an ultimate pressure of 208 kPa (30.2 psi). For comparison, the passenger cabin is designed to an ultimate pressure of only 124 kPa (18 psi). It is much more likely, therefore, that the fuel tanks would survive intact in event of a crash, rather than the rest of the fuselage. The fuselage would tend to break in its weakest parts.

Another aspect of the tankage of the cryogenic fuels which results in their being less likely to suffer damage in event of a survivable crash, compared to conventional fuels, is their location in the fuselage. The tank dimension (its width) which is vulnerable in a collision with an obstacle on the ground is significantly less for the fuselage-mounted tanks than for wing tanks. As an example, in the LH_2-fueled aircraft shown in figure 1, the fuselage tank has a width of 6.63 m (21.75 ft). The Jet A-fueled aircraft designed for the same mission, illustrated in figure 3, has a wing span of 58.5 m (192 ft), most of which contains fuel and is vulnerable to damage from impact which could cause fuel spillage. In the LH_2 aircraft, of course, the wings are devoid of fuel except for the engine supply lines which, as explained in section 3.3.1.2, are contained in the structural box between the front and rear spars and are downstream of shut-off valves controlled from the flight station.

An additional factor in this regard is the consideration that the fuselage-mounted tanks of the cryogenic fuels have a significant amount of structure both ahead of and beneath them to absorb impact loads. Examination of figures 1 and 2 shows that the nose structure of both of these aircraft would have to be crushed before a frontal collision would impact the forward tank. Also, the underside of the tanks in both aircraft is protected, by a minimum of 45.7 cm (18 in.) for the forward tank and 35.5 cm (14 in.) for the rear tank, with specially designed structure to preserve their integrity in event of nose gear collapse, a wheels-up landing, or a tail scrape. This protection should assure a better record of crash survival for cryogenic fuel tanks than the conventional fuel wing tanks.

The tanks for both LH_2 and LCH_4 are insulated to minimize heat leak which would cause rapid boiloff of the fuel. Two types of insulation which

have been found to be most promising as a result of detailed analysis[3] are illustrated in figures 6 and 7 as designed for the LH_2-fueled aircraft. These insulation systems are, respectively, rigid closed-cell foam, and microspheres.

Both designs were established on the basis of minimizing direct operating cost for the aircraft by selecting an optimum compromise between insulation system weight and cost of fuel allowed to boil off. The rigid closed-cell foam design must be thicker than the microsphere system because the evacuated microsphere annulus is a more efficient insulator. However, the microsphere system weighs a little more and requires an active pumping system, an extra complication not required by the passive foam system.

NASA has carried out extensive preliminary tests of many candidate foam insulations[28]. Some, such as Stepan Foam and a General Electric polyurethane composition, have been shown to be very efficient for the cryogenic application. The potential life of these materials has yet to be explored, however.

As shown in figure 6 the rigid closed-cell foam is applied directly to the outer surface of the tank. Over that is laid a vapor barrier such as a 0.127 mm (0.005 in.) thick composite sandwich of mylar-aluminum-aluminum-mylar-fabric mesh (MAAMF), the purpose of which is to prevent cryopumping of air into the foam during its operational life, and also to prevent the same occurrence in the event the foam develops a crack or other defect.

A flexible open-cell foam layer is applied over the MAAMF to provide a spring-like cushion between the rigid foam and the Kevlar-syntactic foam panel which serves as the outer surface of the aircraft in the area of the cryogenic fuel tanks. A second MAAMF layer is applied between the flexible foam cushion and the Kevlar panel to provide a sealed annulus occupied by the cushion which is purged with nitrogen.

The microsphere insulation system is illustrated in figure 7. Microspheres are tiny hollow spheres of borosilicate glass. They are contained in an evacuated annulus surrounding the tank which is formed by a 0.127 mm (0.005 in.) thick stainless steel (CRES) outer shell. The annulus is

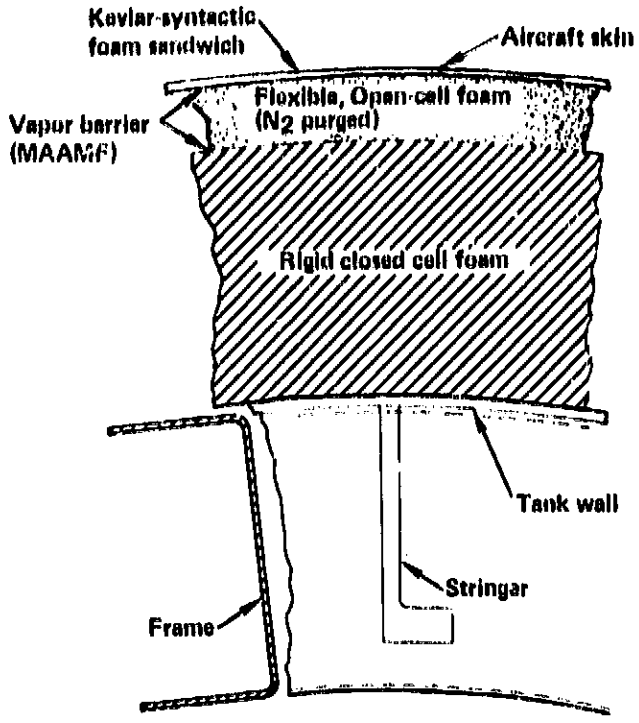

Figure 6. - Rigid, closed-cell plastic foam tank insulation.

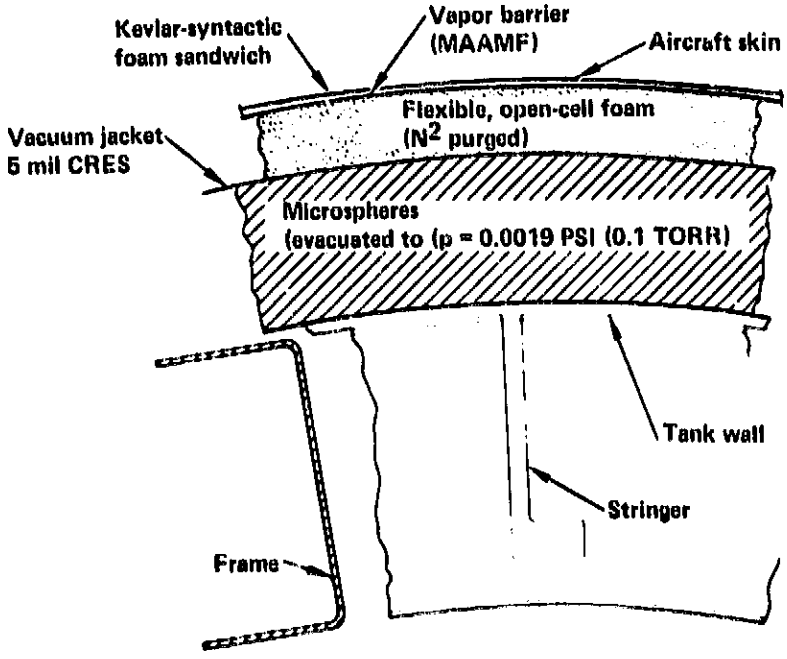

Figure 7. - Evacuated microsphere tank insulation system.

maintained at a soft vacuum of approximately 13.3 Pa (0.1 Torr). The same flexible cushion formed by open-cell foam purged with nitrogen is used to support the Kevlar aircraft skin. This insulation system is 27.9 mm (1.1 in.) thinner than the closed-cell foam design and still results in less fuel boiloff. However, it would be a more expensive system. Experimental testing and development of both systems has been recommended to explore the potential advantages and shortcomings of each.

The volumes forward and aft of each tank in the aircraft (see figures 1 and 2) are intended to be actively flushed with air whenever hydrogen (or methane) sensors located in the space detect leaked fuel. In flight the air purge can be provided by opening vents and using ram air. On the ground the positive air flow can be provided by blowers installed for the purpose.

A unique potential problem posed by the location of the tanks for the cryogenic fuels in the fuselage is the question that surviving passengers and crew could be faced with the hazard of exposure to the fuel itself. Very brief contact with LH_2 produces the effect of a burn on human skin. Exposure of large areas of the body to cryogenic temperatures for even brief periods, of course, would be fatal.

It is always possible to postulate circumstances in which large quantities of fuel are spilled and some of it drains into the passenger compartment. However, in view of the design of the tank and its installation it is considered highly improbable that there would be a survivable crash where this would happen. To illustrate, two pressure bulkheads separate the fuel from the passengers. As previously pointed out, the cryogenic fuel tanks are designed as pressure vessels to an operating pressure of (21 psia). Another pressure bulkhead forms the ends of the passenger compartment adjacent to both the forward and the aft fuel tanks. Both the end of the fuel tank and the adjacent bulkhead leading to the passenger compartment would have to be ruptured to permit direct access of fuel to the passengers. To explore this eventuality an experimental program has been suggested (see Section 7, Recommendations for Future Work) which would involve crashes of suitably modified surplus aircraft.

3.3.2 Passenger cabin wall structure. - One of the important tasks of this study was to evaluate the relative hazard of passengers inside the cabin when the outside of the fuselage is exposed to fire from spilled fuel. To evaluate this hazard it is necessary to know the structural design of a typical section of the fuselage and the materials involved in its construction so the thermal properties can be determined.

View A-A of figure 8 is a representative picture of how the sidewall of a modern passenger transport is constructed. The Lockheed L-1011 design is used as illustration. In the section where the windows are located the aircraft skin is reinforced with a doubler. Frames are located 20 inches on center. Above and below this window belt is a section where fail-safe straps of titanium are employed to reinforce the aluminum skin. A cross section through the wall in this area of the fuselage is illustrated in figure 9 with material callouts noted.

The aircraft skin is clad 2024-T3 aluminum of 2.29 mm (0.09 inch) thickness. A layer of AA fiberglass insulation 57.2 mm (2.25 in.) thick is retained about 12.7 mm (0.5 in.) from the inside surface of the skin. In turn, spaced about 9.5 mm (3/8 in.) from the inside surface of the fiberglass insulation is a honeycomb panel which serves as the interior wall of the cabin. The honeycomb panel consists of a core of crushed nomex with surface sheets of hard fiberglass on both sides. The total thickness of the honeycomb panel is 3.18 mm (0.125 in.).

A section showing the construction of a window is presented in figure 10. The 825 cm^2 (128 in^2) clear area consists of three panels, the outer two being structural members, the innermost being simply a protective layer to prevent scratching of the more critical panes. It also serves a function of permitting circulation of warm dry air to prevent fogging.

The thermal characteristics of the cabin wall section are presented in section 5.5, along with an analysis of heat transfer through the wall as a function of time as a result of exposure to various fire conditions.

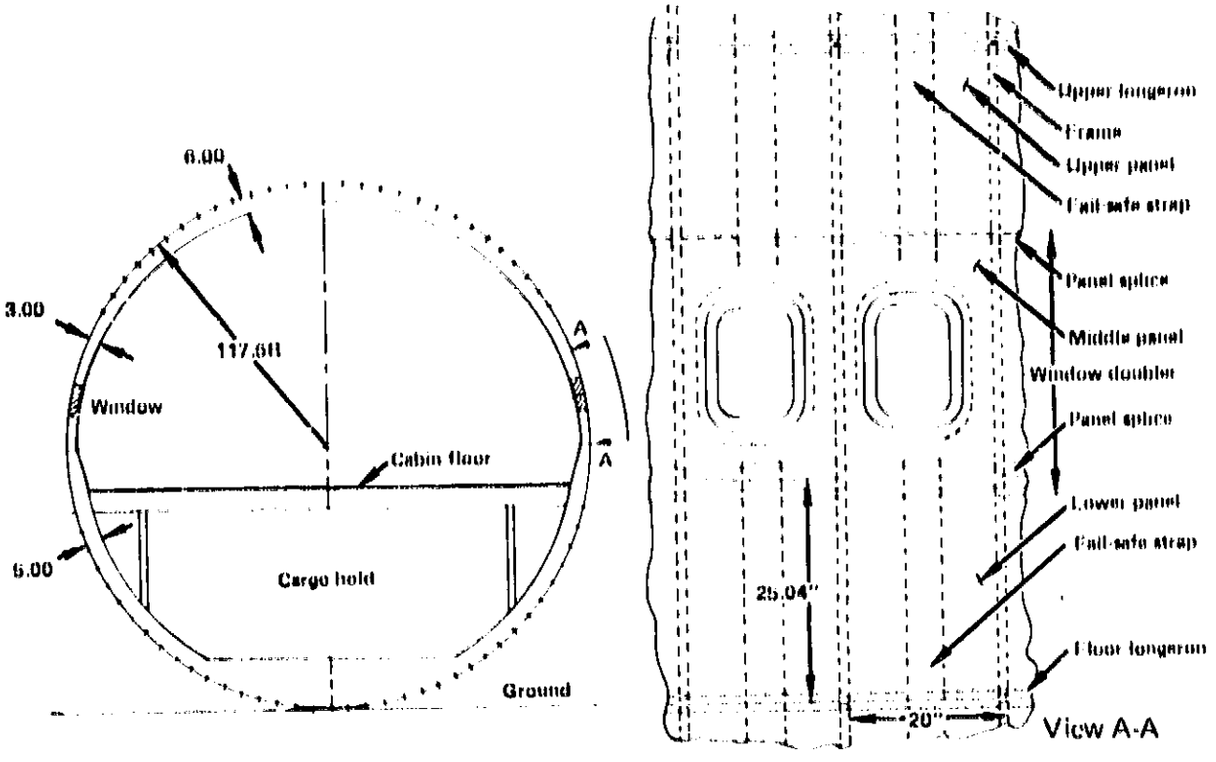

Figure 8. - L-1011 typical fuselage cross section.

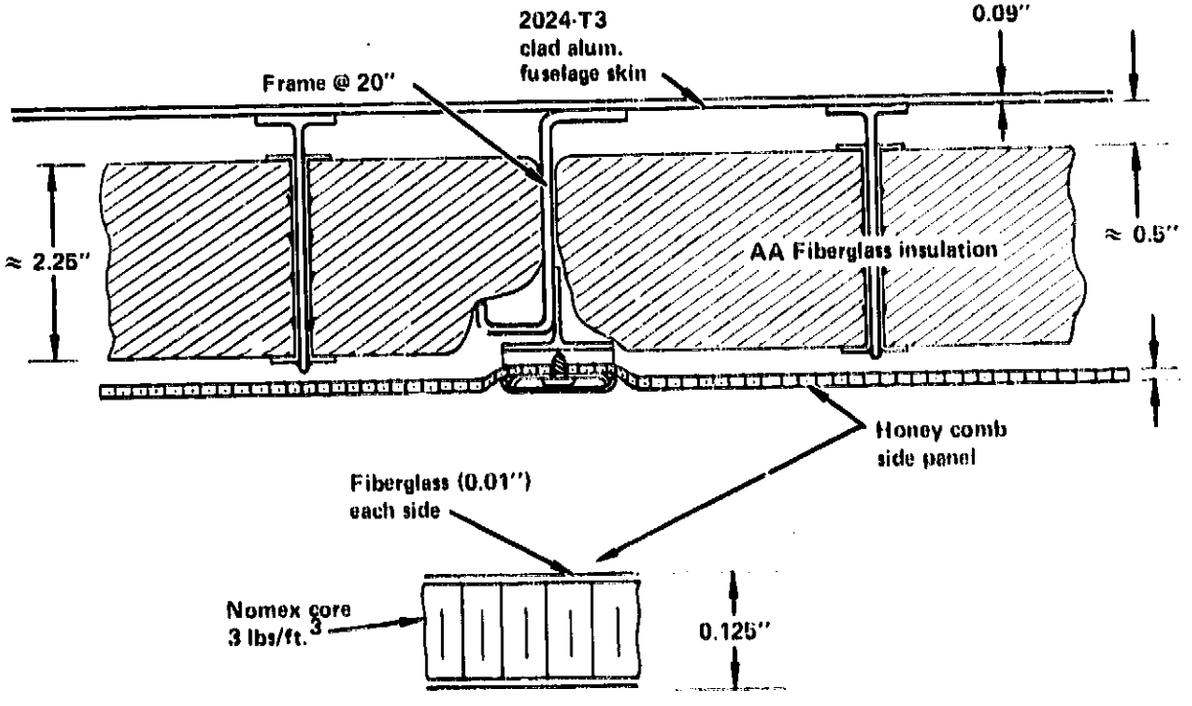

Figure 9. - L-1011 fuselage sidewall (typical cross section).

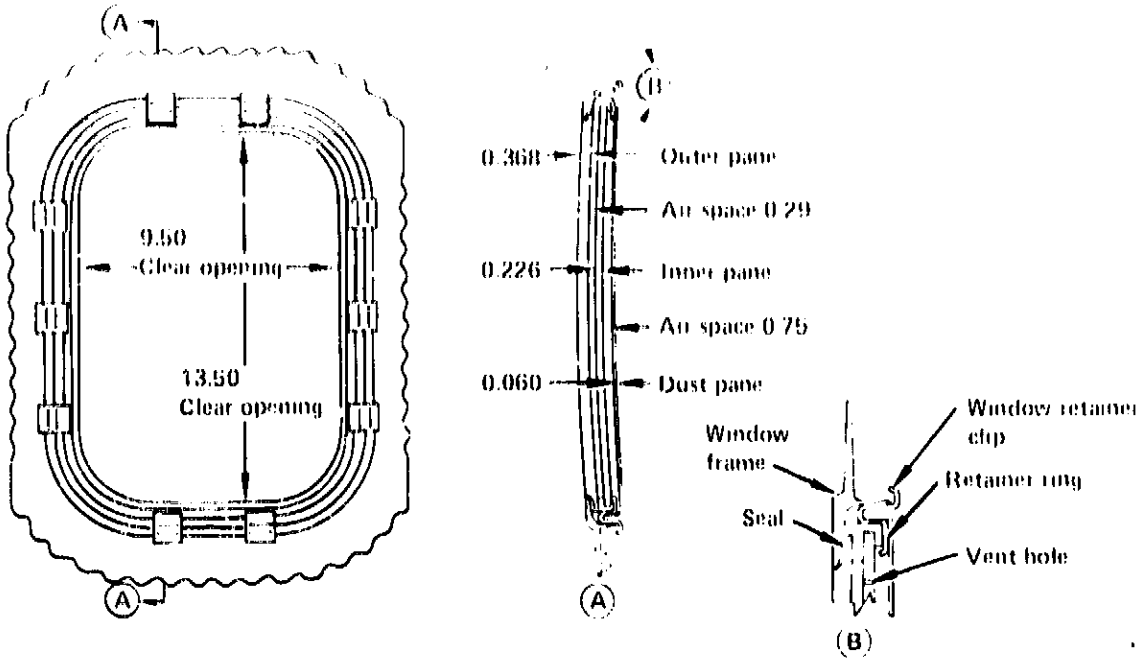

Figure 10. - L-1011 cabin window assembly.

3.4 Aircraft Accident Records

The sources of accident data used in this review were:

a. National Transportation Safety Board (NTSB)

b. International Civil Aviation Organization (ICAO)

c. World Airline Accident Summary - Civil Aviation Authority (CAA)

d. Lockheed Company Accident Files

e. Miscellaneous Reports, Articles.

The NTSB records, particularly accident summaries (references 15 and 16) for the years 1964-1977, were the primary source of information for compiling statistics. The other data sources, as well as more current accident reports, were used to augment the NTSB records. A complete evaluation of the accident data is provided in reference 17.

Table 3 provides a summary of 783 NTSB accidents for the period 1964-1977 as functions of injury index and operational mode. This total was reduced to 341 since many of the accidents were not pertinent for the purposes of this study. Those accidents eliminated from further consideration were:

- Small aircraft (TOGW < 5670 kg (12,500 lb))
- Nondesign-related items (turbulence, hail, sabotage)
- Improper safety practices (unfastened seat belt, passenger/attendant aisle injuries)
- Unrealistic impact conditions (in-air aircraft collisons, collision with on-ground personnel)
- Miscellaneous accidents (inadvertent door opening, static operations).

The reduced number of accidents is shown in table 4. They consist of accidents due to:

- Controlled and uncontrolled collisions with ground/water
- Undershoot
- Stall
- Hard landing
- Wheels up, retracted gear, gear collapse
- Overshoot
- Swerve
- Obstacle impact or collision.

Figure 11 shows a comparison of the number of occurrences of fatal, serious injury and minor/non-injurious accidents for the original 783 data set and the reduced 341 accident data set. As can be noted in figure 11, both sets of data are consistent with each other in that both show uncontrolled and controlled collisions with ground resulting in a substantial number of fatal and serious injury accidents; while stalls, overshoots, undershoots and accidents involving obstacles result in a moderate number of fatal and serious

TABLE 3. – SUMMARY OF ACCIDENT TYPES BY OPERATIONAL MODE

1964-77 NTSB Data

Primary Accident Type	Takeoff X	Y	Z	Landing X	Y	Z	Taxi X	Y	Z	Flight X	Y	Z	Static X	Y	Z	Other X	Y	Z	Totals (T)	X	Y	Z
I. Severe Impact																			(96)	54	12	30
A. Controlled collision	2	0	0	15	4	1				9	1	0							(32)	26	5	1
B. Uncontrolled Collision	2	1	1	7	1	0				11	0	0							(23)	20	2	1
C. Undershoot				4	2	20													(26)	4	2	20
D. Stall	1	2	8	2	1	0				1	0	0							(15)	4	3	8
II. Moderate-High Sink Speed																			(176)	9	15	152
A. Hard landing				2	1	27													(30)	2	1	27
B. Gear Collapse	1	1	4	0	2	25	0	0	11				1	2	0				(47)	2	6	40
C. Wheels up	0	0	1	0	1	18													(20)	0	1	19
D. Retracted Gear	0	0	3	0	0	11	0	0	2										(16)	0	0	16
E. Swerve	1	1	7	0	0	25	0	1	2										(37)	1	2	34
F. Overshoot				4	6	16													(26)	4	6	16
III. System Malfunction																			(131)	20	40	171
A. Engine Malfunction	1	9	11	0	4	3	0	1	0	2	3	20	4	6	0				(54)	3	17	34
B. Prop/rotor malfunction	2	0	2	1	0	1	0	1	0	3	0	1	4	6	0				(21)	10	7	4
C. Airframe failure	0	5	1	0	0	3	0	0	3	4	0	5							(21)	4	5	12
D. Fire/explosion	0	2	2	0	1	4	0	3	3	3	0	7	0	5	5				(35)	3	11	21
IV. Collision With																			(95)	30	9	56
A. Trees		–		5	0	3				1	0	1							(10)	6	0	4
B. Ditches, fence, seawall	1	3	1	1	0	0													(6)	2	3	1
C. App. lights, wires	0	1	2	0	2	4				0	0	1							(10)	0	3	7
D. Obstacles (bldg., auto)	1	0	3	1	0	9	0	0	9	0	0	2	0	0	1				(26)	2	0	24
E. People	2	0	0	1	1	0	1	0	0				1	0	0				(6)	5	1	0
F. Aircraft	2	0	0	0	1	0	3	0	17	10	1	1	0	0	2				(37)	15	2	20
V. Miscellaneous unknowns	0	2	5	1	4	8	0	4	1	3	15	2	1	18	2	1	1	0	(68)	6	44	18
VI. Turbulence and misc. flight occurrences	1	0	1	0	4	1				1	203	6							(217)	2	207	8
Totals	17	27	52	44	35	179	4	10	48	48	223	46	7	31	10	1	1	0		121	327	335
	96			258			62			317			48			2			(783)			

X = No. of accidents involving fatalities
Y = No. of accidents in which highest injury index is severe injury
Z = No. of accidents in which only minor/no injuries were sustained

(T) = Total no. of accidents

TABLE 4. - REDUCED SUMMARY OF ACCIDENT TYPES BY OPERATIONAL MODE BASED ON REDUCED NUMBER OF ACCIDENT CANDIDATES

1964-77 NTSB Data

Primary Accident Type	Takeoff			Landing			Taxi			Flight			Totals			
	X	Y	Z	X	Y	Z	X	Y	Z	X	Y	Z	(T)	X	Y	Z
I. Severe Impact													(70)	37	9	24
A. Controlled collision	2	0	0	15	4	1				6	1	31	(28)	23	4	1
B. Uncontrolled collision	2	1	1	2	1	0				4	0	0	(11)	8	2	1
C. Undershoot				4	2	18							(14)	4	2	18
D. Stall	0	1	4	2	0	0							(7)	2	1	4
II. Moderate-High Sink Speed													154)	8	12	134
A. Hard landing				2	1	24							(27)	2	1	24
B. Gear Collapse	1	1	4	0	2	23	0	0	11				(42)	1	3	38
C. Wheels up	0	0	1	0	0	15							(16)	0	0	16
D. Retracted gear	0	0	3	0	0	10	0	0	1				(14)	0	0	14
E. Swerve	1	1	6	0	0	18	0	1	2				(29)	1	2	26
F. Overshoot				4	6	16							(26)	4	6	16
III. System Malfunction													(80)	8	15	57
A. Engine malfunction	1	6	9	0	2	2				1	1	16	(38)	2	9	27
B. Prop/rotor malfunction	2	0	2	1	0	1				1	0	0	(7)	4	0	3
C. Airframe failure	0	3	1	0	0	3	0	0	3	1	0	5	(16)	1	3	12
D. Fire/explosion	0	1	1	0	1	4	0	1	3	1	0	7	(19)	1	3	15
IV. Collision With													(37)	10	6	21
A. Trees				5	0	3				1	0	1	(10)	6	0	4
B. Ditches, fence, seawall	1	3	0	1	0	0							(5)	2	3	0
C. App. lights, wires	0	1	2	0	2	4				0	0	1	(10)	0	3	7
D. Obstacles (bldg., auto)	1	0	1	1	0	2	0	0	6	0	0	1	(12)	2	0	10
Totals	11	18	35	37	21	144	0	2	26	15	1	31		63	42	236
		64			202			28			47			(341)		

X = No. of accidents involving fatalities
Y = No. of accidents in which highest injury index is severe injury
Z = No. of accidents in which only minor/no injuries were sustained

(T) = Total No. of accident.

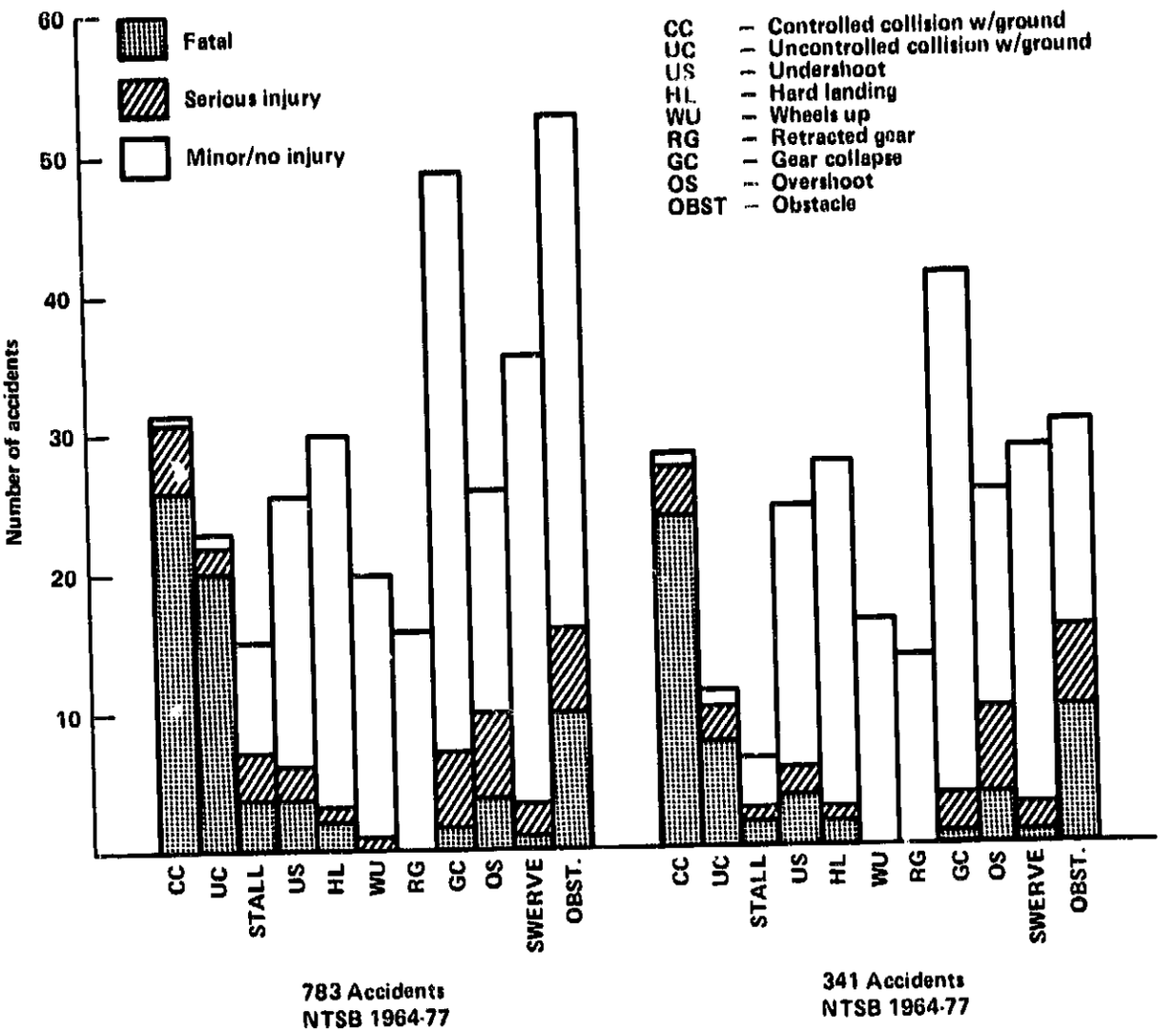

Figure 11. - Comparison of NTSB summaries.

injury accidents on or around airports. Conversely, wheels-up, retracted gear, swerve, hard landing and gear collapse result in few fatal or serious injury accidents.

The NTSB data represents less than 29 percent of the total world accidents during the 1964-1977 period. Figure 12 shows a comparison of the reduced 341 NTSB accidents and worldwide accident types. The trend between both accident sets of data indicates that the reduced NTSB accident data is representative of the worldwide accident history insofar as severity of accident types are concerned. Table 5 summarizes the comparison between the original set of NTSB data, the reduced set of NTSB data, and the worldwide data set.

A total of 108 available accident reports were obtained from the reduced NTSB data set. As part of the study described in reference 17 these

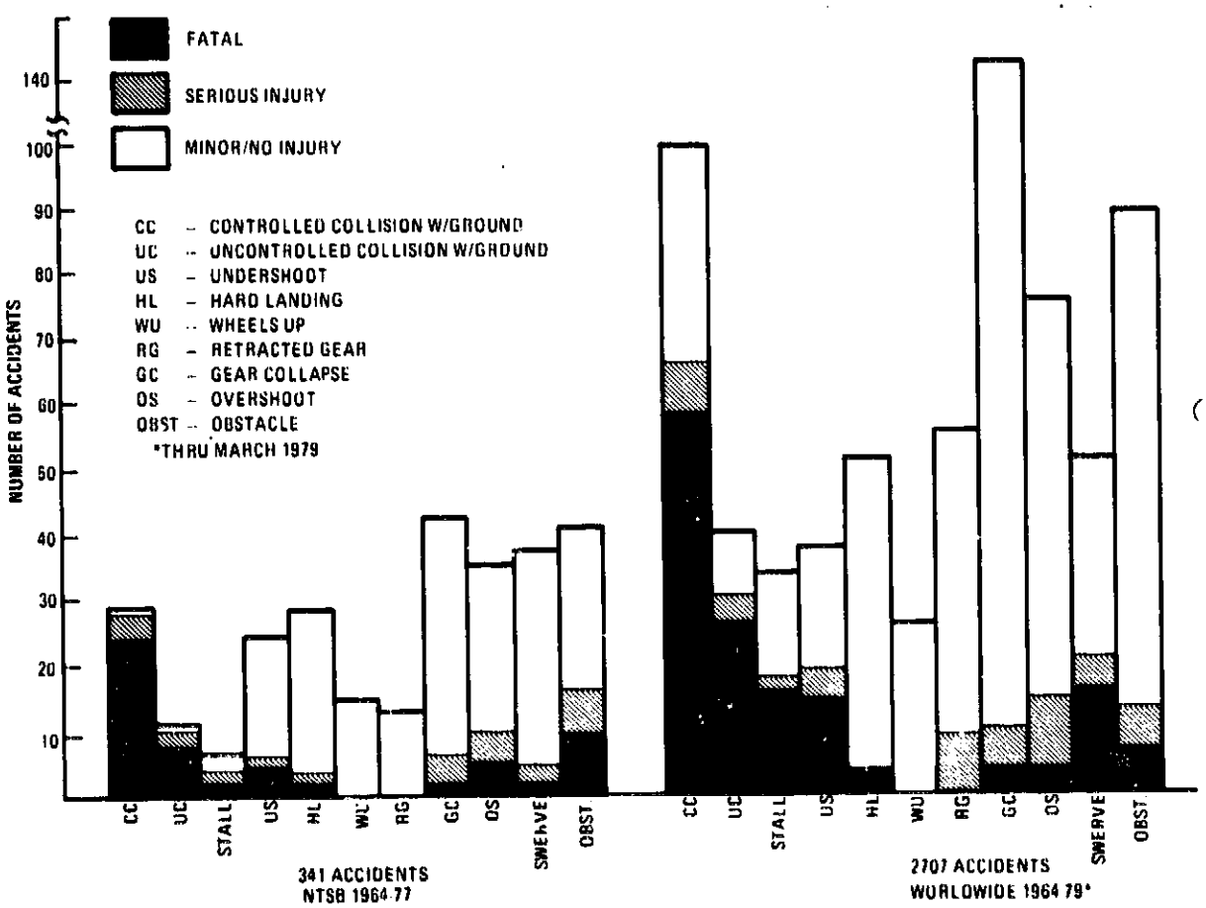

Figure 12. - Comparison of NTSB and worldwide accident summary data.

TABLE 5. - COMPARISON OF FATAL ACCIDENT PERCENTAGES FOR NTSB AND WORLDWIDE ACCIDENT SUMMARIES

Accident Type	NTSB 1964 – 77 (783 Accidents)			NTSB 2964 – 77 (341 Accidents)			Worldwide (1964 – 79)* (2707 Accidents)		
	No. Fatal Accidents	No. Total Accidents	% Fatal:	No. Fatal Accidents	No. Total Accidents	% Fatal:	No. Fatal Accidents	No. Total Accidents	% Fatal:
Controlled collision	26	32	81.3	23	28	82.1	58	100	58
Uncontrolled collision	20	23	87	8	11	72.7	27	40	67.5
Stall	4	15	26.7	2	7	28.6	16	33	48.5
Undershoot	4	26	15.4	4	24	16.7	14	37	37.8
Hard landing	2	30	6.7	2	27	7.4	2	51	3.9
Wheels up	0	20	0	0	16	0	0	27	0
Retracted gear	0	16	0	0	14	0	0	57	0
Gear collapse	2	47	4.3	1	42	2.4	4	152	2.6
Swerve	1	37	2.7	1	29	3.4	8	88	9
Overshoot	4	46	8.7	4	26	15.4	4	76	5.3
Collision with obstacle	10	52	19.2	10	37	27	16	51	31.4
*Thru March 1979									

accidents were classified in accordance with the accident types noted in figures 10 and 11. The accident types were then classified into three crash situation categories. These crash situations are defined below as:

GGO: Ground-to-Ground Overrun Condition (table 6)

AGHL: Air-to-Ground Hard Landing (table 7)

AGI: Air-to-Ground Impact (table 8)

Thirty-two of the 108 accidents were considered as "impact nonsurvivable" or "wipe-outs"; that is, everyone onboard perished. Since Scenarios 2 and 3 in the subject study are concerned only with crash fire hazard in otherwise survivable accidents these 32 accidents were eliminated from further consideration. In addition, ten miscellaneous accidents, which yielded little or no useful information as to causal data were eliminated from the accident files leaving a total of 66 accidents available for data analysis in the three selected crash situations: GGO, AGHL, AGI.

TABLE 6. - GROUND-TO-GROUND, OVERRUN CONDITION, GGO

Type	Characteristics	Accident Description	A/P Definition Required	Hazards and Terrains
GG1 (20 accidents)	• Low Sink Speed or ENV. (1) (1.52 m/sec) • Low Fwd. Vel ≤ T.O. V_R / ≤ Ldg. T/D (Range 40-130 Kts, Avg. 80 Kts) • Symmetrical Impact Conditions Level Attitude • On Runway or Within 500m	• T.O. Abort • Ldg. Overrun	a) Configuration Weight (Ldg./T.O.) CG (Fwd/Aft) Gear Extended Controls Availability (full)	Hazards GG1 (6) Ditch/Storm drain (2) (4) Service Road/Mound (2) each; raised sidewalk fence, light stanchion (1) each; concret slab, upsloped hill, metal bldg. Terrain (4) Runway/Taxiway (4) Hard dirt (8) Unstated (1) each; grassy dirt, mud/soft, water, sand/water Average Overrun 239m Range 26.8 – 498m
GG2 (9 accidents)	• Low Sink Speed or ENV. (1.52 m/sec) • Low Fwd. Vel. ≤ T.O. V_R / ≤ Ldg. T/O (Range 60-100 Kts, Avg 74 Kts) • Symmetrical Impact Conditions Level Attitude • Within 1000m. of Runway	• T.O. Abort • Ldg. Overrun	a) Configuration Weight (Ldg/T.O.) CG (Fwd/Aft) Gear Extended Controls Availability (full)	Hazards GG2 (5) Ravine Embankment (3) Lights/Poles (2) each; fence, drainage ditch vehicles (1) each: service station, hill, trees, rocks Terrain (5) Ravine (1) each; grassy dirt, sand, sod, rough Average Overrun 293m. Range 36.6 – 1036m.

1 ENV = effective normal velocity
(2) (X) = number of occurrences
(3) GG2 accidents include hazards not usually involved in GG1 accidents

TABLE 7. - AIR-TO-GROUND, HARD LANDING, AGHL

Type	Characteristics	Accident Description	A/P Configuration	Hazards and Terrains
Air to Ground AG1 (11 accidents)	• High Sink Speed or ENV. (1) (>3.1 m/sec) (<10 m/sec) Avg ~ 6 m/sec. • Fwd. Vel. <Final Approach >L.O/TD 126-160 Kts • Symmetrical Impact Conditions ≤15° Nose UP • On Runway or Within 100m.	• Hard Landing • Undershoot	a) Configuration Weight (Landing) CG (Fwd./Aft) Gear Extended Control Availability (full)	Hazards None Terrain Impact / Final (4) Runway (2) / (8) Runway (2) Grassy dirt / (6) Grass (1) Soft ground / (1) Soft dirt (4) Unstated Average undershot 64m. Range 6-102m.

(1) ENV = effective normal velocity

(2) (X) = number of occurrences

TABLE 8. - AIR-TO-GROUND, IMPACT, AGI

Type	Characteristics	Accident Description	A/P Configuration	Hazards and Terrain
AG2 (4 accidents)	• High/Sink Speed or ENV. (1) (>3.1 m/sec.) (<10 m/sec.) • Fwd. Vel. (<Final Approach, >L.O./TD, 126 – 160 Kts.) • Symmetrical Impact Conditions ≤5° Nose Up • 150 to 1200m. off runway	• Undershoot	a) Configuration Weight (Landing) CG (Fwd/Aft) Gear Extended Control Availability (full)	Hazards (2) Ravine/Embankment (2) (2) Lights/Poles (1) each; tree, fence, dike, rocks Terrain (4) Unstated Average Undershoot 574m. Range 152 – 1175m.
AG3 (7 accidents)	• Moderate to High (>1.52 m/sec) Sink Speed or ENV. (<10 m/sec.) • High Fwd. Vel. ≥Final Approach ≥T.O. Climb <Descent 110-200 Kts • Symmetrical Unsymmetrical Impact Conditions pitch (θ) 0 to +5° roll (Φ) ±5° to ±45° yaw Ψ = 0 to ±10° flight path (γ) = -4° to -7° • Occurs On or Off-Airport Runway	• Controlled & Uncontrolled Grnd. Collision • Stall • Collision with Obstacle • Undershoot	a) Configuration Weight (Ldg./T.O.) CG Fwd/Aft) Gear Extended/ Retracted	Hazards None Terrain (4) Slope/Mountain (1) Runway (1) Marshland (1) Runway/Rough–Rocky Average distance from airport – 10203m. Range 2414 – 20094m.
AG4 (14 accidents) Total: 25 accidents	• Moderate to High (>1.5 m/sec) Sink Speed or ENV. (<10 m/sec) • High Fwd. Vel. [<Final Approach, >T.O. Climb, <Descent, 100-200 Kts] • Symmetrical and Unsymmetrical Impact Conditions Pitch (θ) 0 to +5° Roll (Φ) ±5° to ±45° Yaw (ψ) = 0 to ±10° Flt. Path (γ) = -4° to -7°	• Controlled & Uncontrolled Ground Collision • Stall • Collision with Obstacle • Undershoot	a) Configuration Weight (Ldg/T.O.) CG (Fwd/Aft) Gear Extended/ Retracted	Hazards (8) Trees (8) Bldgs. (2) Lights, Poles (1) each; Ravine/Embankment, Vehicle, Seawall Terrain Not Stated Average distance from airport – 4410m. Range – 335 to 9656m.

(1) ENV = effective normal velocity (2) (X) = number of occurrences (3) AG4 accidents include hazards usually not involved in AG2 and AG3 accidents

It is appropriate to explain that different investigative bodies have different definitions of what constitutes a survivable accident. The National Transportation Safety Board (NTSB) defines a survivable accident as one in which the occupiable volume is considered sufficiently intact following a crash to have provided protection for the occupants and the loads are deemed to have been within tolerable limits. Thus, by NTSB rules, accidents which some people survive are sometimes categorized as non-survivable and conversely, accidents which produce no survivors are sometimes labeled survivable. On the other hand, the Federal Aviation Authority (FAA) employs a straightforward definition which results in a classification of survivable if at least one person survives a crash. For the present study we are using the FAA definition.

Again as part of the study described in reference 17, the accident data was then assembled in accordance with the type of airplane engine arrangement employed: wing pylon-mounted engines, aft fuselage-mounted engines, and combined aft fuselage/wing pylon-mounted engines. The distribution of accidents, as they relate to these different engine mounting arrangements, is shown in table 9. Of the total of 66 accidents, 30 had an engine mounted in or on the rear of the fuselage and thus had fuel lines running axially through the fuselage which were subject to damage from fuselage breakage/separation.

TABLE 9. - DISTRIBUTION OF ACCIDENT DATA AS RELATED TO AIRPLANE ENGINE ARRANGEMENT

Engine Arrangement	Candidate Crash Situation*							Totals
	GG0			AGHL	AG1			
	GG1							
	Landing	Takeoff	GG2	AG1	AG2	AG3	AG4	
Aft fuselage	4	2	4	7	2	3	3	25
Wing	6	6	5	3	1	4	11	36
One Aft Fuselage – Two Wing Pylon	–	2	–	1	1	1	–	5
Totals	10	10	9	11	4	8	14	66

*Defined in Tables 6, 7, and 8

Tables 10, 11 and 12 show the frequency of occurrence of fuel spillage in relation to the occurrence of fuselage separation for the different engine configured airplanes. As can be noted by the data in these tables fuselage separation/break occurs at well defined hard points, i.e., wing leading edge (L.E.), wing trailing edge (T.E.), forward of empennage, and aft of cabin. In the accidents involving the 30 aircraft with aft-mounted engines only one instance of fuselage separation was noted as a possible cause of fuel spill.

Tables 13 and 14 show the relative fire hazard and structural system damage involvement for all the aircraft as a function of their engine arrangement. Of a total of 36 accidents involving airplanes with wing pylon-mounted engines, 24 accidents show fire occurrences or the potential of a fire hazard from fuel spillage. Wing fuel tank rupture occurred as the stated cause in 10 of the 24 fire hazard accidents, followed by 8 occurrences of wing fuel line severence. Miscellaneous or unstated causes account for 6 fire hazard accidents. Generally the miscellaneous cause is associated with a wing root separation or wing tank rupture.

TABLE 10. - RELATIONSHIP BETWEEN FUSELAGE BREAK AND FUEL SPILL OCCURRENCE - GGO CK. II SITUATION -

Engine Arrangement	Number of Accidents Involved	Occurrence of Fuselage Break and Fuel Spill	Occurrence of Fuel Spill and No Fuselage Break	Occurrence of Fuselage Break and No Fuel Spill
Aft fuselage	7	1 ③ 1 ④ 2 ⑥ 1 ⑦	1	1 ⑤
Wing/pylon	9	1 ⑧ 1 ⑨	4	2 ① 1 ②
One aft fuselage/ two wing pylon	2	–	2	–

(1) Break occurred at wing L.E.
(2) Breaks occurred at wing L.E. and T.E.
(3) Break occurred forward of empennage, fuel spill occurred from wing fuel tank.
(4) Breaks occurred at wing L.E. and T.E., fuel spill occurred at wing root.
(5) Break occurred forward of empennage.
(6) Breaks occurred at wing L.E. and T.E., fuel spill from wing fuel tank or engine fuel line.
(7) Breaks occurred at wing L.E. and T.E., fuel spill from wing fuel tank.
(8) Break occurred at wing L.E., fuel spill from wing fuel tank.
(9) Break occurred at wing L.E., unknown leak source.

TABLE 11. - RELATIONSHIP BETWEEN FUSELAGE BREAK AND FUEL SPILL OCCURRENCE - AGIL CRASH SITUATION -

Engine Arrangement	Number of Accidents Involved	Occurrence of Fuselage Break and Fuel Spill	Occurrence of Fuel Spill and No Fuselage Break	Occurrence of Fuselage Break and No Fuel Spill
Aft fuselage	5	1 ④	1	1 ① 1 ② 1 ③
Wing/pylon	2	–	1	1 ③
One aft fuselage/ two wing pylon	1	–	1	–

① Break occurred forward of empennage.
② Breaks occurred aft of cabin and forward of empennage.
③ Break occurred at wing T.E.
④ Break occurred forward of empennage, full spill occurred at wing root.

TABLE 12. - RELATIONSHIP BETWEEN FUSELAGE BREAK AND FUEL SPILL OCCURRENCE - AGI CRASH SITUATION -

Engine Arrangement	Number of Accidents Involved	Occurrence of Fuselage Break and Fuel Spill	Occurrence of Fuel Spill and No Fuselage Break	Occurrence of Fuselage Break and No Fuel Spill
Aft fuselage	8	1 ① 4 ② 1 ③	2	
Wing/pylon	16	1 ⑤ 1 ⑥ 12 ⑦	2	
One aft fuselage/ two wing pylon	2	1 ② 1 ④		

① Breaks occurred aft of cabin and at wing L.E. and T.E., fuel spill due to engine line or fuselage separation.
② Fuselage destroyed or broke up into several sections and fuel spill attributed to wing tank rupture.
③ Breakup occurred forward of empennage, fuel spill unknown, could be fuel tank or fuel line rupture.
④ Breakup occurred forward of wing L.E., fuel spill from wing tank.
⑤ Breakup occurred forward of empennage, fuel spill due to engine separation.
⑥ Breakup occurred at wing T.E., fuel spill due to engine separation.
⑦ Aircraft were destroyed in 4 accidents, breakup occurred aft of cabin 3 times, forward of empennage 2 times, aft of cabin and forward of empennage 2 times and at wing L.E. once. All spills are associated with fuel tank rupture, engine separation, or wing separation except in 2 cases where spillage cause is unknown.

TABLE 13. – FIRE HAZARD SUMMARY, ALL AIRPLANE CONFIGURATIONS

	Candidate Crash Situations*						
	GG1	GG2	AG1	AG2	AG3	AG4	Total
Number of Accidents	20	9	11	4	8	14	66
FIRE HAZARD							
Total Number Fires Occurred	8	6	5	4	7	11	41
Fuel Containment, Struc. Related (Fuel Spill)	6	5	3	4	5	8	31
Friction, Ground, Hydraulic Line Related	2		1 (8)				3
Unstated		1	1 (10)		2 (6)	3 (6)	7
Fuel Spill, No Fire	2	1			1	3	7
Total Number of Fires and Potential Fires	10	7	5	4	8	14	48
ESTIMATED CONTRIBUTIONS TO FIRE HAZARDS (7)							
• Wing Fuel Line Severed							
a. Engine/Pylon Separation	2		2				4
b. Wing Root/Inboard Failure		3 (4)(9)		1 (4)(9)		4 (9)	8
c. Wing Outboard Failure						1 (9)	1
d. L.G. Penetration							0
e. Wing L.E.							0
f. Miscellaneous						1 (9)	1
• Fuselage Fuel Line Severed							
a. Fuselage Separation					1 (4)		1
b. Engine Separation		1 (4)		1 (4)	2 (4)		4
c. Landing Gear Penetration			1 (5)				1
• Wing Fuel Tank Rupture							
a. L.G. Collapse/Penetration	3						3
b. Columnar Impact (1)		1		3	1	2	7
c. Contour Impact (2)	2				3		5
d. Frontal Obstruction (3)		1				2	3
e. L.G. Collapse and Fus. Impact							0
f. L.G. Trunnion Attach Fitting	1						1
g. Miscellaneous						1	1

* Defined in Tables 6, 7, and 8

(1) Pole, Tree, Pier, Light

(2) Ditch, Ravine, Hill, Embankment

(3) Fence, Building, Wall

(4) Includes possibility of either or both occurrences on same accident

(5) Fuselage Line/routing designed as a result of accident in 1965

(6) Obstacles involved, wing separation occurred

(7) Fuel containment related fires and spills

(8) Nose gear collapse, severed hydraulic line

(9) Possible fuel tank rupture

(10) Wing Root Area

TABLE 14. - STRUCTURAL DAMAGE SUMMARY, ALL AIRPLANE CONFIGURATIONS

	Candidate Crash Situations*						
	GG1	GG2	AG1	AG2	AG3	AG4	Total
Number of Accidents	20	9	11	4	8	14	66
Fuselage Break/Separation							
a. Aft of Cockpit Fwd. Fuselage						3	3
b. Wing, Leading Edge (L.E.)	2	1				1	4
c. Wing, Trailing Edge (T.E.)			2	1	1		4
d. Forward of Empennage	1	1	2		1	3	8
e. Wing, L.E. and T.E.	2	3	1				6
f. Aft of Cockpit and Fwd. of Empennage						2	2
g. Three or Four Breaks		2			2	1	5
h. Fuselage Destroyed				1	2	4	7
Engine Separation							
Fuselage Mounted Configuration	2	2	3	2	1	2	12
Wing Mounted Configuration	6	1	2	1	4	6	20
Fuselage and Wing Mounted	2		1	1	1		5
Wing Failures							
Root-Inboard	2	3		2	3	11	21
Outboard-Tip	2	3		2	1	1	9
Miscellaneous/Unknown	2	1			1	2	6
Landing Gear Collapse							
MLG Collapse Only	4	2	6			3	15
NLG Collapse Only	5	1	1				7
MLG and NLG Collapse	7	3	1	3	3	3	20
Occurrences of:							
Floor Buckling	1	3	4	3	1	3	15
Cockpit Crushing	1	1			1	5	8
Lower Fuselage Crushing/Abrasion	5	3	4	2		2	16
Overhead Racks/Panel FAilures	3	4	3			1	11
Jammed and/or Deformed Doors	5	3	1	1		3	13
Slide Related Failure	3	1				2	6
Galley Equipment Failures		1					1
Tire/Wheel Damage	5	1					6

*Defined in Tables 6, 7, and 8
**Numbers in table indicate number of accidents in which stated events occurred

Of a total of 25 accidents involving aft-mounted engine airplanes, 15 accidents show fire occurrence, or fire potential from a fuel spill. In these 15 fire hazard accidents, aft fuselage break-up occurred 12 times. However, in only one of these 12 instances is it noted that the fuselage separation/break may have led to the fuel spill. Again wing fuel tank rupture is a prevalent occurrence (8); followed by fuselage fuel line severence, usually engine separation (4), and wing fuel line severence, particularly at the root (3).

The explanation of the cause of fuel leakage or fire is oft times unclear in the accident reports. For example, in table 13 it is reported that in seven instances the cause of fire was unstated in the NTSB reports. Since specific causes of fires which were not related to fuel spills are identified (three cases) it can be presumed that the seven unstated cases involve fuel spills but that the source of the spill was in question. On the basis of this conjecture, it would be valid to conclude that 82 percent of the time fuel is spilled, fire results. On the other hand, if the seven unstated causes of fires are divided in the same ratio as the number of fires known to be due to fuel spills (31) to fires known to be due to nonfuel causes (3), then only 6.3 of the seven unstated fires would be due to fuel spills and the above percentage would drop to 81.2 percent. It therefore seems appropriate to conclude that in more than 80 percent of the time when fuel is spilled in an aircraft crash, fire results when the fuel is Jet A. Further, since all the other fuels being considered in this study will ignite at least as readily as Jet A, the statement could be expanded by saying it would be true regardless of the fuel.

Table 15 summarizes the fuel containment related fire potential and structural system damage data. Fuselage break, engine separation, wing failure, and landing gear collapse occurrences, in terms of relative frequency, are similar for wing pylon or aft fuselage engine-mounted configurations. While some percentages differ for the two different configurations, they are generally within ±10 percent of the total of all 66 accidents.

TABLE 15. - SUMMARY OF FUEL CONTAINMENT HAZARDS AND STRUCTURAL DAMAGE AS A FUNCTION OF ENGINE ARRANGEMENT CONFIGURATION

	Engine Arrangement		
	Wing Pylon	Aft Fuselage	All
Number of Accidents	36	25	66
Fire Potential Fuel Containment Related	18 (50) (5)	15 (60) (4)	38 (57.6)
Wing Fuel Line Severance (2)	8 (22.2)	3 (12)	14 (21.2)
Fuselage Fuel Line Severence	--	4 (16) (3)	5 (7.6)
Wing Fuel Tank Rupture (2)	10 (27.8)	8 (32)	21 (31.8)
Structural System Damage (1)			
Fuselage Break/Separation	20 (55.6)	16 (64)	39 (59.1)
Engine Separation	20 (55.6)	12 (48)	37 (56.0)
Wing Failures	20 (55.6)	11 (44)	36 (54.5)
Root-Inboard	13 (36.1)	5 (20)	21 (31.8)
Outboard Tip	5 (13.9)	4 (16)	9 (13.6)
Miscellaneous	2 (5.6)	2 (8)	6 (9.1)
Landing Gear Collapse	22 (61.1)	15 (60)	42 (13.6)

( ) Denotes Fuel Containment and Structural Damage Data in percentages; based on total number of accidents for the particular engine arrangement configurations noted at the top of the respective columns.

(1) More than one system can be damaged in an accident, therefore, percentages can total more than 100%.

(2) Seven fire potentials noted as wing fuel line severence could also be wing fuel tank ruptures.

(3) Only one due to fuselage separation.

(4) Does not include 1 fire occurrence in which containment relationship is unclear.

(5) Does not include 6 fire occurrences in which containment relationship is unclear.

The location of the engines on the wing, or on the aft fuselage, does not significantly alter the accident statistics with regard to overall structure participation.

A detailed evaluation of the crash conditions postulated for the subject study indicates that the three crash situations and their subsets (GG1, GG2, AG1, AG2, AG3, AG4), are applicable to crash scenarios 2 and 3 as follows:

Crash scenario No. 2, defined as follows: "A survivable crash landing, or failed take-off, where damage to fuel tankage or lines results in massive release of liquid hydrogen after the aircraft has come to rest," would result in damage similar to crash situations GG1 and GG2, which are essentially ground-to-ground accidents occurring on the runway or as a result of over-running the runway. The accidents in these scenarios involve airplanes running off the runway at a speed in the vicinity of 80 kts and impacting terrain, or obstacles, at lower speeds; e.g., 40 kts. On an average, the airplane comes to rest within 300 meters past the runway threshold. For these types of accidents, 14 of the 29 accidents involved fuel leakage. Wing tank ruptures account for 11 of the 14 spills distributed as follows:

7 contour, columnar, or frontal impacts*

4 landing gear penetration

Two of the 14 spills were associated with wing engine/pylon fuel line breaks and one of the spills was associated with a fuselage fuel line break (could be either a fuselage break or engine separation).

Fuel spill from only one side of the aircraft is characteristic of this type of accident. Fuselage breaks are generally not severe and the separation usually isn't complete.

Crash scenario 3, defined as follows: "A survivable crash landing, or failed take-off, where damage to fuel tankage or lines results in massive release of liquid hydrogen upon impact and during aircraft deceleration", would produce damage similar to AG1, AG2, AG3 and AG4 crash situations. The

*3 of these spills could be wing root/inboard failures.

air-to-ground accidents in these situations involve high forward and sink speeds. A forward speed of at least 120 kts was assumed for the purpose of estimating credible damage leading to fuel spillage rates and quantities.

AG1 and AG2 accidents occur in the proximity of the airport, while AG3 and AG4 accidents oft-times occur substantial distances from airports and in hostile surroundings. For these types of crashes, 24 of the 37 accidents involved fuel leakage. Wing fuel tank ruptures accounted for 18 spills. In the majority of the accidents, columnar (tree), contour (embankment, hill) and frontal (house) impacts caused failure of the wing either inboard at the wing root or outboard of the nacelle. Fuel line leakage occurred in two instances due to wing engine pylon separation, two instances of fuselage engine pylon separation, and two instances involving rupture of a line in the wing leading edge.

Fuel spillage from both sides of the aircraft is characteristic of this type of accident due to the density of obstacles in the crash environment. The severity of the crash conditions for this situation is such that complete separation of fuselage sections on break-up can be expected.

In summary, in the accidents studied it was found that although fuselage breakage/separation occurred just as frequently as did wing damage, the fuselage damage did not usually result in fuel spillage, whereas wing damage did. Further, in the case of cryogenic fuels, it must be recognized that they will be contained in tanks designed to an ultimate pressure significantly greater (30.2 psi vs. 18 psi) than that of the rest of the fuselage in which they are mounted. Therefore, it can be concluded that the fuselage-mounted tanks of the cryogenic fuels will be more likely to survive a crash than the rest of the fuselage, i.e., breakage will occur in the weaker sections. This should lead to markedly better survival statistics for the cryogenic fuels. Fuel spillage will occur, generally, only if fuselage sections separate so far that lines are pulled apart. Engine separation from the aircraft, whether wing or fuselage-mounted, will be the principal source of fuel spillage for the cryogenic-fueled aircraft. In contrast, the conventionally fueled aircraft will continue to have both this problem, plus the vulnerability of wing tanks which has been shown, in the foregoing analysis, to be the major factor leading to fuel spillage.

The other two crash scenarios, Nos. 1 and 4, represented cases in which crash damage was not relevant.

Crash scenario No. 1, stated as follows: "A normal landing, or ground accident, which results in fuel system insulation damage and/or fuel system damage permitting liquid hydrogen to vent, escape, leak, or run out of a punctured tank or broken line," should be considered an accident in which only small leakage rates could occur because control of flow via shutoff valves and boost pump usage are controllable by the crew. This situation would come about as a result of a long developing problem (metal fatigue) or, it could be maintenance related as opposed to crash damage.

Crash scenario No. 4 is a situation where the aircraft plunges to the ground and all on board are killed by the impact. The question to be resolved is, what is the hazard to the surrounding community represented by the instantaneous release of the fuel aboard at the moment of impact.

3.5 Scenario Damage Definition

In light of the damage which is apt to be inflicted on the subject aircraft in the postulated scenarios, as described in the preceding section, an analysis was made to determine what fuel leakage might be expected to result with each of the four fuels.

By way of review, the cryogenic fuels (LH_2 and LCH_4) are stored in insulated tanks located both forward and aft of the passenger compartment. The non-cryogenic fuels (Jet A and JP-4) are stored in the wing and in center section tanks. As listed in table 2, the subject aircraft carry the following total fuel loads:

LH_2	25,600 kg (56,460 lb)
LCH_4	69,040 kg (152,200 lb)
Jet A	84,780 kg (186,900 lb)
JP-4	84,780 kg (186,900 lb)

All of the aircraft have four engines mounted on pylons below the wing.

The location of the fuel tanks and engines dictates the primary effect of impact damage on fuel leakage. When fuel tanks are located in the wing, impact damage to fuel lines within the wing is of little concern because

of the excessive fuel tank damage that must occur before the fuel lines are impacted. In all other areas, such as engines, engine pylons, and fuel lines external to fuel tanks, fuel line leakage is of concern.

Each engine is assumed to be supplied fuel from its own individual fuel tank. Two fuel pumps were used in each noncryogenic fuel tank and three in each cryogenic tank.

Although as has been pointed out, the fuselage tanks of the cryogenic fuels are considered less apt to be seriously damaged so as to leak fuel in an impact survivable crash, compared with the wing tanks of the conventionally fueled aircraft, the problem at this juncture was not to assess probabilities but to decide on credible damage which could occur in order to analyze the consequences of fuel spillage. Accordingly, fuel tank damage was assumed to vary from a small puncture or a cracked weldment permitting a leak of 0.5 kg per second, to a major tank rupture. In the latter case, an average spill rate was determined by assuming that all of the fuel tanks in the designated area released their fuel within a 30-second period.

Fuel line leakage is significantly affected by the operation of boost pumps. If the pump power source is turned off prior to the crash, spillage would be the result of gravity drain through a severed fuel line. For use in the subsequent analyses, minimum leakage was established by assuming one broken line only, fed by gravity or siphon action. Maximum leakage assumed all fuel lines in the area were broken with all boost pumps operating when applicable.

Table 16 provides a summary of leak rates and quantities which were adopted to represent the LH_2-fueled aircraft in the analyses of Scenarios 1, 2, 3, and 4 described in the following sections. The fuel quantities listed in the table for Scenario 4 represent the amounts of hydrogen assumed to remain in the aircraft after, in the first case, a crash following taxi, take-off, and climb to about 1.8 km (6000 ft). The second value listed is for the situation where the aircraft has flown its design mission and is near its destination when it crashes with only a little more than reserve fuel on board.

TABLE 16. – CRASH SITUATION AND FUEL SPILLAGE FOR LH_2-FUELED AIRCRAFT

	Situation	Damage	LH_2 Spill	
			Rate (kg/sec.)	Quantity (kg)
Scenario 1	Aircraft at rest. Small internal leak.	Cracked weld on tank	0-0.5	1,000
Scenario 2	Aircraft stopped by impact at ≈40 kts. Radial spill.	Engine separation or fuselage line break.		12,600
		• Boost Pumps Off	0.5	
		• Boost Pumps On	2.3	
		Tank punctured or ripped.	900	
Scenario 3	Damage occurs at ≈120 kts. Long axial spill as aircraft decelerates	(Same as Scenario 2)		
Scenario 4	Catastrophic crash. Large radial spill.	All tanks ruptured.	∞	21,600 2,160

Corresponding leakage rates and spill quantities for the other fuels were arbitrarily assumed to be in the ratios of the fuel quantities tanked, viz.,

$$\frac{69,040}{25,600} = 2.7 \text{ for } LCH_4, \text{ and}$$

$$\frac{84,780}{25,600} = 3.3 \text{ for Jet A and JP-4.}$$

4. COMPUTER MODELS AND METHODOLOGY

The computer models and methodology used to calculate the spread, vaporization, and dispersion of spilled aircraft fuels into the atmosphere are provided in this Section. For a fuel leak within the aircraft, a method is provided for calculating the required air purge rate in the compartment to reduce the air/fuel mixture ratio below its flammable limit. Finally, a thermal model is described for calculating heat transfer rates and temperatures of an aircraft fuselage (both external and internal) that is exposed to flames from spilled liquid fuel.

4.1 Aircraft Fuel Liquid Spill, Spreading and Vaporization Models

An analytical model was initially developed to solve for the liquid spill, spreading and vaporization processes that would occur following the rupture of aircraft tanks or lines. Two models were developed, one for axial spread of the liquid perpendicular to the direction of aircraft motion, and the other for radial spread of the liquid from a fixed aircraft position. A flat, horizontal spill surface was assumed, and no dikes or boundaries were present to limit the extent of the liquid spread. Concrete and soil (with 10% moisture) were the two spill surfaces considered in these programs. These models are applicable to all liquids, including the cryogenic fuels and the conventional petroleum-based fuels considered in this study.

The liquid spreading and vaporization processes were modelled using open channel, hydraulic flow methods of analysis. In this analysis, no combustion is assumed to occur over the liquid spill and spread, and hence the unburned fuel vapors will disperse into the atmosphere. Applying both conservation of mass and horizontal momentum, two partial differential equations are obtained which define the liquid flow, as shown below for the axial spreading model case:

Conservation of Mass:

$$\frac{\partial \delta}{\partial t} + \frac{\partial(\delta V)}{\partial x} + V_E = 0 \qquad (1)$$

Conservation of Momentum:

$$\frac{\partial(\delta V)}{\partial t} + \frac{\partial(\delta V^2)}{\partial x} + g\delta \frac{\partial \delta}{\partial x} + \frac{f}{2} V|V| = 0 \qquad (2)$$

where

t = time from the start of the spill

x = axial distance from the center of the spill line

V = mean horizontal velocity of the liquid flow

δ = liquid flow depth

g = acceleration of gravity

V_E = rate of fall of still liquid surface, due to evaporation, etc.

f = Fanning friction factor for open channel flow

These partial differential equations were then converted to ordinary differential equations with respect to time, using the method of characteristics, as presented in Reference (18). These ordinary differential equations are then grouped in terms of the positive and negative characterisitcs of the $\frac{dx}{dt}$ slope, as shown below:

$$\left.\begin{aligned} \delta \frac{dV}{dt} + \lambda \frac{d\delta}{dt} + \lambda V_E - V V_E + \frac{f}{2} V|V| = 0 \\ \frac{dx}{dt} = V + \lambda \end{aligned}\right\} \quad \text{Positive characteristic} \qquad (3)$$

$$\left.\begin{aligned} \delta \frac{dV}{dt} - \lambda \frac{d\delta}{dt} - \lambda V_E - V V_E + \frac{f}{2} V|V| = 0 \\ \frac{dx}{dt} = V - \lambda \end{aligned}\right\} \quad \text{Negative characteristic} \qquad (4)$$

where $\lambda = \pm\sqrt{g\delta}$ = wave velocity.

Computer solutions of the above differential equations were then programmed for a Univac 1100 computer, using an explicit specified time interval method of solution, similar to Section 15.4 of Reference (18).

In the above formulations, only the evaporation term V_E and the friction factor f are dependent on fluid properties. The evaporation term V_E represents the rate of fall of a still liquid surface due to evaporation, boiling, or seepage of liquid into soil, etc. For cryogenic liquid boiling on a surface, the evaporation term V_E can be found from the following relationship,

$$V_E = \frac{q''}{\rho_L h_{fg}} \tag{5}$$

where

ρ_L = liquid density

h_{fg} = latent heat of vaporization

q" = heat rate per unit area from the solid surface

The transient heat flux q" from a semi-infinite spill surface can be predicted from Section 13-3 of Reference (19). For an initial time period, this heat rate is limited by the boiling burn-out heat flux of the spilled cryogenic liquid. After that, the heat flux depends on the solid surface thermal properties, and varies inversely with the square-root of time t.

The term f represents a Fanning friction factor for open channel flow, derived from Section 4.2 of Reference (20), which must be expressed in the following form,

$$\sqrt{f} = \left\{ -4 \log_{10} \left[\frac{d_s}{12\delta} + \frac{1.25}{Re\sqrt{f}} \right] \right\}^{-1} \tag{6}$$

where

$d_s = \left(\frac{n}{0.03779}\right)^6$ = length parameter defining surface roughness.

n = Manning's roughness coefficient, see References (20), (21), etc.

$Re = \frac{4\delta V\rho_L}{\mu_L}$ = Reynolds number of the flow

μ_L = liquid viscosity

The first term in the logarithm bracket represents the effect of surface roughness, while the second represents the effects of flow Reynolds number for turbulent flows. The Fanning friction factor for laminar flow, $f = 16/Re$, was only used for low Reynolds number flows, where the laminar flow f exceeded the above turbulent flow f value. Hence, the flow friction factor and shear stress were defined for the full range of surface roughnesses and flow Reynolds numbers.

In order to make a time integration of the characteristic differential equations, the boundary and initial conditions must be specified. Figure 13 shows the inlet flow boundary and initial conditions at the spill location. Two inlet boundary conditions are possible, depending on whether the Froude number ratio of inlet velocity to wave velocity is less or greater than unity. At the initial time $t = 0$, the spill surface is completely dry, while the initial inlet Froude number must be ≥ 1.0.

The advancing free leading edge boundary condition is presented on Figure 14. With Froude number $Fr \geq 1.0$ at the advancing leading edge of the flow, this fluid boundary cannot influence the method of characteristics solution interior to the liquid flow body. The total time derivatives of the depth δ and the flow per unit width (δV) were obtained from the partial differential equations, and expressed in terms of partial derivatives with respect to distance x. These equations both follow the characteristic velocity $\frac{dx}{dt} = V$, which is the velocity of the advancing leading edge.

A final boundary condition, that involving receding free liquid edges in the final stages of fluid flow and vaporization, is shown on Figure 15. At a receding liquid edge, both the liquid depth δ and velocity V are zero, and the momentum effects are small. The edge will recede due to vaporization, and the location of the edge can be computed by conservation of mass in the triangular wedge shaped edge elements. Receding edges can develop at a leading edge that stops advancing, or at the liquid inlet position, $x = 0$, after the inlet liquid flow has ceased.

- Inlet conditions, at X = 0, depend upon the inlet flow froude number.

$$FR = \frac{V}{\lambda} = \frac{V}{\sqrt{g\delta}}$$

- For sub-critical inlet flow, with FR $\leq$ 1.0:
  - Only the inlet liquid flowrate can be specified
  - The inlet velocity and depth are variables, and are computed in combination with the method of characteristics.
- For super-critical inlet flow, with FR $>$ 1.0:
  - Both the inlet flowrate and velocity head must be specified
  - The inlet velocity and depth are fixed and independent of the liquid flow field at X $>$ 0
- The initial liquid inlet flow must be one of these conditions:
  - Critical flow, Fr = 1.0
  - Super-critical flow, Fr $>$ 1.0

Figure 13. - Inlet flow boundary conditions.

- Froude number FR ≥ 1.0 at the advancing leading edge.
- Conserving mass and momentum, the partial differential equations are used to form this leading edge model:

$$\frac{d\delta}{dt} = \frac{\partial \delta}{\partial t} + V \frac{\partial \delta}{\partial x} = -V_e - \frac{\partial (\delta V)}{\partial x} + V \frac{\partial \delta}{\partial x}$$

$$\frac{d(\delta V)}{dt} = \frac{\partial (\delta V)}{\partial t} + V \frac{\partial (\delta V)}{\partial x} = -\frac{f}{2} V|V| - \frac{\partial}{\partial x}\left(\delta V^2 + \frac{g}{2}\delta^2\right) + V \frac{\partial (\delta V)}{\partial x}$$

$$\frac{dx}{dt} = V_e \qquad \text{Leading edge velocity}$$

- For FR ≥ 1.0, the advancing leading edge does not influence the method of characteristics solution in the liquid body.

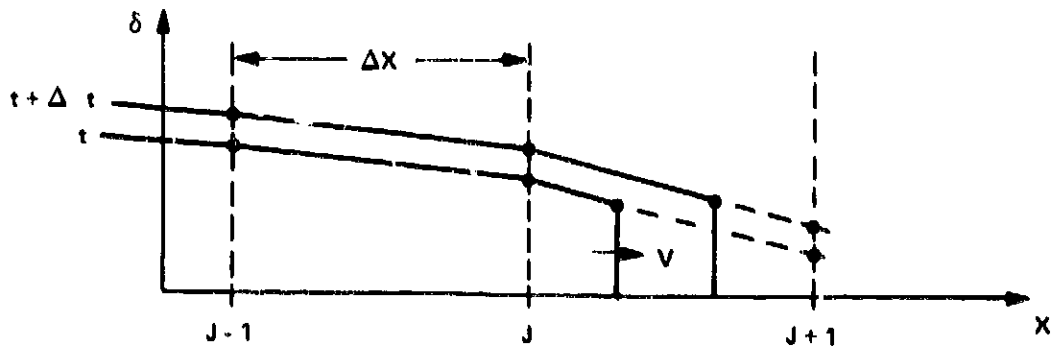

Figure 14. - Advancing leading edge boundary condition.

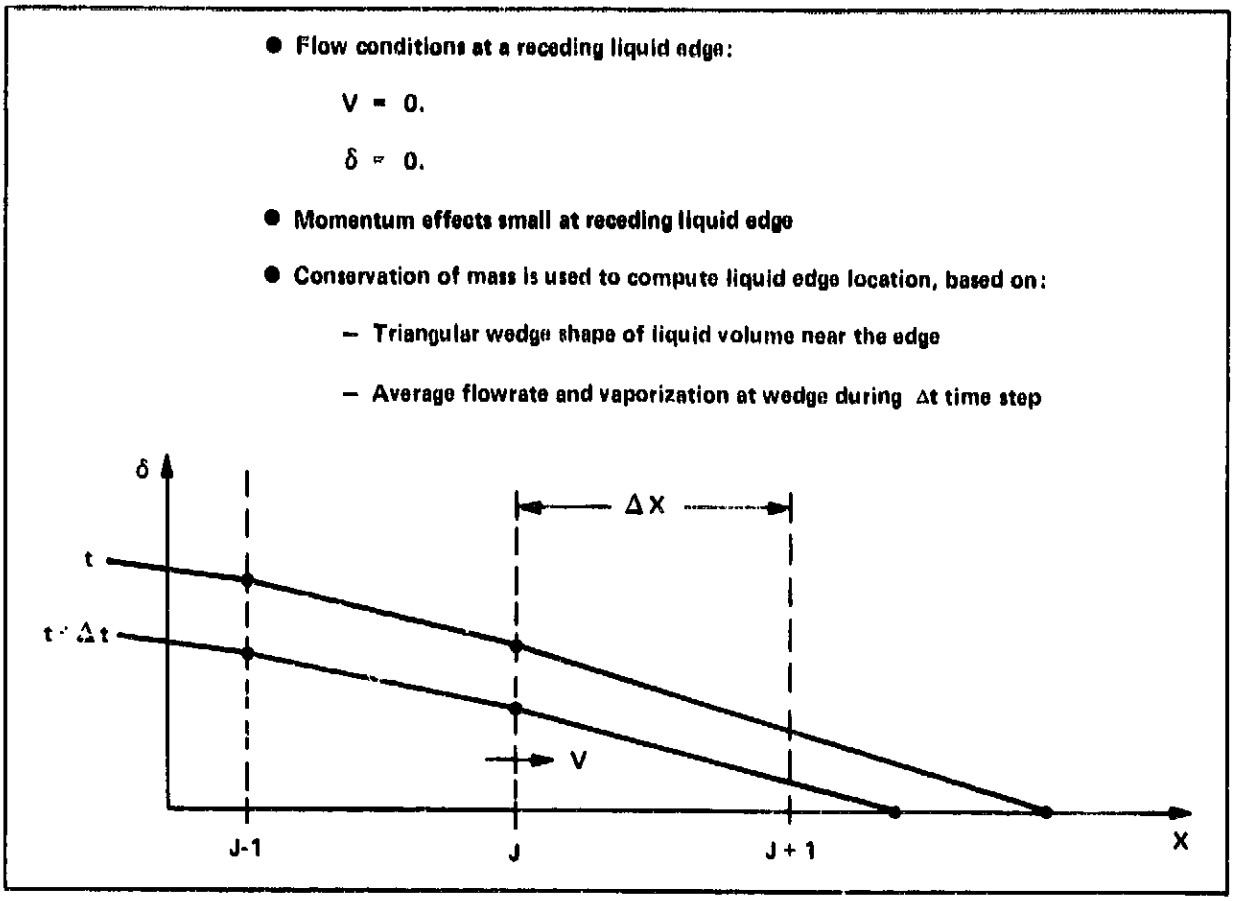

Figure 15. - Receding free edge boundary condition.

Computer programs were developed and run for both the axial spreading model presented above and for a similar radial liquid spill, spreading and vaporization model. Even though some cases have been run successfully on both programs, most cases run on these programs have shown computational instabilities. This problem appears at the free edge boundaries, and it is apparently due to the finite differencing techniques needed to match the edge boundary conditions to the characteristic solution in the liquid pool. Many different approaches have been tried to solve this problem, but none have been successful to date.

Two stably computed runs, with LH_2 spilling on a concrete runway, are presented for an axial spread, figure 16, and for a radial spread, figure 17. The axial spread resulted from a 900 kg/sec spill of hydrogen occurring from an aircraft skidding along the runway at 120 knots. Figure 16 shows the axial extent of the spread x measured perpendicular to the spill center line as a function of time t at one spot on the runway. The outer curve (square-dots) shows the advancing outer edge of the spread out to where it stops and starts to recede as the liquid evaporates. The inner receding edge (circle-dots) starts with dry-up near the center at $t \approx 9$ seconds and then recedes out to a final dry-up at $x \approx 5$ meters and $t \approx 11.5$ seconds.

Figure 17 shows the results of a 108 kg radial spill of LH_2, which occurs over a 10 second time span at a fixed position. The center dries up soon after the flow ceases, while the final dry-up occurs at $r \approx 4$ meters and $t \approx 17$ seconds. For both the radial and axial flow cases, central dry-up may or may not occur, depending on the central liquid depth, the liquid inlet flow momentum, the rate of vaporization, etc.

For comparison, the results of simple constant depth slab evaporation models are plotted as dashed lines on figures 16 and 17, based upon the work of Fay, reference 22. These Fay models assume the leading edge Froude number is ≈ 1.4, since $V = \sqrt{2g\delta}$, and hence they overpredict the spread of the leading edge, by up to $\approx 20\%$. Vaporization stops instantaneously with these constant depth models, and the wider liquid spread yields a faster dry-up time, by up to $\approx 40\%$. Based upon these and other comparisons, it appears that the

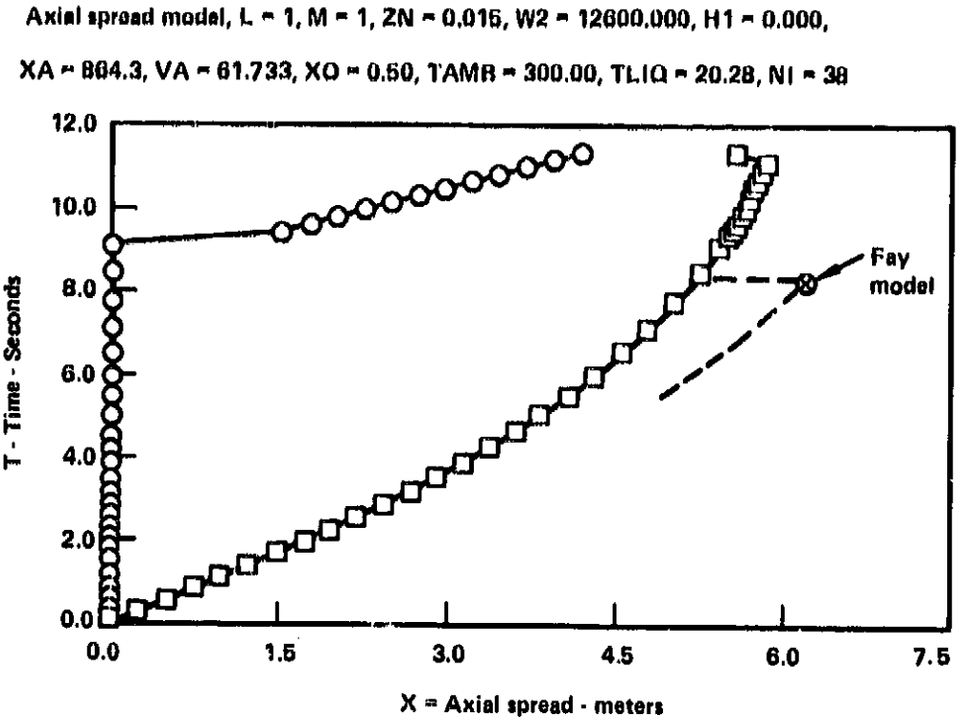

Figure 16. - Axial spread model comparison with Fay model.

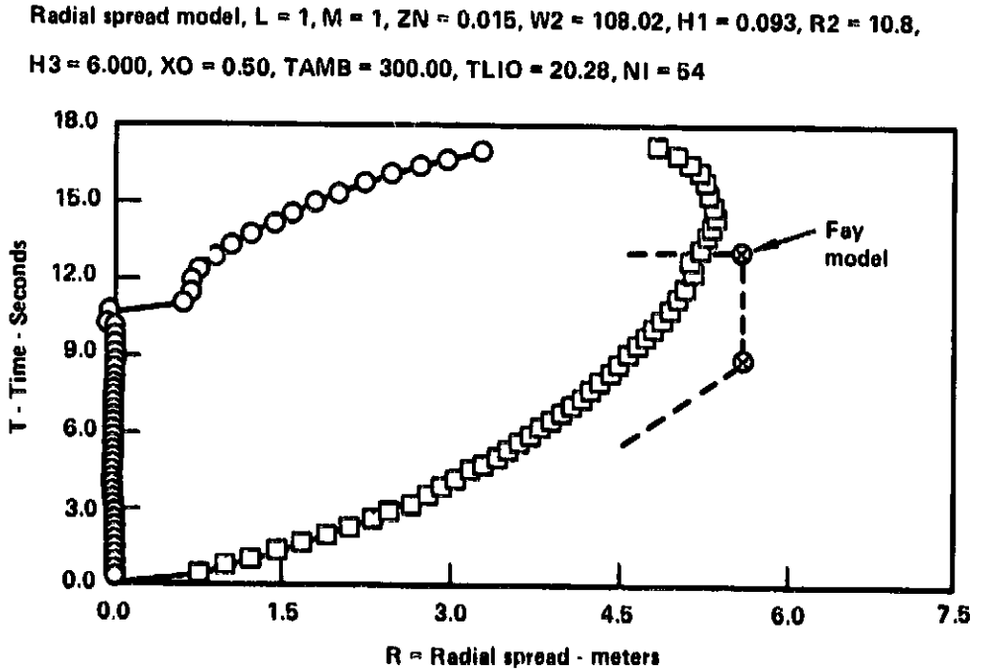

Figure 17. - Radial spread model comparison with Fay model.

Fay models can predict the extent and time of the liquid spread within the limits presented above. With the Fay models, the maximum rate of evaporation occurs when the liquid first reaches its point of maximum spread, and this rate may be up to ≈ 50% greater than the computer model results.

Because of our inability to make more than a few stable runs with the spill, spreading and vaporization computer programs, it was finally decided to use slab models to predict the behavior of the Scenario spills in this study. Based upon similar approaches as Fay, reference (22), slab spreading models were derived which predict the maximum extent of the spread, the time to reach the maximum extent, and the maximum rate of vaporization from the liquid spread at this time. These models were developed for an instantaneous axial spill at one location along the spill centerline, and for both an instantaneous and a continuous radial spill at a fixed location on the spill surface.

The instantaneous axial spill corresponds to a spread at a fixed point, perpendicular to the spill centerline velocity of the aircraft. The following Fay model equations were derived for this instantaneous axial spill and spread.

$$X_m = \left\{ \frac{5}{3} \cdot \frac{\sqrt{2g}}{V_E} \cdot \left(\frac{Q'_o}{2} \right)^{3/2} \right\}^{2/5}$$

$$t_m = \frac{1.4\ Q'_o}{V_E\ X_m} \qquad (7)$$

$$\dot{m}'_E = 2\rho_L\ V_E\ X_m$$

where

X_m = maximum half axial spread, from spill centerline

t_m = time to maximum axial spread

$\dot{m}'_E$ = maximum mass rate of vaporization per unit spill length.

Q'_o = volume of liquid spill per unit of spill centerline length.

The Fay model equations for an instantaneous radial spill at one location on the spill surface are given below.

$$r_m = \left\{ \frac{8}{3} \cdot \frac{\sqrt{2g}}{V_E} \cdot \left(\frac{Q_o}{\pi} \right)^{3/2} \right\}^{1/4} \tag{8}$$

$$t_m = 0.7 \left[\frac{4\, r_m^2}{3g\, V_E} \right]^{1/3}$$

$$\dot{m}_E = \pi\, r_m^2\, V_E\, \rho_L$$

where

r_m = maximum radius of the spread from the center.

Q_o = total volume of the liquid spilled

$\dot{m}_E$ = maximum rate of vaporization from the liquid spread.

For a continuous (steady-flow) radial spill at a fixed location, the following experessions were obtained for a slab spreading model,

$$r_m = \left(\frac{\dot{Q}_o}{\pi V_E} \right)^{1/2} \tag{9}$$

$$t_m = 0.7 \left[\frac{4\, r_m^2}{3g\, V_E} \right]^{1/3}$$

$$\dot{m}_E = \pi r_m^2\, V_E\, \rho_L$$

where

r_m = maximum radius of the spread (also the steady-state radius)

$\dot{Q}_o$ = volume rate of the liquid spill

The above Fay models for predicting the maximum extent, time, and vaporization rate for the various spill types are most applicable when the still rate of liquid fall due to evaporation, V_E, has a constant value. If the term V_E varies with distance and time, as it does with vaporization due to conduction heat transfer from the base surface, then care must be used in applying these models. In this case, an average heat flux must be used for the extent of the spread at the maximum time, and a trial and error solution is required to match this average heat flux to the assumed liquid vaporization rates. Hence, these Fay models only provide an estimate of the liquid spill performance, but they do allow comparisons of different liquids as to types and scale of the spreading and vaporization.

For the radial spreads, the instantaneous model was used for spill times smaller than the maximum spread time, while the continuous model was used for all other cases. In this study, axial spills were only computed with the aircraft in motion so only an instantaneous spill model was needed to predict this spill performance.

4.2 Aircraft Fuel Gaseous Dispersion Model

An aircraft fuel gaseous dispersion model (AFGASDM) was designed to predict the position and fuel vapor concentration at any time after the spill is on the ground and until the vapor concentration drops below the lowest flammable concentration.

Although the literature contains complex grid models using the partial differential equations of motion and conservation (reference 23) and traditional gaussian dispersion models (reference 24), none of these were suitable to solve the problem of aircraft fuel spills. This new, innovative model was developed on basic physical principles and knowledge of turbulent entrainment (reference 25). The gaussian models are unsuitable because they compute concentrations based on averaging times of at least 10 minutes, a requirement set by the empirical development of the Pasquill-Gifford diffusion coefficients (reference 26). NASA spills of liquid hydrogen indicated dispersion times of less than 1 minute (13). The complex grid models are unsuitable because they require implemention on large computers like the Cray-1 and each run of such models costs many thousands of dollars.

The approach described here was designed to predict the spatial position of the gaseous fuel at each second in time as the liquid fuel vaporizes. The concern is the maximum distance downwind and maximum height above the spill at which the gas is flammable. The lowest detonable concentration is higher than the lowest flammable concentration, hence the maximum distance of detonable gas is less than the maximum distance of flammable gas. One second was chosen as a convenient interval of time to repeat the computations of energy, mass and momentum conservation. The model can easily be adjusted for any other interval of time. For the cases reported here, much smaller time intervals are expected to increase the computing cost without appreciable increase in accuracy of the predictions, while much larger time intervals are expected to reduce the accuracy and resolution of the predictions. The accuracy is defined as the closeness with which the model can predict the measured results of field experiments. The resolution is the difference in predicted results the model can compute for cases with different input conditions.

The model can be run repetitively for each 1 second "puff" of gaseous fuel that vaporizes from the liquid. For economy of computer time and cost, only the largest puff is followed by the model for the present work. This 1-second-long puff is largest when the liquid spill has its maximum area and the liquid vaporization rate is highest. All other puffs travel smaller distances before the gaseous fuel concentration is dispersed below the lowest flammable concentration.

An important aspect of this puff model is that the "observer" travels with the puff in a Lagrangian coordinate system whose origin is the center of the puff volume. Ambient air is turbulently entrained into the puff through the sides and part of the top and bottom. The behavior of this turbulent entrainment is taken from the similar appearing turbulent dynamics of cumulus clouds. The gaseous hydrogen dynamics in the NASA White Sands experiments were marked with cloud water droplets and observed in movies and in transparencies supplied by NASA.

The proportion of puff top and bottom available for entrainment is determined by the ascent angle of the puff. There are other puffs before and after the largest puff tracked by the model. If the ascent is vertical, then no part of the top or bottom is an entrainment surface. If the puff motion is horizontal along the ground, then part of the top but none of the bottom is available for entrainment.

After all the conservation equations are solved, the resulting acceleration and velocity determine the vertical and horizontal displacement of the puff center in a set of Eulerian (fixed) coordinates with the origin at the center of the top surface of the liquid spill pool.

The model is designed to handle four fuels: hydrogen, methane, Jet A and JP-4. The initiation of the model is the maximum liquid fuel area and evaporation rate. The evaporation rate is the depth of liquid lost per unit time to vaporization. The initial temperature of the gaseous hydrogen or methane is set at the boiling point at ambient pressure. The model is currently designed to accept an input ground elevation of mean sea level. The model can easily be adjusted for any other ground elevation.

The initial puff horizontal geometry is set equal to the liquid spill geometry. In Scenarios 2 and 4, the hypothetical aircraft is at rest and the liquid spill is circular. In Scenario 3, the aircraft is spilling liquid fuel while decelerating from 120 knots, heading into the wind. These Scenario 3 spills are axial and the model is developed on a unit length of 1 meter down the runway. We assume that every other unit length will have similar gaseous puffs arising from the liquid. In the axial spills, the puff tracked by the model has other puffs in front and in back, as well as on top and underneath. This geometry of adjacent puffs is important to modeling the entrainment of ambient air because no entrainment is assumed across interfaces with adjacent puffs. This assumption is equivalent to assuming the properties of adjacent puffs are close enough to those of the tracked puff that mixing across the interface would change no properties being conserved.

For each Scenario, a model of the liquid spreading and vaporization dynamics (see previous Section) is used to provide the liquid evaporation

rate and the spill maximum radius or maximum axial width, the critical input variables for the dispersion model.

Other input variables are the atmospheric stability, wind speed at 10 meters, surface temperature and relative humidity. The surface temperature is used as the initial temperature of the Jet A and JP-4 spills. The relative humidity is assumed constant throughout the layer in which the gaseous fuel puffs are entraining ambient air. This layer is no deeper than 782 meters in the Scenarios. The wind speed is assumed to have a power law profile of the form:

$$u(z) = u(z_o) \left(\frac{z}{z_o}\right)^p \qquad (10)$$

where

z_o = reference height above ground

$u(z_o)$ = wind speed at reference height

p = power law exponent.

The reference height is the meteorological standard height of 10 meters. The power law exponent is set equal to 0.2 based on field measurements in a neutrally stable atmosphere. The wind speed at the reference height is set by the model user only for a neutral atmosphere. It is constrained to reasonable values selected for the other five stability categories. The six categories are labeled A through F, with A being the most unstable and F being the most stable (reference 26). The reference height wind speeds in meters per second are given in table 17.

The temperature profile is different for each stability, decreasing with height most rapidly for stability category A and increasing most rapidly for category F. The stability is chosen by the model user for the mixing layer, assumed here to be the lowest 200 meters of the atmosphere, above which the stability is assumed to be neutral.

TABLE 17. - ATMOSPHERIC STABILITY CONDITIONS

Stability Class		Reference Height Wind Speed (m/sec)	Lapse Rate (K/km)
Letter	Number		
A	1	2	-40
B	2	3	-30
C	3	5	-20
D	4	Any	-10
E	5	3	0
F	6	2	+10

The puff to be tracked with the model is defined when the liquid spill achieves maximum area. For liquid hydrogen or methane, the vaporization during the first second determines the vertical thickness of the puff. The mass of fuel vaporized is given by:

$$m_f = E\rho_\ell \, A_\ell \, \Delta t \text{ or } E\rho_\ell \, A_\ell \, (1.0 \text{ sec}) \qquad (11)$$

where

m_f = mass of gaseous fuel in puff (g)

E = evaporation rate (m/sec)

ρ_ℓ = density of liquid fuel (g/m^3)

A_ℓ = maximum area of liquid (m^2)

The rapid vaporization rate of the cryogenic fuels is our justification for assuming the initial puff is pure gaseous fuel, not yet containing ambient air to be turbulently entrained. Hence, the volume of this puff is given by:

$$V = m_f/\rho_g \qquad (12)$$

where

V = puff volume (m^3)

ρ_g = density of gaseous fuel at 1 atmosphere pressure and boiling point temperature (g/m^3)

and its thickness is:

$$\Delta z_p = V/A_\ell \tag{13}$$

where Δz_p = vertical thickness of puff (m).

For circular spills, the radius is the horizontal measure of the total puff. For axial spills, the down runway length of the spill is many times larger than the transverse spill width, hence the puff is given a unit length of 1 meter.

The initial puff above Jet A or JP-4 is not pure gaseous fuel because the saturation vapor pressure of these fuels is small. In order to make the dispersion of gaseous fuel above these conventional fuels comparable with the dispersion of the gaseous cryogenic fuels, an initial puff thickness is set at 7 cm, roughly the thickness of initial 1 second long puffs above the cryogenic liquids. The conventional fuels evaporate into a slab of ambient air brought over the liquid at the wind speed for mid puff height for the length of time it takes to cross the liquid in the up runway direction. If the resulting gaseous fuel concentration reaches saturation, then the saturation vapor pressure determines the concentration. If the initial concentration is smaller than the lowest flammable concentration, then no model run is made.

Once the initial puff is defined in shape, temperature, and gaseous fuel concentration, dispersion begins by the entrainment of ambient air and overall motion of the puff. The puff of a gaseous cryogenic fuel starts at the boiling point of the cryogenic liquid, much colder than its surroundings. The puff of conventional gaseous fuel is assumed to always have the same temperature as the surroundings.

Modeling the turbulent entrainment is the critical part. Early computations demonstrated that molecular diffusion of heat, mass or momentum was

orders of magnitude smaller than turbulent diffusion. This finding was supported by the movies of the NASA White Sands hydrogen spills, where the vigorous turbulence was marked visually by the motion of condensed water droplets. The model accounts for two possible contributions to the entrainment velocity, the rate at which ambient air penetrates the puff-air interface normal to the surface. The first contribution is proportional to the relative velocity between the overall puff and the air around it:

$$u_1 = 0.124 \left[w^2 + \left(u(z_p) - u_p \right) \right]^{0.5} \tag{14}$$

where

u_1 = first term of entrainment velocity (m/s)

w = vertical ascent velocity of puff (m/s)

$u(z_p)$ = horizontal wind speed at height of puff center (m/s)

u_p = horizontal velocity of puff (m/s).

The constant (0.124) was taken directly from reference 25. In the vertical direction the puff is moving through quiescent air, while in the horizontal plane the wind is moving air past the puff. The puff is dragged along by the wind through the process of entraining air, subject to the conservation of horizontal momentum. Horizontal momentum must be conserved because there is no net horizontal force applied to the ambient air system surrounding the puff.

The second contribution to the entrainment velocity only applies to the cryogenic fuels. It is based on the vigorous mixing induced just above the liquid surface by the high boiling (vaporization) rate. This term is given by:

$$u_2 = E(\rho_\ell / \rho_g) \ (V_o / V) \tag{15}$$

where

u_2 = second term of entrainment velocity (m/s)

V_o = initial volume of puff (m^3)

E = evaporation rate (m/s)

This second term was made proportional to the evaporation rate. The ratio of densities gives the volume expansion of a unit mass of cryogenic liquid as it vaporizes. The puff volume ratio reduces the influence of this term as the puff grows and moves away from the liquid surface.

The sum of the two terms gives the total entrainment velocity:

$$u_e = u_1 + u_2 \tag{16}$$

where

u_e = entrainment velocity (m/s).

The entrainment velocity is multiplied by the time increment (1 second) and the entrainment surface of the puff to get the volume of air entrained into the puff each second:

$$V_e = u_e \, \Delta t \, A_e \tag{17}$$

where

Δt = time increment (sec.)

A_e = entrainment area of puff.

The entrainment area of the puff is less than the total area of the puff. The entrainment area is the sum of the puff side area and the exposed parts of the puff top and bottom:

$$A_e = A_s + A_T + A_B \tag{18}$$

where

A_s = entraining side area of puff (m^2)

A_T = entraining top area of puff (m^2)

and A_B = entraining bottom area of puff (m^2)

Only if the puff rises from the ground can the bottom be exposed to turbulent entrainment of surrounding air. The top of the puff is partially exposed for entrainment except if it rises straight up. For a circular spill:

$$A_s = \Delta z_p(t)\ 2\pi\ r(t) \tag{19}$$

$$A_T = A_B = \pi r^2(t)\ \left(\Delta x(t)/2r(t)\right) \tag{20}$$

$$= \frac{\pi r\ (t)\ \Delta x(t)}{2}$$

where

$r(t)$ = puff radius (m) as a function of time t

$\Delta x(t)$ = amount of downwind movement of puff center (m).

The ratio $\Delta x(t)/2r(t)$ gives the proportion of the puff top or bottom exposed to surrounding air. The other parts of the top or bottom are covered by the preceding and following puffs. For an axial spill, there are similar relations:

$$A_s = 2\Delta z_p(t)\ L_x(t) \tag{21}$$

$$A_T = A_B = L_x(t)L_y(t)\frac{\Delta x(t)}{L_x(t)} \tag{22}$$

where

$L_x(t)$ = up runway length of axial puff (m)

$L_y(t)$ = crosswind (cross runway) width of puff (m)

In the axial cases, the puff has neighboring puffs on its downwind and upwind sides, as well as above and below.

Solving the above equations for the entrainment area and entrained volume of air allows computation of the entrained mass:

$$m_e = V_e \rho_a(z_p) \tag{23}$$

where

m_e = mass (g) of air entrained during a time increment

$\rho_a(z_p)$ = density of air at height of puff (g/m^3)

This entrained mass of air is added to the existing puff mass to get the new puff mass. The initial puff mass for the cryogenic spills was given by Equation 11. The initial puff mass for the conventional fuels is given by:

$$m_{po} = \frac{V_o P\ (z_{po}) M_p}{R^* T_a(z_{po})} \tag{24}$$

where

m_{po} = initial puff mass (g)

P = pressure of atmosphere ($dyne/cm^2$)

z_{po} = initial puff height (m)

M_p = puff molecular weight (g/mole)

R^* = universal gas constant (cal/mole K)

T_a = temperature of ambient air (K)

The puff molecular weight depends on the molecular fractions of gaseous fuel and air:

$$M_p = M_f F + M_a (1-F) \tag{25}$$

where

M_f = fuel molecular weight (g/mole)

M_a = air molecular weight = 28.9 g/mole

F = fuel mole fraction

The fuel mole fraction is an output of the model after the computations for each time increment:

$$F = \frac{F_o}{\left(1 + \frac{\sum_t^t m_e}{m_f}\frac{M_f}{M_a}\right)} \tag{26}$$

where

F_o = initial fuel mole fraction

$\sum_t^t m_e$ = total entrained air mass.

Now the information derived from the conservation of mass allows application of the conservation of enthalpy. The entrained enthalpy is given by:

$$H_e = m_e C_{pa} T_a(z_p) \tag{27}$$

where

H_e = enthalpy of air entrained during time increment (calories)

C_{pa} = specific heat capacity of air at constant pressure (calories/g K)

$T_a(z_p)$ = temperature of air at puff height (K).

Conservation of enthalpy proceeds stepwise for each thermodynamic process occurring during each time increment. This stepwise solution of the new puff temperature between each thermodynamic process provides a higher degree of accuracy in specifying the temperature. The thermodynamic processes that are handled in the model are: 1) the heating of the gaseous fuel by the warmer entrained air, 2) the condensation of water vapor in the entrained air as it is cooled by the gaseous fuel, 3) the freezing of the water droplets upon further cooling, 4) the melting of these same frozen hydrometeors later in the life of the puff, and 5) the evaporation of the water droplets still later.

Conceivably the initial cryogenic temperature (20.3 K) of the liquid hydrogen can cause atmospheric oxygen to condense at 90 K and nitrogen to condense at 78 K. The condensation of these molecules would cause a rapid local depression in the pressure and collapse of the volume affected. The heating of the cryogenic temperature gaseous fuel to temperatures above these boiling points is so rapid, a few seconds, that the latent heat released in the condensation is almost immediately reabsorbed by the subsequent evaporation. There is, hence, no effect on the overall enthalpy conservation.

Just considering the first thermodynamic process, heating the gaseous fuel and cooling the entrained air, the intermediate puff temperature is given by:

$$T'_p = \frac{H_e + H_p}{C_{pp}(m_p + m_e)} \tag{28}$$

where

T'_p = puff temperature resulting from heating of cryogenic gaseous fuel (K)

H_p = puff enthalpy before adding air entrained during time increment (calories)

C_{pp} = specific heat capacity of puff at constant pressure (calories/g K)

The specific heat capacity of the puff is:

$$C_{pp}(F,T_p) = \frac{C_{pf}(T_p)M_f F + C_{p\,a} M_a(1-F)}{M_p} \tag{29}$$

where

$C_{pp}(F,T_p)$ = puff specific heat capacity at constant pressure as a function of fuel mole fraction and puff temperature (cal/g K)

$C_{pf}(T_p)$ = gaseous fuel specific heat capacity at constant pressure as a function of puff temperature (cal/g K)

In order to compute if water vapor in the entrained air will condense, the water vapor pressure in the ambient air is found from

$$e = h\ 10^{\left[\left\{a - b/T_a(z_p)\right\}\right]} \tag{30}$$

where

e = water vapor pressure in ambient air (millibars)

h = relative humidity in ambient air

a = constant = 9.4051

b = constant = 2353

The saturation water vapor pressure in the puff at temperature T_p' is:

$$e_{sp} = 10^{\left[a - (b/T_p')\right]} \tag{31}$$

where

e_{sp} = saturation water vapor pressure in puff (millibars)

The entrained water vapor will condense if $e_{sp} < e$. If the water vapor condenses, then the latent heat of condensation will provide enthalpy to further warm the puff:

$$T_p'' = \frac{H_e + H_p + m_w L_w}{C_{pp}(F,T_p')\ (m_p + m_e)} \tag{32}$$

where

T_p'' = intermediate puff temperature after condensation (K)

m_w = water vapor mass in entrained air (g)

L_w = latent heat of water vapor condensation (cal/g)

Note the similarity of this equation with (28). The water vapor mass entrained and available for condensation is:

$$m_w = e\ V_e\ M_w / R^*\ T_a$$

where

M_w = molecular weight of water (g/mole)

The condensation of entrained water vapor leads to a test of the intermediate puff temperature T_p'' in order to see if it is low enough to induce freezing of the water droplets. If $T_p'' < 253$ K, the droplets are assumed to freeze. This temperature is chosen as a compromise between 233 K, when all liquid water will freeze, and 273 K, when water with many impurities will freeze. The presence of ice nuclei in the atmosphere will encourage the freezing process, facilitating its occurrence at a higher temperature within the range of 233 K to 273 K. There is no need to put this nuclei dependence in the model because the required input information does not relate directly to the aircraft fuel questions of interest here. Again, the puff temperature is recomputed, using the relation:

$$T_p''' = \frac{H_e + H_p + m_w\ (L_w + L_w')}{C_{pp}(F, T_p'')\ (m_p + m_e)} \qquad (33)$$

where

T_p''' = intermediate puff temperature after fusion (K)

L_w' = latent heat of fusion of water (cal/g).

The conservation of enthalpy part of the model also keeps track of the melting of frozen hydrometeors and the evaporation of condensed water droplets later in the dispersion of the puff when it becomes sufficiently warm. The frozen hydrometeors are melted when the temperature of the puff rises above 273 K and the condensed water droplets evaporate when $e < e_{sp}$. The temperature after these processes is T_p''''.

At the end of the conservation of enthalpy computations, the final puff temperature is used to compute the puff density from:

$$\rho_p = \frac{p(z_p)M_p}{R^* T_p''''} \tag{34}$$

The new volume of the puff is given by:

$$V' = \frac{m_p(t) + m_e(t)}{\rho_p(t)} \tag{35}$$

The new linear dimensions of the puff are computed from the new volume assuming the previous ratios of the linear dimensions are preserved. For a circular spill,

$$\frac{r'}{r} = \frac{\Delta z'_p}{\Delta z_p} \tag{36}$$

$$V' = \pi (r')^2 \Delta z'_p \tag{37}$$

$$r' = \left(\frac{r V'}{\pi \Delta z'_p}\right)^{1/3} \tag{38}$$

and

$$\Delta z'_p = \Delta z_p (r'/r) \tag{39}$$

where

r' = new puff radius (m)

$\Delta z'_p$ = new puff thickness (m)

V' = new puff volume (m^3).

Similarly, for an axial spill,

$$\frac{L'_y}{L_y} = \frac{L'_x}{L_x} \tag{40}$$

$$\frac{\Delta z'_p}{\Delta z_p} = \frac{L'_x}{L_x} \tag{41}$$

$$V' = L'_x L'_y \Delta z'_p \tag{42}$$

$$L_x' = \left(V' L_x^2 / L_y \Delta z_p \right)^{1/3} \tag{43}$$

$$L'_y = L_y \left(L'_x / L_x \right) \tag{44}$$

$$\Delta z'_p = \Delta z_p (L'_x / L_x) \tag{45}$$

where the primed variables are the new linear dimensions as a result of the puff expansion with entrained air.

The next part of the model computes the mass motion of the puff. The buoyancy acceleration determines both the vertical motion of the puff and its level of turbulence. Telford (reference 25) found that three-fourths of the buoyancy potential energy resulted in turbulence in cumulus clouds and the remaining one-fourth resulted in vertical motion. Therefore, the net vertical acceleration of the puff is

$$A = \frac{1}{4} \left(\frac{\rho_a}{\rho_p} - 1 \right) g \tag{46}$$

where

A = net upward acceleration of puff (m/s^2)

g = acceleration of gravity (m/s^2)

The net buoyant acceleration provides the impulse that must equal the change in vertical momentum according to Newton's Second Law of Motion. The impulse is the net upward force times the time increment. The initial vertical momentum is the puff mass times the beginning vertical velocity while

the final vertical momentum is the combined mass of puff and entrained air times the final vertical velocity:

$$m_p A \Delta t = (m_p + m_e) w' - m_p w$$

Rearranging, we solve for the final vertical velocity:

$$w' = (w + A \Delta t) \frac{m_p}{m_p + m_e} \tag{47}$$

where

w' is final vertical velocity after the net acceleration A has acted on the puff during the time increment (m/s).

The new vertical position of the puff is found from

$$z_p' = z_p + \left(\frac{w' + w}{2}\right) \Delta t \tag{48}$$

The computation of the new horizontal position in response to the drag of the wind must also take into account conservation of horizontal momentum because there is no net horizontal force on the puff/air system. Hence,

$$u_p' = \left(m_p u_p + m_e u (z_p)\right)/(m_p + m_e) \tag{49}$$

where

u_p' = new horizontal puff velocity after entraining air during time increment (m/s)

and

$$x_p' = x_p + \left(\left(u_p + u_p'\right)/2\right) \Delta t \tag{50}$$

The overall ascent angle of the puff relative to its starting point is computed from

$$= \tan^{-1}(z_p/x_p) \tag{51}$$

Once the new vertical position of the puff is computed with (48), the puff temperature is corrected by the dry adiabatic cooling it experiences as the ambient pressure drops during ascent. The corrected puff temperature is:

$$T_p = T_p'''' - \Gamma'\left(z_p' - z_p\right) \tag{52}$$

where

T_p = final puff temperature corrected for adiabatic cooling of ascent (K)

Γ' = dry adiabatic lapse rate of the atmosphere (K/m).

The dry adiabatic lapse rate is used here because any release of latent heat from the condensation of water vapor has already been handled in the computation of puff temperature during the conservation of enthalpy. The lapse rate of the atmosphere is set in the lowest 200 meter layer for each stability class as shown in table 17.

The lapse rate for class D (neutral stability) is set equal to the dry adiabatic value. The equal increments between classes is assumed for convenience, but the sequence is in the correct order with the correct sign.

4.3 Vapor Purge Model

This section describes a vapor purge model to be used with Scenario 1, small-scale liquid spills into fuselage or wing compartments within the aircraft. These small-scale liquid leaks are assumed to be continuous, and they may occur from either fuel tanks or fuel lines into adjacent fuselage or wing structural compartments. These compartments are assumed to have liquid drain holes at their bottoms, so that liquid pooling should not occur in the compartment volume. In order to reduce the hazard of combustion, it is desirable to purge the combustible vapors from these compartments at a rate that would maintain the vapor concentration below combustible limits. This purge could

be accomplished with ram air flow through the various compartments during flight, or with pumped air purge if the aircraft is on the ground. The objective of this section is to develop some simple models that will predict the required air purge rates as a function of the assumed fuel leakage rates.

For the cryogenic liquids, with small-scale leaks into compartments above the boiling point temperature, complete vaporization of the liquid fuel should occur at the leakage rate. Except in the immediate vicinity of the liquid leak, the purge air rate required to keep the compartment volume below the minimum combustible limit of the fuel volume ratio or mole fraction ratio, y_{min}, can be expressed as a volume flowrate ratio:

$$\frac{\dot{V}_A}{\dot{V}_F} = \left(\frac{1}{y_{min}} - 1\right) \tag{53}$$

where

$\dot{V}$ = volumetric flowrate at atmospheric temperature and pressure.

y_{min} = minimum combustible mole fraction of fuel in the air.

Subscripts: F refers to fuel and A refers to air.

The above equation can be converted to a mass flowrate ratio by multiplying by the appropriate molecular weight ratio.

$$\frac{\dot{m}_A}{\dot{m}_F} = \left(\frac{1}{y_{min}} - 1\right) \cdot \frac{M_A}{M_F} \tag{54}$$

where

$\dot{m}$ = mass flowrate of fuel vapor or air.

M = molecular weight of fuel vapor or air.

Values greater than or equal to the above limiting flowrate ratios will ensure a noncombustible mixture in the bulk of the compartment. If the liquid does not completely vaporize and some drains from the compartment, then the above

purge air flowrates will be conservative. However, there will always be a combustible mixture in the immediate vicinity of the cryogenic liquid phase.

For the conventional petroleum-based fuels, the purge air flow requirement is much more difficult to estimate. For example, for Jet A the fuel vapor pressure is less than atmospheric, so the fuel vapor must diffuse through a boundary layer into the purge air flow. This heat and mass transfer process is a function of compartment geometry and flow conditions, the area of liquid vaporization, the temperature and pressure levels, etc. Because of limits in study resources, it was decided not to attempt to model and solve for air purge requirements with the conventional fuels. Generally speaking, purge airflow requirements for the lower vapor pressure conventional aircraft fuels will be less than for leaks of the highly volatile cryogenic fuels.

4.4 Heat Transfer Analysis in Aircraft Fuel Fires

This section is concerned with an aircraft mishap or crash that will result in a large-scale fuel spill with combustion occurring adjacent to an intact fuselage cabin. The closed fuselage is assumed to be completely or partially imbedded in some large-scale pool burning flames. The objective of this section is to develop a heat transfer model that could be used to predict the time required either to breach the fuselage cabin or to create life threatening internal cabin conditions for the passengers.

In this study, the Lockheed L-1011 fuselage design was used as a representative model of the fuselage cabin of a long-range subsonic aircraft. As discussed in section 3.3.2, figure 8 presented a cross section and view of the fuselage cabin design, while figure 9 illustrated a typical cross section of the fuselage skin and stringers, the fiberglass insulation, and the interior honeycomb side panel.

Based upon this figure 9 cross section, a thermal model of the fuselage side-wall was developed to compute the transient temperatures of this cross section to flame heating absorbed on the outer fuselage skin. The fuselage skin and stringers were combined as the outer thermal node, absorbing heat from the flames, while the internal honeycomb side panel node exchanged heat

by free convection with an air node in the cabin. The fiberglass insulation was represented by four thermal nodes in series, with conduction resistance between them. Both thermal radiation and free convection heat transfer was modeled in the air gaps on each side of the fiberglass insulation. An explicit solution of the node temperatures as a function of time was then solved on a digital computer for a range of absorbed heat rates on the fuselage skin.

A cabin window assembly and cross section was shown on figure 10. Three plastic window panes are present, which should have radiation transmission properties similar to glass. A thermal model of the window panes was not developed, however, because it would have required development of the spectral wavelength distribution of the various flames and modeling of the wavelength-dependent radiation transmission and absorption of the window panes. The task was considered to be beyond study resources and schedule limitations and not of the importance to justify deleting other tasks.

Detailed thermal modeling of the windows and the flame heat sources would yield an estimate of the radiation heat flux transmitted through the windows and the time required for the various fuel flames to breach the windows. There is an obvious hazard to passengers posed by radiation heat transfer through the windows, plus the susceptability of the plastic windows to melt long before the aluminum structure of the cabin wall. However, a simple solution to the problem is to provide heat resistant window shades with a reflective coating on the outside surface. In event of a crash in which fire results, passengers exposed to high radiation heat flux would thereby have a means of protecting themselves.

5. ANALYSIS OF CRASH SCENARIOS

The results of the analyses for all four fuels are presented here for the internal leak (Scenario 1); the liquid spill spreading and vaporization which occurs in Scenarios 2, 3 and 4; the gaseous dispersion into the atmosphere associated with Scenarios 2, 3 and 4 and the heat transfer rates and the effects of liquid pool fires surrounding an intact fuselage.

5.1 Small Internal Leak Results - Scenario 1

For the small internal fuel leaks of Scenario 1, leakage is assumed to occur from the fuel tanks or fuel lines into fuselage or wing compartments within the aircraft. The leaks might be due to cracks developing in welds or joints of the fuel system, and they could develop either in flight or on the ground. These small fuel leaks will then vaporize in the structural compartments, and may create a combustible fuel vapor/air mixture throughout the compartment. If an ignition source were present, an explosion could result that would severely damage the aircraft.

Running a purge air flow through compartments critical for fuel leaks and/or ignition sources is a way to reduce the fire and explosion hazard. The purge air flowrate is set so that the fuel vapor/air mixture is maintained below the lower combustible limit of the fuel. Hence, only a small region near the liquid fuel will be combustible, with an adequate purge air flow through the compartment. Normally, fuselage or wing compartments which are susceptable to fuel leaks have drains holes at their bottoms to allow any nonevaporated liquid fuel to drain from the compartment.

The liquid fuel spill rates which were established for consideration in Scenario 1 for LH_2 spills are tabulated below:

1A - 1.0×10^{-4} kg/s

1B - 1.0×10^{-3} kg/s

1C - 1.0×10^{-2} kg/s

These same small leakage rates were also used for the other fuels (LCH_4, JP-4 and Jet A) analyzed in this study.

The purge air flow requirements for the above fuel leakage rates were computed using the purge air model presented in Section 4.3. This model assumes that all the fuel leakage vaporizes, and computes an air flow that will maintain the fuel vapor mole fraction, y_{min}, at or below the minimum combustible limit in most of the compartment volume. The results of this analysis, for the four fuels, are shown on table 18, where the air flowrate to fuel leakage rate ratio is computed to keep the compartment volume in a non-combustible state.

For small-scale leaks of the boiling cryogenic fuels, the assumption of complete fuel evaporation is good, and the computed flowrate ratio will be needed to obtain a noncombustible mixture. For example, for LH_2, a fuel leakage rate in the range of 10^{-4} to 10^{-2} kg/s would require a purge air flowrate in the range of 3.45×10^{-2} to 3.45 kg/s respectively, to obtain a safe gas mixture. For the conventional fuels, the situation is more complex, since fuel vaporization can only occur by diffusion into the air stream. The liquid fuel may or may not completely vaporize. It is a complex problem to analyze, involving liquid areas and flow geometry, vapor and air pressures, temperature, and vapor mass diffusion into the air flow. The table 18 air-to-fuel flow ratios for the conventional fuels are conservative since it is assumed that all of the fuel leak vaporizes. For either JP-4 or Jet A leaking at a flowrate of 1.0×10^{-2} kg/s, an air flowrate of about 0.29 kg/s will yield a noncombustible gas mixture in the compartment.

For the low vapor pressure, nonvolatile fuels, a certain temperature must be present before a combustible vapor/air mixture can exist, even with no air flow. For Jet A (kerosine) vaporizing into a one atmosphere air pressure, a temperature of 311 K (100°F) is required for a combustible

TABLE 18. - AIR FLOW TO FUEL LEAKAGE RATIOS FOR NON-COMBUSTIBLE GASES

Parameter \ Fuel	LH_2	LCH_4	JP-4	Jet A
M_F, Molecular Wt.	2.016	16.04	132	168
y_{min}, Non-Combustible Mole Fraction	0.04	0.05	0.008	0.006
$\frac{\dot{m}_A}{\dot{m}_F}$, Air To Fuel Flow Ratio	≥345.	≥ 34.3	27.24	28.6

From Section 4.3:

$$\frac{\dot{m}_A}{\dot{m}_F} = \left[\frac{1}{y_{min}} - 1\right] \cdot \frac{M_A}{M_F}$$

where

M_A = Molecular Weight of Air = 28.97 g/g mole

vapor/air mixture with y≥0.006. To obtain a combustible mixture with the more volatile JP-4 (gasoline) in sea level air, a lower temperature of ≥237.8 K (-32°F) would yield the combustible mole fractions y≥0.008. Hence, for the less volatile conventional fuels, the temperature and air pressure may determine if an air purge flow is required for a compartment.

In conclusion, the purge air requirements for a boiling cryog c fuel leak in an aircraft compartment are more severe than for a less volatile conventional fuel. The purge air requirements for LH_2 are an order of magnitude higher than for the same LCH_4 leakage rate. The conventional fuels evaporate by diffusion, and purge air may not be necessary to maintain a noncombustible mixture if the fuel vapor pressure is low enough. Even if the conventional fuel leak completely vaporized, the air purge rate is less for the higher molecular weight conventional fuels. Hence, the problems of fuel leaks into aircraft compartments are more severe with the cryogenic fuels, but they should be relatively safe with purge air flows which are reasonably obtainable.

C-2

5.2 Liquid Spill, Spreading, and Vaporization Results for Scenarios 2, 3 and 4

5.2.1 Scenario 2 - Radial spills. - In the Scenario 2 spills, liquid flows from either a fuel tank or fuel line onto a fixed position on the base surface, resulting in a radial liquid spread. The liquid hydrogen (LH_2) spills were supplied from a single 12,600 kg capacity tank. Three representative Scenario 2 spill rates were specified, as tabulated below:

2A - 0.5 kg/s, line leak due to gravity flow.

2B - 2.3 kg/s, line leak due to pumped flow.

2C - 900 kg/s, leak due to tank puncture.

Both the Scenario 2A and 2B leakage rates are small; hence these leaks appear continuous with spill times >1.0 hour unless appropriate shut-off valves are closed by the flight crew. The Scenario 2C spill occurs over a 14-second time span, and this may approach an instantaneous spill depending on the liquid spread and vaporization time.

In this study, the liquid methane (LCH_4) tank loadings and spill rates were taken as 2.7 times those given for LH_2 above. For the conventional fuels (JP-4 and Jet A), the tank loadings and spill rates were fixed at 3.3 times those chosen for LH_2. Hence, the spill times are the same for all of the fuels considered in this Scenario, which effectively compares fuel leaks based upon the same degree of damage for each of the fuels considered.

For the Scenario 2 spills, the maximum radius of spread, r_m; the earliest time of the maximum spread, t_m; and the maximum rate of liquid evaporation, $\dot{m}_{EVAP}$, were all calculated based upon the Fay models for radial spread presented near the end of Section 4.1. Usually, an iterative solution of these three parameters is required, to match the liquid evaporation rate to the average of a variable heat flux occurring to the liquid pool. In this case, the Scenario 2A and 2B cases were computed using the continuous radial spill equations while Scenario 2C was solved using the instantaneous radial spill relations of the Fay model.

Two spill spreading, and vaporization conditions were considered in this and the remaining Scenarios. The first condition considered was either boiling vaporization due to heat transfer from the base surface for the cryogenic liquids, or constant temperature vaporization controlled by vapor diffusion into the atmosphere for the conventional fuels. No burning was assumed to occur above the liquid pool for this condition; hence, the extent of spread and the fuel vaporization rates computed here formed the input data for the Vapor Dispersion Models presented in Section 4.2. For this and the remaining Scenarios, concrete was chosen as the spill surface, with a sea level atmosphere pressure at 297 K (75^{o}F) temperature and a 2 m/s wind condition. For the cryogenic liquids, a variable heat flux was considered from the base surface, while the vaporizaton rate of the conventional fuels was considered constant, based upon a large scale 100 meter liquid spread with a 2 m/s wind blowing over it.

The second condition considered was the spill, spreading and vaporization of the liquid fuels with pool burning occurring above the liquid spread. With ignition at the start of the spill, radiation from the flames would be the major source of heat to a large-scale liquid fuel pool. Table 19 shows the radiant heat flux q''_F expected to large-scale spills and the rate of liquid drop V_E due to boiling at this heat flux for the various fuels considered. These data are based upon the flame temperatures T_F and the flame emissivities ϵ_F presented by the A. D. Little, Inc. representatives at the oral presentations held at NASA-Lewis on September 2, 1981. For the cryogenic liquids, this vertically downward radiant heat flux for the equilibrium flame temperature would be completely absorbed by the liquid or base surface, and would result in vaporization of these boiling liquids. For the conventional fuels, this radiant heat flux would first increase the liquid temperature, which would also transfer heat to the base surface, and finally the boiling temperature would be reached. A detailed transient mass and heat flow analysis would be required to estimate the time and extent of the conventional fuel spreads with pool burning above them. Hence, these calculations were only made for the spreading of the cryogenic boiling liquids with pool burning flames above.

TABLE 19. - EXPECTED RADIANT HEAT FLUX FROM VARIOUS FLAMES

Fuel	T_F K	ϵ_F	q''_F kW/m^2	V_E m/s
LH_2	1700.	0.4	189.4	6.0×10^{-3}
LCH_4	1500.	0.8	229.6	1.1×10^{-3}
JP-4	1100.	0.9	74.7	2.6×10^{-4}
Jet A	1100.	0.9	74.7	2.6×10^{-4}

NOTE: The temperature T_F and emissivity ϵ_F of these flames are based upon the A.D. Little, Inc. combustion analysis presented at the NASA-Lewis oral presentations, Sept 2, 1981.

The results of the spreading and vaporization solutions with no burning are shown on table 20. For the cryogenic liquids, the radius r_m and time t_m to evaporate the LH_2 spills are less than those for LCH_4. Vaporization of the conventional fuels requires much larger radii and times, although the more volatile JP-4 (gasoline) is considerably faster than the less volatile Jet A (kerosine) fuel. Scenarios 2A and 2B, which used the continuous radial spill model, show the same rate of vaporization as the spill rate $\dot{m}$. Scenario 2C, which uses the instantaneous radial spill equations, shows a lower maximum vaporization rate than the spill rate which occurred during the 14 second spill duration.

Table 21 shows the results of spreading and vaporization solutions for the cryogenic fuels with pool burning flames above. Once again, the extent and times of the LH_2 spills are less than those for LCH_4, especially for the larger rate Scenario 2C spill. Comparing these solutions with flames to those without flames, table 20 shows that burning decreases the radius and time of the spread, while increasing the maximum rate of vaporization for the instantaneous Scenario 2C spill.

Hence, for the range of radial spills considered here, the cryogenic liquids would evaporate much faster, with less radial spread, than the conventional fuels. Comparing the high rate Scenario 2C spills with no flames,

TABLE 20. - SCENARIO 2, RADIAL SPILL, SPREADING AND VAPORIZATION, NO FLAMES.

Scenario No., Fuel	m kg	$\dot{m}$ kg/sec	Q_0 m3	$\dot{Q}_0$ m^3/sec	V_E m/sec	r_m m	t_m sec	$\dot{m}_{EVAP}$ kg/sec
2A, LH_2	12,600	0.5	117.8	0.0071	2.5×10^{-3}	1.0	1.8	0.5
2B, LH_2	12,600	2.3	117.8	0.0324	2.5×10^{-3}	2.0	3.0	2.3
2C, LH_2	12,600	900	117.8	12.70	2.5×10^{-3}	35	32	630
2A, LCH_4	34,398	1.37	81.13	0.0032	6.0×10^{-4}	1.3	3.6	1.37
2B, LCH_4	34,398	6.28	81.13	0.0148	4.0×10^{-4}	3.4	8.0	6.28
2C, LCH_4	34,398	2,457	81.13	5.795	1.1×10^{-4}	61	117	550
2A, JP-4	42,210	1.68	54.12	0.0021	2.0×10^{-6}	18.5	143	1.68
2B, JP-4	42,210	7.71	54.12	0.0099	2.0×10^{-6}	40	237	7.71
2C, JP-4	42,210	3,015	54.12	3.865	2.0×10^{-6}	143	785	100
2A, Jet A	42,210	1.68	54.12	0.0021	7.0×10^{-8}	99	1,330	1.68
2B, Jet A	42,210	7.71	54.12	0.0099	7.0×10^{-8}	212	2,220	7.71
2C, Jet A	42,210	3,015	54.12	3.865	7.0×10^{-8}	331	4,180	18.8

the LH_2 would completely vaporize in 32 seconds, compared to an LCH_4 vaporization time of ≈117 seconds, while the maximum hydrogen radius is approximately half that for methane. Burning above these cryogenic fuels decreases both the radii and times of the spills by comparable ratios for both LH_2 and LCH_4. The noburning vaporization times of the conventional fuels may seem short, but it should be remembered that these models have a completely flat surface, with no small-scale liquid pools. Although we did not solve spreading of the conventional fuels with flames above, a burning Jet A, Scenario 2C spill might last for approximately an hour based on aircraft crash experience.

TABLE 21. - SCENARIO 2, RADIAL SPILL, SPREADING AND VAPORIZATION, FLAMES ABOVE

Scenario No., Fuel	m kg	$\dot{m}$ kg/sec	Q_0 m^3	$\dot{Q}_0$ m^3/sec	V_E m/sec	r_m m	t_m sec	$\dot{m}_{EVAP}$ kg/sec
2A, LH_2	12,600	0.6	117.8	0.0071	6.0×10^{-3}	0.6	1.0	0.6
2B, LH_2	12,600	2.3	117.8	0.0324	6.0×10^{-3}	1.3	1.7	2.3
2C, LH_2	12,600	900	117.8	12.70	6.0×10^{-3}	26	15	900
2A, LCH_4	34,398	1.37	81.13	0.0032	1.1×10^{-3}	1.0	2.5	1.37
2B, LCH_4	34,398	6.28	81.13	0.0148	1.1×10^{-3}	2.1	4.1	6.28
2C, LCH_4	34,398	2,457	81.13	5.795	1.1×10^{-3}	35	38	1,710

The largest Jet A aircraft spill (the Tenerife crash of two fully tanked 747s on March 27, 1977) burned for more than 10 hours.

5.2.2 Scenario 3 - Axial spills. - For the Scenario 3 spills, liquid flows from either a fuel tank or fuel line onto the base surface while the aircraft decelerates from a velocity of 61.7 m/s (120 knots) along the spill line. The tank loadings and leakage rates are exactly the same as those used for the Scenario 2 spills. The axial spread considered was a one-dimensional spread perpendicular to the spill line. With the high aircraft velocity, V_A, a constant rate of spill will yield a near instantaneous spill of Q'_o (volume per unit length of spill line) at a fixed position along the spill line. Neglecting the velocity along the spill line, this instantaneous spill will then create a unit width spread, out perpendicular from both sides of the spill centerline. In this model, the axial distance, x, will be half the full spread distance, measured perpendicularly from the spill center line to one edge of the axial spread. Based upon the Fay model equations for instantaneous axial spills presented in Section 4.1, the maximum axial half-spread distance, x_m; the earliest time of the maximum spread, t_m; and the

maximum rate of evaporation per unit width of spread, $\dot{m}'_{EVAP}$ were calculated. The same methods of solution and both the burning and non-burning conditions were computed for the Scenario 3 spills, as was done for Scenario 2. For Scenario 3, only an instantaneous axial spill model was required, considering the aircraft velocity.

The results of the axial spreading and vaporization solutions with no burning are shown on table 22, while those with pool burning above the liquid spread are given in table 23. It should be noticed that the low spill rates of Scenarios 3A and 3B yield very short axial spreads, x_m. Considering the high aircraft velocity, V_A = 61.7 m/s, the liquid would actually spray upon falling and/or striking the spill surface. This would tend to increase the extent of the spread and decrease the time to complete evaporation compared to those values presented in the tables. This instantaneous axial spread model best simulates the high spill rate cases, such as Scenario 3C, where the one-dimensional axial spread extends for a considerable distance.

Generally speaking, the same observations made for the Scenario 2 spill data pertains here. The extent and time of the maximum spreads increase in this order: LH_2, LCH_4, JP-4 and Jet A, the order of decreasing volatility. As expected, flames above the liquid spill decrease the time and extent of the vaporization, which occurs at an increased rate.

In conclusion, a fuel spill from a moving aircraft distributes the liquid along a long spill line. The spread perpendicular to this line is then shorter in distance and time than for a fixed location radial spill. For example, the Scenario 3C, LH_2 spill with no flame extends 864 meters down and 6.2 meters on each side of the spill line, with the aircraft moving 61.7 m/s. The total time of spill along the spill line length is 14 seconds, while the evaporation time at any point along the spill line is ≈13 seconds. In comparison, the Scenario 2C, LH_2 radial spill with no burning, had a maximum radial spread of 35 meters and required ≈32 seconds to evaporate. Hence, the aircraft motion in the axial spills increases the surface area of the spread, which substantially decreases the time required for evaporation at any location along the spill line.

TABLE 22. - AXIAL SPILL, SPREADING AND VAPORIZATION, NO FLAMES

Scenario No., Fuel	m kg	$\dot{m}$ kg/sec	Q_0 m^3	Q_0' m3/m	V_E m/sec	Xm m	t_m sec	$\dot{m}'_{EVAP}$ kg/msec
3A, LH_2	12,600	0.5	117.8	1.14×10^{-4}	2.5×10^{-3}	0.07	0.7	0.026
3B, LH_2	12,600	2.3	117.8	5.26×10^{-4}	2.5×10^{-3}	0.17	1.3	0.061
3C, LH_2	12,600	900	117.8	0.2056	2.5×10^{-3}	6.2	12.9	2.21
3A, LCH_4	34,398	1.37	81.13	5.22×10^{-5}	1.0×10^{-3}	0.06	0.8	0.054
3B, LCH_4	34,398	6.28	81.13	2.40×10^{-4}	1.0×10^{-3}	0.16	1.5	0.134
3C, LCH_4	34,398	2,457	81.13	0.0939	2.3×10^{-4}	10	41	1.95
3A, JP-4	42,210	1.68	54.12	3.48×10^{-5}	2.0×10^{-6}	0.6	29	0.0018
3B, JP-4	42,210	7.71	54.12	1.60×10^{-4}	2.0×10^{-6}	1.5	53	0.0046
3C, JP-4	42,210	3,015	54.12	0.0626	2.0×10^{-6}	53	580	0.165
3A, Jet A	42,210	1.68	54.12	3.48×10^{-5}	7.0×10^{-8}	2.3	217	0.00025
3B, Jet A	42,210	7.71	54.12	1.60×10^{-4}	7.0×10^{-8}	5.6	400	0.00062
3C, Jet A	42,210	3,015	54.12	0.0626	7.0×10^{-8}	203	4,330	0.0221

Initial aircraft velocity along the spill line, V_A = 61.73 m/sec (120 knots)

5.2.3 Scenario 4 - Radial spills, catastrophic crash. - The Scenario 4 spills are the result of a nonsurvivable crash of the aircraft, in which all of the tanks rupture and spill instantaneously, resulting in an assumed radial spreading and vaporization of the liquid fuel. Scenario 4A represents a crash shortly after takeoff, where the nearly full tank loadings would be spilled instantaneously, while Scenario 4B simulates a crash just before landing, with an instantaneous spill of ≈10% of the total tank capacity.

TABLE 23. - AXIAL SPILL, SPREADING AND VAPORIZATION, FLAMES ABOVE

Scenario No., Fuel	m kg	$\dot{m}$ kg/sec	Q_0 m^3	Q_0' m3/m	V_F m/sec	x_m m	t_m sec	$\dot{m}'_{EVAP}$ kg/msec
3A, LH_2	12,600	0.5	117.8	1.14×10^{-4}	6.0×10^{-3}	0.05	0.4	0.042
3B, LH_2	12,600	2.3	117.8	5.26×10^{-4}	6.0×10^{-3}	0.12	0.7	0.104
3C, LH_2	12,600	900	117.8	0.2056	6.0×10^{-3}	4.4	7.7	3.74
3A, LCH_4	34,398	1.37	81.13	5.22×10^{-5}	1.1×10^{-3}	0.06	0.8	0.055
3B, LCH_4	34,398	6.28	81.13	2.40×10^{-4}	1.1×10^{-3}	0.15	1.4	0.137
3C, LCH_4	34,398	2,457	81.13	0.0939	1.1×10^{-3}	5.5	15.	4.94

Initial aircraft velocity along the spill line, V_A = 61.73 m/sec (120 knots).

The total fuel spillage for 4A for LH_2 was 21,600 kg. and the same weight ratios as used in Scenarios 2 and 3 were used here for the various fuels.

Since all these spills are instantaneous, the Fay model equations for instantaneous radial spills presented near the end of Section 4.1 were used in this analysis. The maximum radius of the spread, r_m; the earliest time of the maximum spread, t_m; and the maximum rate of vaporization, $\dot{m}_{EVAP}$, were computed for both the conditions of no flames and pool burning flames above the liquid spreads. These data are presented in table 24 for the no-burning condition and in table 25 for the liquid pool burning condition.

Once again, these data show the same ranking of the fuels relative to the radial extent of the spread and time for vaporization as occurred for the Scenario 2 radial spills. With no flames, the maximum Scenario 4A spills would find a maximum radius of 49 meters and a vaporization time of 39 seconds for LH_2, compared to 77 meters and 140 seconds for LCH_4. With flames above the liquid spill, a 37-meter maximum radious and a 22 second vaporization time is predicted for LH_2, compared to 43 meters and 43 seconds for LCH_4, when the maximum Scenario 4A spill is considered. The extent of spread and time of

TABLE 24. SCENARIO 4, RADIAL SPILL, SPREADING AND VAPORIZATION, NO FLAMES

Scenario No., Fuel	m kg	$\dot{m}$ kg/sec	Q_0 m^3	$\dot{Q}_0$ m^3/sec	V_E m/sec	r_m m	t_m sec	$\dot{m}_{EVAP}$ kg/sec
4A, LH_2	21,600	∞	304.74	∞	1.9×10^{-3}	49	39	1,040
4B, LH_2	2,160	∞	30.474	∞	2.5×10^{-3}	20	19	210
4A, LCH_4	58,968	∞	139.08	∞	1.0×10^{-4}	77	140	790
4B, LCH_4	5,896	∞	13.908	∞	1.5×10^{-4}	29	64	170
4A, JP-4	72,360	∞	92.77	∞	2.0×10^{-6}	175	895	160
4B, JP-4	7,236	∞	9.277	∞	2.0×10^{-6}	74	505	26.8
4A, Jet A	72,360	∞	92.77	∞	7.0×10^{-8}	406	4,790	28.2
4B, Jet A	7,236	∞	9.277	∞	7.0×10^{-8}	171	2,690	5.02

TABLE 25. - SCENARIO 4, RADIAL SPILL, SPREADING AND VAPORIZATION, FLAMES ABOVE

Scenario No., Fuel	m kg	$\dot{m}$ kg/sec	Q_0 m^3	$\dot{Q}_0$ m^3/sec	V_E m/sec	r_m m	t_m sec	$\dot{m}_{EVAP}$ kg/sec
4A, LH_2	21,600	∞	304.74	∞	6.0×10^{-3}	37	22	1,830
4A, LH_2	2,160	∞	30.474	∞	6.0×10^{-3}	16	12	330
4A, LCH_4	58,968	∞	139.08	∞	1.1×10^{-3}	43	43	2,560
4B, LCH_4	5,896	∞	13.908	∞	1.1×10^{-3}	18	24	465

vaporization for the Scenario 4A conventional fuel spills is greater than those above for the no flame condition, table 24, and for the flame condition, where experience shows burn times greater than an hour as representative of Scenario 4A spills of Jet A.

The above predictions of Scenarios 2 through 4 spills have shown that the extent of spread and time of vaporization is much less for the cryogenic fuels than the conventional fuels, in both the burning and no burning condition. Comparing the cryogenic fuels, the extent of the spread for LH_2 can be down to half as far, while the evaporation time can be one-fourth to one-half that of LCH_4. Hence, from the standpoint of minimum liquid spread and fast evaporation, liquid hydrogen is the safest fuel, presenting least hazard to the surroundings in event of a crash.

5.3 Gaseous Dispersion Results for Scenarios 2, 3 and 4

A complete listing of the gaseous dispersion results (for LH_2, LCH_4, and JP-4 fuels) for Scenarios 2, 3, and 4 is given in Appendix A. A summary of the results is presented in table 26. The significance of the results are discussed in this Section.

Scenario 2A is a small circular spill. The final time, downwind distance, and height above ground are listed for the different fuels in table 26 for comparison. The listing for the LH_2 case in Appendix A shows that both the buoyancy acceleration (column 5), and vertical speed of the puff rise from zero to maximum and then decrease. The overall angle of ascent is about 30°. The first entrainment speed (u_1 in column 10) also increases from zero to a maximum before decreasing, following its dependence on the relative velocity between the puff and the surrounding air. The second entrainment speed (u_s in column 11) decreases monotonically after its initial maximum because the volume dilution quickly reduces the creation of turbulence by the vigorous evaporation rate. The puff radius and thickness increase monotonically as the puff continually entrains air.

The next two sheets in Appendix A, a plot and listing for the methane case for Scenario 2A, show the LCH_4 puff lasts almost twice as long as the

TABLE 26. - GASEOUS DISPERSION SUMMARY FOR SCENARIOS 2, 3 AND 4

Scenario	Fuel	Final Time (seconds)	Downwind Distance (meters)	Height Above Ground (meters)
2A	LH_2	30	61	26
2A	LCH_4	54	42	5
2A	JP-4	206	63	0.05
2B	LH_2	42	80	52
2B	LCH_4	122	83	11
2B	JP-4	942 (16 min)	397	0.06
2C	LH_2	146	411	676
2C	LCH_4	1,624 (27 min)	713	72
2C	JP-4	11,736 (3.26 hr)	6,816	0.09
3A	LH_2	16	21	7
3A	LCH_4	11	10	1
3A	JP-4	412	321	0.23
3B	LH_2	21	31	12
3B	LCH_4	20	18	2
3B	JP-4	538 (9 min)	420	0.23
3C	LH_2	30	47	23
3C	LCH_4	40	21	1
3C	JP-4	216	142	0.14
4A	LH_2	173	512	782
4A	LCH_4	1,998 (33 min)	851	
4A	JP-4	17,318 (4.8 hr)	10.4 km	83
4B	LH_2	119	320	399
4B	LCH_4	831 (14 min)	404	46
4B	JP-4	3,211 (54 min)	1.6 km	0.07

hydrogen cane and travels along the ground for most of its lifetime. As entrainment continues, the initial negative buoyancy becomes slightly positive and lifts the puff a few meters off the ground. The listing shows how entrainment does not occur through the bottom of the puff when it travels along the ground. The general behavior of ascending hydrogen puffs and ground-level travel of methane puffs predicted by the model is supported by the liquid hydrogen tests conducted at White Sands (13) and the liquid natural gas tests conducted at China Lake (14).

The next plot and listing in Appendix A show how the JP-4 in Scenario 2A never rises off the ground because of its negative buoyancy. It travels slowly for a long time because it hugs the ground where the wind speed is very low. In fact, the power law wind profile requires that the wind speed go to zero right at the surface, a boundary condition usually imposed in all fluid flow models that have friction at the walls. There is also no contribution to entrainment from the second term because it is computed only if there is a vigorous evaporation rate. There is no mixing of air through the bottom surface because the JP-4 hugs the ground in stable air. The second line for time equal to 1 second in the Appendix A listing for JP-4 shows a slight decrease in the puff radius and half thickness before these puff dimensions monotonically increase. The initial decrease is not real, but results from computational error in the program. This error is small enough to neglect in assessing the model results.

There are no plots or listings for any Jet A cases because no flammable concentration is ever produced when the surface temperature is 294 K (70°F). Only if the surface temperature is increased to at least 314 to 322 K (105 - 120°F) can a flammable concentration be produced from the increased evaporation rate.

The results for Scenario 2B (for hydrogen) in Appendix A show how a bigger spill increases the trajectory time, dimensions (also see table 26), and ascent angle. The JP-4 puff for Scenario 2B lasts 16 minutes as it hugs the ground and slowly moves almost 400 meters.

The Scenario 2C for hydrogen shows the puff moving 575 meters above ground during a downwind travel of 411 meters. In comparison, the methane in Scenario 2C travels along the ground 713 meters and doesn't get off the ground except briefly just before it dilutes to its lowest flammable concentration. In the listing for this case in Appendix A the ascent angle of 85° at the one second time results from the vertical expansion of the puff before it starts moving downwind.

The JP-4 case for Scenario 2C shows that vapor from a large (143 m radius) spill of conventional fuel can theoretically move a long distance (6.8 km) downwind close to the ground for a long time (over 3 hours). In reality, the JP-4 vapor would disperse more quickly when it moved off the downwind end of the runway, which probably won't be longer than about 4 km (13,126 feet).

On an airport the trajectory of the flammable gaseous fuels in all cases would move towards incoming aircraft. Safety considerations would dictate that measures must be taken to prevent any aircraft from flying, or trying to land, through a cloud (many puffs) of any flammable gaseous fuel.

For the axial geometry Scenarios 3A, 3B, and 3C, the model follows a puff emanating from a spill of 1 meter unit axial length. The spill rates in Scenarios 3A and 3B are small enough to allow an aircraft to spill fuel over the entire length of runway. This might amount to 4000 unit spills, each starting with a 1-meter length, following each other downwind. In addition, for each unit length of spill there will be puffs that precede and follow this largest puff being tracked by the model.

Data for the hydrogen case for Scenario 4A in Appendix A shows the flammable puff moving off the ground in 20 seconds after spreading to 54.2 m radius. It persists for 173 sec. and during that time rises to 782 meters above ground before being diluted to less than 4 percent hydrogen. The rapid rise rate means the vapor cloud from a hydrogen spill will not endanger persons or property in the surrounding area in event of a catastrophic crash of a LH_2 fueled airplane. On the other hand, the methane in Scenario 4A moves along the ground for more than one-half hour to cover 851 meters, and it only rises off the ground during the last 1 to 2 minutes. The JP-4 gas puff could theoretically move 10.4 km downwind along the ground in almost

5 hours. However, after 4 km at most, it would move off the end of the runway onto grass, water, etc. Therefore, the boundary conditions will probably change dramatically, invalidating these computed distances and travel time. However, the potential exists for the flammable JP-4 cloud to move off airport property onto the land of other owners.

Plots of the movement and size of the puffs for each of the fuels are presented in figures 18 and 19. Figure 18 shows altitude versus drift distance with indications of elapsed time marked on the path of each of the fuels. Figure 19 illustrates the growth of the puff diameter as a function of time for all three fuels.

The hydrogen case for Scenario 4A was also run with each atmospheric stability class. As shown in table 27, from data in Appendix A, the puff rose least and traveled furthest downwind in the least time with stability classes 3 and 4 (C and D). The wind speed was at the maximum 5 m/s for both classes and its effect probably outweighed the effect of temperature profile, determined by the lapse rate.

The effect of relative humidity on the Scenario 4A LH_2 spill can be seen in the bottom part of table 27. More water vapor reduces the travel time and downwind distance monotonically but the maximum height is achieved by a puff rising through air with 50% relative humidity.

5.4 Heat Transfer to the Passenger Cabin

Consider an aircraft crash with a fuel spill beneath and flames around the fuselage, but with an intact and closed passenger cabin. For the various fuels considered in this study, what time period would be required for the flames to breach the cabin, or create a life threatening environment for the passengers in the cabin? In Section 4.4, a thermal model was described to compute the transient temperatures through the fuselage cabin wall cross section. The objective of this section is to present results of an analysis of this cabin wall model to estimate the survivability time for passengers inside the fuselage cabin imbedded in the flames of various fuels.

In order to compare the various fuels, the heat absorbed on the fuselage skin from the adjacent flames must be estimated. A large scale fuel spill

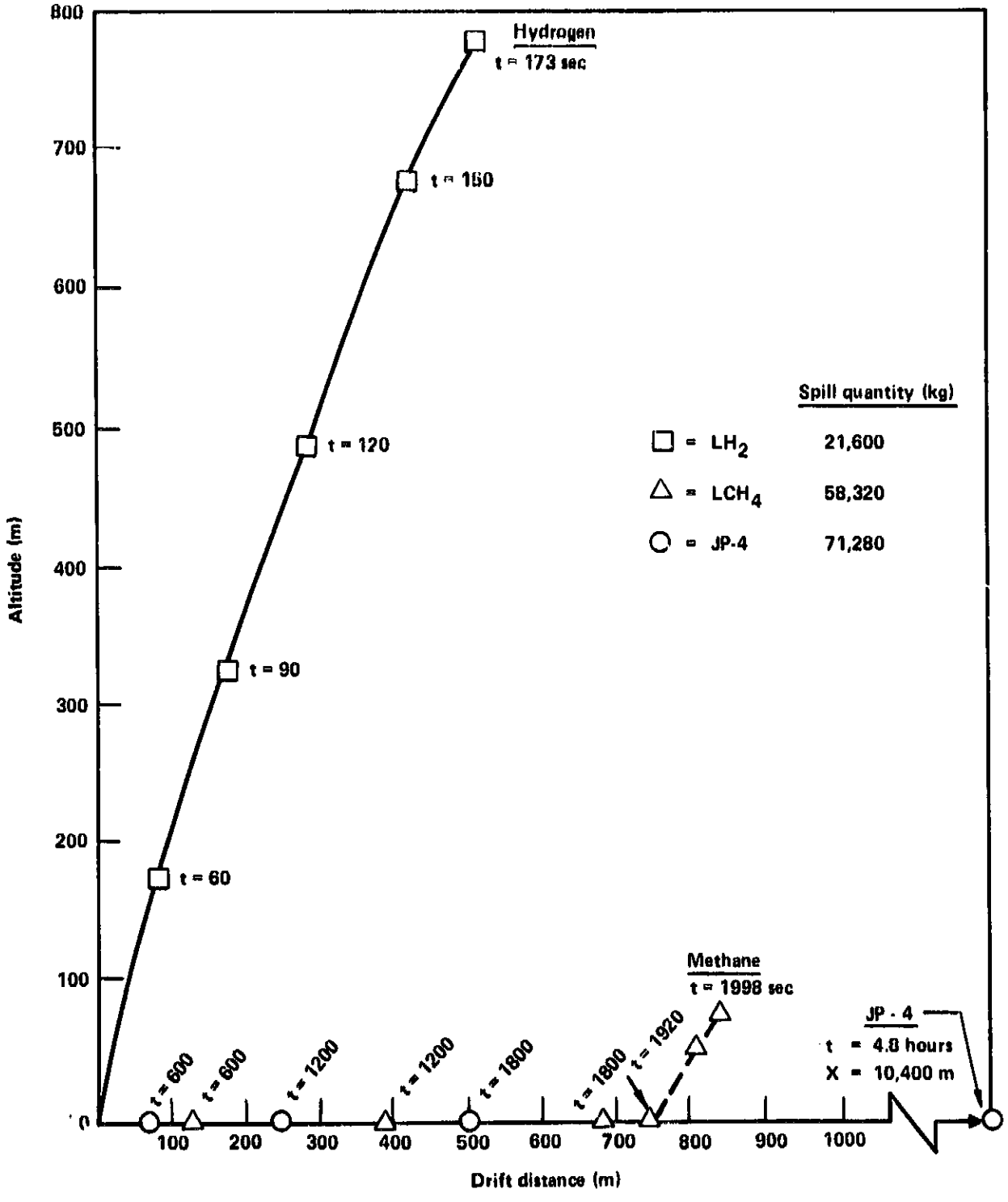

Figure 18. - Altitude vs. drift distance for flammable puffs of liquid hydrogen, liquid methane, and JP-4 (Scenario 4A, wind speed = 2 m/s).

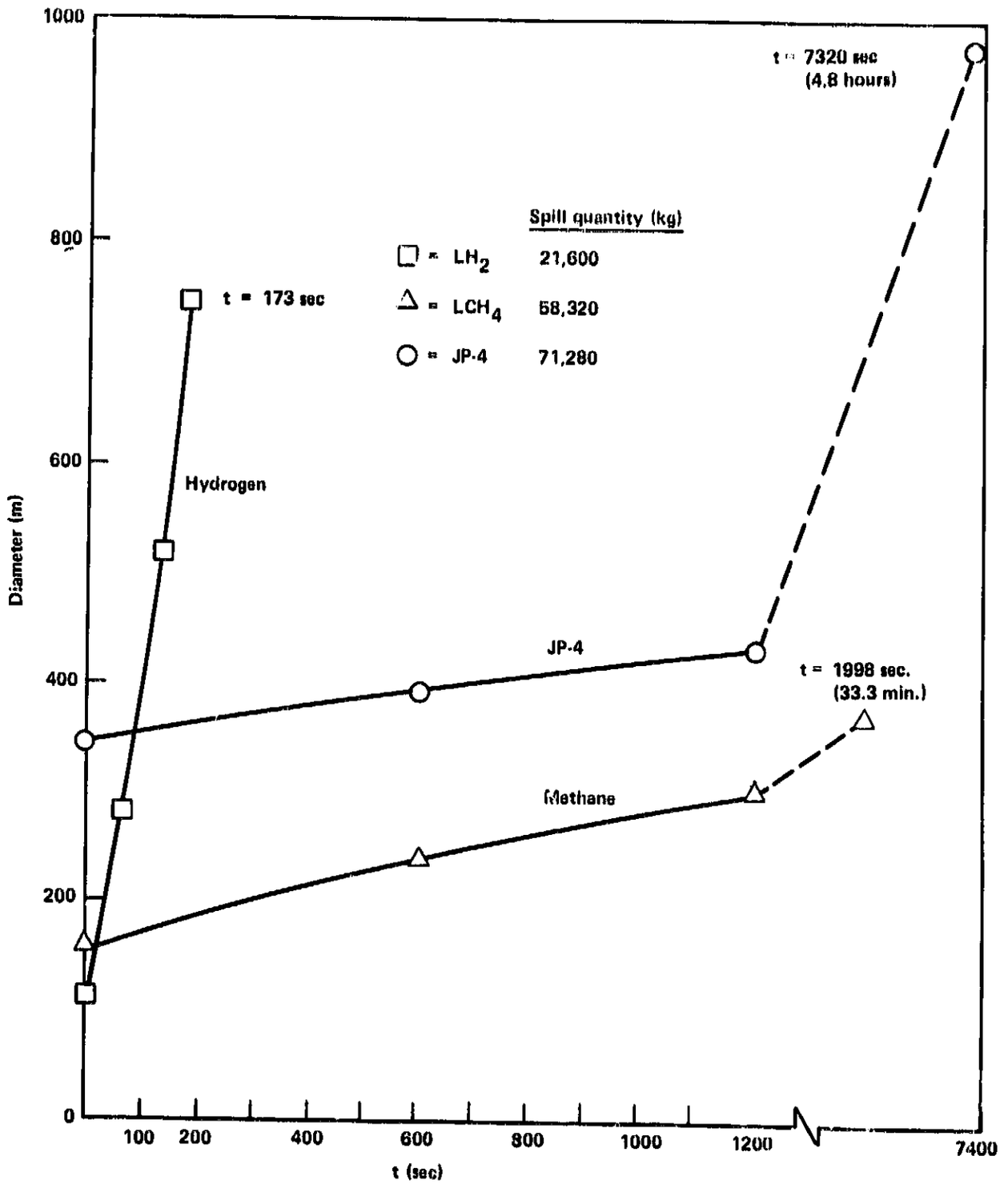

Figure 19. - Flammable puff diameter vs time for liquid hydrogen, liquid methane, and JP-4 (Scenario 4A, wind speed = 2 m/s).

TABLE 27. - GASEOUS DISPERSION RESULTS FOR DIFFERENT ATMOSPHERIC STABILITIES AND RELATIVE HUMIDITIES

Fuel = Hydrogen. Scenario 4A					
Stability	Relative Humidity (%)	Final Time (seconds)	Downwind Distance (meters)	Height Above Ground (meters)	Wind Speed (m/s)
6	50	173	512	782	2
5	50	148	580	537	3
4	50	119	703	347	5
3	50	119	702	344	5
2	50	153	635	557	3
1	50	186	536	739	2
6	0	267	842	763	2
6	25	222	684	774	2
6	50	173	512	782	2
6	75	151	431	770	2
6	100	138	357	718	2

was assumed which would result in a large scale pool burning. The fuselage was assumed to be directly imbedded in the flames, so that both radiation and convection heat transfer occur to the outer surface of the fuselage skin. The incident radiation heat flux from each of the large scale fuel flames can be taken from table 19. The radiation view factor from the vertical fuselage skin wall to the large scale flames should be ~0.5. Although the bare aluminum skin could have a low emissivity, ~0.1, a painted skin or one subjected to corrosive flames could have emissivity $\varepsilon \sim 0.9$, which was assumed in this analysis. Hence, the absorbed radiant heat flux on the fuselage skin q''_R, is shown on table 28 for the various fuels.

With flames next to the external fuselage skin, turbulent convection heat transfer will occur from the hot flames. The turbulent convection heat

TABLE 28. - ABSORBED FUSELAGE SKIN HEAT FLUX IN THE VARIOUS FLAMES

Fuel	q''_F kW/m^2	q''_R kW/m^2	q''_c kW/m^2	q'' kW/m^2
LH_2	189.4	85.2	31.8	117.0
LCH_4	229.6	103.3	27.2	130.5
JP-4	74.7	33.6	18.2	51.8
JET A	74.7	33.6	18.2	51.8

transfer coefficient, h, opposite the vertical fuselage skin wall, is estimated as $h \approx 23$ W/m^{2}K (4.0 Btu/hr ft^2 $^\circ$R). Using this heat transfer coefficient, the convective heat flux, q''_c, to the skin is shown on table 28 for each of the fuels. The estimated maximum heat flux absorbed by the skin, q", was then obtained by adding the absorbed radiant and convective heat fluxes, which yields the data in the last column of table 28.

The transient thermal model of the fuselage cabin wall, briefly described in Section 4.4, was run over a range of absorbed heat fluxes, q", on the fuselage skin. The solid curves of figure 20 show the outer fuselage wall temperature as a function of the absorbed heat fluxes labeled on those curves. Plotted as dashed lines on the same graph is the temperature response to the estimated maximum absorbed heat flux q" for each of the fuel flames considered in table 28. The dotted curve at the bottom of this graph shows the inner cabin wall temperature, which only rises one or two $^\circ$C (two to four $^\circ$F) over this short time span.

When the aluminum skin and stringer temperatures are in the range of 430°C (805°F) to 480°C (896°F), the fuselage should collapse due to its own weight. This fuselage collapse temperature band is shown in figure 20. Based upon the maximum expected absorbed heat fluxes from the various flames, the fuselage should collapse after ~40 seconds in a methane flame, and after ~50 seconds in hydrogen flame, and after ~120 seconds in a JP-4 or Jet A flame. The inner cabin wall temperature barely rises over short time spans, and hence this temperature is no threat to human survival.

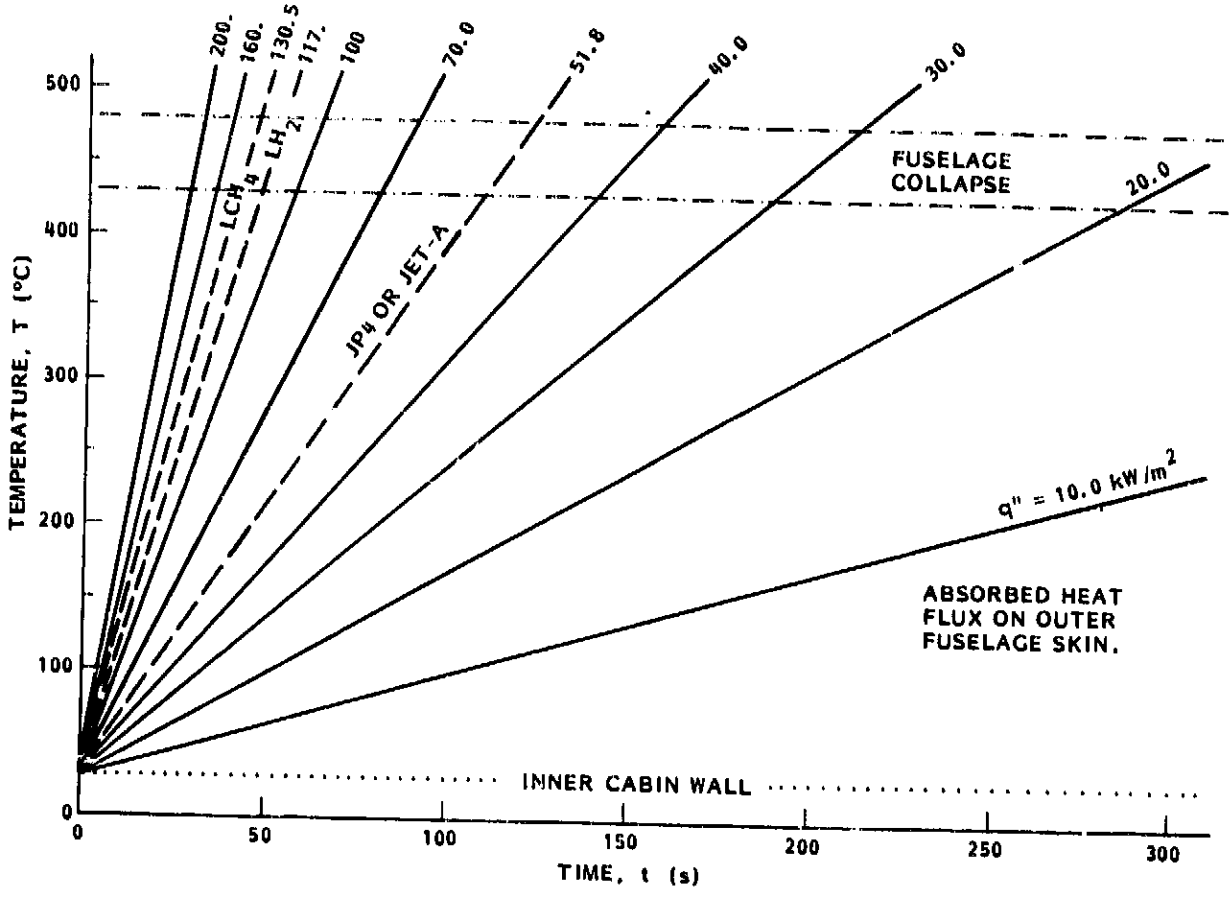

Figure 20. - Outer fuselage wall temperature in flames.

To evaluate the possibility of fuselage collapse in large scale spill flames, the expected burning times for Scenario 2C, 4A and 4B radial spills with flames above, as given in tables 21 and 25 were investigated. For LH_2, the fuselage collapse time is ~ 50 seconds, much greater than the largest predicted burn time of 22 seconds. For LCH_4, the fuselage collapse time is ~ 40 seconds, which is comparable to the largest predicted burn time of 43 seconds. For either JP-4 or JET A, the fuselage collapse time of ~ 120 seconds is much less than the expected conventional fuels burn times of approximately an hour. Hence, based upon this study of large scale fires, the fuselage structure should survive a hydrogen fire, be marginal for collapse in a methane fire, and should definitely collapse in JP-4 or JET A fire about the fuselage.

Although a thermal analysis was not done on the cabin windows, a few observations should be made. A good fraction of the high radiant heat flux from the flames would be transferred through the plastic windows, say ~50 kW/m^2. Since a radiant heat flux of ~10 kW/m^2 can cause skin burn within a few seconds exposure, the passengers would appear to be at risk to radiation burns through the windows, especially with the cryogenic fuel fires. Although the thermal capacity of window panes appears to be similar to that of the fuselage wall cross-section and only a fraction of the radiant heating will be absorbed by the window panes, the softening temperature of these plastic window panes should be in the range of 90°C (193°F) to 150°C (302°F). This low structural failure temperature of the window pane materials may mean that flames would breach the window panes before the fuselage would collapse. Hence, because of the possibilities of radiation skin burns through the window panes and structural collapse due to the low softening temperature of the plastic window panes, a transient thermal and radiation analysis should be done on the cabin windows and means of alleviating the high heat flux (such as reflective coatings on the outside surfaces of the window panes) investigated.

6. CONCLUSIONS

Conclusions reached as a result of this crash fire hazard study of various aircraft fuels are as follows:

1. Cryogenic fuels will be carried in fuselage tanks which inherently are more resistant to damage than is the rest of the fuselage.

2. Fuselage tanks for cryogenic fuels are less susceptible to damage which would result in spilled fuel than are tanks for conventional fuels which are located in the wing.

3. Tanks of conventionally-fueled aircraft are vented to the atmosphere; therefore a combustible mixture can exist inside the tanks. Cryogenic fuel tanks are pressurized with gaseous fuel. No oxygen is present within the tanks so there is no fire or explosion hazard. This represents added safety for cryogenic fuels.

4. The extent of spreading of the liquid fuels, and the time required for them to vaporize, varies inversely with the volatility of the various fuels. Ranking the fuels in the order of increasing vaporization time and extent of spread, for conditions both with and without flames above the pools, yields the following order: LH_2, LCH_4, JP-4, JET A.

5. The probability of fire in event of a survivable crash where fuel is spilled is quite high (greater than 80%), regardless of the type of fuel involved.

6. The ground level hazard to the surrounding community represented by spilled hydrogen in event of a crash where fire does not immediately result is dissipated within about 40 seconds in the worst case analyzed. Since a flammable cloud rises to a height of about 800 m, it poses a threat to low flying aircraft for a few minutes. With LCH_4 the ground level hazard would persist for more than half an hour and the flammable cloud would be blown 851 m before it is dissipated. It therefore poses a substantial threat to people, vehicles, and structures on the ground ir this area. The cloud of flammable vapor from the corresponding JP-4 spill never leaves the ground, persists for 4.8 hours, and theoretically could drift 10.4 km. Jet A and JP-4 vaporize by diffusion at the normal ambient temperature condition analyzed; however, Jet A does not have a high enough vapor pressure to form a combustible mixture at standard atmospheric conditions.

7. A fire resulting from crash of a LH_2-fueled aircraft will be very small in area and short in duration compared to other fuels. Passengers in LH_2 aircraft can probably best survive a crash fire by staying in their seats until the fire burns out (less than 30 seconds for the worst case studied). With all the other fuels a fire would require immediate evacuation of the fuselage.

8. Liquid drain holes and purge air flow will reduce the hazard of fires caused by small fuel leaks into aircraft compartments for both the cryogenic and conventional fuels.

9. Conventional gaussian dispersion models cannot be used to predict the time/space dynamics of gaseous hydrogen and methane originating from cryogenic liquids which disperse sometimes in less than one minute. Complex, expensive models using the partial differential equations of motion for a large number of 3-dimensional grid cells are unnecessarily detailed and expensive. The methodology of a numerical model developed for this study to solve the energy, mass and momentum conservation equations for individual puffs of gaseous fuel evaporated from the liquid spill has proved to be very satisfactory. Each puff is created during a time span of one second and it is followed at every one second interval until it is no longer flammable. For the subject study the model was run on the puff produced by the maximum evaporation rate from the spill when it has its maximum area. Any other puff can be followed. The model accounts for all thermodynamic processes of water vapor phase changes and sensible heat balance. Molecular diffusion is negligible compared to turbulent diffusion. Turbulent entrainment is modeled on the current understanding of the similar turbulent entrainment occuring in cumulus clouds.

10. Considering the spill, spreading, vaporization, dispersion, and burning phenomena of these fuels in the subject crash scenarios, liquid hydrogen (LH_2) fuel appears to offer many advantages when compared to LCH_4, JP-4, or JET A.

7. RECOMMENDATIONS FOR FUTURE WORK

The recommendations for future work relative to hazard comparisons of possible aircraft fuels can be divided into two categories; analytical studies and experimental tests.

7.1 Analytical Studies

1. Obtain stable solutions of the method of characteristics models of the spill, spreading and vaporization programs. These programs will provide more accurate, representative data for the design and performance prediction of the consequences of liquid spills.

2. Include heat transfer due to surface conduction, flame radiation and convection, atmospheric heat and mass convection, and thermal capacity effects in the liquid vaporization model.

3. Include flow resistance due to boiling in the liquid spreading model as it may significantly impede a cryogenic liquid spreading flow.

4. Calibrate the gaseous dispersion model with input conditions provided from NASA supported test spills of liquid hydrogen at White Sands (13), Arthur D. Little Co. spills of liquid hydrogen in 1958 (reference 12), and the LNG spill test program conducted by Lawrence Livermore National Laboratory at China Lake (14). The early calibration runs against the White Sands spills are not presented in this report because of lack of data on the actual test conditions. These calibration runs are critical to validating the model, although subjective agreement already exists between the model predictions and the movies of the test spills.

5. Run the gaseous dispersion model over different surface temperatures varying from 233K(-40°F) to 322K (120°F) and surface elevations varying from sea level up to 1.5 km (4922 ft), and wind speeds varying from dead calm to 30 m/s (approximately 60 mph).

6. Run the gaseous dispersion model for spills of fuel from storage tanks that contain much larger masses and have specific surrounding ground topography.

7. Extend the gaseous dispersion model to handle other hazardous or toxic substances like chlorine, hydrogen chloride and chemical warfare gases.

8. Perform analytical studies of the expected flame temperatures and flame emissivities of different fuel flames of various scale sizes to evaluate flame damage to the aircraft structure or surviving passengers in an expected crash scenario.

9. Develop an analytical model to predict the transmitted radiant heat flux and the transient temperatures of the cabin window panes to evaluate the hazards to passengers from flames outside the fuselage.

7.2 Experimental Tests

1. More cryogenic fuel spill tests, both burning and non-burning, would provide valuable experience and data to compare against analytical models of the spill spreading, vaporization and dispersion phenomena. The analytical models can be used to help design the tests. In addition, burning tests could provide experimental verification of flame temperatures and radiation fluxes from various size conflagrations. The spill tests should include both large "instantaneous" spills, and spills to simulate pipeline rupture where long durations are involved.

2. Some flow friction tests of a boiling cryogenic liquid spreading on a hot surface should be run to see if the boiling phenomena significantly impedes the liquid spread.

3. Tests of the radiant heat transmission, temperature rise, and structural failure temperatures should be run on cabin window panes and typical aircraft fuselage structure to evaluate the passenger hazards, especially with cryogenic fuel flames adjacent to the fuselage.

4. Crash tests of surplus aircraft with representative cryogenic tankage. This should be done to provide a basis for comparison with similar tests which have already been conducted by the FAA using surplus P2 aircraft with conventional fuels.

5. Demonstrate the effectiveness of purge systems to eliminate fire hazard in event of onboard fuel leaks, especially with the cryogenic fuels. Also, demonstrate the effectiveness of candidate systems to detect the presence of fuel leaks.

APPENDIX A

ANALYTICAL RESULTS OF THE AIRCRAFT FUEL GASEOUS DISPERSION MODEL

For each of the scenarios listed in table 29, there is a plot of altitude (Z) versus distance (X) of the trajectory of the largest puff. The time in seconds at which the gaseous fuel concentration drops below its lowest flammable limit is plotted at the end of the trajectory. Each plot shows the fuel, its lowest flammable mole fraction, circular spill radius or axial spill width in meters, wind speed at 10 meters height in meters per second, surface temperature in kelvin, and relative humidity (dimensionless).

Each plot is followed by a tabular listing of time, downwind distance of puff center, puff temperature, atmospheric temperature at puff height minus puff temperature, buoyancy acceleration, puff vertical speed, puff height above ground, overall angle of ascent of puff from starting point, puff volume, 3 entrainment speed terms, gaseous fuel mole fraction in puff, incremental entrainment volumes through puff sides, top and bottom, radius of circular puff, half thickness of puff, and the length and width of an axial puff.

The listing also contains the input conditions: the circular spill radius or the axial spill width in meters, the fuel, the surface elevation in meters above sea level, the evaporation rate in meters per second, the surface temperature in kelvin, the relative humidity, the atmospheric stability class number, the wind speed at 10 meters above the ground in meters per second, and the gaseous fuel lower flammable concentration expressed as a mole fraction.

All scenarios in this report were run at zero surface elevation (sea level) and surface temperature of 294°K. Also, all scenarios except for extra runs of Scenario 4A with LH_2 were run with the most stable atmosphere (class 6) and 50% relative humidity (= 0.5).

TABLE 29. - GASEOUS DISPERSION SCENARIOS ANALYZED

Scenario	Fuel	Maximum Radius (m)	Maximum Axial Width (m)	Evaporation Rate (m/s)	Comments
2A	LH_2	1	--	2.24×10^{-3}	
2A	LCH_4	1.3	--	6.06×10^{-4}	
2A	JP-4	18.5	--	2.00×10^{-6}	
2A	Jet A	99	--	7.00×10^{-8}	No flammable concentration
2B	LH_2	2	--	2.58×10^{-3}	
2B	LCH_4	3.4	--	4.08×10^{-4}	
2B	JP-4	40	--	2.00×10^{-6}	
2B	Jet A	212	--	7.00×10^{-8}	No flammable concentration
2C	LH_2	35	--	1.94×10^{-3}	
2C	LCH_4	61	--	1.11×10^{-4}	
2C	JP-4	143	--	2.00×10^{-6}	
2C	Jet A	331	--	7.00×10^{-8}	No flammable concentration
3A	LH_2	--	0.14	2.50×10^{-3}	
3A	LCH_4	--	0.12	1.06×10^{-3}	
3A	JP-4	--	1.18	2.00×10^{-6}	
3A	Jet A	--	4.52	7.00×10^{-8}	No flammable concentration
3B	LH_2	--	0.34	2.50×10^{-3}	
3B	LCH_4	--	0.32	9.87×10^{-4}	
3B	JP-4	--	2.94	2.00×10^{-6}	
3B	Jet A	--	11.28	7.00×10^{-8}	No flammable concentration
3C	LH_2	--	12.4	2.51×10^{-3}	
3C	LCH_4	--	20	2.30×10^{-4}	
3C	JP-4	--	106	2.00×10^{-6}	
3C	Jet A	--	406	7.00×10^{-8}	No flammable concentration
4A	LH_2	49	--	1.94×10^{-3}	
4A	LCH_4	77	--	1.00×10^{-4}	
4A	JP-4	175	--	2.00×10^{-6}	
4A	Jet A	406	--	7.00×10^{-8}	No flammable concentration
4B	LH_2	20	--	2.36×10^{-3}	
4B	LCH_4	29	--	1.62×10^{-4}	
4B	JP-4	74	--	2.00×10^{-6}	
4B	Jet A	171	--	7.00×10^{-8}	No flammable concentration

In addition to the above, the last two series of computer results listed in Appendix A are for the following cases involving Scenario 4A with LH_2 fuel:

- Six cases, all identical, except for variations of atmospheric stability. The runs are listed in order of class as follows: 6, 5, 4, 3, 2, and 1.

- Five cases, all identical, except for variations of relative humidity. The runs appear in order; 0, 25, 50, 75 and 100 percent.

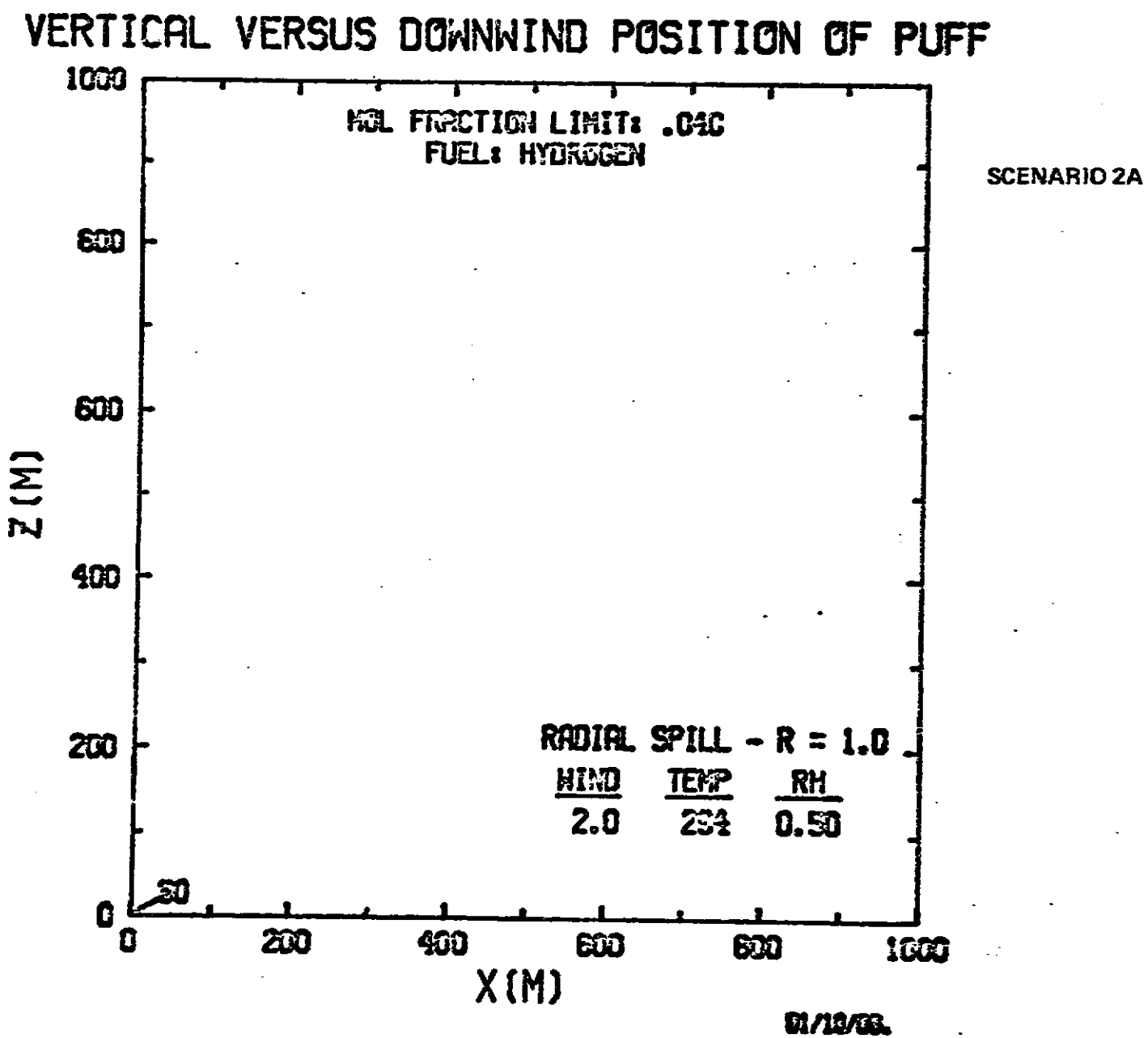
VERTICAL VERSUS DOWNWIND POSITION OF PUFF
MOL FRACTION LIMIT: .04C
FUEL: HYDROGEN
SCENARIO 2A
RADIAL SPILL - R = 1.0
WIND TEMP RH
2.0 294 0.50
Z(M)
X(M)
0
200
400
600
800
1000
01/10/88.

LOOKING AT LARGEST PUFF ONLY

SCENARIO 2A

INITIAL CONDITIONS

RADIAL SPILL - RADIUS: 1.0 FUEL: HYDROGEN SURFACE ELEVATION: 0.

EVAPORATION RATE: 2.240E-3 TEMP: 294 RELATIVE HUMIDITY: .50

STABILITY: 6 WIND: 2.0 M/S FMF LOWER LIMIT: .040

IT	XP	T	DELTEN	A	U	ZP	ANG	VP	U1	U2	U4	FMF	VES	VET	VEB	R	ZTZP	LL	LW
	M	K	K	M/S^2	M/S	M	DEG	CU.M	M/S	M/S	M/S		CU.M	CU.M	CU.M	M	M	M	M
0	0.	20.3	0.0	0.00	0.0	.06	0.	.371E+00	0.000	0.000	0.000	1.000	0.00	0.00	0.00	1.0	.06	0.00	0.00
1	0.	30.5	263.5	1.13	.2	.16	34.	.635E+00	.039	.118	0.000	.975	.15	0.00	0.00	1.2	.07	0.00	0.00
2	1.	48.2	245.8	2.13	.5	.51	33.	.105E+01	.083	.069	0.000	.930	.16	.07	.07	1.4	.08	0.00	0.00
3	2.	73.0	221.0	2.42	.7	1.09	35.	.172E+01	.093	.042	0.000	.861	.20	.16	.16	1.7	.10	0.00	0.00
4	3.	101.2	192.9	2.14	.8	1.82	35.	.267E+01	.103	.025	0.000	.771	.26	.27	.27	1.9	.11	0.00	0.00
5	4.	129.1	164.9	1.77	.8	2.61	34.	.389E+01	.107	.016	0.000	.675	.34	.38	.38	2.2	.13	0.00	0.00
6	5.	154.4	139.6	1.45	.8	3.42	34.	.538E+01	.108	.011	0.000	.583	.42	.49	.49	2.4	.14	0.00	0.00
7	7.	176.3	117.7	1.22	.8	4.24	33.	.715E+01	.108	.008	0.000	.502	.50	.58	.58	2.7	.16	0.00	0.00
8	8.	195.0	99.1	1.05	.8	5.08	32.	.919E+01	.108	.006	0.000	.431	.60	.68	.68	2.9	.17	0.00	0.00
9	10.	210.7	83.3	.93	.8	5.92	32.	.115E+02	.108	.005	0.000	.371	.70	.77	.77	3.1	.18	0.00	0.00
10	11.	224.1	69.9	.85	.9	6.76	31.	.142E+02	.109	.004	0.000	.321	.81	.86	.86	3.3	.20	0.00	0.00
11	13.	235.5	58.6	.80	.9	7.62	31.	.172E+02	.110	.003	0.000	.279	.93	.95	.95	3.5	.21	0.00	0.00
12	15.	245.2	48.9	.76	.9	8.49	30.	.205E+02	.111	.003	0.000	.243	1.06	1.05	1.05	3.8	.22	0.00	0.00
13	16.	253.4	40.7	.73	.9	9.38	30.	.242E+02	.113	.002	0.000	.213	1.20	1.16	1.16	4.0	.23	0.00	0.00
14	18.	260.4	33.7	.70	.9	10.29	30.	.284E+02	.114	.002	0.000	.187	1.36	1.27	1.27	4.2	.25	0.00	0.00
15	20.	266.5	27.6	.69	.9	11.21	29.	.329E+02	.116	.002	0.000	.165	1.53	1.39	1.39	4.4	.26	0.00	0.00
16	22.	271.8	22.4	.67	1.0	12.15	29.	.380E+02	.119	.001	0.000	.146	1.72	1.51	1.51	4.6	.27	0.00	0.00
17	24.	275.2	18.9	.62	1.0	13.11	29.	.434E+02	.121	.001	0.000	.129	1.93	1.65	1.65	4.8	.28	0.00	0.00
18	26.	279.3	14.8	.62	1.0	14.09	29.	.494E+02	.123	.001	0.000	.115	2.13	1.77	1.77	5.0	.30	0.00	0.00
19	28.	282.9	11.3	.62	1.0	15.09	29.	.560E+02	.125	.001	0.000	.103	2.36	1.91	1.91	5.2	.31	0.00	0.00
20	30.	284.0	10.1	.55	1.0	16.10	29.	.627E+02	.128	.001	0.000	.092	2.62	2.06	2.06	5.4	.32	0.00	0.00
21	32.	285.0	9.1	.49	1.0	17.11	28.	.700E+02	.129	.001	0.000	.083	2.84	2.19	2.19	5.6	.33	0.00	0.00
22	34.	285.9	8.3	.44	1.0	18.12	28.	.776E+02	.129	.001	0.000	.075	3.05	2.30	2.30	5.8	.34	0.00	0.00
23	36.	286.6	7.5	.40	1.0	19.13	28.	.856E+02	.128	.001	0.000	.068	3.24	2.39	2.39	6.0	.36	0.00	0.00
24	38.	287.3	6.9	.36	1.0	20.12	28.	.940E+02	.127	.001	0.000	.062	3.43	2.48	2.48	6.2	.37	0.00	0.00
25	40.	287.9	6.4	.33	1.0	21.10	28.	.103E+03	.126	.000	0.000	.057	3.61	2.56	2.56	6.4	.38	0.00	0.00
26	42.	288.4	5.9	.30	1.0	22.07	28.	.112E+03	.124	.000	0.000	.053	3.78	2.63	2.63	6.6	.39	0.00	0.00
27	44.	288.8	5.4	.27	1.0	23.03	28.	.121E+03	.123	.000	0.000	.049	3.95	2.69	2.69	6.8	.40	0.00	0.00
28	46.	289.2	5.1	.25	.9	23.97	27.	.131E+03	.121	.000	0.000	.045	4.11	2.75	2.75	6.9	.41	0.00	0.00
29	48.	289.5	4.7	.23	.9	24.90	27.	.141E+03	.119	.000	0.000	.042	4.27	2.81	2.81	7.1	.42	0.00	0.00
30	51.	289.8	4.4	.22	.9	25.82	27.	.151E+03	.118	.000	0.000	.039	4.42	2.87	2.87	7.3	.43	0.00	0.00

VERTICAL VERSUS DOWNWIND POSITION OF PUFF

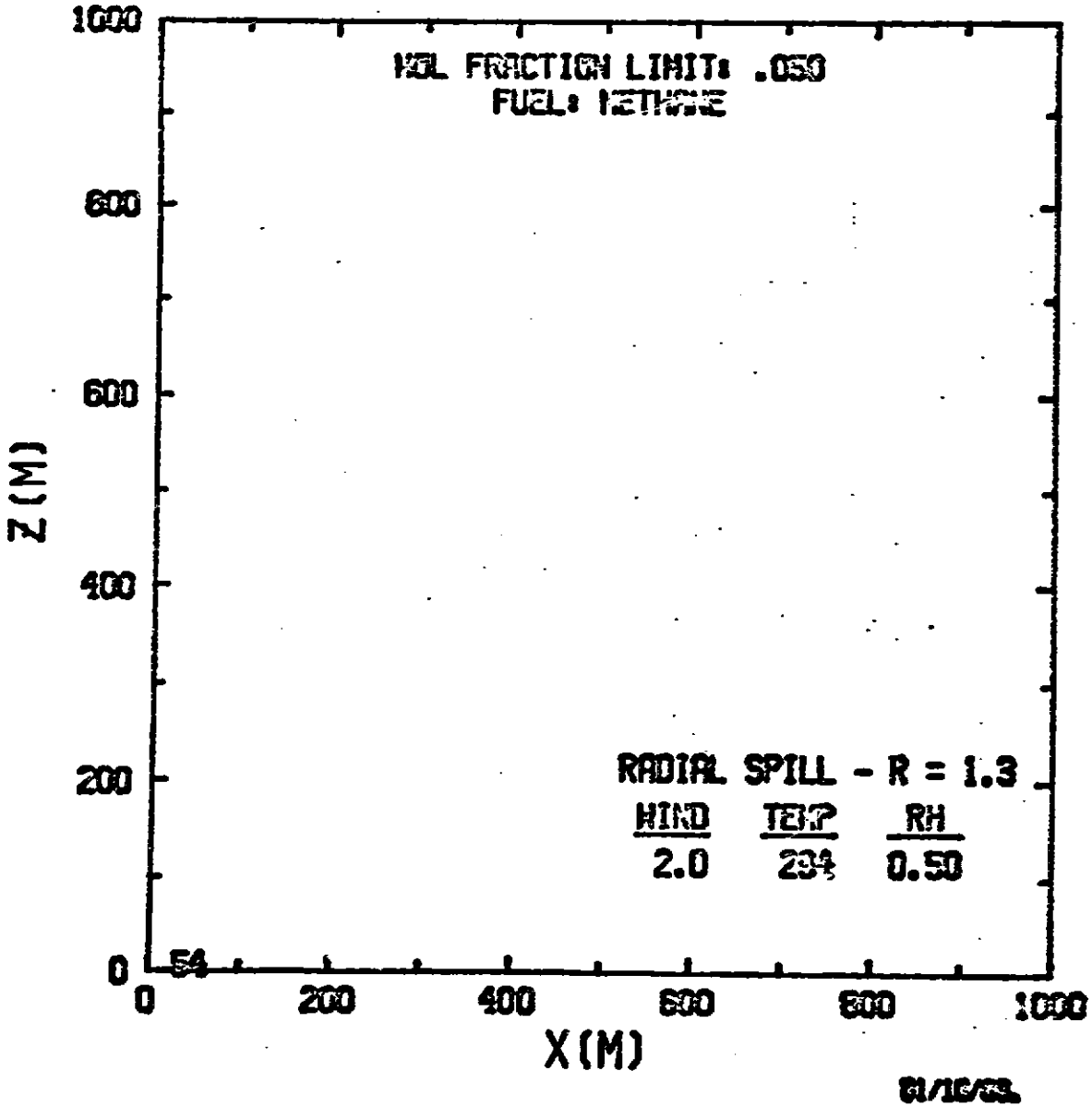

LOOKING AT LARGEST PUFF ONLY

INITIAL CONDITIONS

SCENARIO 2A

RADIAL SPILL - RADIUS: 1.3 FUEL: METHANE SURFACE ELEVATION: 0.

EVAPORATION RATE: 6.060E-4 TEMP: 294 RELATIVE HUMIDITY: .50

STABILITY: 6 WIND: 2.0 M/S FMF LOWER LIMIT: .050

IT	XP M	T K	DELTEM K	A	W M/S	ZP M	ANG DEG	VP CU.M	U1 M/S	U2 M/S	U4 M/S	FMF	VES CU.M	VET CU.M	VEB CU.M	R M	ZTZP M	LL M	LW M
0	0.	111.7	0.0	0.00	0.0	.07	0.	.741E+00	0.000	0.000	0.000	1.000	0.00	0.00	0.00	1.3	.07	0.00	0.00
1	0.	132.4	161.6	-2.50	0.0	.08	29.	.104E+01	.092	.140	0.000	.886	.26	0.00	0.00	1.5	.08	0.00	0.00
2	0.	151.7	142.3	-2.03	0.0	.09	12.	.135E+01	.076	.099	0.000	.782	.25	.06	0.00	1.6	.08	0.00	0.00
4	1.	181.4	112.6	-1.41	0.0	.10	5.	.202E+01	.065	.061	0.000	.625	.23	.11	0.00	1.8	.10	0.00	0.00
6	2.	201.5	92.5	-1.05	0.0	.11	3.	.270E+01	.043	.044	0.000	.520	.21	.12	0.00	2.0	.11	0.00	0.00
8	3.	216.0	78.0	-.80	0.0	.11	2.	.337E+01	.036	.034	0.000	.447	.20	.12	0.00	2.1	.11	0.00	0.00
10	4.	227.0	67.0	-.62	0.0	.12	2.	.403E+01	.031	.028	0.000	.393	.19	.12	0.00	2.3	.12	0.00	0.00
12	6.	235.5	58.5	-.49	0.0	.13	1.	.467E+01	.028	.024	0.000	.352	.19	.11	0.00	2.4	.13	0.00	0.00
14	7.	242.4	51.6	-.38	0.0	.13	1.	.530E+01	.026	.021	0.000	.319	.19	.11	0.00	2.5	.13	0.00	0.00
16	8.	248.0	46.0	-.29	0.0	.14	1.	.592E+01	.024	.018	0.000	.292	.18	.11	0.00	2.6	.14	0.00	0.00
18	9.	252.6	41.4	-.22	0.0	.14	1.	.653E+01	.022	.017	0.000	.270	.18	.11	0.00	2.7	.14	0.00	0.00
20	11.	256.5	37.5	-.17	0.0	.15	1.	.713E+01	.021	.015	0.000	.251	.18	.11	0.00	2.7	.15	0.00	0.00
22	12.	259.9	34.1	-.12	0.0	.15	1.	.772E+01	.020	.014	0.000	.235	.18	.10	0.00	2.8	.15	0.00	0.00
24	14.	262.9	31.1	-.08	0.0	.15	1.	.830E+01	.019	.013	0.000	.221	.18	.10	0.00	2.9	.15	0.00	0.00
26	15.	265.5	28.5	-.04	0.0	.16	1.	.888E+01	.018	.012	0.000	.209	.17	.10	0.00	2.9	.16	0.00	0.00
28	17.	267.8	26.2	-.01	0.0	.16	1.	.946E+01	.018	.011	0.000	.198	.17	.10	0.00	3.0	.16	0.00	0.00
30	18.	269.9	24.1	.02	.0	.17	1.	.100E+02	.017	.011	0.000	.188	.17	.10	0.00	3.1	.16	0.00	0.00
32	20.	272.6	21.4	.06	.0	.20	1.	.108E+02	.018	.010	0.000	.176	.18	.10	.10	3.1	.17	0.00	0.00
34	21.	274.2	19.8	.06	.0	.28	1.	.117E+02	.023	.009	0.000	.163	.22	.12	.12	3.2	.17	0.00	0.00
36	23.	277.2	16.8	.10	.1	.41	1.	.129E+02	.030	.008	0.000	.150	.28	.15	.15	3.3	.18	0.00	0.00
38	24.	280.5	13.5	.15	.1	.64	2.	.144E+02	.039	.008	0.000	.136	.36	.20	.20	3.5	.19	0.00	0.00
40	26.	284.0	10.1	.20	.2	1.00	2.	.164E+02	.049	.007	0.000	.121	.47	.26	.26	3.6	.19	0.00	0.00
42	28.	285.2	8.8	.18	.3	1.48	3.	.188E+02	.059	.006	0.000	.106	.60	.34	.34	3.8	.20	0.00	0.00
44	30.	286.3	7.7	.15	.3	2.05	4.	.216E+02	.065	.005	0.000	.092	.71	.41	.41	4.0	.21	0.00	0.00
46	32.	287.3	6.7	.13	.3	2.67	5.	.252E+02	.069	.004	0.000	.080	.81	.48	.48	4.2	.22	0.00	0.00
48	34.	288.2	5.9	.11	.3	3.32	6.	.291E+02	.070	.004	0.000	.069	.90	.55	.55	4.4	.23	0.00	0.00
50	37.	288.9	5.1	.10	.3	3.98	6.	.334E+02	.070	.003	0.000	.060	.98	.60	.60	4.6	.24	0.00	0.00
52	39.	289.5	4.5	.08	.3	4.64	7.	.380E+02	.069	.003	0.000	.053	1.05	.65	.65	4.9	.26	0.00	0.00
54	42.	290.0	4.0	.07	.3	5.29	7.	.430E+02	.068	.003	0.000	.047	1.12	.70	.70	4.9	.27	0.00	0.00

VERTICAL VERSUS DOWNWIND POSITION OF PUFF

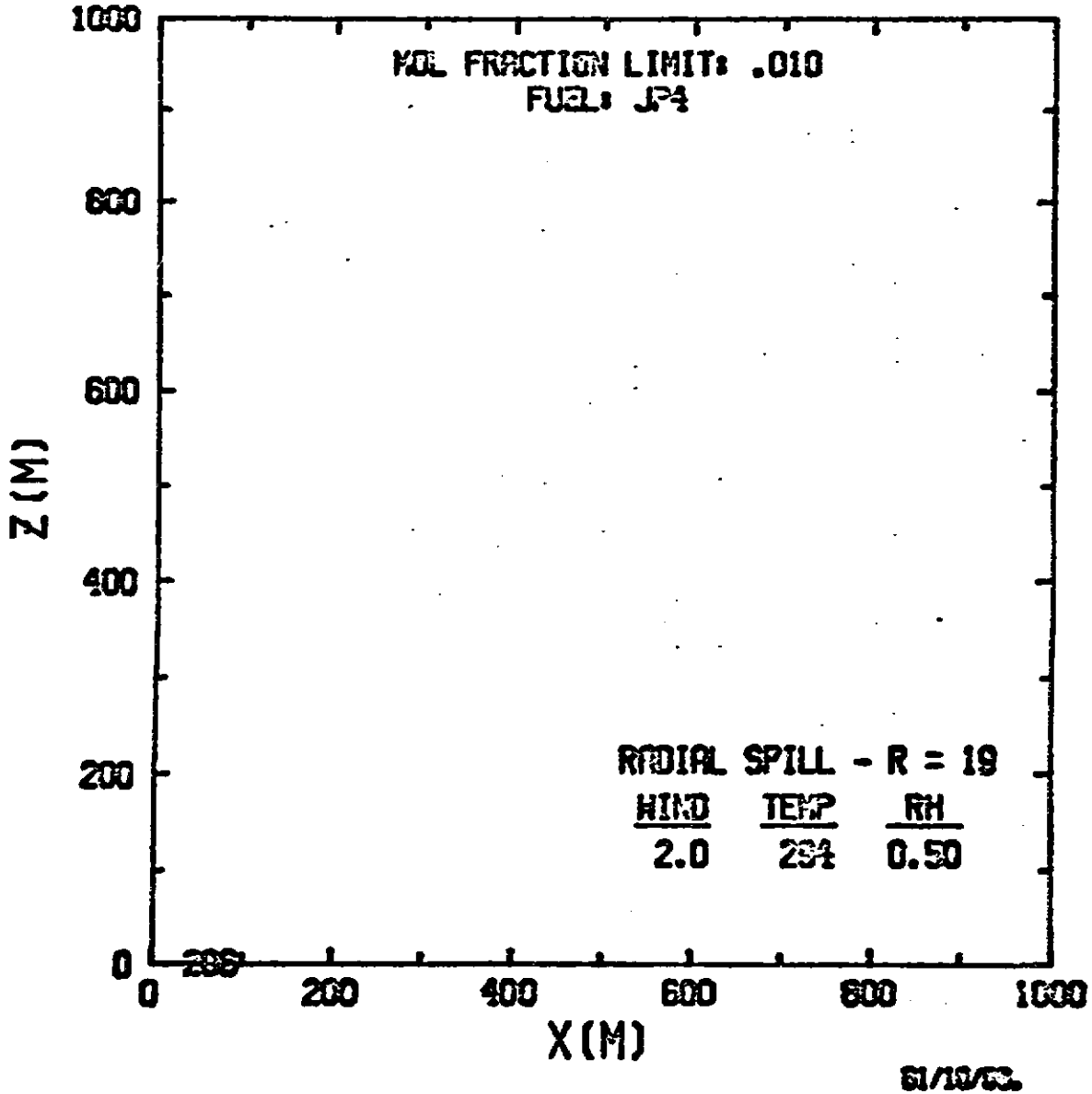

SCENARIO 2A

01/10/83

LOOKING AT LARGEST PUFF ONLY

INITIAL CONDITIONS

SCENARIO 2A

RADIAL SPILL - RADIUS: 18.5 FUEL: JP4 SURFACE ELEVATION: 0.

EVAPORATION RATE: 2.000E-6 TEMP: 294 RELATIVE HUMIDITY: .50

STABILITY: 6 WIND: 2.0 M/S FMF LOWER LIMIT: .010

IT	XP M	T K	DELTEM K	A	W M/S	ZP M	ANG DEG	VP CU.M	U1 M/S	U2 M/S	U4 M/S	FMF	VES CU.M	VET CU.M	VEB CU.M	R M	ZTZP M	LL M	LW M
0	0.	294.0	0.0	0.00	0.0	.04	0.	.752E+02	0.000	0.000	0.000	.109	0.00	0.00	0.00	18.5	.04	0.00	0.00
1	0.	294.0	-.0	-2.32	-.6	.03	83.	.763E+02	.080	0.000	0.000	.106	.65	0.00	0.00	18.1	.03	0.00	0.00
10	0.	294.0	.0	-1.90	0.0	.03	8.	.811E+02	.075	0.000	0.000	.082	.60	.08	0.00	18.4	.03	0.00	0.00
20	1.	294.0	.0	-1.56	0.0	.04	2.	.873E+02	.070	0.000	0.000	.064	.59	.17	0.00	18.9	.04	0.00	0.00
30	2.	294.0	.0	-1.30	0.0	.04	1.	.945E+02	.066	0.000	0.000	.052	.58	.24	0.00	19.4	.04	0.00	0.00
40	3.	294.0	.0	-1.11	0.0	.04	1.	.102E+03	.061	0.000	0.000	.044	.57	.31	0.00	19.9	.04	0.00	0.00
50	5.	294.0	.0	-.96	0.0	.04	0.	.111E+03	.057	0.000	0.000	.037	.57	.36	0.00	20.4	.04	0.00	0.00
60	7.	294.0	.0	-.84	0.0	.04	0.	.120E+03	.054	0.000	0.000	.032	.56	.40	0.00	21.0	.04	0.00	0.00
70	10.	294.0	.0	-.74	0.0	.04	0.	.130E+03	.050	0.000	0.000	.028	.55	.44	0.00	21.5	.04	0.00	0.00
80	13.	294.0	.0	-.67	0.0	.04	0.	.139E+03	.047	0.000	0.000	.025	.54	.47	0.00	22.0	.04	0.00	0.00
90	16.	294.0	.0	-.60	0.0	.04	0.	.149E+03	.045	0.000	0.000	.022	.54	.49	0.00	22.5	.04	0.00	0.00
100	19.	294.0	.0	-.55	0.0	.04	0.	.160E+03	.042	0.000	0.000	.020	.53	.51	0.00	23.0	.04	0.00	0.00
110	22.	294.0	.0	-.50	0.0	.04	0.	.170E+03	.040	0.000	0.000	.018	.52	.52	0.00	23.5	.04	0.00	0.00
120	26.	294.0	.0	-.46	0.0	.05	0.	.180E+03	.038	0.000	0.000	.017	.52	.53	0.00	24.0	.05	0.00	0.00
130	30.	294.0	.0	-.43	0.0	.05	0.	.191E+03	.036	0.000	0.000	.016	.51	.54	0.00	24.4	.05	0.00	0.00
140	34.	294.0	.0	-.40	0.0	.05	0.	.201E+03	.035	0.000	0.000	.015	.51	.55	0.00	24.9	.05	0.00	0.00
150	38.	294.0	.0	-.38	0.0	.05	0.	.212E+03	.033	0.000	0.000	.014	.51	.55	0.00	25.3	.05	0.00	0.00
160	43.	294.0	.0	-.36	0.0	.05	0.	.222E+03	.032	0.000	0.000	.013	.50	.56	0.00	25.7	.05	0.00	0.00
170	47.	294.0	.0	-.34	0.0	.05	0.	.233E+03	.031	0.000	0.000	.012	.50	.56	0.00	26.1	.05	0.00	0.00
180	51.	294.0	.0	-.32	0.0	.05	0.	.243E+03	.030	0.000	0.000	.011	.50	.56	0.00	26.5	.05	0.00	0.00
190	56.	294.0	.0	-.30	0.0	.05	0.	.254E+03	.029	0.000	0.000	.011	.50	.56	0.00	26.8	.05	0.00	0.00
200	60.	294.0	.0	-.29	0.0	.05	0.	.264E+03	.028	0.000	0.000	.010	.49	.56	0.00	27.2	.05	0.00	0.00
206	63.	294.0	.0	-.28	0.0	.05	0.	.271E+03	.028	0.000	0.000	.010	.49	.56	0.00	27.4	.05	0.00	0.00

VERTICAL VERSUS DOWNWIND POSITION OF PUFF

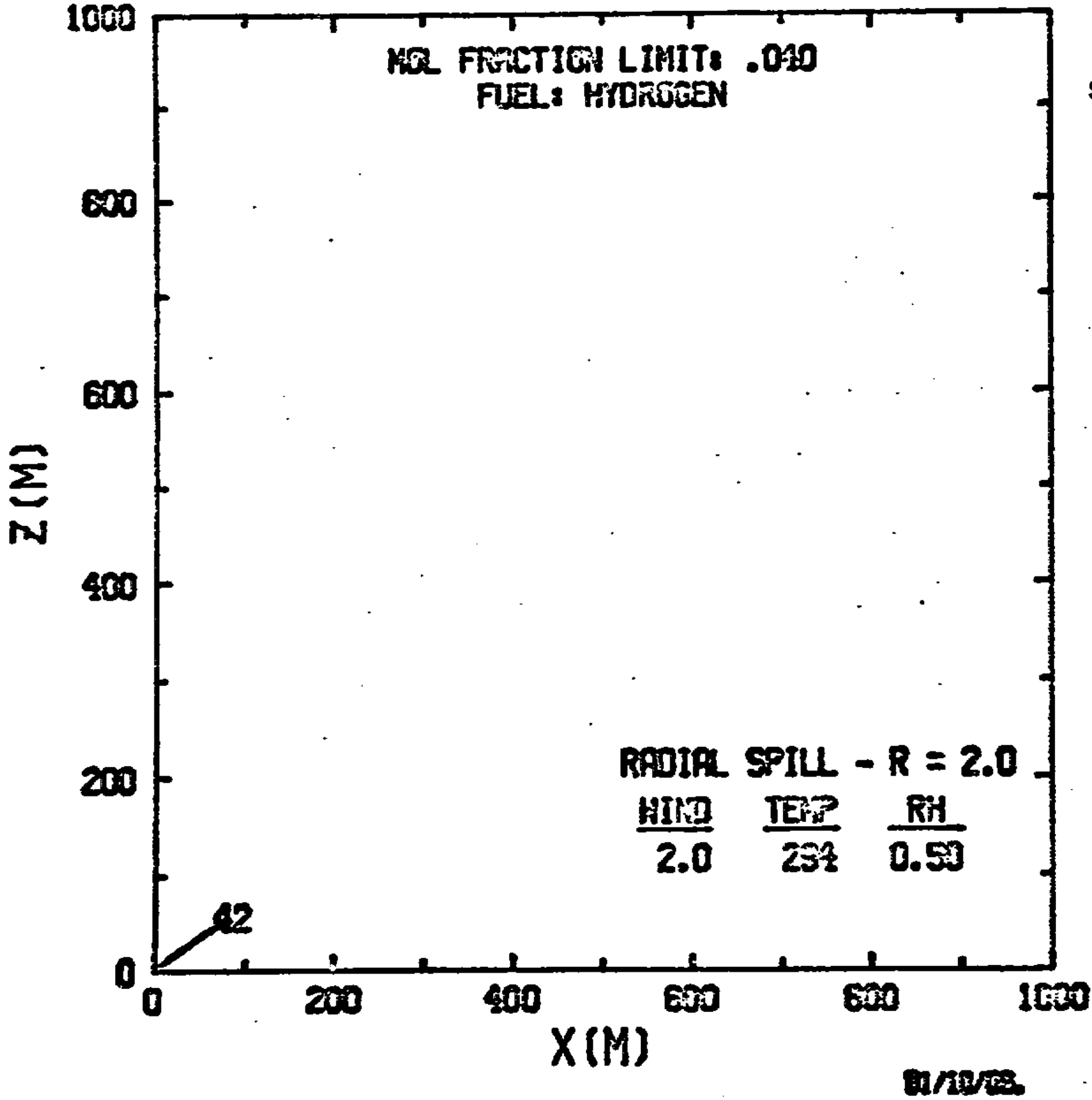

SCENARIO 2B

LOOKING AT LARGEST PUFF ONLY

INITIAL CONDITIONS

SCENARIO 2B

RADIAL SPILL - RADIUS: 2.0 FUEL: HYDROGEN SURFACE ELEVATION: 0.

EVAPORATION RATE: 2.580E-3 TEMP: 294 RELATIVE HUMIDITY: .50

STABILITY: 6 WIND: 2.0 M/S FMF LOWER LIMIT: .040

IT	XP M	T K	DELTEN K	A	U M/S	ZP M	ANG DEG	VP CU.M	U1 M/S	U2 M/S	U4 M/S	FMF	VES CU.M	VET CU.M	VEB CU.M	R M	ZTZP M	LL M	LW M
0	0.	20.3	0.0	0.00	0.0	.07	0.	.171E+01	0.000	0.000	0.000	1.000	0.00	0.00	0.00	2.0	.07	0.00	0.00
1	0.	26.0	268.0	.69	.1	.14	44.	.247E+01	.091	.136	0.000	.986	.39	0.00	0.00	2.2	.08	0.00	0.00
2	0.	34.1	259.9	1.41	.4	.41	41.	.330E+01	.089	.094	0.000	.966	.39	.09	.09	2.5	.09	0.00	0.00
4	2.	61.4	232.6	2.44	1.0	1.77	45.	.643E+01	.122	.051	0.000	.895	.56	.41	.41	3.1	.10	0.00	0.00
6	4.	100.8	193.2	2.14	1.2	3.94	45.	.122E+02	.153	.026	0.000	.772	.90	.96	.96	3.8	.13	0.00	0.00
8	7.	141.0	153.0	1.62	1.2	6.36	43.	.209E+02	.159	.014	0.000	.632	1.29	1.51	1.51	4.5	.15	0.00	0.00
10	10.	174.7	119.4	1.23	1.2	8.82	42.	.323E+02	.159	.009	0.000	.507	1.71	1.99	1.99	5.2	.18	0.00	0.00
12	13.	201.3	92.8	1.00	1.2	11.29	40.	.463E+02	.158	.006	0.000	.407	2.17	2.43	2.43	5.9	.20	0.00	0.00
14	17.	222.1	72.1	.86	1.2	13.77	39.	.635E+02	.158	.004	0.000	.329	2.68	2.86	2.86	6.5	.22	0.00	0.00
16	21.	238.4	55.7	.78	1.3	16.28	38.	.834E+02	.159	.003	0.000	.269	3.26	3.31	3.31	7.2	.24	0.00	0.00
18	25.	251.4	42.8	.74	1.3	18.83	37.	.107E+03	.162	.002	0.000	.221	3.91	3.80	3.80	7.8	.26	0.00	0.00
20	29.	261.6	32.6	.70	1.3	21.45	37.	.134E+03	.165	.002	0.000	.183	4.67	4.33	4.33	8.4	.29	0.00	0.00
22	33.	269.9	24.3	.68	1.4	24.14	36.	.166E+03	.170	.002	0.000	.153	5.52	4.91	4.91	9.0	.31	0.00	0.00
24	38.	275.4	18.9	.62	1.4	26.89	36.	.201E+03	.174	.001	0.000	.129	6.42	5.49	5.49	9.6	.33	0.00	0.00
26	42.	281.1	13.2	.62	1.4	29.71	35.	.241E+03	.177	.001	0.000	.109	7.43	6.11	6.11	10.2	.35	0.00	0.00
28	47.	284.3	10.0	.57	1.5	32.60	35.	.286E+03	.183	.001	0.000	.093	8.60	6.80	6.80	10.8	.37	0.00	0.00
30	51.	285.7	8.7	.48	1.5	35.53	35.	.334E+03	.184	.001	0.000	.080	9.65	7.38	7.38	11.3	.39	0.00	0.00
32	56.	286.8	7.6	.41	1.5	38.45	35.	.386E+03	.184	.001	0.000	.070	10.69	7.86	7.86	11.9	.40	0.00	0.00
34	61.	287.7	6.7	.36	1.4	41.33	34.	.441E+03	.182	.001	0.000	.061	11.45	8.27	8.27	12.4	.42	0.00	0.00
36	65.	288.4	6.0	.31	1.4	44.17	34.	.499E+03	.179	.000	0.000	.054	12.30	8.61	8.61	12.9	.44	0.00	0.00
38	70.	289.1	5.4	.28	1.4	46.95	34.	.561E+03	.175	.000	0.000	.049	13.07	8.92	8.92	13.4	.46	0.00	0.00
40	75.	289.6	4.9	.25	1.3	49.67	33.	.624E+03	.172	.000	0.000	.044	13.79	9.19	9.19	13.9	.47	0.00	0.00
42	80.	290.0	4.5	.22	1.3	52.35	33.	.691E+03	.169	.000	0.000	.040	14.49	9.43	9.43	14.4	.49	0.00	0.00

VERTICAL VERSUS DOWNWIND POSITION OF PUFF

SCENARIO 2B

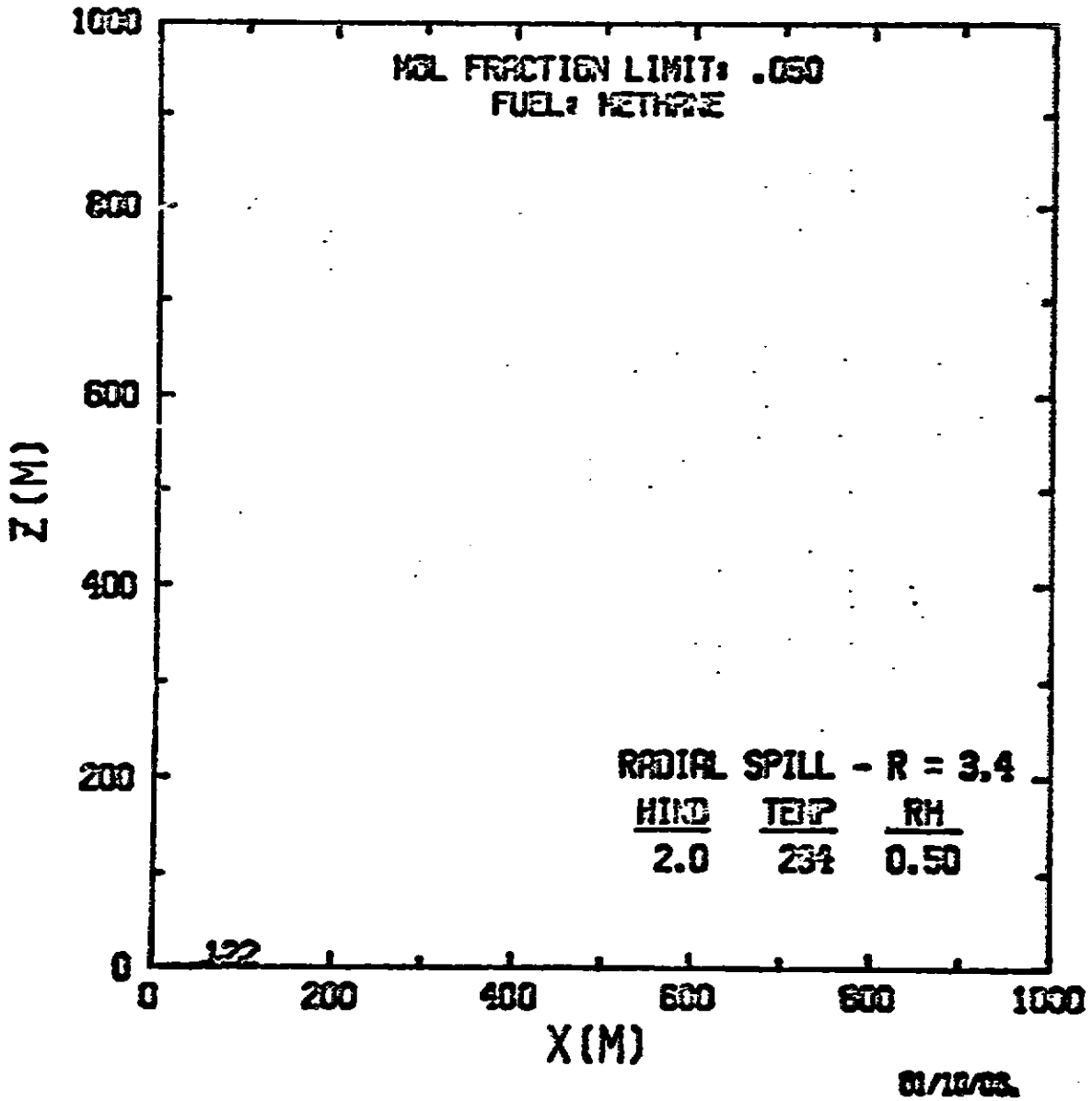

01/10/88

LOOKING AT LARGEST PUFF ONLY

INITIAL CONDITIONS

RADIAL SPILL - RADIUS: 3.4 FUEL: METHANE SURFACE ELEVATION: 0.

EVAPORATION RATE: 4.080E-4 TEMP: 294 RELATIVE HUMIDITY: .50

STABILITY: 6 WIND: 2.0 M/S FMF LOWER LIMIT: .050

SCENARIO 2B

IT	XP M	T K	DELTEN K	A	W M/S	ZP M	ANG DEG	VP CU.M	U1 M/S	U2 M/S	U4 M/S	FMF	VES CU.M	VET CU.M	VEB CU.M	R M	ZTOP M	LL M	LB M
0	0.	111.7	0.0	0.00	0.0	.05	0.	.341E+01	0.000	0.000	0.000	1.000	0.00	0.00	0.00	3.4	.05	0.00	0.00
1	0.	118.3	175.7	-2.88	0.0	.05	48.	.395E+01	.085	.094	0.000	.963	.36	0.00	0.00	3.5	.05	0.00	0.00
6	1.	150.6	143.4	-2.06	0.0	.06	4.	.614E+01	.063	.057	0.000	.788	.33	.15	0.00	4.1	.06	0.00	0.00
12	3.	180.6	113.4	-1.43	0.0	.06	1.	.922E+01	.047	.037	0.000	.630	.30	.21	0.00	4.7	.06	0.00	0.00
18	5.	201.2	92.8	-1.06	0.0	.07	1.	.124E+02	.038	.027	0.000	.522	.29	.23	0.00	5.1	.07	0.00	0.00
24	8.	216.1	77.9	-.80	0.0	.08	1.	.156E+02	.032	.021	0.000	.447	.28	.23	0.00	5.5	.08	0.00	0.00
30	11.	227.4	66.6	-.62	0.0	.08	0.	.187E+02	.028	.018	0.000	.391	.27	.22	0.00	5.9	.08	0.00	0.00
36	15.	236.2	57.8	-.48	0.0	.09	0.	.218E+02	.025	.015	0.000	.349	.26	.22	0.00	6.2	.09	0.00	0.00
42	18.	243.2	50.8	-.36	0.0	.09	0.	.248E+02	.023	.013	0.000	.315	.26	.22	0.00	6.5	.09	0.00	0.00
48	22.	248.9	45.1	-.28	0.0	.09	0.	.278E+02	.022	.012	0.000	.288	.26	.21	0.00	6.7	.09	0.00	0.00
54	26.	253.6	40.4	-.21	0.0	.10	0.	.307E+02	.020	.011	0.000	.265	.25	.21	0.00	6.9	.10	0.00	0.00
60	29.	257.5	36.5	-.16	0.0	.10	0.	.336E+02	.019	.010	0.000	.246	.25	.21	0.00	7.1	.10	0.00	0.00
66	33.	261.0	33.0	-.11	0.0	.10	0.	.365E+02	.018	.009	0.000	.230	.25	.20	0.00	7.3	.10	0.00	0.00
72	37.	264.0	30.0	-.06	0.0	.10	0.	.393E+02	.017	.008	0.000	.216	.25	.20	0.00	7.5	.10	0.00	0.00
78	41.	266.6	27.4	-.03	0.0	.11	0.	.422E+02	.017	.008	0.000	.203	.25	.20	0.00	7.7	.11	0.00	0.00
84	45.	269.0	25.0	.01	.0	.11	0.	.450E+02	.016	.007	0.000	.192	.25	.20	0.00	7.9	.11	0.00	0.00
90	49.	272.6	21.5	.06	.1	.24	0.	.498E+02	.027	.007	0.000	.176	.38	.30	.30	8.1	.11	0.00	0.00
96	54.	277.0	17.0	.10	.1	.74	1.	.590E+02	.051	.006	0.000	.151	.72	.57	.57	8.6	.12	0.00	0.00
102	59.	283.9	10.2	.20	.3	2.02	2.	.754E+02	.076	.004	0.000	.121	1.18	1.00	1.00	9.3	.13	0.00	0.00
108	65.	286.3	7.8	.15	.4	4.35	4.	.101E+03	.094	.003	0.000	.092	1.72	1.60	1.60	10.3	.14	0.00	0.00
114	72.	288.2	5.9	.11	.5	7.17	6.	.135E+03	.097	.002	0.000	.068	2.14	2.14	2.14	11.3	.16	0.00	0.00
120	80.	289.5	4.6	.08	.5	10.07	7.	.178E+03	.094	.002	0.000	.052	2.48	2.57	2.57	12.4	.17	0.00	0.00
122	83.	289.9	4.2	.07	.5	11.03	8.	.194E+03	.092	.002	0.000	.048	2.58	2.69	0.00	12.7	.18	0.00	0.00

VERTICAL VERSUS DOWNWIND POSITION OF PUFF

SCENARIO 2B

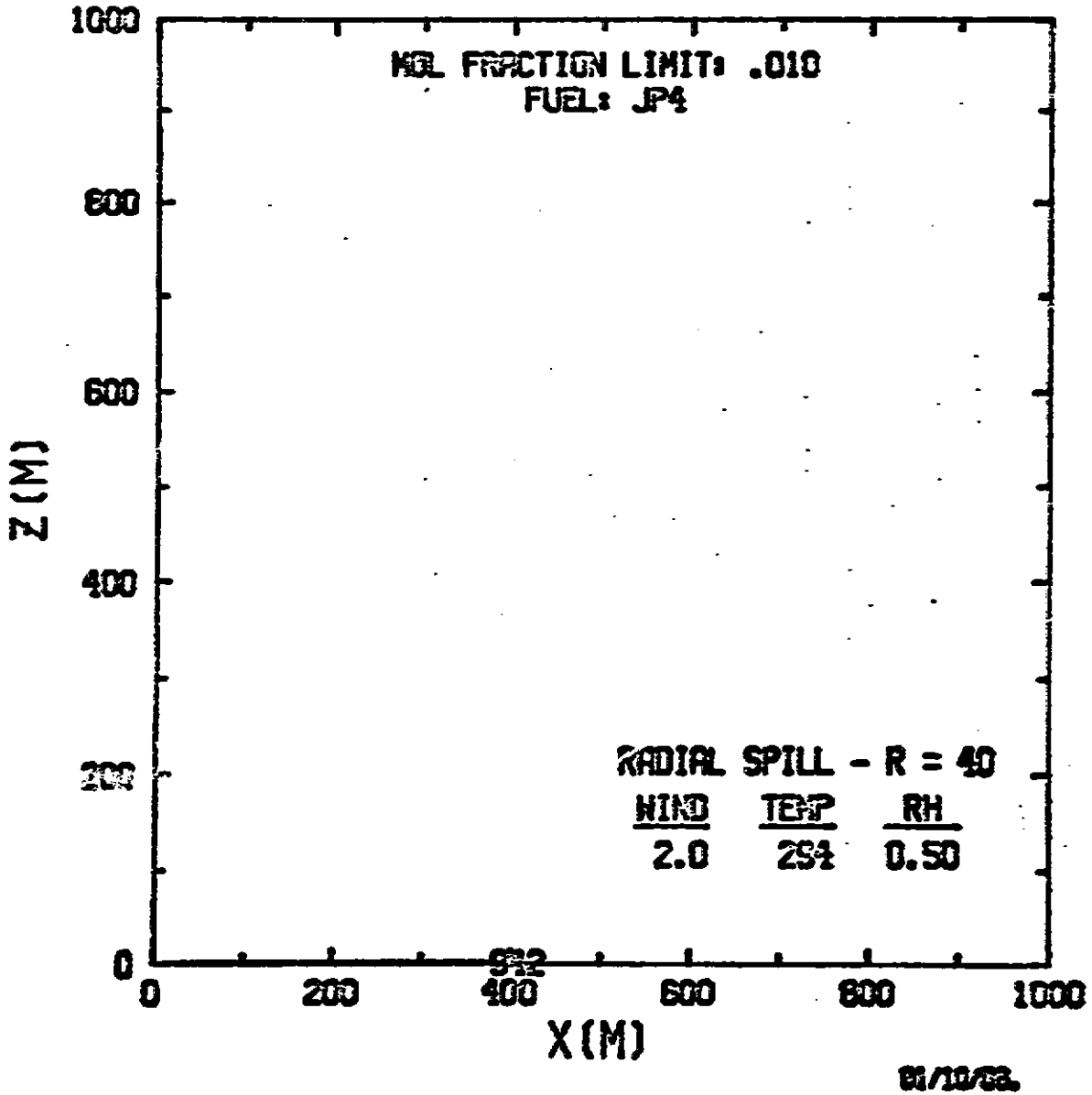

01/10/83.

LOOKING AT LARGEST PUFF ONLY

INITIAL CONDITIONS

RADIAL SPILL - RADIUS: 40.0 FUEL: JP4 SURFACE ELEVATION: 0.

EVAPORATION RATE: 2.000E-6 TEMP: 294 RELATIVE HUMIDITY: .50

STABILITY: 6 WIND: 2.0 M/S FMF LOWER LIMIT: .010

SCENARIO 2B

IT	XP M	T K	DELTEM K	A	W M/S	ZP M	ANG DEG	VP CU.M	U1 M/S	U2 M/S	U4 M/S	FMF	VES CU.M	VET CU.M	VEB CU.M	R M	ZTZP M	LL M	LW M
0	0.	294.0	0.0	0.00	0.0	.04	0.	.352E+03	0.000	0.000	0.000	.109	0.00	0.00	0.00	40.0	.04	0.00	0.00
1	0.	294.0	-.0	-2.36	-.6	.03	87.	.353E+03	.080	0.000	0.000	.108	1.41	0.00	0.00	38.6	.03	0.00	0.00
30	1.	294.0	.0	-2.05	0.0	.03	2.	.386E+03	.073	0.000	0.000	.090	1.27	.24	0.00	39.8	.03	0.00	0.00
60	3.	294.0	.0	-1.78	0.0	.04	1.	.427E+03	.067	0.000	0.000	.075	1.24	.47	0.00	41.1	.04	0.00	0.00
90	7.	294.0	.0	-1.55	0.0	.04	0.	.474E+03	.061	0.000	0.000	.064	1.22	.65	0.00	42.6	.04	0.00	0.00
120	13.	294.0	.0	-1.36	0.0	.04	0.	.527E+03	.056	0.000	0.000	.055	1.19	.80	0.00	44.1	.04	0.00	0.00
150	20.	294.0	.0	-1.20	0.0	.04	0.	.584E+03	.051	0.000	0.000	.048	1.17	.91	0.00	45.6	.04	0.00	0.00
180	28.	294.0	.0	-1.07	0.0	.04	0.	.644E+03	.047	0.000	0.000	.042	1.15	.99	0.00	47.1	.04	0.00	0.00
210	37.	294.0	.0	-.97	0.0	.04	0.	.706E+03	.044	0.000	0.000	.037	1.14	1.06	0.00	48.5	.04	0.00	0.00
240	47.	294.0	.0	-.88	0.0	.04	0.	.770E+03	.041	0.000	0.000	.034	1.12	1.10	0.00	49.9	.04	0.00	0.00
270	58.	294.0	.0	-.81	0.0	.04	0.	.835E+03	.038	0.000	0.000	.031	1.11	1.14	0.00	51.3	.04	0.00	0.00
300	69.	294.0	.0	-.74	0.0	.05	0.	.901E+03	.036	0.000	0.000	.028	1.10	1.16	0.00	52.6	.05	0.00	0.00
330	81.	294.0	.0	-.69	0.0	.05	0.	.967E+03	.034	0.000	0.000	.026	1.09	1.18	0.00	53.8	.05	0.00	0.00
360	94.	294.0	.0	-.64	0.0	.05	0.	.103E+04	.032	0.000	0.000	.024	1.08	1.19	0.00	55.0	.05	0.00	0.00
390	107.	294.0	.0	-.60	0.0	.05	0.	.110E+04	.031	0.000	0.000	.022	1.07	1.20	0.00	56.2	.05	0.00	0.00
420	120.	294.0	.0	-.57	0.0	.05	0.	.117E+04	.030	0.000	0.000	.021	1.06	1.21	0.00	57.3	.05	0.00	0.00
450	134.	294.0	.0	-.53	0.0	.05	0.	.124E+04	.028	0.000	0.000	.020	1.06	1.21	0.00	58.4	.05	0.00	0.00
480	148.	294.0	.0	-.51	0.0	.05	0.	.130E+04	.027	0.000	0.000	.019	1.05	1.21	0.00	59.4	.05	0.00	0.00
510	163.	294.0	.0	-.48	0.0	.05	0.	.137E+04	.026	0.000	0.000	.018	1.05	1.21	0.00	60.4	.05	0.00	0.00
540	178.	294.0	.0	-.46	0.0	.05	0.	.144E+04	.025	0.000	0.000	.017	1.04	1.21	0.00	61.3	.05	0.00	0.00
570	193.	294.0	.0	-.44	0.0	.05	0.	.150E+04	.024	0.000	0.000	.016	1.04	1.21	0.00	62.3	.05	0.00	0.00
600	208.	294.0	.0	-.42	0.0	.06	0.	.157E+04	.024	0.000	0.000	.015	1.04	1.21	0.00	63.2	.06	0.00	0.00
630	224.	294.0	.0	-.40	0.0	.06	0.	.164E+04	.023	0.000	0.000	.014	1.03	1.21	0.00	64.0	.06	0.00	0.00
660	240.	294.0	.0	-.38	0.0	.06	0.	.170E+04	.022	0.000	0.000	.014	1.03	1.21	0.00	64.9	.06	0.00	0.00
690	256.	294.0	.0	-.37	0.0	.06	0.	.177E+04	.022	0.000	0.000	.013	1.03	1.20	0.00	65.7	.06	0.00	0.00
720	272.	294.0	.0	-.36	0.0	.06	0.	.184E+04	.021	0.000	0.000	.013	1.03	1.20	0.00	66.5	.06	0.00	0.00
750	288.	294.0	.0	-.34	0.0	.06	0.	.190E+04	.021	0.000	0.000	.012	1.03	1.20	0.00	67.3	.06	0.00	0.00
780	305.	294.0	.0	-.33	0.0	.06	0.	.197E+04	.020	0.000	0.000	.012	1.03	1.20	0.00	68.1	.06	0.00	0.00
810	322.	294.0	.0	-.32	0.0	.06	0.	.204E+04	.020	0.000	0.000	.011	1.03	1.19	0.00	68.8	.06	0.00	0.00
840	339.	294.0	.0	-.31	0.0	.06	0.	.210E+04	.019	0.000	0.000	.011	1.03	1.19	0.00	69.6	.06	0.00	0.00
870	356.	294.0	.0	-.30	0.0	.06	0.	.217E+04	.019	0.000	0.000	.011	1.03	1.19	0.00	70.3	.06	0.00	0.00
900	373.	294.0	.0	-.29	0.0	.06	0.	.224E+04	.019	0.000	0.000	.010	1.03	1.19	0.00	71.0	.06	0.00	0.00
930	390.	294.0	.0	-.28	0.0	.06	0.	.230E+04	.018	0.000	0.000	.010	1.03	1.18	0.00	71.7	.06	0.00	0.00
942	397.	294.0	.0	-.28	0.0	.06	0.	.233E+04	.018	0.000	0.000	.010	1.03	1.18	0.00	71.9	.06	0.00	0.00

VERTICAL VERSUS DOWNWIND POSITION OF PUFF

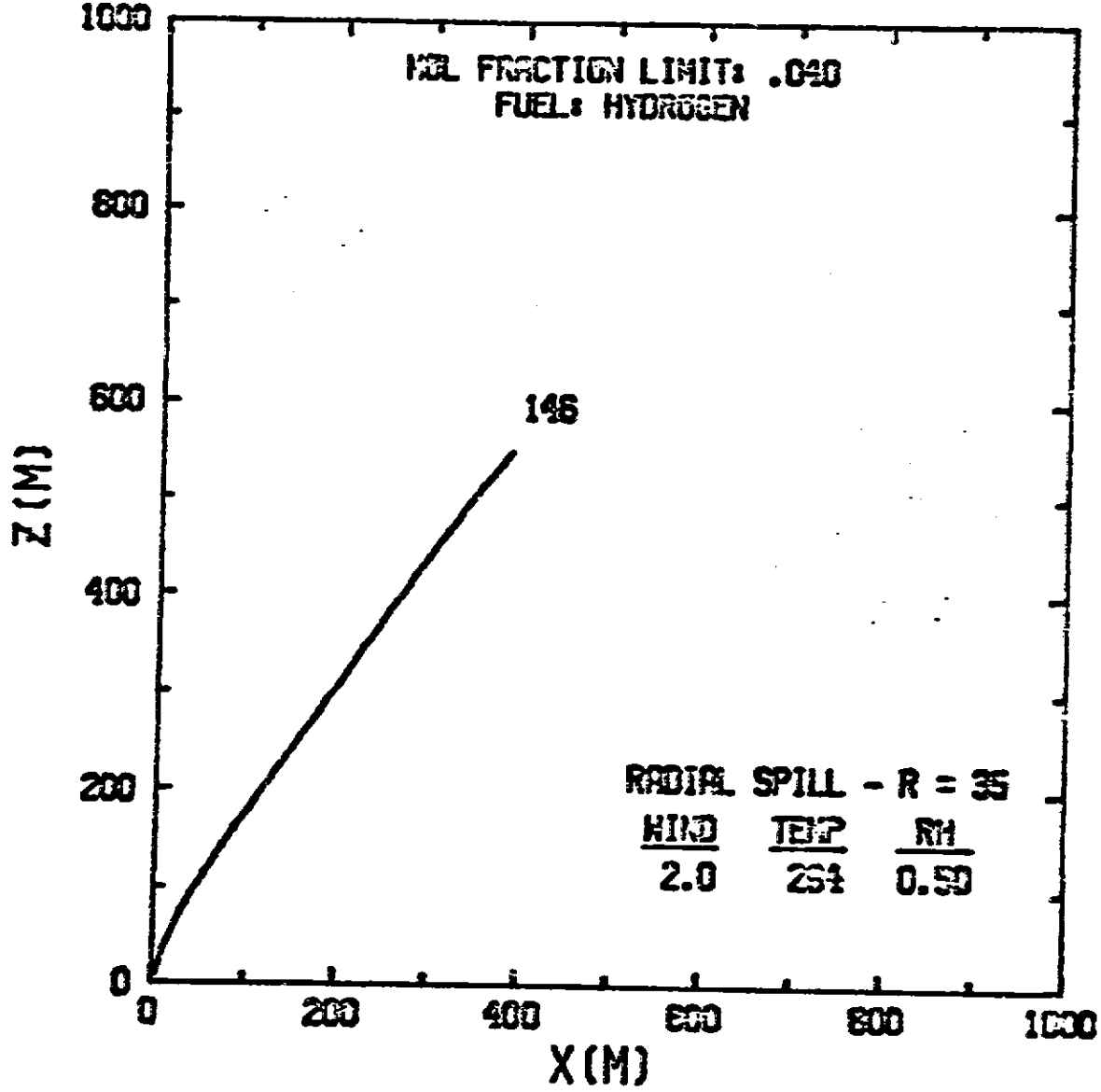

SCENARIO 2C

81/10/02.

LOOKING AT LARGEST PUFF ONLY

INITIAL CONDITIONS

SCENARIO 2C

RADIAL SPILL - RADIUS: 35.0 FUEL: HYDROGEN SURFACE ELEVATION: 0.

EVAPORATION RATE: 1.940E-3 TEMP: 294 RELATIVE HUMIDITY: .50

STABILITY: 6 WIND: 2.0 M/S FMF LOWER LIMIT: .040

IT	XP	T	DELTEM	A	W	ZP	ANG	VP	U1	U2	U4	FMF	VES	VET	VEB	R	ZTZP	LL	LW
	M	K	K		M/S	M	DEG	CU.M	M/S	M/S	M/S		CU.M	CU.M	CU.M	M	M	M	M
0	0.	20.3	0.0	0.00	0.0	.05	0.	.394E+03	0.000	0.000	0.000	1.000	0.00	0.00	0.00	35.0	.05	0.00	0.00
1	0.	20.5	273.5	-.05	0.0	.05	83.	.443E+03	.086	.102	0.000	.999	4.24	0.00	0.00	35.1	.05	0.00	0.00
6	0.	22.0	272.0	.17	.1	.20	54.	.476E+03	.078	.086	0.000	.996	4.32	.35	.35	36.0	.05	0.00	0.00
12	1.	24.8	269.2	.54	.6	2.13	71.	.541E+03	.168	.076	0.000	.989	6.29	1.78	1.78	37.5	.05	0.00	0.00
18	2.	30.9	263.2	1.15	1.7	8.83	74.	.684E+03	.263	.062	0.000	.974	9.48	7.24	7.24	40.5	.06	0.00	0.00
24	7.	47.0	247.3	2.04	3.1	23.33	74.	.109E+04	.401	.041	0.000	.933	17.00	27.89	27.89	47.3	.07	0.00	0.00
30	15.	81.5	212.9	2.31	4.1	45.47	71.	.212E+04	.510	.021	0.000	.834	31.42	77.58	77.58	58.9	.09	0.00	0.00
36	28.	124.1	170.6	1.80	4.2	70.57	68.	.389E+04	.532	.011	0.000	.692	48.58	131.84	131.84	72.0	.11	0.00	0.00
42	43.	161.7	133.2	1.35	4.2	95.94	66.	.633E+04	.528	.007	0.000	.556	66.71	177.26	177.26	84.5	.12	0.00	0.00
48	59.	191.4	103.8	1.06	4.2	121.05	64.	.939E+04	.521	.005	0.000	.446	85.73	216.84	216.84	96.2	.14	0.00	0.00
54	77.	214.5	81.0	.90	4.1	145.96	62.	.131E+05	.517	.003	0.000	.360	106.25	254.62	254.62	107.3	.16	0.00	0.00
60	95.	232.4	63.3	.81	4.2	170.90	61.	.174E+05	.519	.002	0.000	.294	129.10	293.48	293.48	117.9	.17	0.00	0.00
66	114.	246.7	49.3	.76	4.2	196.10	60.	.224E+05	.526	.002	0.000	.243	155.68	335.34	335.34	128.2	.19	0.00	0.00
72	134.	258.0	37.8	.73	4.3	221.82	59.	.282E+05	.538	.001	0.000	.202	184.97	381.56	381.56	138.3	.20	0.00	0.00
78	154.	267.1	28.6	.72	4.5	248.26	58.	.348E+05	.554	.001	0.000	.170	219.29	432.75	432.75	148.3	.22	0.00	0.00
84	175.	272.9	22.6	.65	4.6	275.55	58.	.422E+05	.571	.001	0.000	.144	256.84	486.83	486.83	158.0	.23	0.00	0.00
90	196.	279.0	16.3	.65	4.7	303.51	57.	.508E+05	.585	.001	0.000	.123	297.27	541.33	541.33	167.9	.25	0.00	0.00
96	217.	284.0	11.1	.66	4.9	332.28	57.	.604E+05	.603	.001	0.000	.105	343.96	603.00	603.00	177.8	.26	0.00	0.00
102	239.	285.7	9.2	.57	5.0	361.91	57.	.706E+05	.619	.001	0.000	.091	391.97	664.21	664.21	187.2	.27	0.00	0.00
108	262.	286.6	8.1	.49	5.0	391.92	56.	.816E+05	.623	.001	0.000	.079	434.62	713.79	713.79	196.4	.29	0.00	0.00
114	284.	287.3	7.2	.42	5.0	421.88	56.	.934E+05	.620	.000	0.000	.070	473.56	755.10	755.10	205.4	.30	0.00	0.00
120	307.	287.9	6.5	.37	4.9	451.58	56.	.106E+06	.614	.000	0.000	.062	509.55	790.30	790.30	214.1	.31	0.00	0.00
126	331.	288.3	5.9	.32	4.8	480.88	55.	.119E+06	.605	.000	0.000	.055	543.10	820.80	820.80	222.5	.33	0.00	0.00
132	355.	288.6	5.4	.29	4.8	509.71	55.	.133E+06	.595	.000	0.000	.050	574.59	847.60	847.60	230.6	.34	0.00	0.00
138	378.	288.8	5.0	.26	4.7	538.05	55.	.147E+06	.585	.000	0.000	.045	604.28	871.37	871.37	238.5	.35	0.00	0.00
144	403.	289.0	4.7	.23	4.6	565.88	55.	.162E+06	.574	.000	0.000	.041	632.37	892.63	892.63	246.1	.36	0.00	0.00
146	411.	289.0	4.6	.22	4.6	575.05	54.	.167E+06	.571	.000	0.000	.040	641.41	899.22	0.00	248.6	.36	0.00	0.00

VERTICAL VERSUS DOWNWIND POSITION OF PUFF

SCENARIO 2C

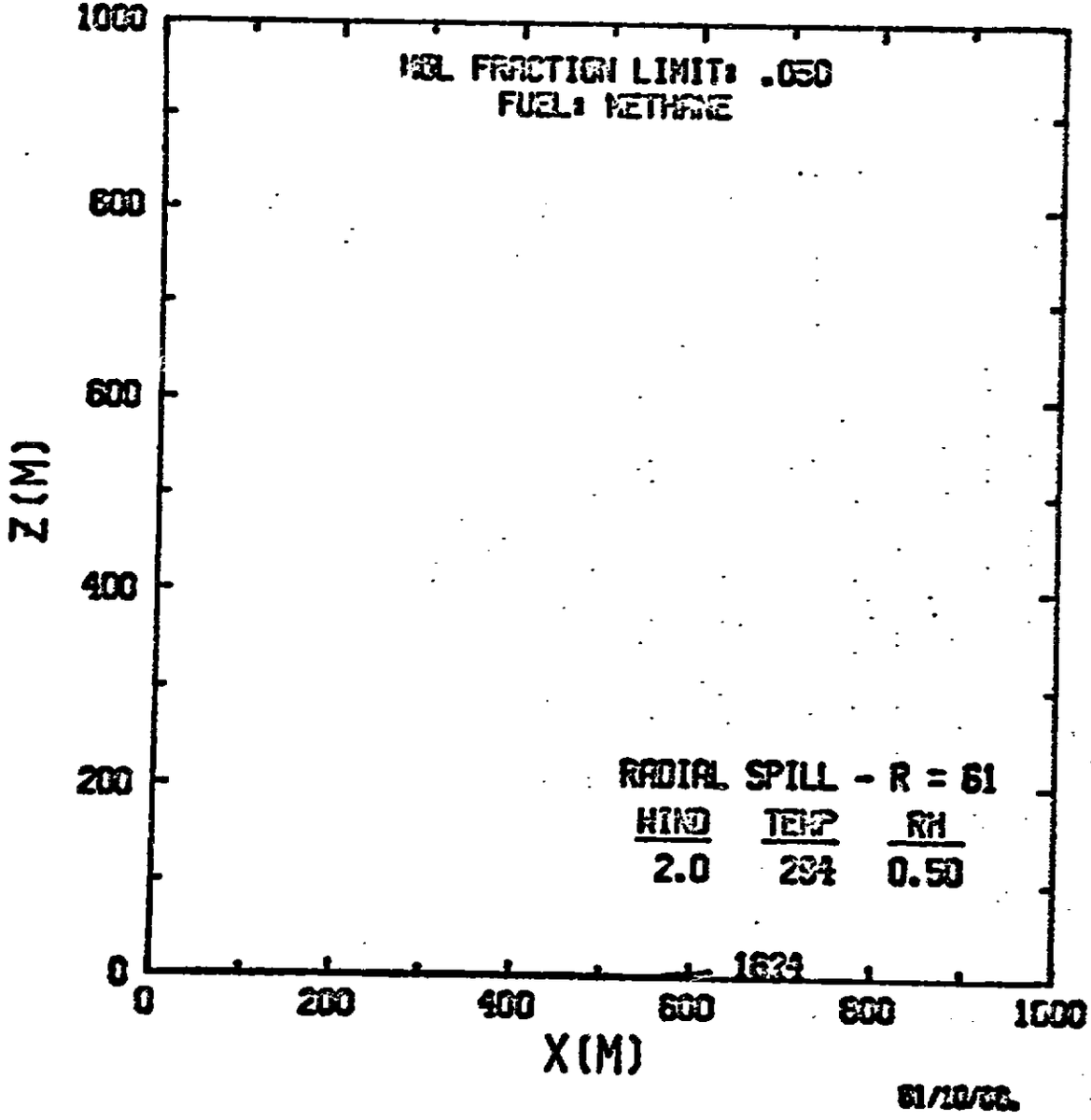

LOOKING AT LARGEST PUFF ONLY

INITIAL CONDITIONS

RADIAL SPILL - RADIUS: 61.0 FUEL: METHANE SURFACE ELEVATION: 0.

EVAPORATION RATE: 1.110E-4 TEMP: 294 RELATIVE HUMIDITY: .50

STABILITY: 6 WIND: 2.0 M/S FMF LOWER LIMIT: .050

SCENARIO 2C

IT	XP M	T K	DELTEM K	A	W M/S	ZP M	ANG DEG	VP CU.M	U1 M/S	U2 M/S	U4 M/S	FMF	VES CU.M	VET CU.M	VEB CU.M	R M	ITZP M	EL M	LW M
0	0.	111.7	0.0	0.00	0.0	.01	0.	.299E+03	0.000	0.000	0.000	1.000	0.00	0.00	0.00	61.0	.01	0.00	0.00
1	0.	111.9	182.1	-3.07	-.8	.01	85.	.315E+03	.065	.026	0.000	.999	.89	0.00	0.00	59.8	.01	0.00	0.00
120	8.	141.1	152.9	-2.28	0.0	.01	0.	.474E+03	.050	.016	0.000	.839	.81	.96	0.00	62.1	.01	0.00	0.00
240	32.	172.9	121.1	-1.58	0.0	.02	0.	.726E+03	.037	.011	0.000	.670	.77	1.50	0.00	78.5	.02	0.00	0.00
360	68.	196.7	97.3	-1.13	0.0	.02	0.	.102E+04	.029	.008	0.000	.545	.75	1.68	0.00	87.7	.02	0.00	0.00
480	111.	214.1	79.9	-.84	0.0	.02	0.	.132E+04	.025	.006	0.000	.457	.73	1.73	0.00	95.5	.02	0.00	0.00
600	158.	227.0	67.0	-.62	0.0	.02	0.	.163E+04	.021	.005	0.000	.393	.72	1.73	0.00	102.4	.02	0.00	0.00
720	210.	237.0	57.0	-.46	0.0	.02	0.	.193E+04	.019	.004	0.000	.345	.71	1.71	0.00	108.4	.02	0.00	0.00
840	264.	244.8	49.2	-.34	0.0	.02	0.	.224E+04	.017	.003	0.000	.308	.70	1.69	0.00	113.7	.02	0.00	0.00
960	320.	250.9	43.1	-.25	0.0	.02	0.	.254E+04	.016	.003	0.000	.278	.70	1.67	0.00	118.6	.02	0.00	0.00
1080	377.	255.9	38.1	-.18	0.0	.03	0.	.284E+04	.015	.003	0.000	.254	.70	1.66	0.00	123.0	.03	0.00	0.00
1200	436.	260.1	33.9	-.12	0.0	.03	0.	.313E+04	.014	.002	0.000	.234	.70	1.64	0.00	127.1	.03	0.00	0.00
1320	497.	263.8	30.2	-.07	0.0	.03	0.	.343E+04	.013	.002	0.000	.217	.70	1.62	0.00	130.9	.03	0.00	0.00
1440	558.	266.9	27.1	-.02	0.0	.03	0.	.372E+04	.013	.002	0.000	.202	.71	1.61	0.00	134.5	.03	0.00	0.00
1560	624.	277.7	16.4	.11	.4	6.82	1.	.530E+04	.143	.001	0.000	.148	8.62	25.58	25.58	151.1	.03	0.00	0.00
1624	713.	289.6	5.1	.05	1.1	72.32	6.	.165E+05	.182	.000	0.000	.050	23.01	126.59	0.00	220.1	.05	0.00	0.00

VERTICAL VERSUS DOWNWIND POSITION OF PUFF

SCENARIO 2C

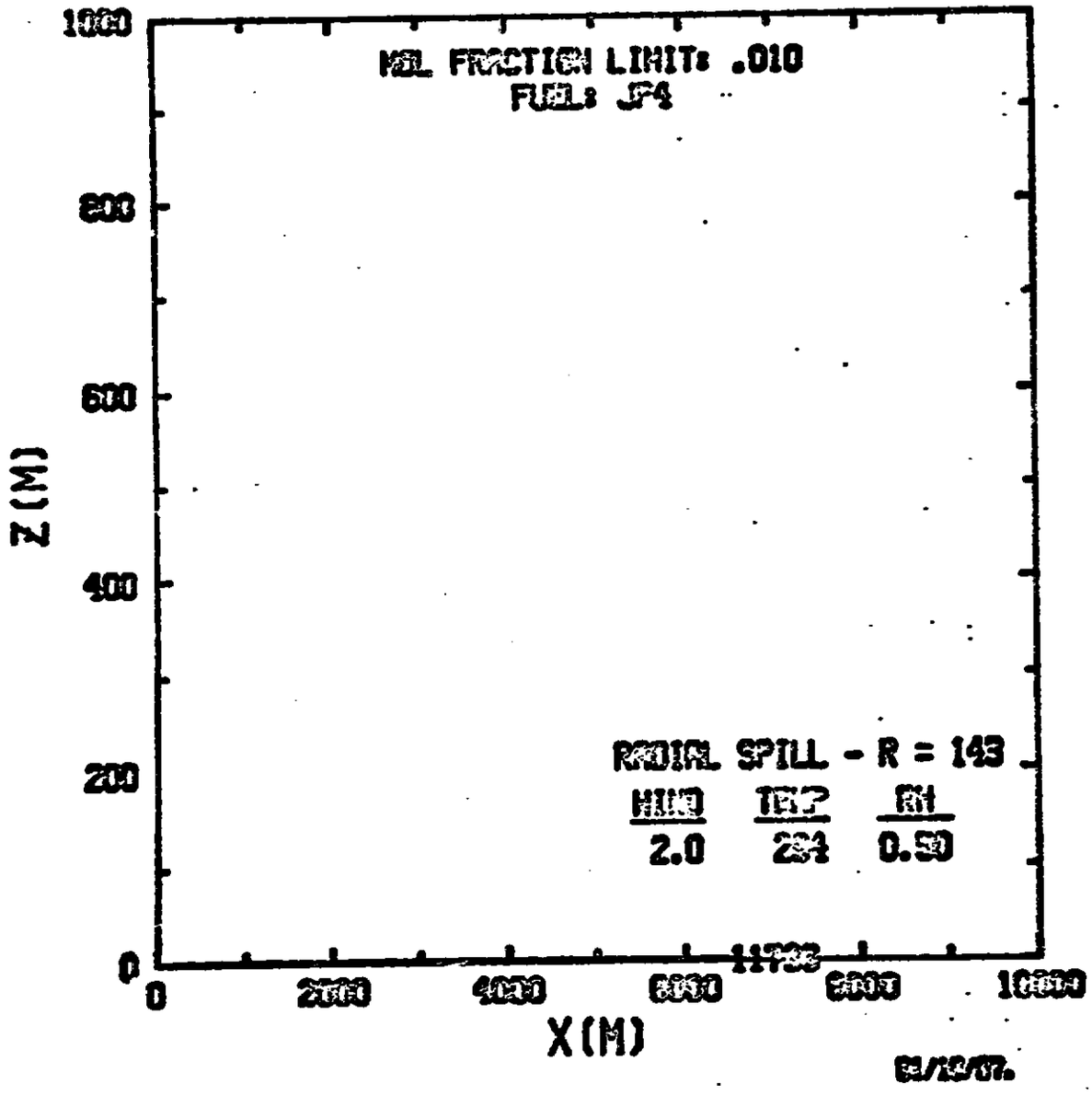

LOOKING AT LARGEST PUFF ONLY

INITIAL CONDITIONS

RADIAL SPILL - RADIUS: 143.0 FUEL: JP4 SURFACE ELEVATION: 0.

EVAPORATION RATE: 2.000E-6 TEMP: 294 RELATIVE HUMIDITY: .50

STABILITY: 6 WIND: 2.0 M/S FMF LOWER LIMIT: .010

SCENARIO 2C

IT	XP	T	DELTEM	A	W	ZP	ANG	VP	U1	U2	U4	FMF	VES	VET	VEB	R	ZTZP	LL	LW
	M	K	K		M/S	M	DEG	CU.M	M/S	M/S	M/S		CU.M	CU.M	CU.M	M	M	M	M
0	0.	294.0	0.0	0.00	0.0	.04	0.	.449E+04	0.000	0.000	0.000	.109	0.00	0.00	0.00	143.0	.04	0.00	0.00
1	0.	294.0	-.0	-2.37	-.6	.03	89.	.450E+04	.080	0.000	0.000	.109	5.03	0.00	0.00	136.1	.03	0.00	0.00
600	82.	294.0	.0	-1.83	0.0	.04	0.	.751E+04	.050	0.000	0.000	.078	4.02	3.25	0.00	161.2	.04	0.00	0.00
1200	282.	294.0	.0	-1.42	0.0	.05	0.	.116E+05	.035	0.000	0.000	.058	3.76	4.08	0.00	186.0	.05	0.00	0.00
1800	544.	294.0	.0	-1.16	0.0	.05	0.	.160E+05	.028	0.000	0.000	.046	3.65	4.25	0.00	206.8	.05	0.00	0.00
2400	841.	294.0	.0	-.98	0.0	.05	0.	.205E+05	.023	0.000	0.000	.038	3.60	4.25	0.00	224.4	.05	0.00	0.00
3000	1163.	294.0	.0	-.84	0.0	.06	0.	.250E+05	.020	0.000	0.000	.032	3.60	4.22	0.00	239.8	.06	0.00	0.00
3600	1502.	294.0	.0	-.74	0.0	.06	0.	.296E+05	.018	0.000	0.000	.028	3.61	4.19	0.00	253.4	.06	0.00	0.00
4200	1854.	294.0	.0	-.67	0.0	.07	0.	.341E+05	.017	0.000	0.000	.025	3.64	4.16	0.00	265.7	.07	0.00	0.00
4800	2216.	294.0	.0	-.60	0.0	.07	0.	.387E+05	.016	0.000	0.000	.022	3.67	4.14	0.00	277.0	.07	0.00	0.00
5400	2586.	294.0	.0	-.55	0.0	.07	0.	.434E+05	.015	0.000	0.000	.020	3.72	4.12	0.00	287.5	.07	0.00	0.00
6000	2964.	294.0	.0	-.50	0.0	.07	0.	.480E+05	.014	0.000	0.000	.019	3.77	4.11	0.00	297.4	.07	0.00	0.00
6600	3349.	294.0	.0	-.47	0.0	.08	0.	.527E+05	.013	0.000	0.000	.017	3.82	4.11	0.00	306.7	.08	0.00	0.00
7200	3739.	294.0	.0	-.43	0.0	.08	0.	.575E+05	.013	0.000	0.000	.016	3.88	4.11	0.00	315.5	.08	0.00	0.00
7800	4133.	294.0	.0	-.41	0.0	.08	0.	.622E+05	.012	0.000	0.000	.015	3.94	4.11	0.00	323.9	.08	0.00	0.00
8400	4532.	294.0	.0	-.38	0.0	.08	0.	.670E+05	.012	0.000	0.000	.014	4.00	4.12	0.00	332.0	.08	0.00	0.00
9000	4935.	294.0	.0	-.36	0.0	.08	0.	.719E+05	.011	0.000	0.000	.013	4.07	4.13	0.00	339.7	.09	0.00	0.00
9600	5342.	294.0	.0	-.34	0.0	.08	0.	.768E+05	.011	0.000	0.000	.012	4.13	4.14	0.00	347.2	.09	0.00	0.00
10200	5752.	294.0	.0	-.32	0.0	.09	0.	.818E+05	.011	0.000	0.000	.011	4.20	4.15	0.00	354.5	.09	0.00	0.00
10800	6165.	294.0	.0	-.30	0.0	.09	0.	.868E+05	.011	0.000	0.000	.011	4.27	4.17	0.00	361.5	.09	0.00	0.00
11400	6581.	294.0	.0	-.29	0.0	.09	0.	.919E+05	.010	0.000	0.000	.010	4.34	4.19	0.00	368.3	.09	0.00	0.00
11736	6816.	294.0	.0	-.28	0.0	.09	0.	.947E+05	.010	0.000	0.000	.010	4.38	4.20	0.00	372.1	.09	0.00	0.00

VERTICAL VERSUS DOWNWIND POSITION OF PUFF

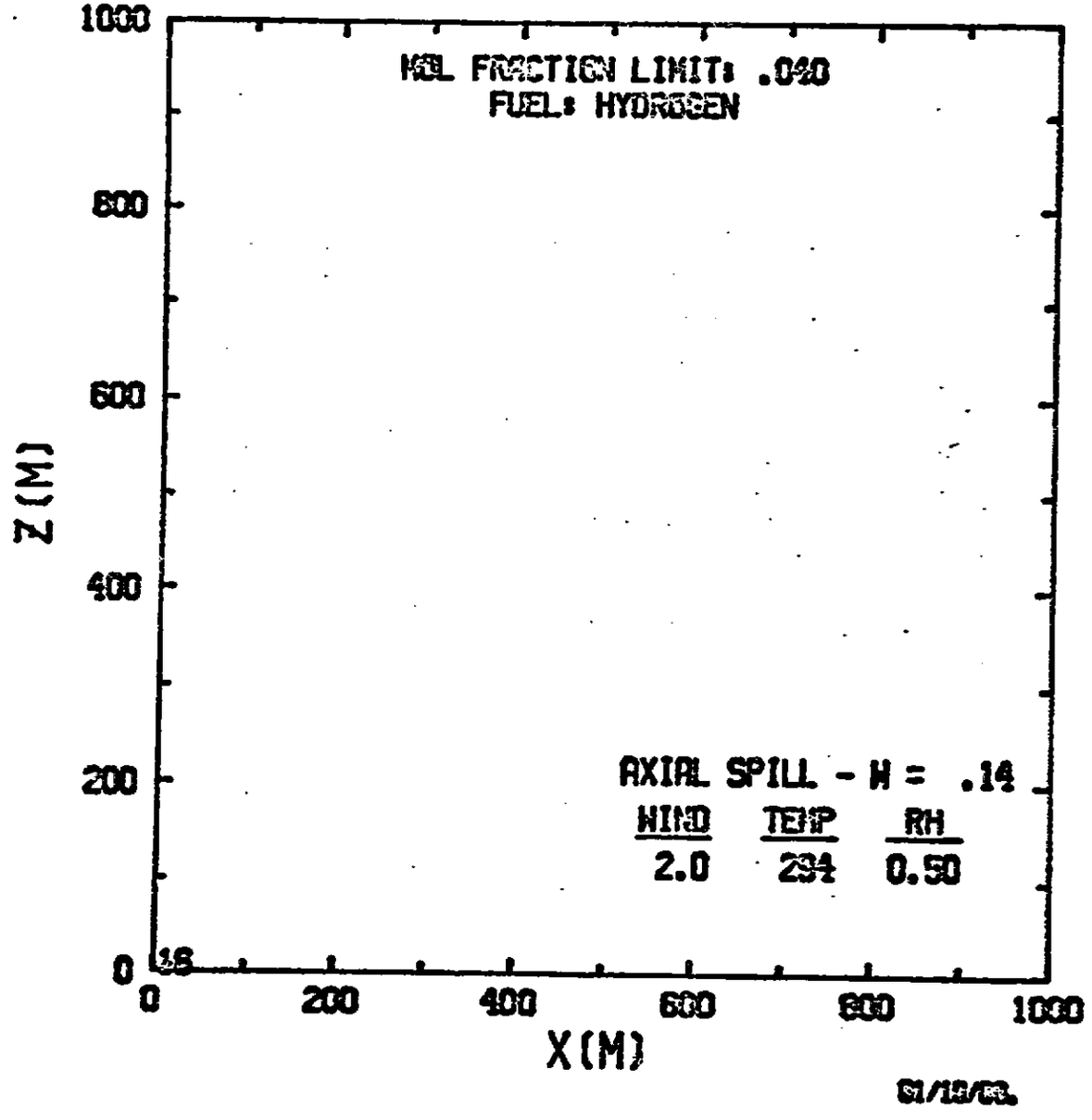

SCENARIO 3A

01/15/88.

LOGGING AT LARGEST PUFF ONLY

INITIAL CONDITIONS

AXIAL SPILL - WIDTH: .1

EVAPORATION RATE: 2.500E-3

STABILITY: 6

SCENARIO 3A

FUEL: HYDROGEN SURFACE ELEVATION: 0.

TEMP: 294 RELATIVE HUMIDITY: .50

WIND: 2.0 M/S FMF LOWER LIMIT: .040

	XP	T	DELTEM	A	W	ZP	ANG	VP	U1	U2	U4	FMF	VES	VEI	VEB	R	ZTZP	LL	LW
	M	K	K		M/S	M	DEG	CU.M	M/S	M/S	M/S		CU.M	CU.M	CU.M	M	M	M	M
1	0.	20.3	0.0	0.00	0.0	.07	0.	.185E-01	0.000	0.000	0.000	1.000	0.00	0.00	0.00	0.0	.07	1.00	.14
2	1.	81.4	212.6	2.36	.2	.14	13.	.985E-01	.091	.132	0.000	.835	.06	0.00	0.00	0.0	.11	1.74	.24
3	1.	120.0	174.5	1.69	.3	.39	15.	.172E+00	.034	.025	0.000	.707	.05	.01	.01	0.0	.14	2.09	.29
4	2.	159.6	134.4	1.40	.4	.77	17.	.286E+00	.052	.014	0.000	.564	.08	.02	.02	0.0	.16	2.47	.35
5	4.	192.6	101.4	1.07	.4	1.17	18.	.442E+00	.056	.009	0.000	.440	.10	.02	.02	0.0	.19	2.85	.40
6	5.	218.3	75.8	.89	.4	1.60	19.	.643E+00	.058	.006	0.000	.343	.14	.03	.03	0.0	.21	3.23	.45
7	6.	238.2	55.9	.79	.4	2.04	19.	.896E+00	.059	.004	0.000	.269	.17	.03	.03	0.0	.24	3.60	.50
8	7.	253.3	40.7	.72	.5	2.50	19.	.121E+01	.060	.003	0.000	.212	.21	.04	.04	0.0	.26	3.97	.56
9	9.	265.1	28.9	.68	.5	2.97	19.	.159E+01	.062	.002	0.000	.169	.27	.05	.05	0.0	.29	4.35	.61
10	10.	273.3	20.7	.62	.5	3.45	19.	.204E+01	.064	.002	0.000	.135	.32	.06	.06	0.0	.31	4.73	.66
11	12.	280.7	13.3	.62	.5	3.95	19.	.259E+01	.065	.001	0.000	.110	.39	.06	.06	0.0	.34	5.11	.72
12	13.	286.6	7.4	.62	.5	4.48	19.	.324E+01	.067	.001	0.000	.090	.47	.07	.07	0.0	.36	5.50	.77
13	15.	288.0	6.1	.50	.5	5.01	19.	.396E+01	.069	.001	0.000	.073	.56	.08	.08	0.0	.39	5.88	.82
14	16.	289.0	5.1	.41	.5	5.53	19.	.478E+01	.069	.001	0.000	.061	.64	.09	.09	0.0	.41	6.26	.88
15	18.	289.8	4.3	.34	.5	6.05	19.	.568E+01	.068	.001	0.000	.052	.71	.10	.10	0.0	.44	6.62	.93
16	20.	290.4	3.7	.29	.5	6.55	18.	.666E+01	.066	.000	0.000	.044	.77	.10	.10	0.0	.46	6.98	.98
17	21.	290.9	3.2	.25	.5	7.03	18.	.770E+01	.065	.000	0.000	.038	.83	.11	.11	0.0	.48	7.32	1.03

SCENARIO 3A

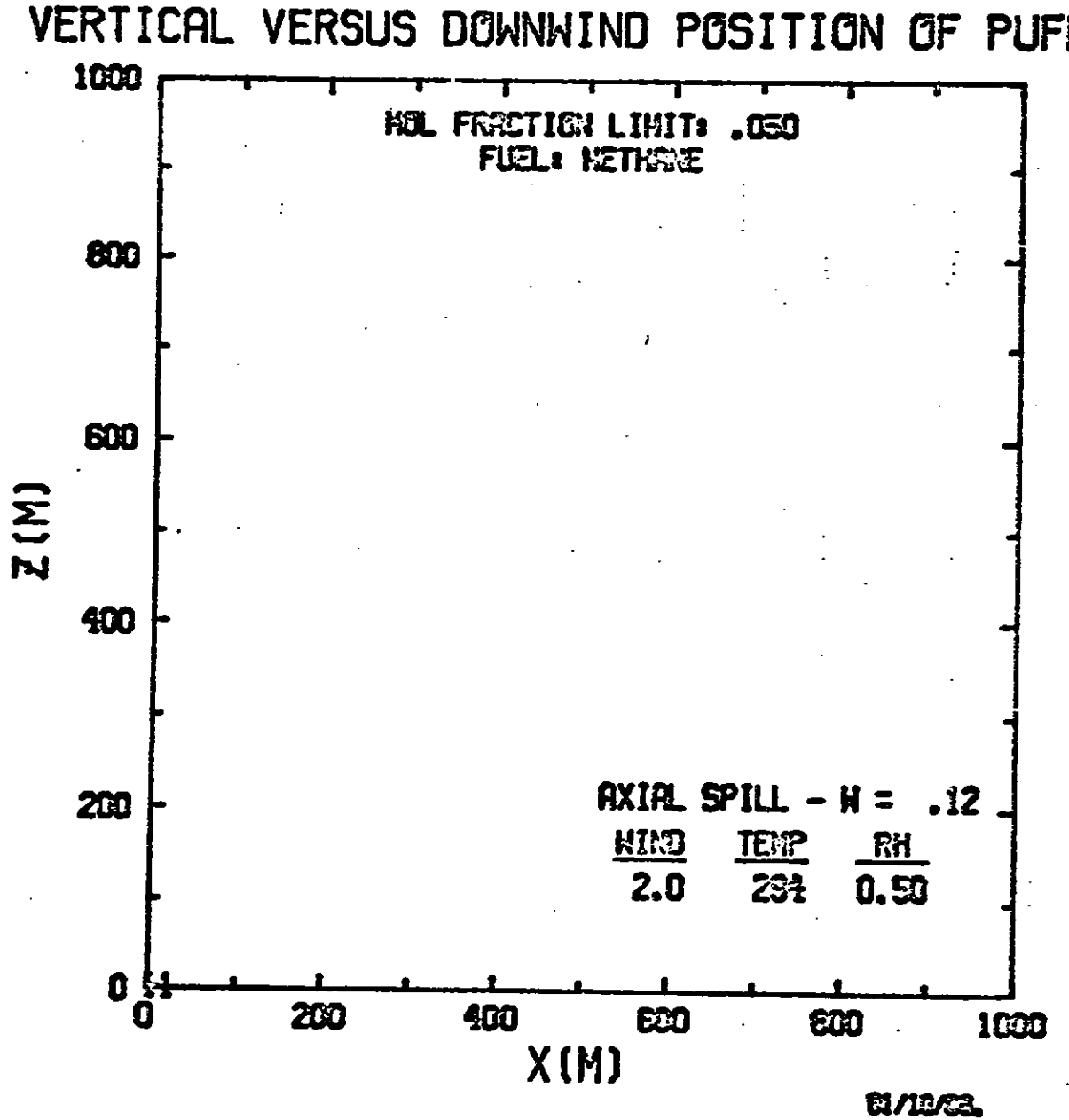
VERTICAL VERSUS DOWNWIND POSITION OF PUFF
MOL FRACTION LIMIT: .050
FUEL: METHANE
AXIAL SPILL - M = .12
WIND 2.0
TEMP 294
RH 0.50
Z(M)
X(M)
0
200
400
600
800
1000

LOOKING AT LARGEST PUFF ONLY

INITIAL CONDITIONS

AXIAL SPILL - WIDTH: .1 FUEL: METHANE SURFACE ELEVATION: 0.

EVAPORATION RATE: 1.060E-3 TEMP: 294 RELATIVE HUMIDITY: .50

STABILITY: 6 WIND: 2.0 M/S FMF LOWER LIMIT: .050

SCENARIO 3A

IT	XP	T	DELTEM	A	U	ZP	ANG	VP	U1	U2	U4	FMF	VES	VET	VEB	R	ZTZP	LL	LW
	M	K	K		M/S	M	DEG	CU.M	M/S	M/S	M/S		CU.M	CU.M	CU.M	M	M	M	M
0	0.	111.7	0.0	0.00	0.0	.12	0.	.293E-01	0.000	0.000	0.000	1.000	0.00	0.00	0.00	0.0	.12	1.00	.12
1	1.	241.5	52.5	-.39	0.0	.23	17.	.206E+00	.103	.214	0.000	.324	.17	0.00	0.00	0.0	.23	1.90	.23
2	2.	262.4	31.6	-.09	0.0	.27	10.	.327E+00	.024	.035	0.000	.222	.10	.01	0.00	0.0	.27	2.22	.27
3	2.	272.0	22.0	.02	.0	.30	7.	.436E+00	.018	.022	0.000	.172	.10	.01	0.00	0.0	.30	2.44	.29
4	3.	279.0	15.0	.13	.0	.32	5.	.543E+00	.016	.016	0.000	.142	.09	.01	0.00	0.0	.32	2.62	.31
5	4.	283.9	10.1	.20	.1	.37	5.	.650E+00	.015	.013	0.000	.121	.09	.01	0.00	0.0	.34	2.75	.33
6	5.	285.4	8.6	.17	.1	.45	5.	.773E+00	.017	.011	0.000	.102	.11	.01	.01	0.0	.36	2.94	.35
7	6.	286.7	7.3	.14	.1	.55	5.	.918E+00	.020	.009	0.000	.086	.12	.01	.01	0.0	.38	3.12	.37
8	7.	287.8	6.2	.12	.1	.66	5.	.109E+01	.023	.008	0.000	.073	.15	.01	.01	0.0	.40	3.29	.40
9	8.	288.7	5.3	.10	.1	.77	5.	.128E+01	.025	.007	0.000	.062	.17	.01	.01	0.0	.42	3.47	.42
10	9.	289.4	4.6	.08	.1	.89	6.	.149E+01	.026	.006	0.000	.054	.18	.01	.01	0.0	.45	3.65	.44
11	10.	290.0	4.0	.07	.1	1.01	6.	.172E+01	.026	.005	0.000	.047	.20	.01	.01	0.0	.47	3.83	.46

VERTICAL VERSUS DOWNWIND POSITION OF PUFF

SCENARIO 3A

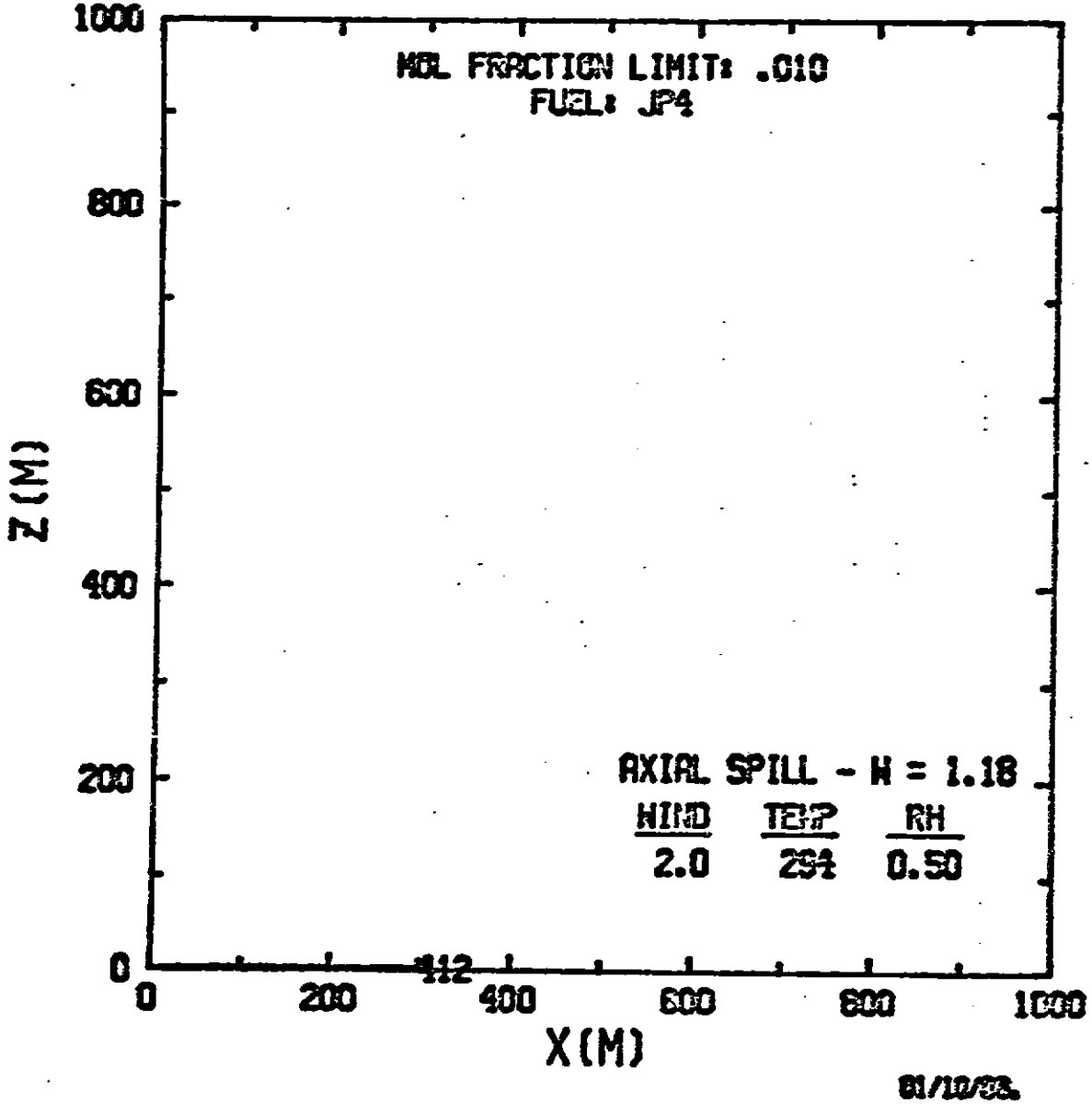

01/10/83

LOOKING AT LARGEST PUFF ONLY

INITIAL CONDITIONS

AXIAL SPILL - WIDTH: 1.2 FUEL: JP4 SURFACE ELEVATION: 0.

EVAPORATION RATE: 2.000E-6 TEMP: 294 RELATIVE HUMIDITY: .50

STABILITY: 6 WIND: 2.0 M/S FMF LOWER LIMIT: .010

SCENARIO 3A

IT	XP M	T K	DELTEM K	A	U M/S	ZP M	ANG DEG	VP CU.M	U1 M/S	U2 M/S	U4 M/S	FMF	VES CU.M	VET CU.M	VEB CU.M	R M	ZTZP M	LL M	LW M
0	0.	294.0	0.0	0.00	0.0	.04	0.	.826E-01	0.000	0.000	0.000	.109	0.00	0.00	0.00	0.0	.04	1.00	1.18
1	0.	294.0	.0	-2.37	0.0	.04	31.	.912E-01	.080	0.000	0.000	.108	.01	0.00	0.00	0.0	.04	1.03	1.22
20	9.	294.0	.0	-2.01	0.0	.06	0.	.539E+00	.018	0.000	0.000	.088	.01	.02	0.00	0.0	.06	1.86	2.19
40	21.	294.0	.0	-1.73	0.0	.08	0.	.106E+01	.012	0.000	0.000	.073	.01	.02	0.00	0.0	.08	2.32	2.74
60	35.	294.0	.0	-1.51	0.0	.09	0.	.163E+01	.010	0.000	0.000	.062	.01	.02	0.00	0.0	.09	2.68	3.16
80	49.	294.0	.0	-1.32	0.0	.10	0.	.226E+01	.009	0.000	0.000	.053	.01	.02	0.00	0.0	.10	2.98	3.52
100	64.	294.0	.0	-1.17	0.0	.11	0.	.296E+01	.009	0.000	0.000	.046	.01	.03	0.00	0.0	.11	3.26	3.84
120	79.	294.0	.0	-1.04	0.0	.12	0.	.372E+01	.009	0.000	0.000	.041	.01	.03	0.00	0.0	.12	3.51	4.14
140	95.	294.0	.0	-.93	0.0	.13	0.	.454E+01	.008	0.000	0.000	.036	.02	.03	0.00	0.0	.13	3.75	4.43
160	110.	294.0	.0	-.84	0.0	.14	0.	.544E+01	.008	0.000	0.000	.032	.02	.03	0.00	0.0	.14	3.98	4.70
180	126.	294.0	.0	-.75	0.0	.15	0.	.642E+01	.008	0.000	0.000	.028	.02	.03	0.00	0.0	.15	4.21	4.96
200	142.	294.0	.0	-.68	0.0	.15	0.	.746E+01	.008	0.000	0.000	.025	.02	.03	0.00	0.0	.15	4.42	5.22
220	158.	294.0	.0	-.62	0.0	.16	0.	.858E+01	.008	0.000	0.000	.023	.02	.04	0.00	0.0	.16	4.63	5.46
240	175.	294.0	.0	-.56	0.0	.17	0.	.977E+01	.008	0.000	0.000	.021	.03	.04	0.00	0.0	.17	4.83	5.70
260	191.	294.0	.0	-.51	0.0	.18	0.	.110E+02	.008	0.000	0.000	.019	.03	.04	0.00	0.0	.18	5.03	5.94
280	208.	294.0	.0	-.47	0.0	.18	0.	.124E+02	.008	0.000	0.000	.017	.03	.04	0.00	0.0	.18	5.23	6.17
300	224.	294.0	.0	-.43	0.0	.19	0.	.138E+02	.008	0.000	0.000	.016	.03	.04	0.00	0.0	.19	5.42	6.39
320	241.	294.0	.0	-.40	0.0	.20	0.	.153E+02	.008	0.000	0.000	.014	.03	.04	0.00	0.0	.20	5.61	6.61
340	258.	294.0	.0	-.37	0.0	.20	0.	.169E+02	.008	0.000	0.000	.013	.04	.05	0.00	0.0	.20	5.79	6.83
360	276.	294.0	.0	-.34	0.0	.21	0.	.186E+02	.008	0.000	0.000	.012	.04	.05	0.00	0.0	.21	5.97	7.05
380	293.	294.0	.0	-.31	0.0	.22	0.	.203E+02	.008	0.000	0.000	.011	.04	.05	0.00	0.0	.22	6.15	7.26
400	310.	294.0	.0	-.29	0.0	.22	0.	.222E+02	.008	0.000	0.000	.010	.04	.05	0.00	0.0	.22	6.33	7.47
412	321.	294.0	.0	-.28	0.0	.23	0.	.233E+02	.008	0.000	0.000	.010	.05	.05	0.00	0.0	.23	6.44	7.60

VERTICAL VERSUS DOWNWIND POSITION OF PUFF

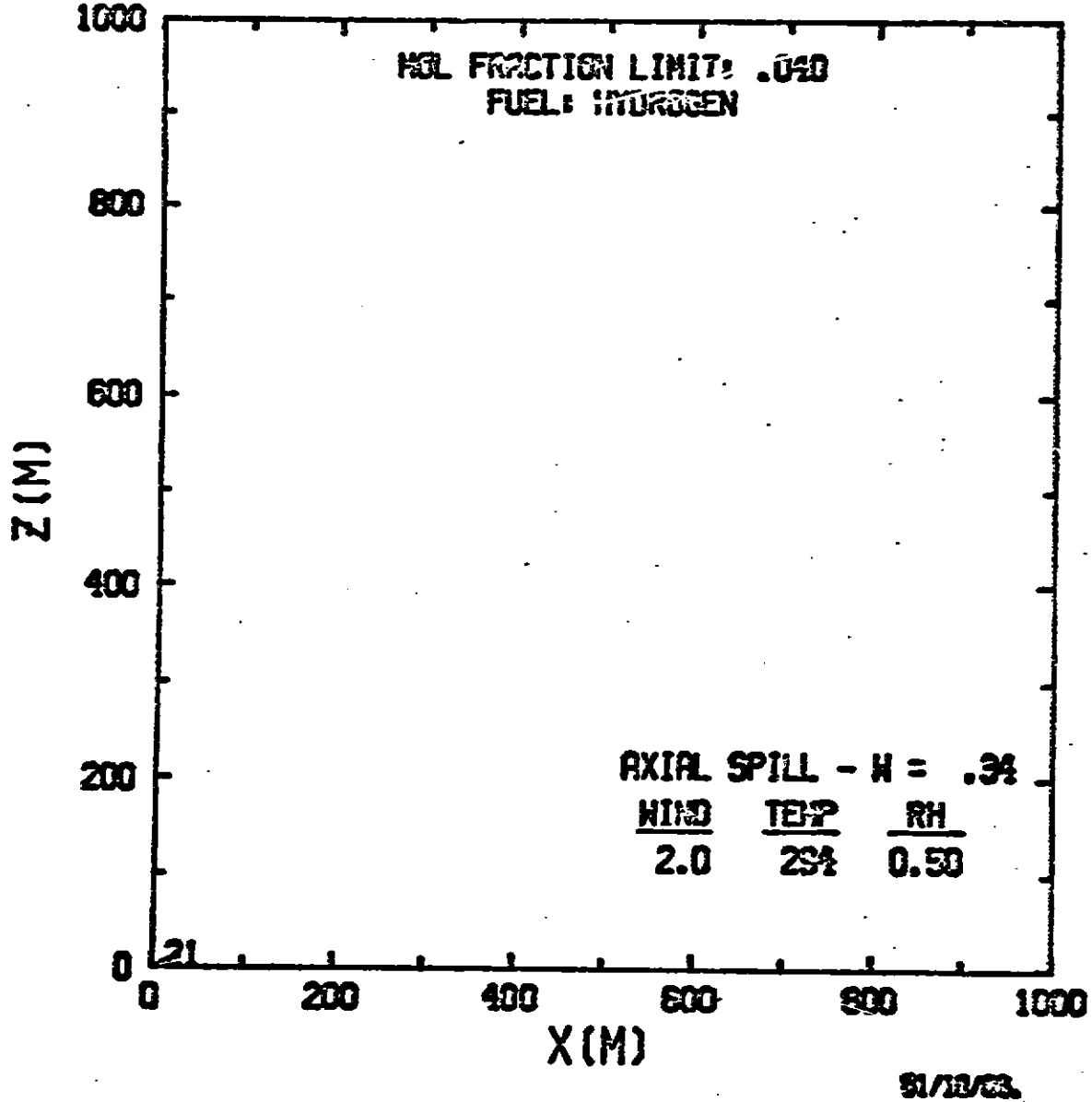

SCENARIO 3B

LOOKING AT LARGEST PUFF ONLY

SCENARIO 3B

INITIAL CONDITIONS

AXIAL SPILL - WIDTH: .3 FUEL: HYDROGEN SURFACE ELEVATION: 0.

EVAPORATION RATE: 2.500E-3 TEMP: 294 RELATIVE HUMIDITY: .50

STABILITY: 6 WIND: 2.0 M/S FMF LOWER LIMIT: .040

IT	XP M	T K	DELTEM K	A	U M/S	ZP M	ANG DEG	VP CU.M	U1 M/S	U2 M/S	U4 M/S	FMF	VES CU.M	VET CU.M	VEB CU.M	R M	ZTZP M	LL M	LU M
0	0.	20.3	0.0	0.00	0.0	.07	0.	.448E-01	0.000	0.000	0.000	1.000	0.00	0.00	0.00	0.0	.07	1.00	.34
1	0.	30.2	243.8	2.19	.3	.19	21.	.133E+00	.091	.132	0.000	.925	.06	0.00	0.00	0.0	.09	1.43	.49
2	1.	88.2	205.8	2.29	.4	.53	22.	.266E+00	.061	.044	0.000	.813	.06	.02	.02	0.0	.12	1.80	.61
3	2.	124.9	139.1	1.83	.5	.99	23.	.445E+00	.065	.022	0.000	.690	.07	.04	.04	0.0	.14	2.13	.72
4	3.	158.1	135.9	1.41	.5	1.51	24.	.682E+00	.071	.013	0.000	.570	.10	.06	.06	0.0	.16	2.46	.83
5	5.	185.9	108.1	1.13	.6	2.05	24.	.981E+00	.073	.009	0.000	.465	.13	.08	.08	0.0	.18	2.77	.94
6	6.	208.5	85.5	.95	.6	2.62	24.	.135E+01	.074	.006	0.000	.380	.16	.09	.09	0.0	.20	3.07	1.05
7	7.	226.7	67.4	.84	.6	3.19	23.	.179E+01	.075	.004	0.000	.312	.20	.11	.11	0.0	.22	3.37	1.15
8	9.	241.4	52.7	.77	.6	3.78	23.	.231E+01	.076	.003	0.000	.257	.24	.13	.13	0.0	.24	3.67	1.25
9	10.	253.1	40.9	.72	.6	4.38	23.	.292E+01	.078	.003	0.000	.213	.29	.15	.15	0.0	.26	3.97	1.35
10	12.	262.7	31.4	.69	.6	5.00	23.	.362E+01	.080	.002	0.000	.178	.34	.17	.17	0.0	.28	4.26	1.45
11	13.	270.3	23.8	.67	.6	5.64	23.	.444E+01	.082	.002	0.000	.150	.40	.19	.19	0.0	.30	4.56	1.55
12	15.	276.0	18.1	.62	.7	6.30	23.	.537E+01	.084	.001	0.000	.126	.47	.21	.21	0.0	.32	4.85	1.65
13	17.	281.4	12.6	.62	.7	6.97	23.	.614E+01	.086	.001	0.000	.107	.54	.23	.23	0.0	.34	5.15	1.75
14	18.	286.0	8.1	.62	.7	7.67	23.	.765E+01	.088	.001	0.000	.092	.62	.26	.26	0.0	.36	5.45	1.85
15	20.	287.1	6.9	.53	.7	8.37	23.	.894E+01	.091	.001	0.000	.079	.72	.29	.29	0.0	.38	5.74	1.95
16	22.	288.1	6.0	.45	.7	9.08	22.	.104E+02	.091	.001	0.000	.068	.80	.31	.31	0.0	.40	6.03	2.05
17	24.	288.8	5.3	.39	.7	9.78	22.	.119E+02	.090	.001	0.000	.060	.87	.33	.33	0.0	.42	6.31	2.14
18	25.	289.4	4.7	.34	.7	10.47	22.	.135E+02	.089	.000	0.000	.053	.94	.35	.35	0.0	.43	6.55	2.24
19	27.	289.8	4.2	.30	.7	11.14	22.	.153E+02	.088	.000	0.000	.047	1.01	.36	.36	0.0	.45	6.85	2.33
20	29.	290.4	3.7	.27	.7	11.81	22.	.171E+02	.086	.000	0.000	.042	1.07	.37	.37	0.0	.47	7.11	2.42
21	31.	290.7	3.4	.24	.6	12.46	22.	.190E+02	.085	.000	0.000	.038	1.13	.39	.39	0.0	.49	7.36	2.50

VERTICAL VERSUS DOWNWIND POSITION OF PUFF

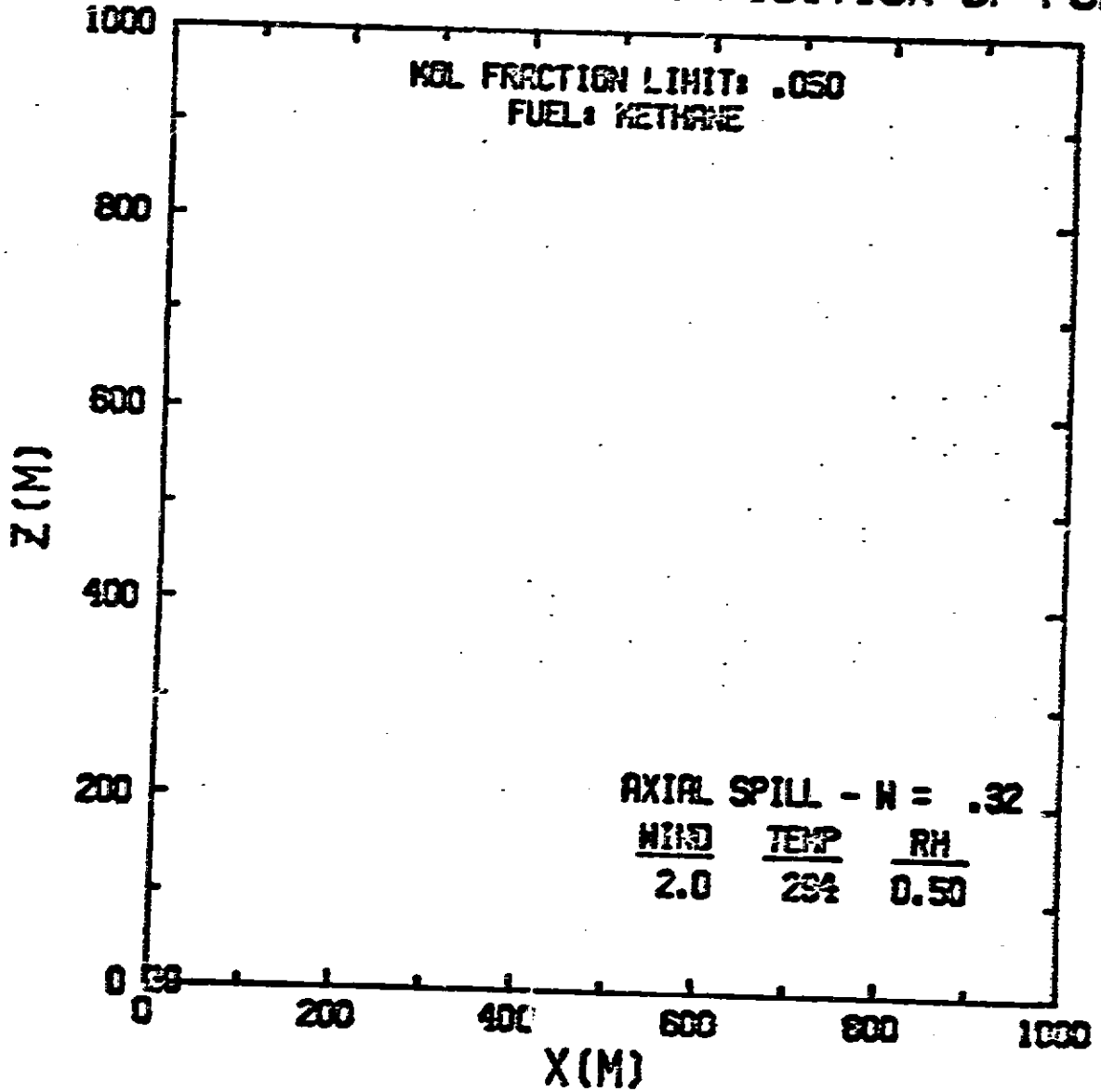

SCENARIO 3B

LOOKING AT LARGEST PUFF ONLY

INITIAL CONDITIONS

AXIAL SPILL - WIDTH: .3 FUEL: METHANE SURFACE ELEVATION: 0.

EVAPORATION RATE: 9.870E-4 TEMP: 294 RELATIVE HUMIDITY: .50

STABILITY: 6 WIND: 2.0 M/S FMF LOWER LIMIT: .050

SCENARIO 3B

IT	XP M	T K	DELTEM K	A	W M/S	ZP M	ANG DEG	VP CU.M	U1 M/S	U2 M/S	U4 M/S	FMF	VES CU.M	VET CU.M	VEB CU.M	R M	ZTZP M	LL M	LL M
0	0.	111.7	0.0	0.00	0.0	.11	0.	.728E-01	0.000	0.000	0.000	1.000	0.00	0.00	0.00	0.0	.11	1.00	.33
1	1.	191.2	102.8	-1.23	0.0	.17	18.	.228E+00	.101	.228	0.000	.574	.15	0.00	0.00	0.0	.17	1.46	.47
2	1.	224.1	69.9	-.67	0.0	.20	10.	.377E+00	.047	.073	0.000	.407	.12	.03	0.00	0.0	.20	1.72	.55
3	2.	241.7	52.3	-.39	0.0	.22	7.	.514E+00	.032	.044	0.000	.322	.10	.03	0.00	0.0	.22	1.91	.61
4	3.	252.7	41.3	-.22	0.0	.23	5.	.642E+00	.026	.032	0.000	.270	.10	.03	0.00	0.0	.23	2.05	.66
5	3.	260.3	33.7	-.12	0.0	.25	4.	.766E+00	.023	.026	0.000	.233	.09	.02	0.00	0.0	.25	2.17	.70
6	4.	266.0	28.0	-.03	0.0	.26	4.	.885E+00	.021	.022	0.000	.206	.09	.02	0.00	0.0	.26	2.28	.73
7	5.	270.6	23.4	.03	.0	.27	3.	.100E+01	.019	.019	0.000	.185	.09	.02	0.00	0.0	.27	2.38	.76
8	6.	273.0	21.0	.04	.0	.28	3.	.111E+01	.018	.017	0.000	.169	.09	.02	0.00	0.0	.28	2.48	.79
9	7.	276.8	17.3	.09	.0	.31	3.	.125E+01	.017	.015	0.000	.152	.09	.02	.02	0.0	.29	2.56	.82
10	8.	279.9	14.1	.14	.1	.35	3.	.139E+01	.017	.013	0.000	.138	.09	.02	.02	0.0	.30	2.65	.85
11	9.	282.9	11.1	.19	.1	.44	3.	.155E+01	.020	.012	0.000	.125	.10	.02	.02	0.0	.31	2.74	.88
12	9.	284.0	10.0	.17	.1	.55	3.	.173E+01	.025	.011	0.000	.113	.12	.03	.03	0.0	.32	2.84	.91
13	10.	285.0	9.0	.15	.1	.68	4.	.194E+01	.029	.010	0.000	.101	.14	.03	.03	0.0	.34	2.95	.94
14	11.	286.0	8.1	.13	.2	.83	4.	.218E+01	.033	.009	0.000	.090	.17	.04	.04	0.0	.35	3.07	.98
15	12.	286.8	7.2	.12	.2	1.00	5.	.245E+01	.036	.008	0.000	.080	.19	.04	.04	0.0	.36	3.19	1.02
16	13.	287.5	6.5	.10	.2	1.17	5.	.274E+01	.038	.007	0.000	.072	.21	.05	.05	0.0	.38	3.31	1.06
17	14.	288.2	5.8	.09	.2	1.34	5.	.306E+01	.039	.006	0.000	.064	.22	.05	.05	0.0	.39	3.44	1.10
18	16.	288.8	5.2	.08	.2	1.51	6.	.341E+01	.039	.005	0.000	.058	.24	.05	.05	0.0	.40	3.56	1.14
19	17.	289.3	4.7	.07	.2	1.68	6.	.378E+01	.040	.005	0.000	.052	.26	.06	.06	0.0	.42	3.68	1.18
20	18.	289.7	4.3	.07	.2	1.86	6.	.417E+01	.040	.004	0.000	.048	.27	.06	.06	0.0	.43	3.80	1.22

VERTICAL VERSUS DOWNWIND POSITION OF PUFF

SCENARIO 3B

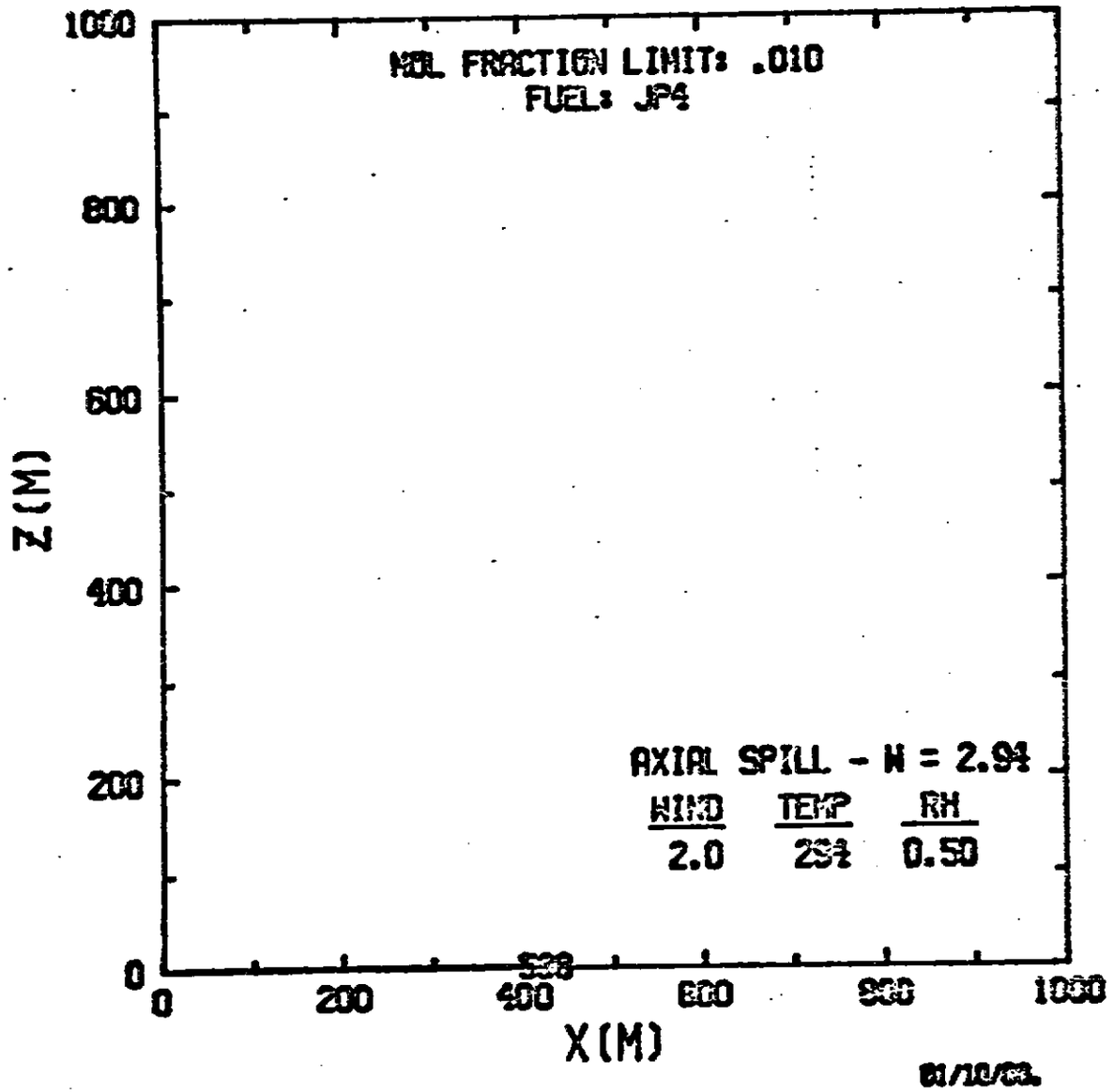

01/10/83

LOOKING AT LARGEST PUFF ONLY

INITIAL CONDITIONS

AERIAL SPILL - WIDTH: 2.9 FUEL: JP4 SURFACE ELEVATION: 0.

EVAPORATION RATE: 2.000E-6 TEMP: 294 RELATIVE HUMIDITY: .50

STABILITY: 6 WIND: 2.0 M/S FMF LOWER LIMIT: .010

SCENARIO 3B

IT	XP M	T K	DELTEM K	A	W M/S	ZP M	ANG DEG	VP CU.M	U1 M/S	U2 M/S	U4 M/S	FMF	VES CU.M	VET CU.M	VEB CU.M	R M	ZTZP M	LL M	LW M
0	0.	294.0	0.0	0.00	0.0	.04	0.	.2[illegible]E+00	0.000	0.000	0.000	.109	0.00	0.00	0.00	0.0	.04	1.00	2.94
1	0.	294.0	.0	-2.37	0.0	.04	54.	.214E+00	.080	0.000	0.000	.109	.01	0.00	0.00	0.0	.04	1.01	2.95
20	7.	294.0	.0	-2.09	0.0	.06	0.	.106E+01	.021	0.000	0.000	.092	.01	.06	0.00	0.0	.06	1.72	5.05
40	17.	294.0	.0	-1.83	0.0	.08	0.	.213E+01	.014	0.000	0.000	.078	.01	.06	0.00	0.0	.08	2.16	6.36
60	33.	294.0	.0	-1.63	0.0	.09	0.	.326E+01	.011	0.000	0.000	.068	.01	.06	0.00	0.0	.09	2.49	7.31
80	47.	294.0	.0	-1.46	0.0	.10	0.	.446E+01	.010	0.000	0.000	.059	.01	.06	0.00	0.0	.10	2.76	8.11
100	61.	294.0	.0	-1.31	0.0	.11	0.	.575E+01	.009	0.000	0.000	.053	.01	.06	0.00	0.0	.11	3.00	8.82
120	76.	294.0	.0	-1.19	0.0	.11	0.	.713E+01	.009	0.000	0.000	.047	.01	.06	0.00	0.0	.11	3.22	9.47
140	91.	294.0	.0	-1.08	0.0	.12	0.	.860E+01	.009	0.000	0.000	.042	.01	.07	0.00	0.0	.12	3.43	10.08
160	106.	294.0	.0	-.99	0.0	.13	0.	.102E+02	.008	0.000	0.000	.038	.02	.07	0.00	0.0	.13	3.62	10.65
180	122.	294.0	.0	-.91	0.0	.13	0.	.118E+02	.008	0.000	0.000	.035	.02	.07	0.00	0.0	.13	3.81	11.21
200	137.	294.0	.0	-.83	0.0	.14	0.	.136E+02	.008	0.000	0.000	.032	.02	.08	0.00	0.0	.14	3.99	11.72
220	153.	294.0	.0	-.77	0.0	.15	0.	.155E+02	.008	0.000	0.000	.029	.02	.08	0.00	0.0	.15	4.16	12.23
240	169.	294.0	.0	-.71	0.0	.15	0.	.174E+02	.008	0.000	0.000	.027	.02	.08	0.00	0.0	.15	4.33	12.72
260	185.	294.0	.0	-.66	0.0	.16	0.	.195E+02	.008	0.000	0.000	.025	.02	.08	0.00	0.0	.16	4.49	13.20
280	201.	294.0	.0	-.61	0.0	.16	0.	.216E+02	.008	0.000	0.000	.023	.02	.09	0.00	0.0	.16	4.65	13.66
300	218.	294.0	.0	-.57	0.0	.17	0.	.239E+02	.008	0.000	0.000	.021	.03	.09	0.00	0.0	.17	4.80	14.11
320	234.	294.0	.0	-.53	0.0	.17	0.	.262E+02	.008	0.000	0.000	.020	.03	.09	0.00	0.0	.17	4.95	14.55
340	251.	294.0	.0	-.50	0.0	.18	0.	.287E+02	.008	0.000	0.000	.018	.03	.10	0.00	0.0	.18	5.10	14.99
360	267.	294.0	.0	-.47	0.0	.18	0.	.312E+02	.008	0.000	0.000	.017	.03	.10	0.00	0.0	.18	5.24	15.42
380	284.	294.0	.0	-.44	0.0	.19	0.	.338E+02	.008	0.000	0.000	.016	.03	.10	0.00	0.0	.19	5.39	15.84
400	301.	294.0	.0	-.41	0.0	.19	0.	.366E+02	.008	0.000	0.000	.015	.03	.11	0.00	0.0	.19	5.53	16.25
420	318.	294.0	.0	-.39	0.0	.20	0.	.394E+02	.008	0.000	0.000	.014	.03	.11	0.00	0.0	.20	5.68	16.65
440	335.	294.0	.0	-.36	0.0	.20	0.	.424E+02	.008	0.000	0.000	.013	.04	.11	0.00	0.0	.20	5.80	17.05
460	352.	294.0	.0	-.34	0.0	.21	0.	.454E+02	.008	0.000	0.000	.012	.04	.12	0.00	0.0	.21	5.93	17.43
480	367.	294.0	.0	-.33	0.0	.21	0.	.485E+02	.008	0.000	0.000	.012	.04	.12	0.00	0.0	.21	6.07	17.83
500	387.	294.0	.0	-.31	0.0	.22	0.	.518E+02	.008	0.000	0.000	.011	.04	.12	0.00	0.0	.22	6.20	18.21
520	404.	294.0	.0	-.29	0.0	.22	0.	.551E+02	.008	0.000	0.000	.010	.04	.13	0.00	0.0	.22	6.33	18.61
536	420.	294.0	.0	-.28	0.0	.23	0.	.582E+02	.008	0.000	0.000	.010	.05	.13	0.00	0.0	.23	6.44	18.93

VERTICAL VERSUS DOWNWIND POSITION OF PUFF

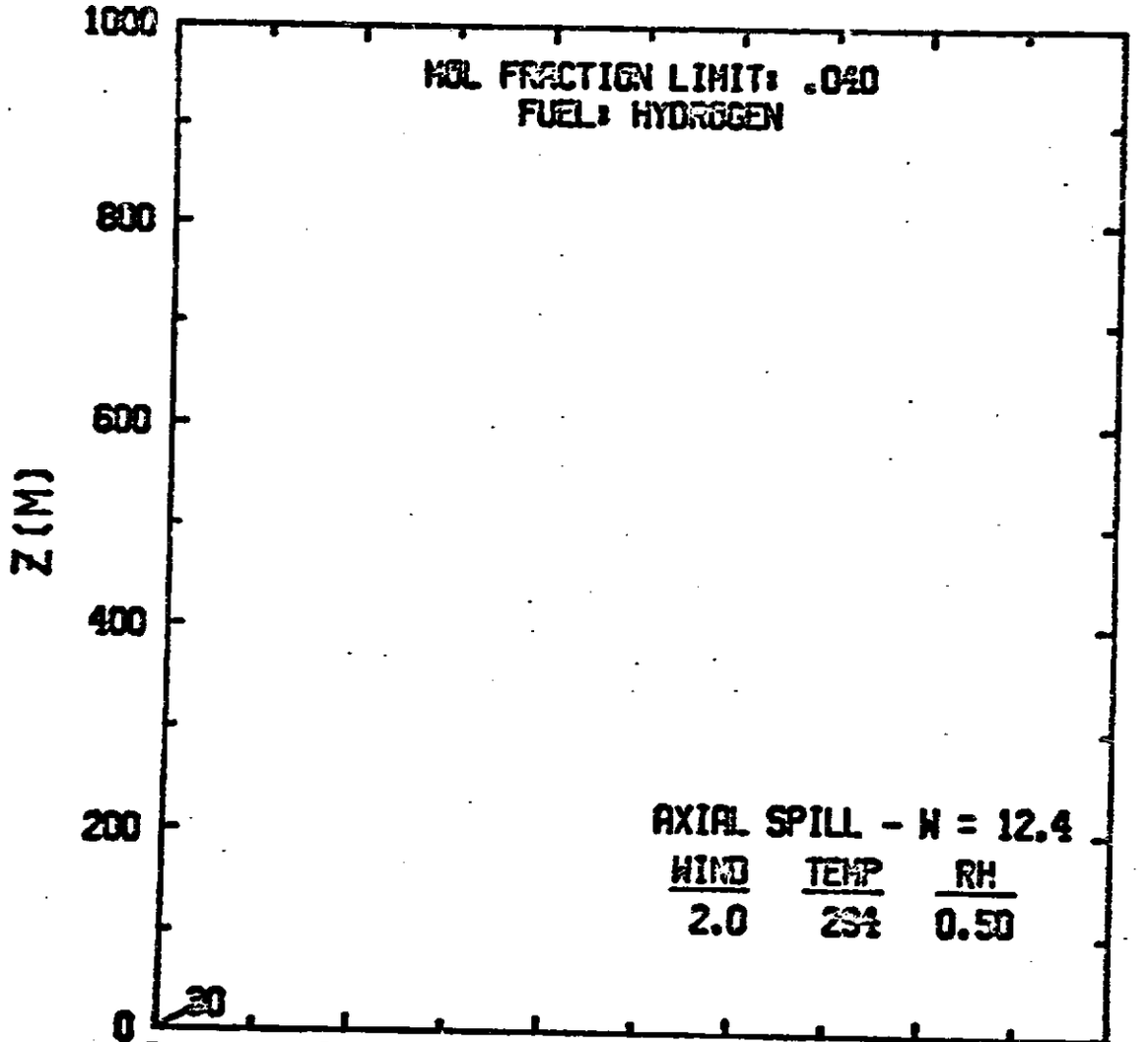

SCENARIO 3C

LOOKING AT LARGEST PUFF ONLY
INITIAL CONDITIONS
AXIAL SPILL - WIDTH: 12.4
EVAPORATION RATE: 2.510E-3
STABILITY: 6

SCENARIO 3C

FUEL: HYDROGEN
TEMP: 294
WIND: 2.0 M/S
SURFACE ELEVATION: 0.
RELATIVE HUMIDITY: .50
FMF LOWER LIMIT: .040

IT	XP M	T K	DELTEM K	A	U M/S
0	0.	20.3	0.0	0.00	0.0
1	0.	21.2	272.8	.05	.0
2	0.	24.0	270.0	.45	.1
4	1.	53.6	240.4	2.29	.6
6	3.	119.3	174.7	1.90	.7
8	6.	173.3	120.7	1.25	.7
10	9.	211.0	83.0	.93	.7
12	12.	237.2	56.9	.79	.8
14	15.	255.5	38.6	.72	.8
16	19.	268.6	25.5	.68	.9
18	23.	277.1	17.0	.62	.9
20	26.	284.5	9.7	.62	1.0
22	30.	286.3	7.8	.49	1.0
24	34.	287.7	6.5	.40	1.0
26	38.	288.7	5.4	.33	1.0
28	42.	289.5	4.7	.28	.9
30	47.	290.1	4.1	.24	.9

ZP M	ANG DEG	VP CU.M	U1 M/S	U2 M/S	U4 M/S	FMF	VES CU.M	VET CU.M	VEB CU.M	R M	ZTZP M	LL M	LW M
.07	0.	.164E+01	0.000	0.000	0.000	1.000	0.00	0.00	0.00	0.0	.07	1.00	12.40
.07	72.	.191E+01	.091	.132	0.000	.998	.06	0.00	0.00	0.0	.07	1.05	13.03
.14	49.	.218E+01	.090	.114	0.000	.991	.06	.06	.06	0.0	.07	1.10	13.61
.82	38.	.526E+01	.101	.073	0.000	.916	.07	.77	.77	0.0	.10	1.47	18.21
2.08	33.	.151E+02	.093	.023	0.000	.710	.10	2.46	2.46	0.0	.14	2.08	25.80
3.47	31.	.304E+02	.092	.010	0.000	.513	.15	3.85	3.85	0.0	.17	2.62	32.49
4.93	29.	.513E+02	.095	.005	0.000	.370	.22	5.20	5.20	0.0	.21	3.11	38.60
6.45	28.	.783E+02	.098	.003	0.000	.273	.30	6.63	6.63	0.0	.24	3.58	44.39
8.05	28.	.112E+03	.102	.002	0.000	.205	.40	8.25	8.25	0.0	.27	4.03	49.99
9.74	27.	.154E+03	.108	.002	0.000	.157	.52	10.08	10.08	0.0	.30	4.46	55.49
11.51	27.	.204E+03	.113	.001	0.000	.123	.66	12.02	12.02	0.0	.32	4.91	60.85
13.38	27.	.263E+03	.118	.001	0.000	.097	.83	14.22	14.22	0.0	.35	5.34	66.25
15.31	27.	.329E+03	.123	.001	0.000	.078	1.01	16.49	16.49	0.0	.38	5.75	71.32
17.26	27.	.403E+03	.124	.001	0.000	.064	1.17	18.20	18.20	0.0	.41	6.15	76.22
19.18	27.	.482E+03	.122	.000	0.000	.054	1.31	19.60	19.60	0.0	.43	6.52	80.90
21.06	26.	.567E+03	.120	.000	0.000	.046	1.44	20.79	20.79	0.0	.46	6.88	85.34
22.91	26.	.657E+03	.118	.000	0.000	.040	1.56	21.83	21.83	0.0	.48	7.22	89.57

VERTICAL VERSUS DOWNWIND POSITION OF PUFF

SCENARIO 3C

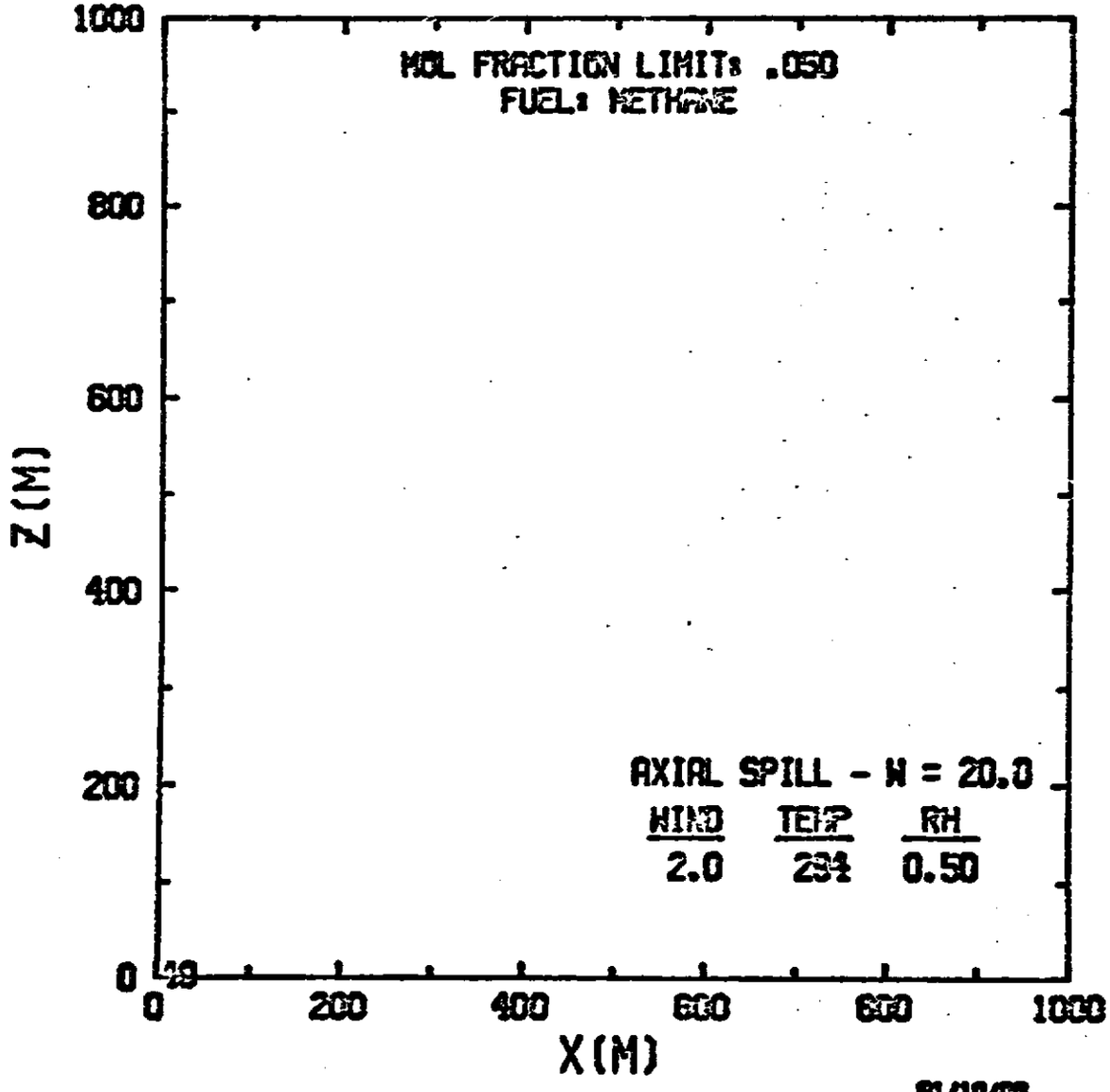

01/10/83

LOOKING AT LARGEST PUFF ONLY

INITIAL CONDITIONS

AXIAL SPILL - WIDTH: 20.0 FUEL: METHANE SURFACE ELEVATION: 0.

EVAPORATION RATE: 2.300E-4 TEMP: 294 RELATIVE HUMIDITY: .50

STABILITY: 6 WIND: 2.0 M/S FMF LOWER LIMIT: .050

SCENARIO 3C

IT	XP M	T K	DELTEM K	A	U M/S	ZP M	ANG DEG	VP CU.M	U1 M/S	U2 M/S	U4 M/S	FMF	VES CU.M	VET CU.M	VEB CU.M	R M	ZTZP M	LL M	LW M
0	0.	111.7	0.0	0.00	0.0	.03	0.	.106E+01	0.000	0.000	0.000	1.000	0.00	0.00	0.00	0.0	.03	1.00	20.00
1	0.	112.6	181.4	-3.05	0.0	.03	79.	.113E+01	.076	.053	0.000	.995	.01	0.00	0.00	0.0	.03	1.02	20.42
2	0.	114.2	179.8	-3.00	0.0	.03	54.	.116E+01	.075	.050	0.000	.986	.01	.01	0.00	0.0	.03	1.03	20.57
4	0.	122.5	171.5	-2.76	0.0	.03	14.	.130E+01	.072	.047	0.000	.940	.01	.08	0.00	0.0	.03	1.07	21.42
6	0.	143.5	150.5	-2.22	0.0	.03	4.	.174E+01	.064	.038	0.000	.836	.01	.25	0.00	0.0	.03	1.16	23.53
8	1.	173.5	120.5	-1.56	0.0	.04	2.	.260E+01	.050	.027	0.000	.667	.01	.46	0.00	0.0	.04	1.34	26.88
10	2.	199.1	94.9	-1.09	0.0	.04	1.	.373E+01	.037	.018	0.000	.533	.01	.56	0.00	0.0	.04	1.51	30.29
12	3.	217.8	76.2	-.77	0.0	.04	1.	.496E+01	.030	.013	0.000	.438	.01	.59	0.00	0.0	.04	1.66	33.28
14	4.	231.3	62.7	-.55	0.0	.05	1.	.620E+01	.025	.010	0.000	.372	.01	.58	0.00	0.0	.05	1.79	35.83
16	5.	241.4	52.6	-.39	0.0	.05	1.	.744E+01	.022	.008	0.000	.324	.01	.57	0.00	0.0	.05	1.90	38.03
18	6.	249.0	45.0	-.28	0.0	.05	1.	.864E+01	.020	.007	0.000	.288	.01	.56	0.00	0.0	.05	2.00	39.97
20	7.	254.9	39.1	-.19	0.0	.06	0.	.983E+01	.018	.006	0.000	.259	.01	.55	0.00	0.0	.06	2.08	41.70
22	8.	259.7	34.3	-.12	0.0	.06	0.	.110E+02	.017	.005	0.000	.236	.01	.54	0.00	0.0	.06	2.16	43.27
24	9.	263.7	30.3	-.07	0.0	.06	0.	.121E+02	.016	.005	0.000	.217	.01	.53	0.00	0.0	.06	2.24	44.71
26	10.	267.1	26.9	-.02	0.0	.06	0.	.133E+02	.015	.004	0.000	.201	.01	.53	0.00	0.0	.06	2.30	46.05
28	12.	270.0	24.0	.02	.0	.07	0.	.144E+02	.014	.004	0.000	.187	.01	.52	0.00	0.0	.06	2.36	47.30
30	13.	274.2	19.8	.06	.0	.10	0.	.163E+02	.017	.004	0.000	.163	.01	.62	.62	0.0	.07	2.47	49.76
32	14.	280.3	13.7	.15	.1	.21	1.	.205E+02	.026	.003	0.000	.137	.02	.97	.97	0.0	.07	2.66	53.15
34	16.	284.8	9.2	.17	.1	.43	2.	.264E+02	.038	.002	0.000	.108	.03	1.59	1.59	0.0	.08	2.89	57.75
36	17.	286.9	7.1	.13	.2	.74	2.	.348E+02	.044	.002	0.000	.082	.04	2.26	2.26	0.0	.08	3.17	63.31
38	19.	288.5	5.5	.10	.2	1.06	3.	.436E+02	.045	.001	0.000	.063	.05	2.81	2.81	0.0	.09	3.46	69.22
40	21.	289.7	4.3	.07	.2	1.39	4.	.584E+02	.044	.001	0.000	.050	.06	3.26	3.26	0.0	.10	3.75	75.08

VERTICAL VERSUS DOWNWIND POSITION OF PUFF

SCENARIO 3C

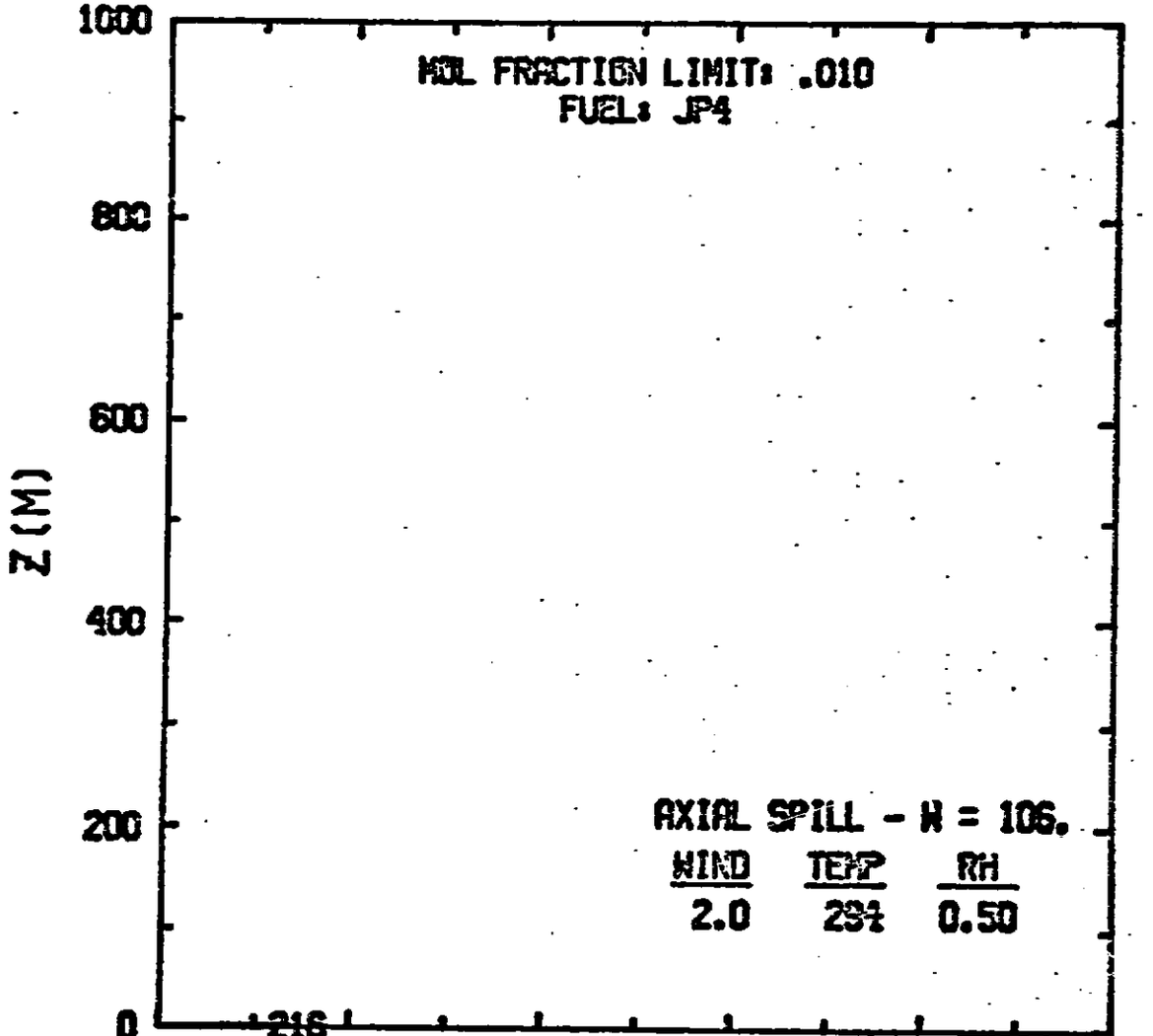

01/10/86.

C JP4

LOOKING AT LARGEST PUFF ONLY

INITIAL CONDITIONS

AXIAL SPILL - WIDTH: 106.0 FUEL: JP4 SURFACE ELEVATION: 0.

EVAPORATION RATE: 2.000E-6 TEMP: 294 RELATIVE HUMIDITY: .50

STABILITY: 6 WIND: 2.0 M/S FMF LOWER LIMIT: .010

SCENARIO 3C

IT	XP M	T K	DELTEM K	A	W M/S	ZP M	ANG DEG	VP CU.M	U1 M/S	U2 M/S	U4 M/S	FMF	VES CU.M	VET CU.M	VEB CU.M	R M	ZTZP M	LL M	LW M
0	0.	294.0	0.0	0.00	0.0	.04	0.	.742E+01	0.000	0.000	0.000	.109	0.00	0.00	0.00	0.0	.04	1.00	106.00
1	0.	294.0	.0	-2.37	0.0	.04	89.	.743E+01	.080	0.000	0.000	.109	.01	0.00	0.00	0.0	.04	1.00	106.04
10	0.	294.0	.0	-2.32	0.0	.04	8.	.856E+01	.073	0.000	0.000	.106	.01	.47	0.00	0.0	.04	1.05	111.11
20	3.	294.0	.0	-1.87	0.0	.05	1.	.210E+02	.035	0.000	0.000	.080	.01	2.06	0.00	0.0	.05	1.41	149.47
30	8.	294.0	.0	-1.47	0.0	.06	0.	.397E+02	.021	0.000	0.000	.060	.01	2.11	0.00	0.0	.06	1.74	184.39
40	14.	294.0	.0	-1.22	0.0	.07	0.	.590E+02	.016	0.000	0.000	.048	.01	2.07	0.00	0.0	.07	1.98	210.15
50	20.	294.0	.0	-1.04	0.0	.08	0.	.786E+02	.014	0.000	0.000	.040	.01	2.05	0.00	0.0	.08	2.18	230.96
60	27.	294.0	.0	-.91	0.0	.08	0.	.984E+02	.013	0.000	0.000	.035	.01	2.06	0.00	0.0	.08	2.35	248.75
70	34.	294.0	.0	-.80	0.0	.09	0.	.119E+03	.012	0.000	0.000	.030	.01	2.08	0.00	0.0	.09	2.50	264.51
80	41.	294.0	.0	-.72	0.0	.09	0.	.139E+03	.011	0.000	0.000	.027	.01	2.10	0.00	0.0	.09	2.63	278.78
90	48.	294.0	.0	-.65	0.0	.10	0.	.160E+03	.010	0.000	0.000	.024	.01	2.13	0.00	0.0	.10	2.75	291.93
100	55.	294.0	.0	-.59	0.0	.10	0.	.181E+03	.010	0.000	0.000	.022	.01	2.16	0.00	0.0	.10	2.87	304.20
110	62.	294.0	.0	-.55	0.0	.10	0.	.203E+03	.010	0.000	0.000	.020	.01	2.20	0.00	0.0	.10	2.98	315.74
120	69.	294.0	.0	-.50	0.0	.11	0.	.225E+03	.009	0.000	0.000	.018	.01	2.24	0.00	0.0	.11	3.08	326.68
130	77.	294.0	.0	-.47	0.0	.11	0.	.247E+03	.009	0.000	0.000	.017	.01	2.28	0.00	0.0	.11	3.18	337.12
140	84.	294.0	.0	-.44	0.0	.11	0.	.270E+03	.009	0.000	0.000	.016	.01	2.32	0.00	0.0	.11	3.27	347.12
150	92.	294.0	.0	-.41	0.0	.12	0.	.293E+03	.009	0.000	0.000	.015	.01	2.36	0.00	0.0	.12	3.37	356.75
160	99.	294.0	.0	-.38	0.0	.12	0.	.317E+03	.009	0.000	0.000	.014	.01	2.40	0.00	0.0	.12	3.45	366.04
170	107.	294.0	.0	-.36	0.0	.12	0.	.341E+03	.009	0.000	0.000	.013	.01	2.44	0.00	0.0	.12	3.54	375.05
180	114.	294.0	.0	-.34	0.0	.13	0.	.366E+03	.008	0.000	0.000	.012	.02	2.48	0.00	0.0	.13	3.62	383.76
190	122.	294.0	.0	-.32	0.0	.13	0.	.391E+03	.008	0.000	0.000	.012	.02	2.53	0.00	0.0	.13	3.70	392.25
200	130.	294.0	.0	-.30	0.0	.13	0.	.417E+03	.008	0.000	0.000	.011	.02	2.57	0.00	0.0	.13	3.78	400.22
210	138.	294.0	.0	-.29	0.0	.13	0.	.443E+03	.008	0.000	0.000	.010	.02	2.61	0.00	0.0	.13	3.85	408.82
216	142.	294.0	.0	-.28	0.0	.14	0.	.459E+03	.008	0.000	0.000	.010	.02	2.64	0.00	0.0	.14	3.90	413.35

VERTICAL VERSUS DOWNWIND POSITION OF PUFF

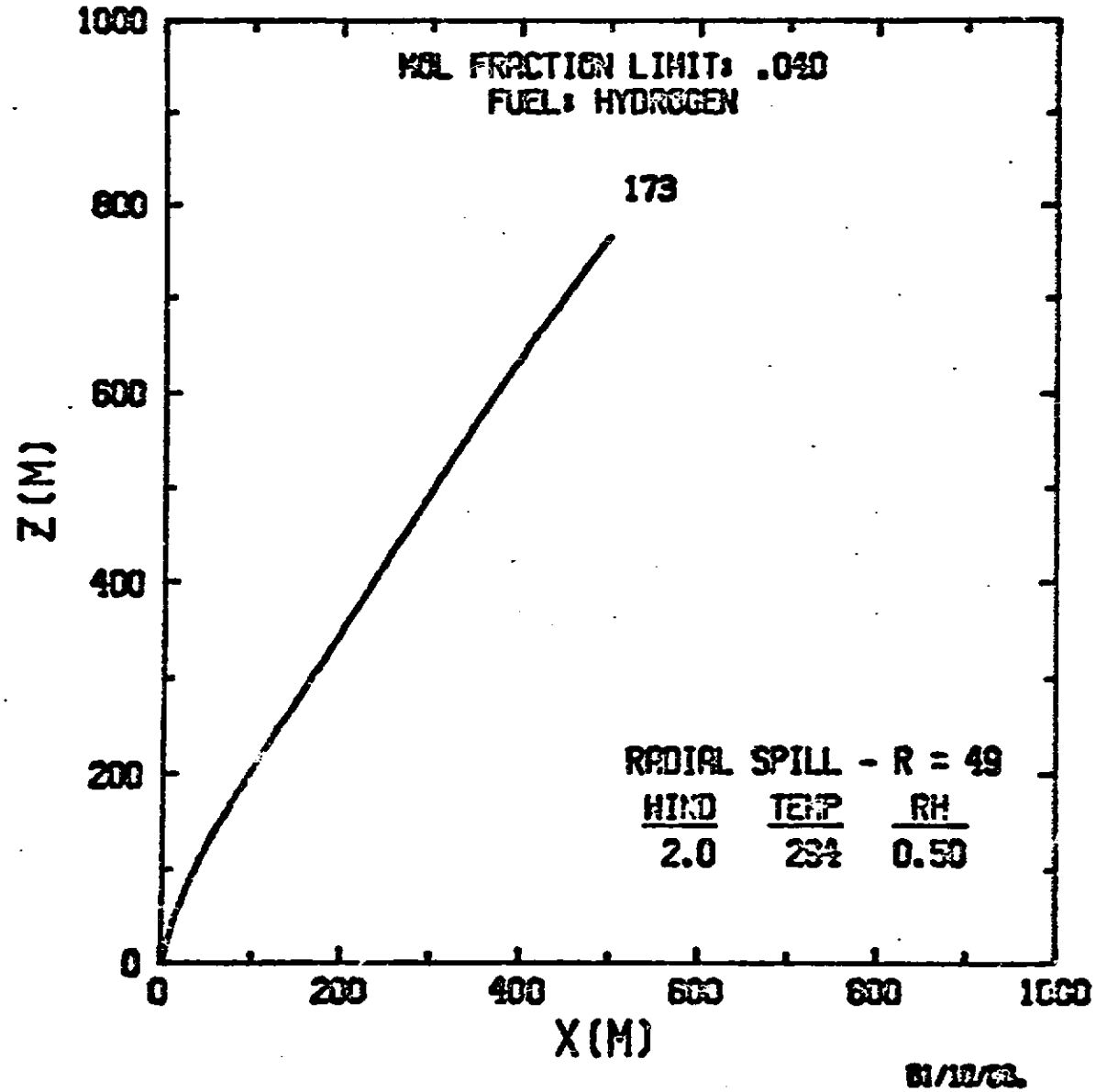

SCENARIO 4A

01/10/83

LOOKING AT LARGEST PUFF ONLY

INITIAL CONDITIONS

SCENARIO 4A

RADIAL SPILL - RADIUS: 49.0 FUEL: HYDROGEN SURFACE ELEVATION: 0.

EVAPORATION RATE: 1.940E-3 TEMP: 294 RELATIVE HUMIDITY: .50

STABILITY: 6 WIND: 2.0 M/S FMF LOWER LIMIT: .040

IT	XP	T	DELTEM	A	W	ZP	ANG	VP	U1	U2	U4	FMF	VES	VET	VEB	R	ZTOP	LL	LW
	M	K	K		M/S	M	DEG	CU.M	M/S	M/S	M/S		CU.M	CU.M	CU.M	M	M	M	M
0	0.	288.3	0.0	0.00	0.0	.05	0.	.771E+03	0.000	0.000	0.000	1.000	0.00	0.00	0.00	49.0	.05	0.00	0.00
1	0.	288.5	273.5	-.06	-.0	.05	85.	.865E+03	.086	.102	0.000	1.000	5.94	0.00	0.00	48.9	.05	0.00	0.00
10	0.	292.4	271.6	.24	.2	.58	64.	.953E+03	.125	.084	0.000	.995	6.94	.84	.84	50.5	.05	0.00	0.00
20	2.	297.4	266.7	.82	1.4	7.66	76.	.118E+04	.247	.069	0.000	.982	11.95	6.67	6.67	54.2	.06	0.00	0.00
30	8.	306.1	248.2	1.99	3.6	32.25	76.	.209E+04	.460	.041	0.000	.935	26.69	47.05	47.05	65.3	.07	0.00	0.00
40	25.	315.0	195.7	2.11	4.8	76.32	72.	.543E+04	.606	.016	0.000	.777	61.88	174.52	174.92	89.7	.09	0.00	0.00
50	50.	336.9	138.4	1.39	4.9	125.22	68.	.117E+05	.611	.007	0.000	.575	103.70	295.41	295.41	115.6	.12	0.00	0.00
60	79.	359.1	96.6	1.00	4.8	173.66	65.	.205E+05	.600	.004	0.000	.418	148.57	393.30	393.30	139.2	.15	0.00	0.00
70	111.	383.4	67.4	.83	4.8	221.75	63.	.319E+05	.600	.003	0.000	.310	199.58	488.52	488.52	161.2	.17	0.00	0.00
80	145.	409.1	46.5	.77	5.0	270.61	62.	.462E+05	.616	.002	0.000	.235	261.88	595.94	595.94	181.9	.19	0.00	0.00
90	180.	436.7	31.5	.73	5.2	321.27	61.	.638E+05	.641	.001	0.000	.181	337.95	719.36	719.36	202.3	.21	0.00	0.00
100	216.	472.9	22.0	.65	5.4	374.21	60.	.847E+05	.670	.001	0.000	.142	426.33	854.72	854.72	222.2	.23	0.00	0.00
110	254.	489.9	13.6	.65	5.6	429.08	59.	.110E+06	.693	.001	0.000	.113	524.94	993.90	993.90	242.3	.25	0.00	0.00
120	293.	494.5	9.7	.56	5.8	486.09	59.	.139E+06	.718	.001	0.000	.092	635.11	1143.08	1143.08	261.6	.27	0.00	0.00
130	332.	495.6	8.1	.45	5.8	544.00	59.	.171E+06	.720	.000	0.000	.075	730.53	1257.27	1257.27	280.0	.29	0.00	0.00
140	373.	496.4	7.0	.36	5.7	601.40	58.	.206E+06	.709	.000	0.000	.063	814.79	1346.16	1346.16	297.7	.31	0.00	0.00
150	414.	496.9	6.1	.30	5.6	657.67	58.	.243E+06	.693	.000	0.000	.054	890.62	1417.90	1417.90	314.5	.33	0.00	0.00
160	456.	497.2	5.5	.25	5.4	712.55	57.	.282E+06	.676	.000	0.000	.047	959.65	1477.21	1477.21	330.6	.35	0.00	0.00
170	499.	497.3	5.0	.22	5.3	765.97	57.	.324E+06	.658	.000	0.000	.041	1022.91	1526.95	1526.95	345.9	.36	0.00	0.00
173	512.	497.4	4.9	.21	5.2	781.71	57.	.337E+06	.652	.000	0.000	.040	1040.86	1540.30	0.00	350.3	.37	0.00	0.00

VERTICAL VERSUS DOWNWIND POSITION OF PUFF

SCENARIO 4A

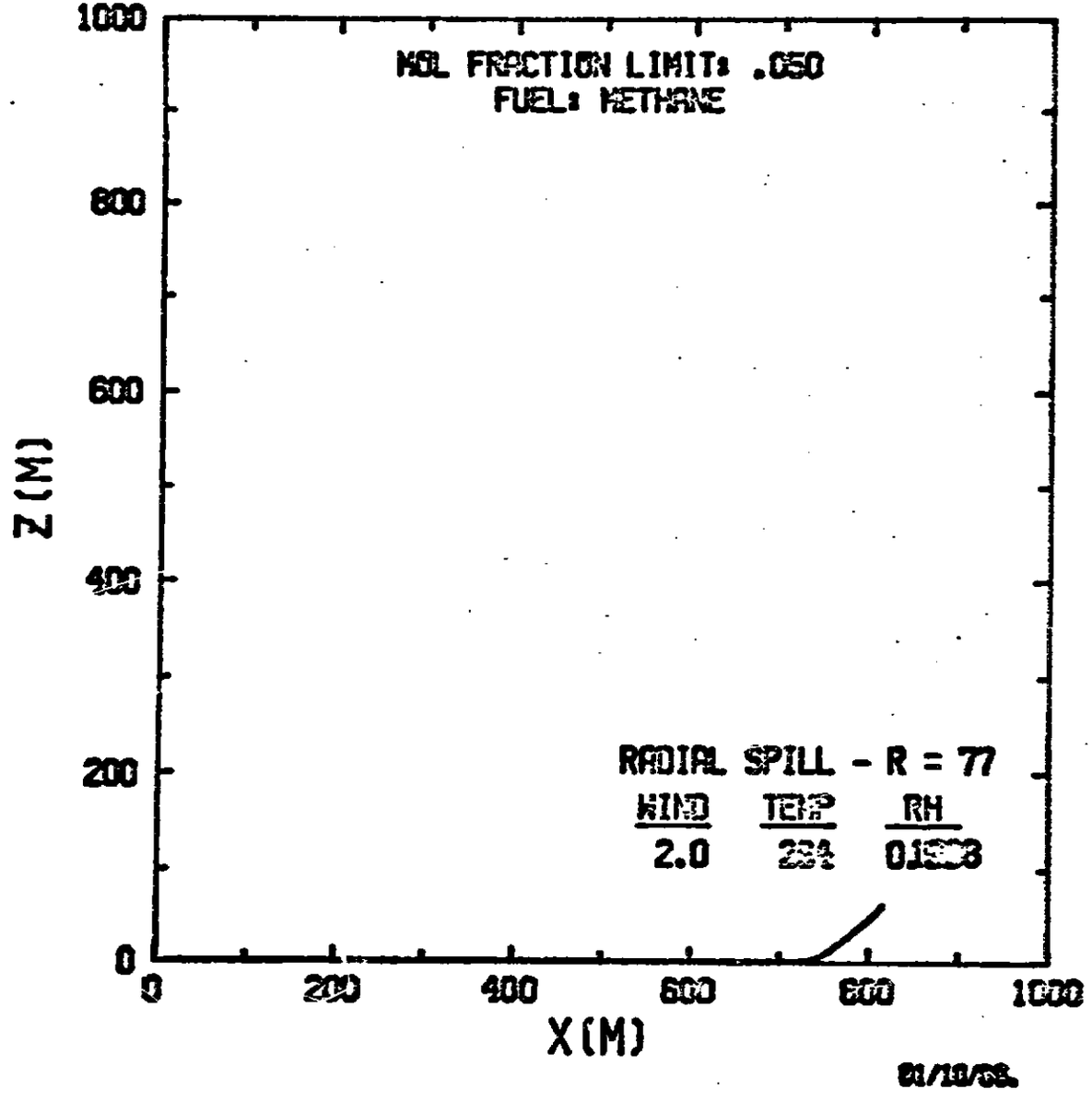

LOOKING AT LARGEST PUFF ONLY

INITIAL CONDITIONS

RADIAL SPILL - RADIUS: 77.0 FUEL: METHANE SURFACE ELEVATION: 0.

EVAPORATION RATE: 1.000E-4 TEMP: 294 RELATIVE HUMIDITY: .50

STABILITY: 6 WIND: 2.0 M/S FMF LOWER LIMIT: .050

SCENARIO 4A

IT	XP	T	DELTEM	A	U	ZP	ANG	VP	U1	U2	U4	FMF	VES	VET	VEB	R	ZTZP	LL	LW
	M	K	K		M/S	M	DEG	CU.M	M/S	M/S	M/S		CU.M	CU.M	CU.M	M	M	M	M
0	0.	111.7	0.0	0.00	0.0	.01	0.	.429E+03	0.000	0.000	0.000	1.000	0.00	0.00	0.00	77.0	.01	0.00	0.00
1	0.	111.9	182.1	-3.07	-.8	.01	56.	.452E+03	.064	.023	0.000	.999	.97	0.00	0.00	75.0	.01	0.00	0.00
60	1.	121.5	172.5	-2.79	0.0	.01	0.	.519E+03	.058	.019	0.000	.946	.90	.46	0.00	75.5	.01	0.00	0.00
120	6.	133.6	160.4	-2.47	0.0	.01	0.	.614E+03	.052	.016	0.000	.879	.89	.91	0.00	83.0	.01	0.00	0.00
180	14.	146.9	147.1	-2.14	0.0	.01	0.	.735E+03	.046	.014	0.000	.808	.87	1.29	0.00	88.0	.01	0.00	0.00
240	25.	160.1	133.9	-1.84	0.0	.01	0.	.876E+03	.041	.011	0.000	.738	.86	1.57	0.00	93.3	.01	0.00	0.00
300	38.	172.1	121.9	-1.59	0.0	.01	0.	.103E+04	.037	.010	0.000	.675	.84	1.76	0.00	98.5	.01	0.00	0.00
360	54.	182.7	111.3	-1.39	0.0	.02	0.	.119E+04	.033	.008	0.000	.618	.83	1.89	0.00	103.3	.02	0.00	0.00
420	72.	192.0	102.0	-1.22	0.0	.02	0.	.136E+04	.030	.007	0.000	.569	.82	1.96	0.00	107.9	.02	0.00	0.00
480	91.	200.3	93.7	-1.07	0.0	.02	0.	.154E+04	.028	.006	0.000	.527	.81	2.01	0.00	112.3	.02	0.00	0.00
540	112.	207.5	86.5	-.95	0.0	.02	0.	.171E+04	.026	.006	0.000	.490	.80	2.04	0.00	116.4	.02	0.00	0.00
600	134.	213.9	80.1	-.84	0.0	.02	0.	.189E+04	.024	.005	0.000	.458	.79	2.05	0.00	120.2	.02	0.00	0.00
660	157.	219.6	74.4	-.74	0.0	.02	0.	.207E+04	.023	.005	0.000	.429	.79	2.06	0.00	123.8	.02	0.00	0.00
720	180.	224.7	69.3	-.66	0.0	.02	0.	.224E+04	.021	.004	0.000	.405	.78	2.06	0.00	127.3	.02	0.00	0.00
780	205.	229.2	64.8	-.59	0.0	.02	0.	.242E+04	.020	.004	0.000	.382	.78	2.05	0.00	130.5	.02	0.00	0.00
840	230.	233.3	60.7	-.52	0.0	.02	0.	.260E+04	.019	.004	0.000	.363	.78	2.05	0.00	133.6	.02	0.00	0.00
900	255.	237.0	57.0	-.46	0.0	.02	0.	.278E+04	.019	.004	0.000	.345	.77	2.04	0.00	136.5	.02	0.00	0.00
960	281.	240.4	53.6	-.41	0.0	.02	0.	.295E+04	.018	.003	0.000	.329	.77	2.03	0.00	139.4	.02	0.00	0.00
1020	308.	243.5	50.5	-.36	0.0	.02	0.	.313E+04	.017	.003	0.000	.314	.77	2.02	0.00	142.1	.02	0.00	0.00
1080	335.	246.3	47.7	-.32	0.0	.02	0.	.331E+04	.017	.003	0.000	.301	.77	2.01	0.00	144.6	.02	0.00	0.00
1140	362.	248.8	45.2	-.28	0.0	.02	0.	.348E+04	.016	.003	0.000	.289	.77	2.00	0.00	147.1	.02	0.00	0.00
1200	390.	251.1	42.9	-.25	0.0	.02	0.	.366E+04	.016	.003	0.000	.277	.77	1.99	0.00	149.5	.02	0.00	0.00
1260	418.	253.3	40.7	-.22	0.0	.02	0.	.383E+04	.015	.003	0.000	.267	.77	1.98	0.00	151.8	.02	0.00	0.00
1320	446.	255.2	38.8	-.19	0.0	.02	0.	.400E+04	.015	.002	0.000	.258	.77	1.98	0.00	154.0	.02	0.00	0.00
1380	475.	257.0	37.0	-.16	0.0	.02	0.	.418E+04	.014	.002	0.000	.249	.77	1.97	0.00	156.2	.02	0.00	0.00
1440	504.	258.8	35.2	-.14	0.0	.02	0.	.435E+04	.014	.002	0.000	.240	.77	1.96	0.00	158.3	.02	0.00	0.00
1500	533.	260.4	33.6	-.11	0.0	.02	0.	.452E+04	.014	.002	0.000	.233	.77	1.95	0.00	160.3	.02	0.00	0.00
1560	562.	261.9	32.1	-.09	0.0	.02	0.	.469E+04	.013	.002	0.000	.226	.77	1.95	0.00	162.3	.02	0.00	0.00
1620	592.	263.3	30.7	-.07	0.0	.02	0.	.486E+04	.013	.002	0.000	.219	.77	1.94	0.00	164.2	.02	0.00	0.00
1680	622.	264.7	29.3	-.05	0.0	.02	0.	.503E+04	.013	.002	0.000	.212	.77	1.93	0.00	166.1	.02	0.00	0.00
1740	652.	265.9	28.1	-.04	0.0	.03	0.	.520E+04	.013	.002	0.000	.206	.77	1.93	0.00	168.0	.03	0.00	0.00
1800	682.	267.1	26.9	-.02	0.0	.03	0.	.537E+04	.012	.002	0.000	.201	.77	1.92	0.00	169.8	.03	0.00	0.00
1860	712.	268.3	25.7	-.00	0.0	.03	0.	.555E+04	.012	.002	0.000	.195	.77	1.92	0.00	171.5	.03	0.00	0.00
1920	745.	275.0	19.1	.07	.3	4.91	0.	.696E+04	.133	.001	0.000	.130	8.72	26.21	26.21	184.9	.03	0.00	0.00
1980	815.	288.1	6.6	.08	1.3	61.25	4.	.177E+05	.207	.001	0.000	.066	24.39	143.81	143.81	251.4	.04	0.00	0.00
1998	851.	289.5	5.3	.04	1.1	82.96	6.	.238E+05	.187	.000	0.000	.050	26.83	188.61	0.00	277.6	.04	0.00	0.00

VERTICAL VERSUS DOWNWIND POSITION OF PUFF

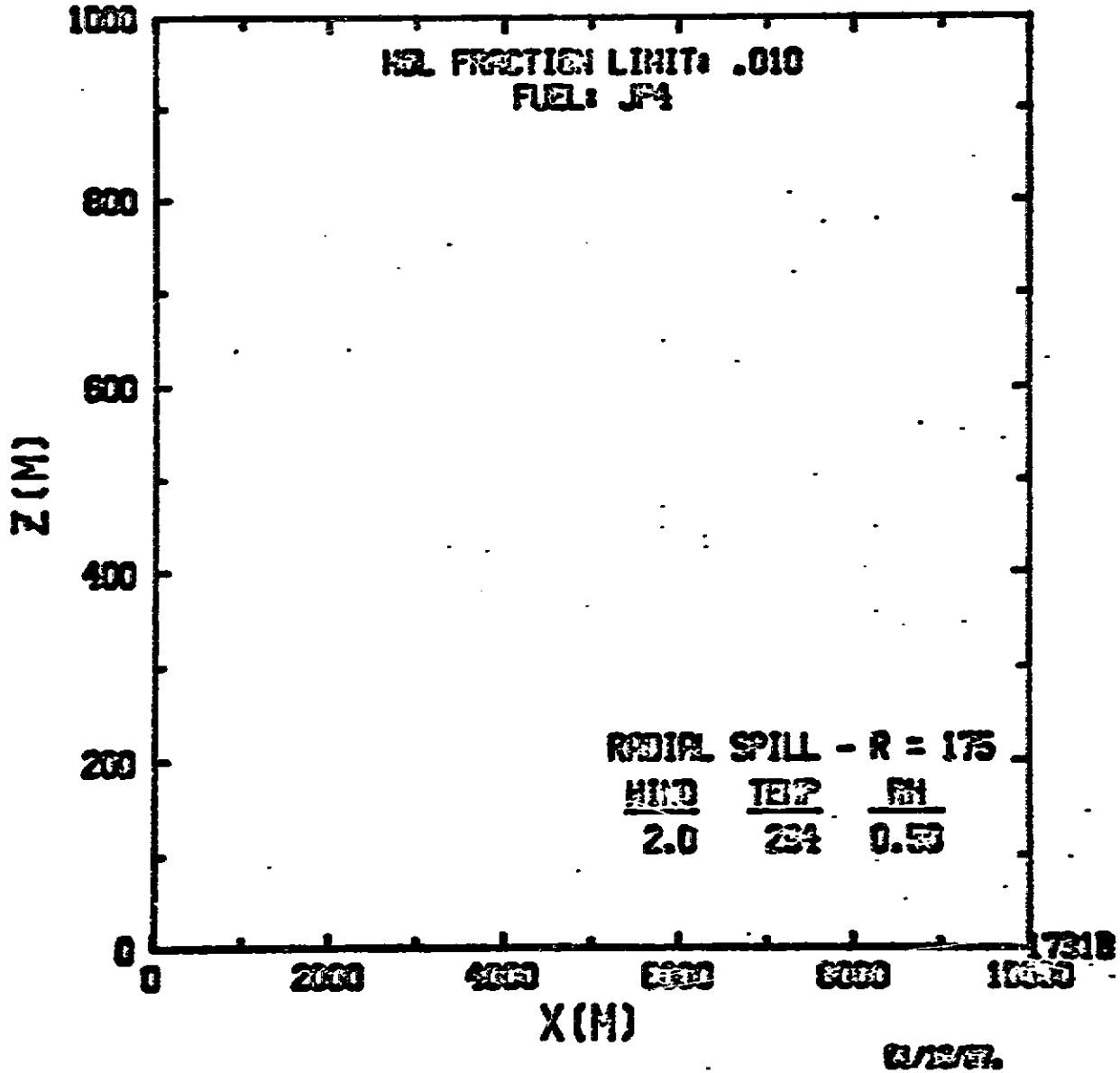

SCENARIO 4A

LOOKING AT LARGEST PUFF ONLY

INITIAL CONDITIONS

RADIAL SPILL - RADIUS: 175.0 FUEL: JP4 SURFACE ELEVATION: 0.

EVAPORATION RATE: 2.000E-6 TEMP: 294 RELATIVE HUMIDITY: .50

STABILITY: 6 WIND: 2.0 M/S FMF LOWER LIMIT: .010

SCENARIO 4A

IT	XP M	T K	DELTEM K	A	W M/S	ZP M	ANG DEG	VP CU.M	U1 M/S	U2 M/S	U4 M/S	FMF	VES CU.M	VET CU.M	VEB CU.M	R M	ZTZP M	LL M	LW M
0	0.	294.0	0.0	0.00	0.0	.04	0.	.673E+04	0.000	0.000	0.000	.109	0.00	0.00	0.00	175.0	.04	0.00	0.00
1	0.	294.0	-.0	-2.37	-.6	.03	89.	.674E+04	.080	0.000	0.000	.109	6.16	0.00	0.00	166.2	.03	0.00	0.00
600	68.	294.0	.0	-1.99	0.0	.04	0.	.102E+05	.055	0.000	0.000	.087	4.98	3.53	0.00	190.6	.04	0.00	0.00
1200	243.	294.0	.0	-1.66	0.0	.04	0.	.149E+05	.040	0.000	0.000	.069	4.67	4.75	0.00	215.8	.04	0.00	0.00
1800	479.	294.0	.0	-1.41	0.0	.05	0.	.200E+05	.032	0.000	0.000	.057	4.50	5.10	0.00	238.1	.05	0.00	0.00
2400	755.	294.0	.0	-1.23	0.0	.05	0.	.253E+05	.027	0.000	0.000	.049	4.42	5.18	0.00	257.4	.05	0.00	0.00
3000	1056.	294.0	.0	-1.08	0.0	.05	0.	.308E+05	.023	0.000	0.000	.042	4.38	5.18	0.00	274.8	.05	0.00	0.00
3600	1376.	294.0	.0	-.97	0.0	.06	0.	.362E+05	.021	0.000	0.000	.038	4.37	5.16	0.00	289.6	.06	0.00	0.00
4200	1711.	294.0	.0	-.88	0.0	.06	0.	.417E+05	.019	0.000	0.000	.034	4.38	5.12	0.00	303.4	.06	0.00	0.00
4800	2057.	294.0	.0	-.81	0.0	.06	0.	.473E+05	.018	0.000	0.000	.031	4.40	5.09	0.00	316.1	.06	0.00	0.00
5400	2412.	294.0	.0	-.74	0.0	.07	0.	.528E+05	.016	0.000	0.000	.028	4.44	5.07	0.00	328.0	.07	0.00	0.00
6000	2776.	294.0	.0	-.69	0.0	.07	0.	.584E+05	.016	0.000	0.000	.026	4.48	5.05	0.00	339.0	.07	0.00	0.00
6600	3146.	294.0	.0	-.64	0.0	.07	0.	.640E+05	.015	0.000	0.000	.024	4.52	5.03	0.00	349.4	.07	0.00	0.00
7200	3522.	294.0	.0	-.60	0.0	.07	0.	.696E+05	.014	0.000	0.000	.022	4.57	5.02	0.00	359.3	.07	0.00	0.00
7800	3904.	294.0	.0	-.56	0.0	.07	0.	.753E+05	.014	0.000	0.000	.021	4.62	5.02	0.00	368.8	.07	0.00	0.00
8400	4290.	294.0	.0	-.53	0.0	.08	0.	.811E+05	.013	0.000	0.000	.020	4.68	5.01	0.00	377.8	.08	0.00	0.00
9000	4681.	294.0	.0	-.50	0.0	.08	0.	.868E+05	.013	0.000	0.000	.018	4.74	5.02	0.00	386.5	.08	0.00	0.00
9600	5075.	294.0	.0	-.48	0.0	.08	0.	.926E+05	.012	0.000	0.000	.017	4.80	5.02	0.00	394.8	.08	0.00	0.00
10200	5473.	294.0	.0	-.45	0.0	.08	0.	.985E+05	.012	0.000	0.000	.017	4.87	5.03	0.00	402.9	.08	0.00	0.00
10800	5875.	294.0	.0	-.43	0.0	.08	0.	.104E+06	.012	0.000	0.000	.016	4.93	5.04	0.00	410.7	.08	0.00	0.00
11400	6279.	294.0	.0	-.41	0.0	.08	0.	.110E+06	.011	0.000	0.000	.015	5.00	5.05	0.00	418.3	.09	0.00	0.00
12000	6687.	294.0	.0	-.39	0.0	.09	0.	.116E+06	.011	0.000	0.000	.014	5.06	5.07	0.00	425.7	.09	0.00	0.00
12600	7097.	294.0	.0	-.38	0.0	.09	0.	.122E+06	.011	0.000	0.000	.014	5.13	5.08	0.00	432.9	.09	0.00	0.00
13200	7509.	294.0	.0	-.36	0.0	.09	0.	.129E+06	.011	0.000	0.000	.013	5.20	5.10	0.00	439.9	.09	0.00	0.00
13800	7924.	294.0	.0	-.35	0.0	.09	0.	.135E+06	.011	0.000	0.000	.013	5.28	5.12	0.00	446.8	.09	0.00	0.00
14400	8342.	294.0	.0	-.33	0.0	.09	0.	.141E+06	.010	0.000	0.000	.012	5.35	5.14	0.00	453.5	.09	0.00	0.00
15000	8761.	294.0	.0	-.32	0.0	.09	0.	.147E+06	.010	0.000	0.000	.012	5.42	5.16	0.00	460.1	.09	0.00	0.00
15600	9183.	294.0	.0	-.31	0.0	.09	0.	.154E+06	.010	0.000	0.000	.011	5.50	5.18	0.00	466.5	.09	0.00	0.00
16200	9606.	294.0	.0	-.30	0.0	.09	0.	.160E+06	.010	0.000	0.000	.011	5.57	5.21	0.00	472.8	.09	0.00	0.00
16800	10031.	294.0	.0	-.29	0.0	.10	0.	.167E+06	.010	0.000	0.000	.010	5.65	5.23	0.00	479.1	.10	0.00	0.00
17318	10400.	294.0	.0	-.28	0.0	.10	0.	.172E+06	.010	0.000	0.000	.010	5.71	5.26	0.00	484.4	.10	0.00	0.00

VERTICAL VERSUS DOWNWIND POSITION OF PUFF

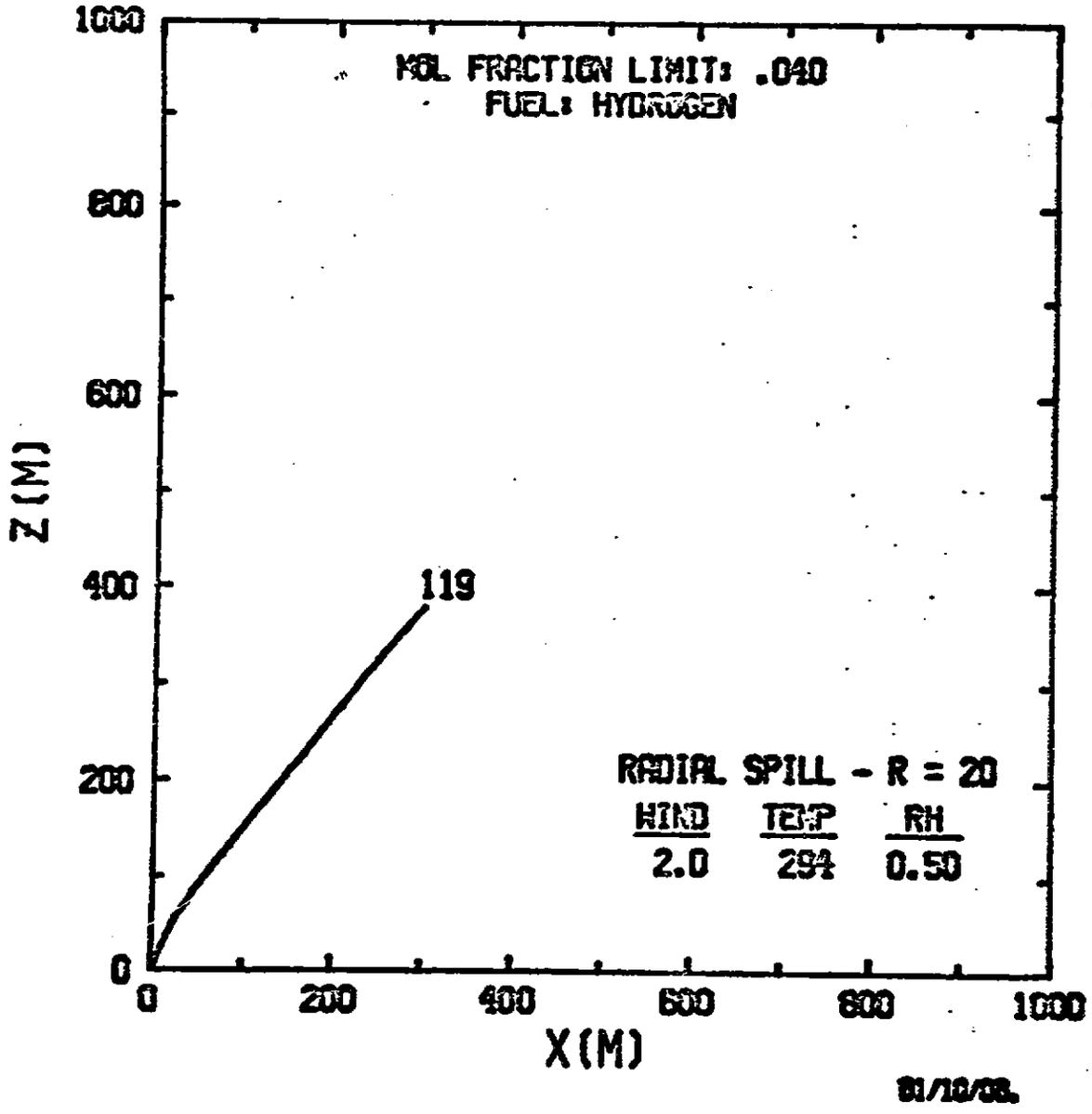

LOOKING AT LARGEST PUFF ONLY

INITIAL CONDITIONS

SCENARIO 4B

RADIAL SPILL - RADIUS: 20.0 FUEL: HYDROGEN SURFACE ELEVATION: 0.

EVAPORATION RATE: 2.360E-3 TEMP: 294 RELATIVE HUMIDITY: .50

STABILITY: 6 WIND: 2.0 M/S FMF LOWER LIMIT: .040

IT	XP M	T K	DELTEM K	A	W M/S	ZP M	ANG DEG	VP CU.M	U1 M/S	U2 M/S	U4 M/S	FMF	VES CU.M	VET CU.M	VEB CU.M	R M	ZTZP M	LL M	LW M
0	0.	20.3	0.0	0.00	0.0	.06	0.	.156E+03	0.000	0.000	0.000	1.000	0.00	0.00	0.00	20.0	.06	0.00	0.00
1	0.	20.8	273.2	-.00	0.0	.06	78.	.178E+03	.090	.124	0.000	.999	3.35	0.00	0.00	20.3	.06	0.00	0.00
6	0.	24.0	270.0	.45	.3	.61	62.	.208E+03	.120	.097	0.000	.991	3.77	.58	.58	21.3	.07	0.00	0.00
12	2.	32.3	261.8	1.27	1.4	5.39	70.	.285E+03	.220	.073	0.000	.970	6.13	3.66	3.66	23.7	.07	0.00	0.00
18	7.	56.6	237.5	2.33	2.9	18.49	70.	.536E+03	.366	.041	0.000	.908	12.41	17.55	17.55	29.1	.09	0.00	0.00
24	16.	103.0	191.4	2.09	3.5	38.32	67.	.116E+04	.443	.019	0.000	.765	23.52	46.41	46.41	37.6	.12	0.00	0.00
30	29.	150.6	144.0	1.48	3.5	59.59	64.	.217E+04	.446	.010	0.000	.597	35.83	72.52	72.52	46.3	.14	0.00	0.00
36	44.	187.8	107.0	1.10	3.5	80.71	61.	.354E+04	.438	.006	0.000	.459	46.82	94.11	94.11	54.3	.17	0.00	0.00
42	60.	215.4	79.7	.90	3.5	101.61	59.	.524E+04	.434	.004	0.000	.356	62.96	114.16	114.16	61.9	.19	0.00	0.00
48	77.	235.9	59.3	.79	3.5	122.52	58.	.732E+04	.436	.003	0.000	.280	79.02	134.85	134.85	69.1	.21	0.00	0.00
54	95.	251.6	43.9	.74	3.6	143.73	57.	.979E+04	.444	.002	0.000	.224	97.76	157.54	157.54	76.0	.24	0.00	0.00
60	114.	263.5	32.2	.70	3.7	165.48	56.	.127E+05	.456	.002	0.000	.181	119.57	182.66	182.66	82.9	.26	0.00	0.00
66	133.	272.9	23.0	.68	3.8	187.93	55.	.161E+05	.471	.001	0.000	.148	144.82	210.39	210.39	89.7	.28	0.00	0.00
72	152.	279.2	16.8	.63	3.9	211.00	54.	.200E+05	.483	.001	0.000	.122	171.25	237.63	237.63	96.3	.30	0.00	0.00
78	172.	285.3	10.5	.64	4.0	234.78	54.	.246E+05	.500	.001	0.000	.102	203.10	269.52	269.52	103.0	.32	0.00	0.00
84	193.	286.7	8.9	.53	4.1	259.31	53.	.294E+05	.512	.001	0.000	.086	234.95	299.88	299.88	109.3	.34	0.00	0.00
90	214.	287.8	7.7	.44	4.1	284.03	53.	.348E+05	.513	.001	0.000	.073	262.92	323.69	323.69	115.5	.36	0.00	0.00
96	235.	288.6	6.7	.38	4.1	309.57	53.	.405E+05	.507	.000	0.000	.063	288.27	343.17	343.17	121.5	.38	0.00	0.00
102	257.	289.2	5.9	.32	4.0	332.74	52.	.467E+05	.499	.000	0.000	.055	311.58	359.56	359.56	127.3	.40	0.00	0.00
108	279.	289.7	5.3	.28	3.9	356.46	52.	.531E+05	.489	.000	0.000	.049	333.24	373.64	373.64	132.5	.41	0.00	0.00
114	301.	290.0	4.8	.25	3.8	379.70	52.	.599E+05	.479	.000	0.000	.043	353.53	385.94	385.94	138.2	.43	0.00	0.00
119	320.	290.3	4.4	.22	3.8	398.68	51.	.657E+05	.471	.000	0.000	.040	369.51	395.08	0.00	142.5	.44	0.00	0.00

VERTICAL VERSUS DOWNWIND POSITION OF PUFF

SCENARIO 4B

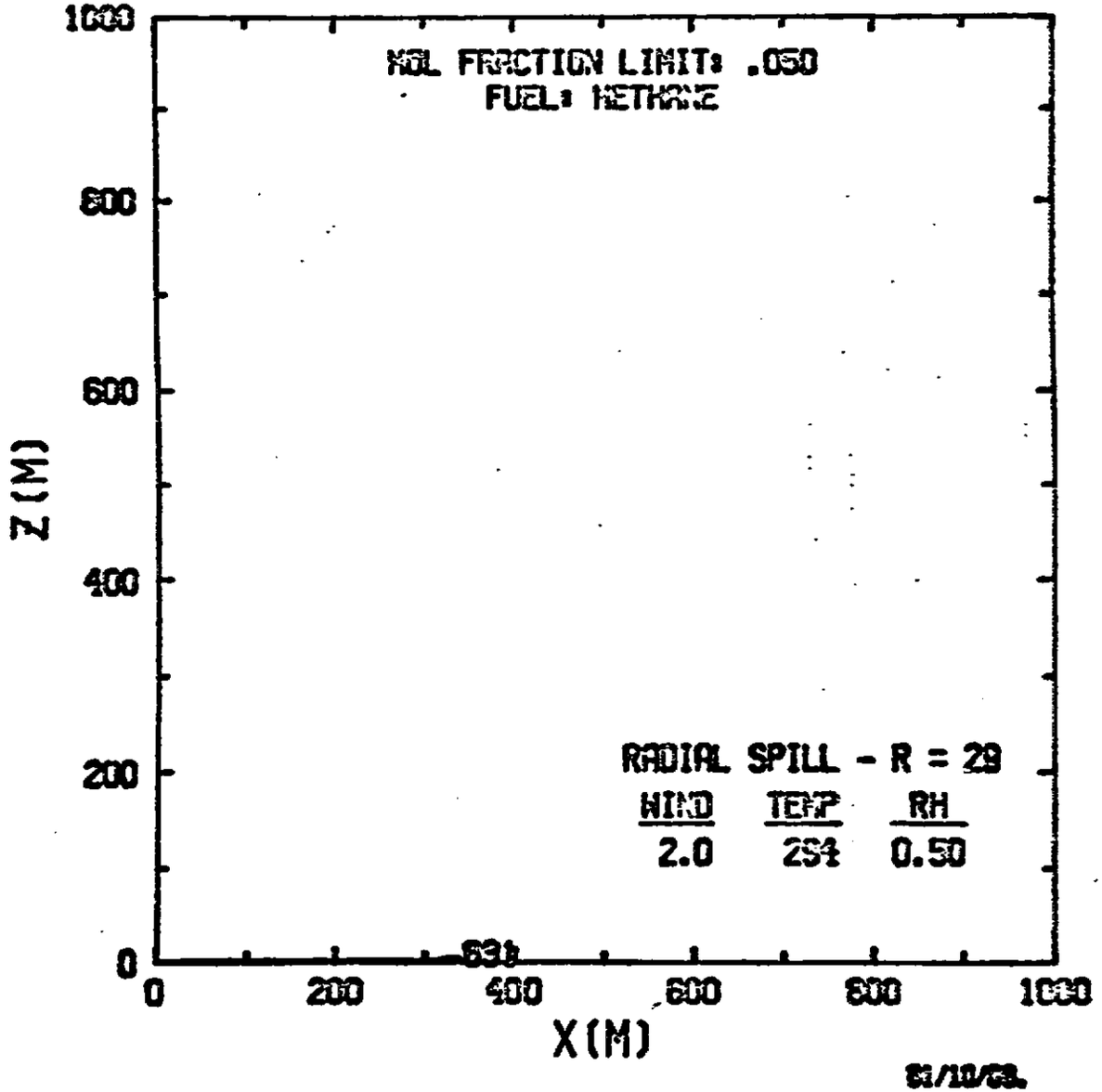

DKI-3 AT LARGEST PUFF ONLY
INITIAL CONDITIONS

RADIAL SPILL - RADIUS: 29.0 FUEL: METHANE SURFACE ELEVATION: 0.
EVAPORATION RATE: 1.520E-4 TEMP: 294 RELATIVE HUMIDITY: .50
STABILITY: 6 WIND: 2.0 M/S FMF LOWER LIMIT: .050

SCENARIO 4B

IT	XP M	T K	DELTEM K	A	U M/S	ZP M	ANG DEG	VP CU.M	U1 M/S	U2 M/S	U4 M/S	FMF	VES CU.M	VET CU.M	VEB CU.M	R M	ZTZP M	LL M	LW M
0	0.	111.7	0.0	0.00	0.0	.02	0.	.925E+02	0.000	0.000	0.000	1.000	0.00	0.00	0.00	29.0	.02	0.00	0.00
1	0.	112.3	181.8	-3.03	-.8	.02	81.	.980E+02	.070	.035	0.000	.997	.67	0.00	0.00	28.6	.02	0.00	0.00
5	5.	145.1	148.9	-2.19	0.0	.02	0.	.155E+03	.052	.021	0.000	.817	.61	.61	0.00	33.2	.02	0.00	0.00
10	19.	177.2	116.8	-1.49	0.0	.02	0.	.238E+03	.038	.014	0.000	.648	.58	.89	0.00	38.3	.02	0.00	0.00
15	39.	200.2	93.8	-1.07	0.0	.03	0.	.331E+03	.030	.010	0.000	.527	.55	.97	0.00	42.7	.03	0.00	0.00
20	62.	216.8	77.2	-.79	0.0	.03	0.	.426E+03	.025	.008	0.000	.443	.54	.99	0.00	46.4	.03	0.00	0.00
25	88.	229.1	64.9	-.59	0.0	.03	0.	.522E+03	.022	.006	0.000	.383	.53	.99	0.00	49.6	.03	0.00	0.00
30	116.	238.6	55.4	-.44	0.0	.03	0.	.617E+03	.020	.005	0.000	.337	.52	.98	0.00	52.4	.03	0.00	0.00
35	145.	246.1	47.9	-.32	0.0	.03	0.	.711E+03	.018	.005	0.000	.302	.52	.96	0.00	54.9	.03	0.00	0.00
40	175.	252.0	42.0	-.23	0.0	.03	0.	.804E+03	.017	.004	0.000	.273	.52	.95	0.00	57.2	.03	0.00	0.00
45	206.	256.8	37.2	-.17	0.0	.04	0.	.896E+03	.016	.004	0.000	.250	.52	.94	0.00	59.3	.04	0.00	0.00
50	237.	260.7	33.1	-.11	0.0	.04	0.	.987E+03	.015	.003	0.000	.230	.52	.93	0.00	61.2	.04	0.00	0.00
55	270.	264.4	29.6	-.06	0.0	.04	0.	.108E+04	.014	.003	0.000	.214	.52	.92	0.00	63.0	.04	0.00	0.00
60	302.	267.4	26.6	-.01	0.0	.04	0.	.117E+04	.013	.003	0.000	.199	.52	.91	0.00	64.7	.04	0.00	0.00
80	337.	277.3	16.7	.10	.3	3.67	1.	.162E+04	.115	.002	0.000	.149	4.57	9.59	9.59	72.1	.04	0.00	0.00
31	404.	289.6	4.8	.06	.9	44.75	6.	.507E+04	.155	.001	0.000	.050	12.90	47.08	0.00	105.1	.06	0.00	0.00

VERTICAL VERSUS DOWNWIND POSITION OF PUFF

SCENARIO 4B

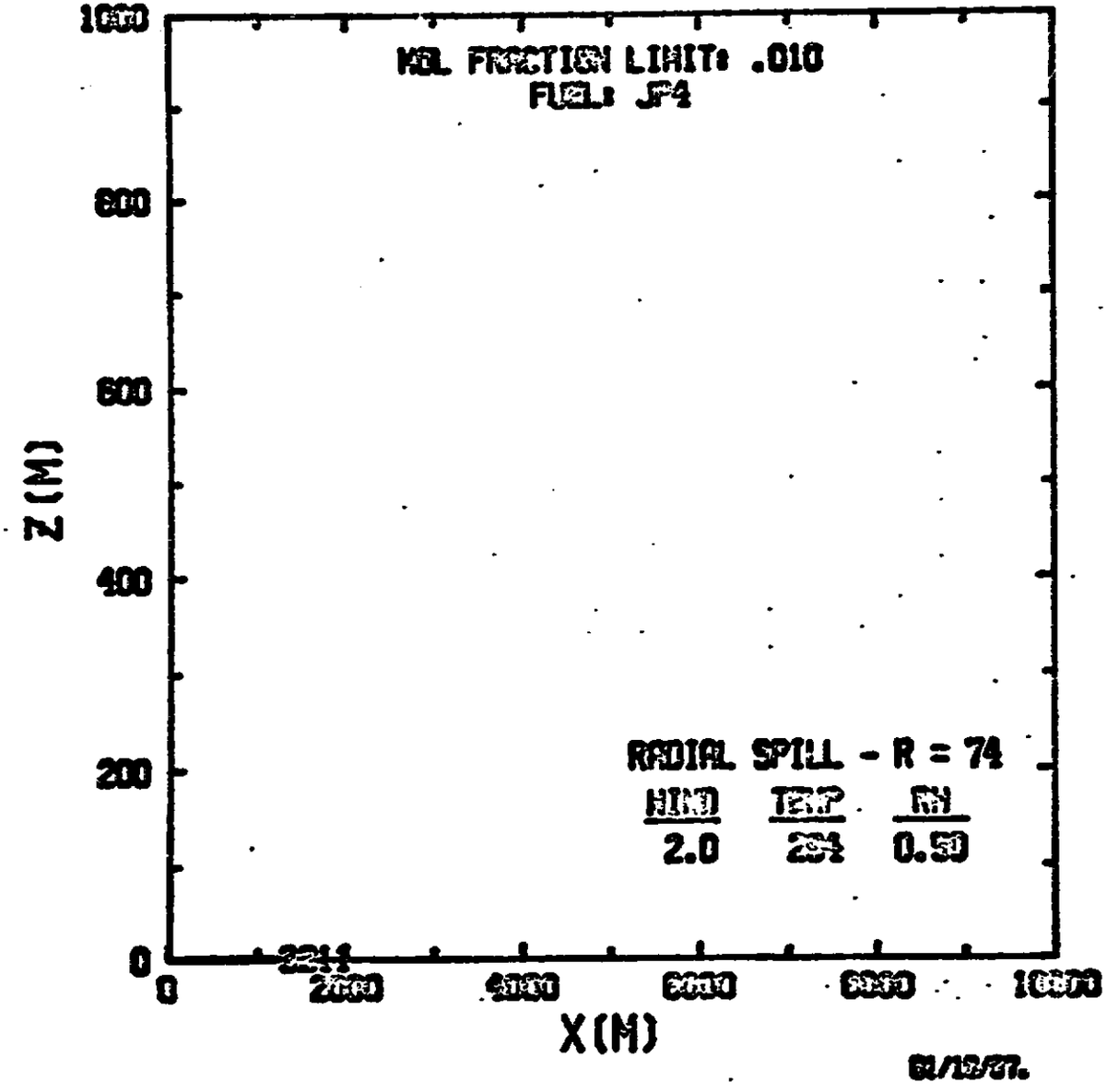

LOOKING AT LARGEST PUFF ONLY

INITIAL CONDITIONS

RADIAL SPILL - RADIUS: 74.0 FUEL: JP4 SURFACE ELEVATION: 0.

EVAPORATION RATE: 2.000E-6 TEMP: 294 RELATIVE HUMIDITY: .50

STABILITY: 6 WIND: 2.0 M/S FMF LOWER LIMIT: .010

SCENARIO 4B

IT	XP	T	DELTEM	A	W	ZP	ANG	VP	U1	U2	U4	FMF	VES	VET	VEB	R	ZTZP	LL	LW
	M	K	K		M/S	M	DEG	CU.M	M/S	M/S	M/S		CU.M	CU.M	CU.M	M	M	M	M
0	0.	294.0	0.0	0.00	0.0	.04	0.	.120E+04	0.000	0.000	0.000	.109	0.00	0.00	0.00	74.0	.04	0.00	0.00
1	0.	294.0	-.0	-2.37	-.6	.03	88.	.121E+04	.080	0.000	0.000	.109	2.60	0.00	0.00	70.9	.03	0.00	0.00
120	7.	294.0	.0	-1.99	0.0	.04	0.	.147E+04	.066	0.000	0.000	.087	2.26	.90	0.00	75.7	.04	0.00	0.00
240	27.	294.0	.0	-1.65	0.0	.04	0.	.182E+04	.055	0.000	0.000	.069	2.16	1.50	0.00	81.3	.04	0.00	0.00
360	58.	294.0	.0	-1.40	0.0	.04	0.	.224E+04	.046	0.000	0.000	.057	2.09	1.85	0.00	87.0	.04	0.00	0.00
480	96.	294.0	.0	-1.20	0.0	.04	0.	.268E+04	.040	0.000	0.000	.047	2.03	2.04	0.00	92.4	.04	0.00	0.00
600	142.	294.0	.0	-1.05	0.0	.05	0.	.315E+04	.035	0.000	0.000	.041	1.99	2.14	0.00	97.4	.05	0.00	0.00
720	191.	294.0	.0	-.93	0.0	.05	0.	.363E+04	.032	0.000	0.000	.036	1.96	2.20	0.00	102.0	.05	0.00	0.00
840	245.	294.0	.0	-.83	0.0	.05	0.	.411E+04	.029	0.000	0.000	.032	1.94	2.22	0.00	106.3	.05	0.00	0.00
960	302.	294.0	.0	-.76	0.0	.05	0.	.459E+04	.027	0.000	0.000	.028	1.92	2.23	0.00	110.3	.05	0.00	0.00
1080	361.	294.0	.0	-.69	0.0	.05	0.	.508E+04	.025	0.000	0.000	.026	1.91	2.23	0.00	114.0	.05	0.00	0.00
1200	423.	294.0	.0	-.64	0.0	.06	0.	.557E+04	.023	0.000	0.000	.024	1.90	2.23	0.00	117.5	.06	0.00	0.00
1320	486.	294.0	.0	-.59	0.0	.06	0.	.605E+04	.022	0.000	0.000	.022	1.89	2.22	0.00	120.8	.06	0.00	0.00
1440	551.	294.0	.0	-.55	0.0	.06	0.	.654E+04	.021	0.000	0.000	.020	1.89	2.21	0.00	123.9	.06	0.00	0.00
1560	618.	294.0	.0	-.52	0.0	.06	0.	.702E+04	.020	0.000	0.000	.019	1.89	2.20	0.00	126.9	.06	0.00	0.00
1680	686.	294.0	.0	-.49	0.0	.06	0.	.751E+04	.019	0.000	0.000	.018	1.89	2.19	0.00	129.7	.06	0.00	0.00
1800	755.	294.0	.0	-.46	0.0	.06	0.	.799E+04	.018	0.000	0.000	.017	1.89	2.18	0.00	132.4	.06	0.00	0.00
1920	825.	294.0	.0	-.44	0.0	.06	0.	.848E+04	.018	0.000	0.000	.016	1.89	2.18	0.00	135.0	.06	0.00	0.00
2040	895.	294.0	.0	-.42	0.0	.07	0.	.896E+04	.017	0.000	0.000	.015	1.90	2.17	0.00	137.5	.07	0.00	0.00
2160	967.	294.0	.0	-.40	0.0	.07	0.	.945E+04	.016	0.000	0.000	.014	1.90	2.16	0.00	139.9	.07	0.00	0.00
2280	1040.	294.0	.0	-.38	0.0	.07	0.	.993E+04	.016	0.000	0.000	.014	1.91	2.16	0.00	142.2	.07	0.00	0.00
2400	1113.	294.0	.0	-.36	0.0	.07	0.	.104E+05	.015	0.000	0.000	.013	1.92	2.15	0.00	144.5	.07	0.00	0.00
2520	1187.	294.0	.0	-.35	0.0	.07	0.	.109E+05	.015	0.000	0.000	.012	1.93	2.15	0.00	146.7	.07	0.00	0.00
2640	1261.	294.0	.0	-.33	0.0	.07	0.	.114E+05	.015	0.000	0.000	.012	1.93	2.14	0.00	148.8	.07	0.00	0.00
2760	1336.	294.0	.0	-.32	0.0	.07	0.	.119E+05	.014	0.000	0.000	.011	1.94	2.14	0.00	150.9	.07	0.00	0.00
2880	1412.	294.0	.0	-.31	0.0	.07	0.	.124E+05	.014	0.000	0.000	.011	1.95	2.13	0.00	152.9	.07	0.00	0.00
3000	1488.	294.0	.0	-.30	0.0	.07	0.	.129E+05	.014	0.000	0.000	.011	1.96	2.13	0.00	154.9	.07	0.00	0.00
3120	1565.	294.0	.0	-.29	0.0	.07	0.	.133E+05	.014	0.000	0.000	.010	1.97	2.13	0.00	156.8	.07	0.00	0.00
3211	1623.	294.0	.0	-.28	0.0	.07	0.	.137E+05	.013	0.000	0.000	.010	1.98	2.13	0.00	158.2	.07	0.00	0.00

VERTICAL VERSUS DOWNWIND POSITION OF PUFF

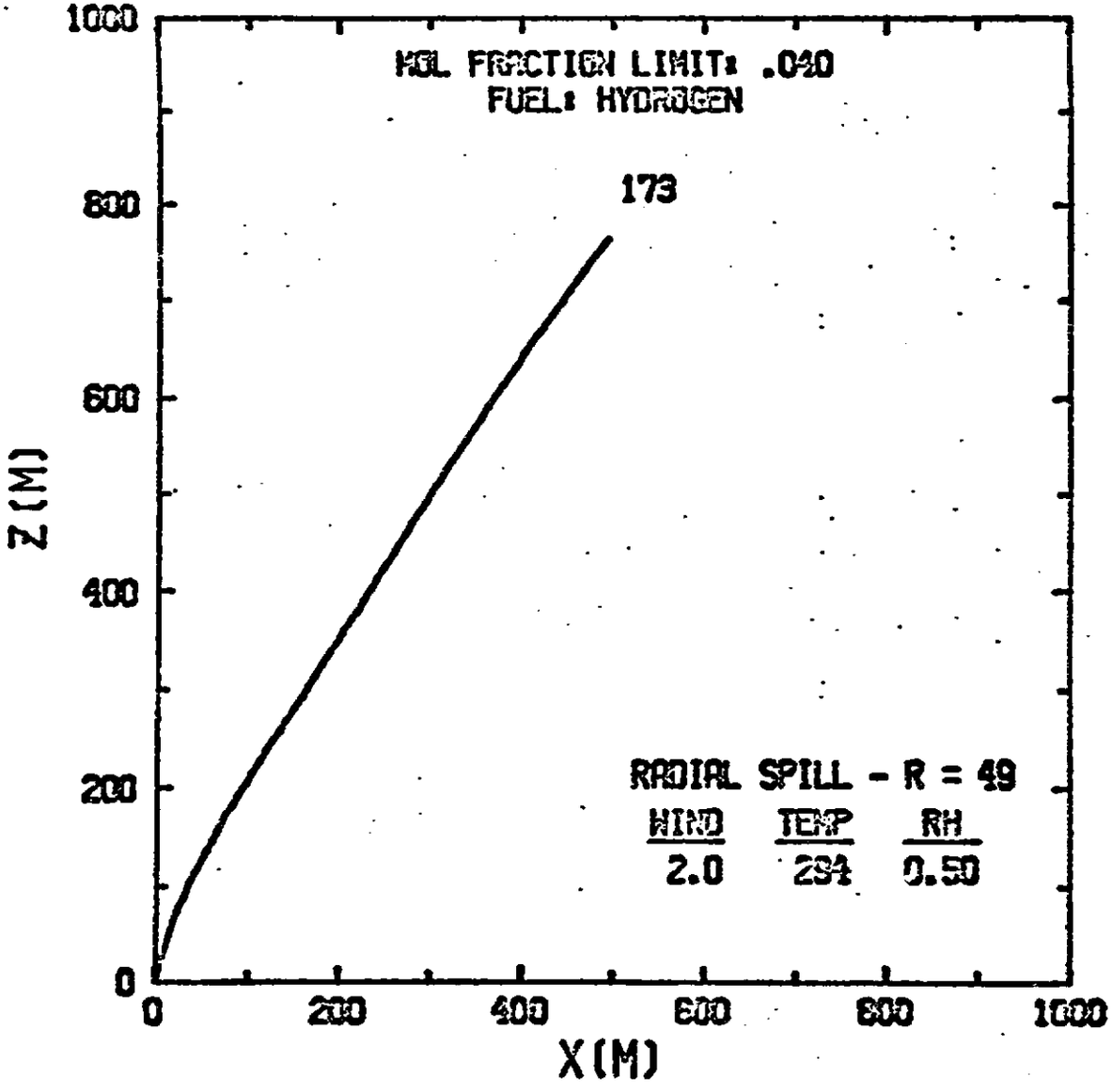

SCENARIO 4A
STABILITY 6

LOOKING AT LARGEST PUFF ONLY

INITIAL CONDITIONS

SCENARIO 4A

RADIAL SPILL - RADIUS: 49.0 FUEL: HYDROGEN SURFACE ELEVATION: 0.

EVAPORATION RATE: 1.940E-3 TEMP: 294 RELATIVE HUMIDITY: .50

STABILITY: 6 WIND: 2.0 M/S FMF LOWER LIMIT: .040

IT	XP M	T K	DELTEM K	A1	W M/S	ZP-ZS M	ANG DEG	VP CU.M	U1 M/S	U2 M/S	U4 M/S	FMF	VES CU.M	VET CU.M	VEB CU.M	R M	ZTZP M	LL M	LZ M
0	0.	20.3	0.0	0.00	0.0	0.0	0.	0.	0.000	0.000	0.000	1.000	0.0	0.0	0.0	0.0	0.00	0.00	0.00
1	0.	20.4	273.6	0.00	0.0	.1	90.	.861E+03	0.000	.102	0.000	1.000	3.2	0.0	0.0	48.9	.05	0.00	0.00
10	0.	22.3	271.7	.05	.2	.5	66.	.946E+03	.121	.084	0.000	.995	6.8	.7	.7	50.4	.05	0.00	0.00
20	2.	26.9	267.2	.16	1.3	6.9	77.	.115E+04	.240	.070	0.000	.984	11.6	5.6	5.6	53.8	.06	0.00	0.00
30	7.	43.4	250.9	.23	3.5	30.1	77.	.195E+04	.447	.044	0.000	.942	25.1	39.9	39.9	64.0	.07	0.00	0.00
40	23.	93.6	201.2	.04	4.8	73.5	73.	.501E+04	.608	.017	0.000	.795	58.9	161.7	161.7	87.4	.09	0.00	0.00
50	47.	152.2	143.0	-.01	4.9	122.6	69.	.110E+05	.615	.008	0.000	.592	100.4	284.6	284.6	113.4	.12	0.00	0.00
60	76.	195.8	99.9	-.01	4.8	171.4	66.	.196E+05	.604	.004	0.000	.430	144.9	383.7	383.7	137.1	.14	0.00	0.00
70	107.	226.1	69.8	.01	4.8	219.6	64.	.308E+05	.602	.003	0.000	.318	195.1	478.5	478.5	159.0	.17	0.00	0.00
80	140.	247.4	48.1	.02	5.0	268.5	62.	.447E+05	.615	.002	0.000	.241	256.2	584.5	584.5	180.0	.19	0.00	0.00
90	175.	262.5	33.7	.02	5.2	319.1	61.	.620E+05	.640	.001	0.000	.186	331.0	706.5	706.5	200.4	.21	0.00	0.00
100	211.	272.0	22.9	.01	5.4	371.9	60.	.825E+05	.670	.001	0.000	.145	420.5	843.9	843.9	220.3	.23	0.00	0.00
110	249.	280.3	14.3	.02	5.6	426.7	60.	.108E+06	.691	.001	0.000	.116	515.6	978.9	978.9	240.4	.25	0.00	0.00
120	287.	284.3	9.8	.01	5.8	483.6	59.	.136E+06	.717	.001	0.000	.093	626.2	1129.7	1129.7	259.8	.27	0.00	0.00
130	327.	285.5	8.2	-.00	5.8	541.5	59.	.168E+06	.721	.000	0.000	.077	723.0	1247.1	1247.1	278.3	.29	0.00	0.00
140	367.	286.3	7.1	-.01	5.7	599.1	58.	.202E+06	.711	.000	0.000	.064	808.3	1338.1	1338.1	296.0	.31	0.00	0.00
150	408.	286.8	6.2	-.01	5.6	655.5	58.	.239E+06	.696	.000	0.000	.055	884.9	1411.4	1411.4	313.0	.33	0.00	0.00
160	450.	287.1	5.5	-.01	5.4	710.6	58.	.279E+06	.678	.000	0.000	.047	954.6	1471.9	1471.9	329.1	.34	0.00	0.00
170	493.	287.3	5.0	-.01	5.3	764.3	57.	.320E+06	.660	.000	0.000	.041	1018.5	1522.6	1522.6	344.5	.36	0.00	0.00

VERTICAL VERSUS DOWNWIND POSITION OF PUFF

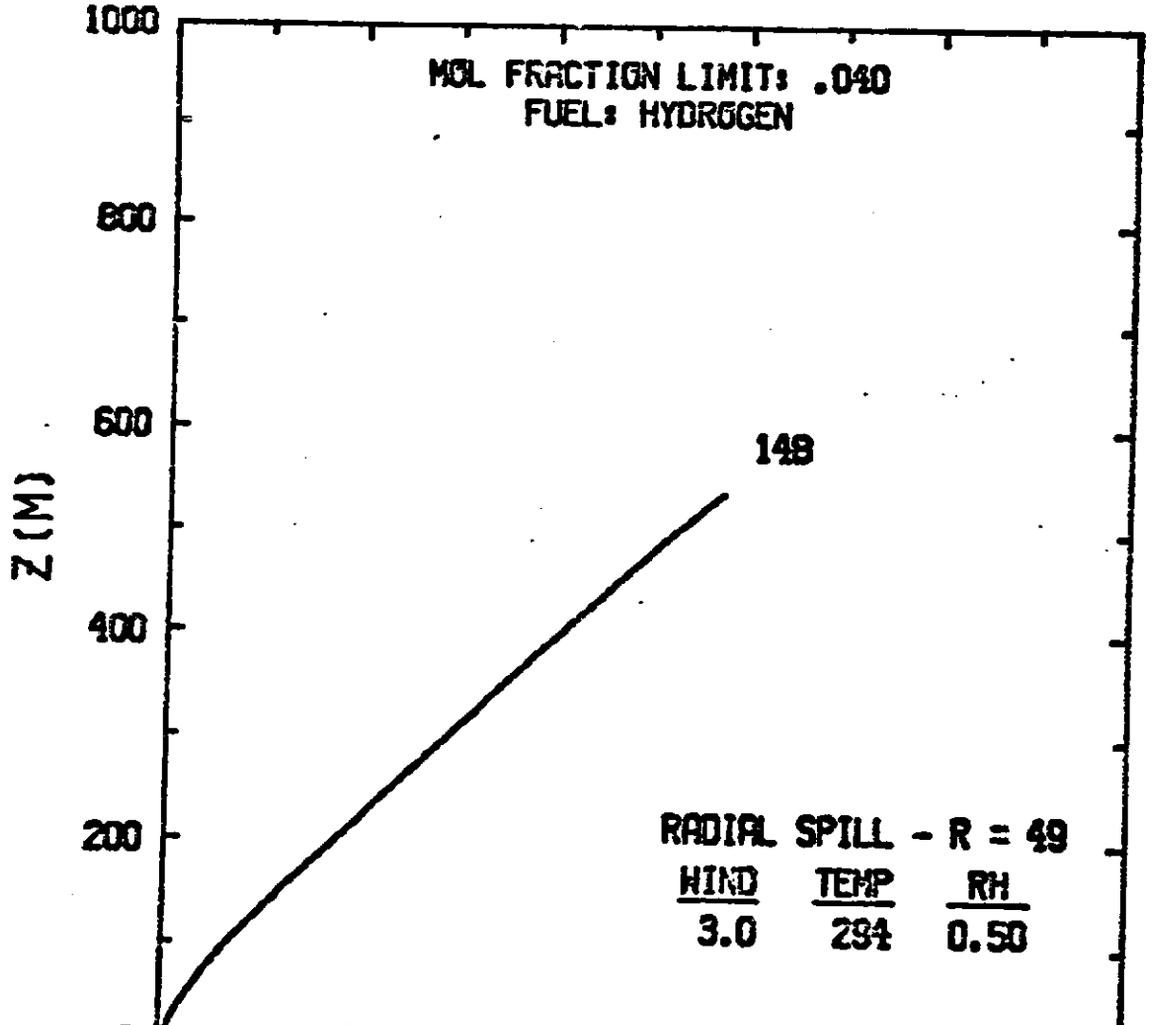

SCENARIO 4A
STABILITY 5

LOOKING AT LARGEST PUFF ONLY

INITIAL CONDITIONS

RADIAL SPILL - RADIUS: 49.0 FUEL: HYDROGEN SURFACE ELEVATION: 0.

EVAPORATION RATE: 1.940E-3 TEMP: 294 RELATIVE HUMIDITY: .50

STABILITY: 5 WIND: 3.0 M/S FMF LOWER LIMIT: .040

SCENARIO 4A

IT	XP M	T K	DELTEM K	A M/S^2	W M/S	ZP M	ANG DEG	VP CU.M	U1 M/S	U2 M/S	U4 M/S	FMF	VES CU.M	VET CU.M	VEB CU.M	R M	ZTZP M	LL M	LW M
0	0.	20.3	0.0	0.00	0.0	.05	0.	.771E+03	0.000	0.000	0.000	1.000	0.0	0.0	0.0	0.0	.05	0.00	0.00
1	0.	20.5	273.5	-.05	-.0	.05	80.	.867E+03	.130	.102	0.000	.999	7.3	0.0	0.0	49.0	.05	0.00	0.00
10	1.	23.4	270.6	.37	.3	.95	57.	.997E+03	.204	.081	0.000	.992	9.7	2.6	2.6	51.3	.05	0.00	0.00
20	5.	35.5	258.5	1.49	2.1	11.96	66.	.156E+04	.362	.054	0.000	.962	18.4	28.9	28.9	59.5	.06	0.00	0.00
30	24.	85.5	208.5	2.27	4.0	44.38	62.	.442E+04	.521	.020	0.000	.821	46.3	172.3	172.3	83.8	.09	0.00	0.00
40	57.	153.2	140.8	1.43	4.2	85.98	56.	.112E+05	.530	.008	0.000	.586	86.7	345.6	345.6	113.8	.12	0.00	0.00
50	98.	201.1	92.9	.97	4.1	127.28	52.	.213E+05	.517	.004	0.000	.406	130.6	481.4	481.4	140.8	.15	0.00	0.00
60	143.	232.1	61.9	.78	4.1	168.35	50.	.346E+05	.517	.002	0.000	.289	180.9	612.0	612.0	165.4	.17	0.00	0.00
70	191.	253.0	41.0	.71	4.2	210.08	48.	.517E+05	.529	.002	0.000	.212	242.1	757.2	757.2	188.8	.20	0.00	0.00
80	241.	267.1	26.6	.67	4.4	253.8	46.	.728E+05	.552	.001	0.000	.159	317.2	924.4	924.4	211.4	.22	0.00	0.00
90	293.	275.8	17.6	.60	4.6	298.68	46.	.983E+05	.575	.001	0.000	.123	403.5	1103.6	1103.6	233.4	.24	0.00	0.00
100	347.	282.7	10.4	.58	4.8	345.76	45.	.129E+06	.00	.001	0.000	.096	504.9	1301.5	1301.5	255.4	.27	0.00	0.00
110	403.	284.3	8.5	.45	4.9	394.41	44.	.163E+06	.611	.000	0.000	.077	601.4	1474.4	1474.4	276.0	.29	0.00	0.00
120	460.	285.4	7.1	.36	4.8	443.02	44.	.202E+06	.605	.000	0.000	.063	685.0	1604.6	1604.6	295.8	.31	0.00	0.00
130	518.	286.1	6.1	.29	4.7	490.75	43.	.243E+06	.592	.000	0.000	.053	759.5	1707.8	1707.8	314.8	.33	0.00	0.00
3min = 140	578.	286.5	5.3	.24	4.6	537.29	43.	.287E+06	.577	.000	0.000	.045	826.9	1792.2	1792.2	332.4	.35	0.00	0.00

VERTICAL VERSUS DOWNWIND POSITION OF PUFF

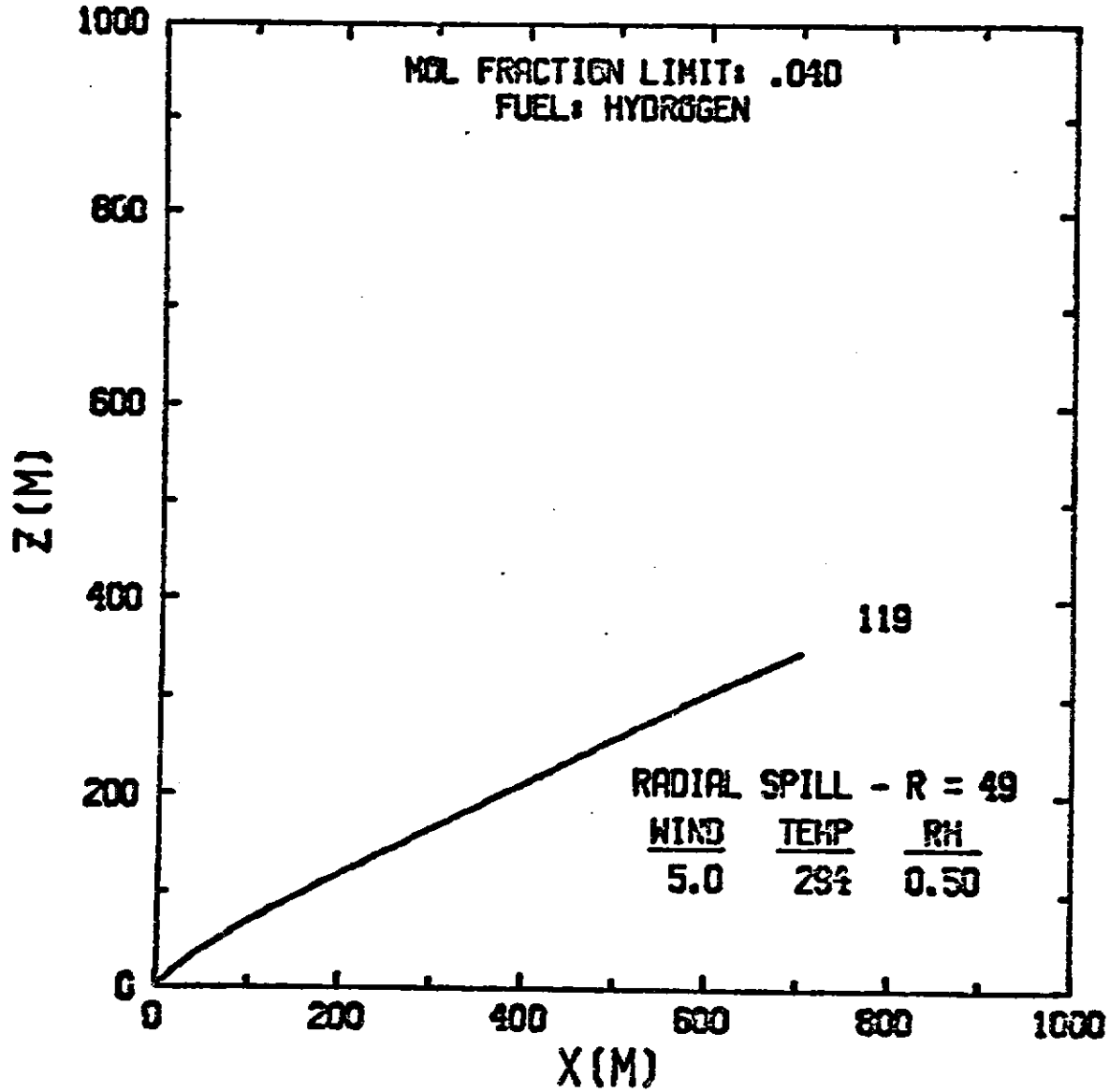

SCENARIO 4A
STABILITY 4

LOOKING AT LARGEST PUFF ONLY

SCENARIO 4A

INITIAL CONDITIONS

RADIAL SPILL - RADIUS: 49.0 FUEL: HYDROGEN SURFACE ELEVATION: 0.

EVAPORATION RATE: 1.940E-3 TEMP: 294 RELATIVE HUMIDITY: .50

STABILITY: 4 WIND: 5.0 M/S FMF LOWER LIMIT: .040

IT	XP M	T K	DELTEM K	A	U M/S	ZP M	ANG DEG	VP CU.M	U1 M/S	U2 M/S	U4 M/S	FMF	VES CU.M	VET CU.M	VEB CU.M	R M	ZTZP M	LL M	LW M
0	0.	20.3	0.0	0.00	0.0	.05	0.	.771E+03	0.000	0.000	0.000	1.000	0.0	0.0	0.0	0.0	.05	0.00	0.00
1	0.	20.6	273.4	-.04	0.0	.05	69.	.871E+03	.216	.102	0.000	.999	10.0	0.0	0.0	49.1	.05	0.00	0.00
10	2.	27.1	266.8	.81	.7	1.93	43.	.117E+04	.367	.072	0.000	.983	16.1	15.4	15.4	54.0	.08	0.00	0.00
20	23.	77.4	216.4	2.37	2.9	20.62	42.	.387E+04	.452	.023	0.000	.847	36.7	187.6	187.6	80.3	.09	0.00	0.00
30	72.	158.3	135.2	1.38	3.3	53.03	36.	.119E+05	.447	.007	0.000	.567	75.7	445.8	445.8	116.2	.12	0.00	0.00
40	134.	211.4	81.7	.90	3.3	86.39	33.	.248E+05	.434	.003	0.000	.364	120.7	652.4	652.4	149.0	.15	0.00	0.00
50	204.	243.0	49.8	.73	3.4	119.92	30.	.425E+05	.438	.002	0.000	.245	175.0	861.0	861.0	177.0	.18	0.00	0.00
60	279.	262.4	30.1	.66	3.6	154.62	29.	.658E+05	.455	.001	0.000	.172	243.6	1101.4	1101.4	204.4	.21	0.00	0.00
70	357.	273.7	18.4	.58	3.7	191.16	28.	.951E+05	.477	.001	0.000	.124	327.2	1373.2	1373.2	230.8	.24	0.00	0.00
80	439.	281.7	10.1	.56	3.9	229.44	28.	.132E+06	.500	.001	0.000	.093	424.8	1664.6	1664.6	256.9	.27	0.00	0.00
90	525.	283.7	7.9	.41	4.0	269.04	27.	.173E+06	.508	.000	0.000	.071	518.2	1918.3	1918.3	281.2	.29	0.00	0.00
100	613.	284.9	6.4	.32	3.9	308.37	27.	.220E+06	.509	.000	0.000	.057	598.9	2107.2	2107.2	304.4	.32	0.00	0.00
110	703.	285.7	5.3	.26	3.8	346.74	26.	.271E+06	.487	.000	0.000	.046	671.1	2257.2	2257.2	326.1	.34	0.00	0.00

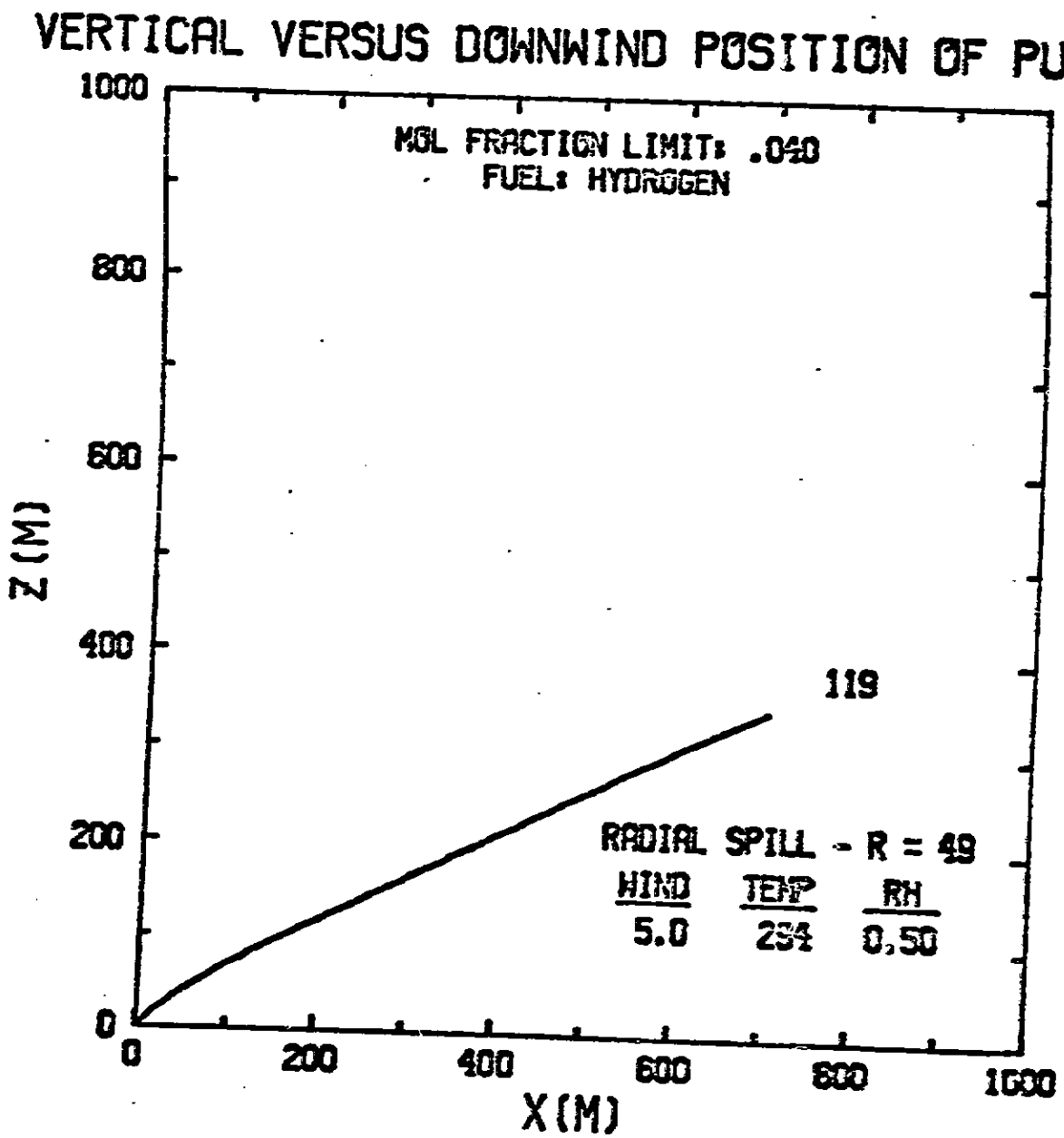
VERTICAL VERSUS DOWNWIND POSITION OF PUFF
MOL FRACTION LIMIT: .040
FUEL: HYDROGEN
SCENARIO 4A
STABILITY 3
119
RADIAL SPILL - R = 49
WIND 5.0
TEMP 294
RH 0.50
Z (M)
X (M)
0
200
400
600
800
1000

LOOPING AT LARGEST PUFF ONLY

INITIAL CONDITIONS

SCENARIO 4A

RADIAL SPILL - RADIUS: 49.0 FUEL: HYDROGEN SURFACE ELEVATION: 0.

EVAPORATION RATE: 1.940E-3 TEMP: 294 RELATIVE HUMIDITY: .50

STABILITY: 3 WIND: 5.0 M/S FMF LOWER LIMIT: .040

IT	XP M	T K	DELTEM K	A	W M/S	ZP M	ANG DEG	VP CU.M	U1 M/S	U2 M/S	U4 M/S	FMF	VES CU.M	VET CU.M	VEB CU.M	R M	ZTZP M	LL M	LW M
0	0.	20.3	0.0	0.00	0.0	.05	0.	.771E+03	0.000	0.000	0.000	1.000	0.0	0.0	0.0	0.0	.05	0.00	0.00
1	0.	20.6	273.4	-.04	0.0	.05	69.	.871E+03	.216	.102	0.000	.999	10.0	0.0	0.0	49.1	.05	0.00	0.00
10	2.	27.1	266.8	.81	.7	1.93	43.	.117E+04	.367	.072	0.000	.983	16.1	15.4	15.4	[illegible]	.06	0.00	0.00
20	23.	77.4	216.2	2.37	2.9	20.62	42.	.387E+04	.452	.023	0.000	.946	36.7	187.6	187.6	[illegible]	.08	0.00	0.00
30	72.	158.0	134.9	1.38	3.3	53.03	36.	.119E+05	.446	.007	0.000	.566	75.6	445.4	445.4	[illegible]	.12	0.00	0.00
40	134.	210.7	81.5	.89	3.3	86.33	33.	.247E+05	.443	.003	0.000	.364	120.2	650.3	650.3	147.9	.15	0.00	0.00
50	204.	241.7	49.9	.72	3.4	119.73	30.	.423E+05	.436	.002	0.000	.245	173.6	855.3	855.3	178.7	.18	0.00	0.00
60	279.	260.7	30.3	.65	3.5	154.19	29.	.652E+05	.452	.001	0.000	.172	240.5	1089.8	1089.8	208.8	.21	0.00	0.00
70	357.	272.6	17.6	.61	3.7	190.39	28.	.944E+05	.475	.001	0.000	.125	323.2	1358.5	1358.5	230.3	.24	0.00	0.00
80	439.	279.5	10.3	.55	3.9	228.29	27.	.130E+06	.494	.001	0.000	.093	415.8	1635.3	1635.3	255.9	.27	0.00	0.00
90	524.	281.5	8.1	.41	3.9	267.40	27.	.171E+06	.502	.000	0.000	.072	507.8	1885.9	1885.9	280.0	.29	0.00	0.00
100	612.	282.8	4.5	.32	3.8	306.27	27.	.217E+06	.495	.000	0.000	.057	586.9	2072.1	2072.1	302.9	.32	0.00	0.00
110	702.	283.6	5.5	.25	3.7	344.21	26.	.267E+06	.482	.000	0.000	.047	657.6	2219.8	2219.8	324.5	.34	0.00	0.00

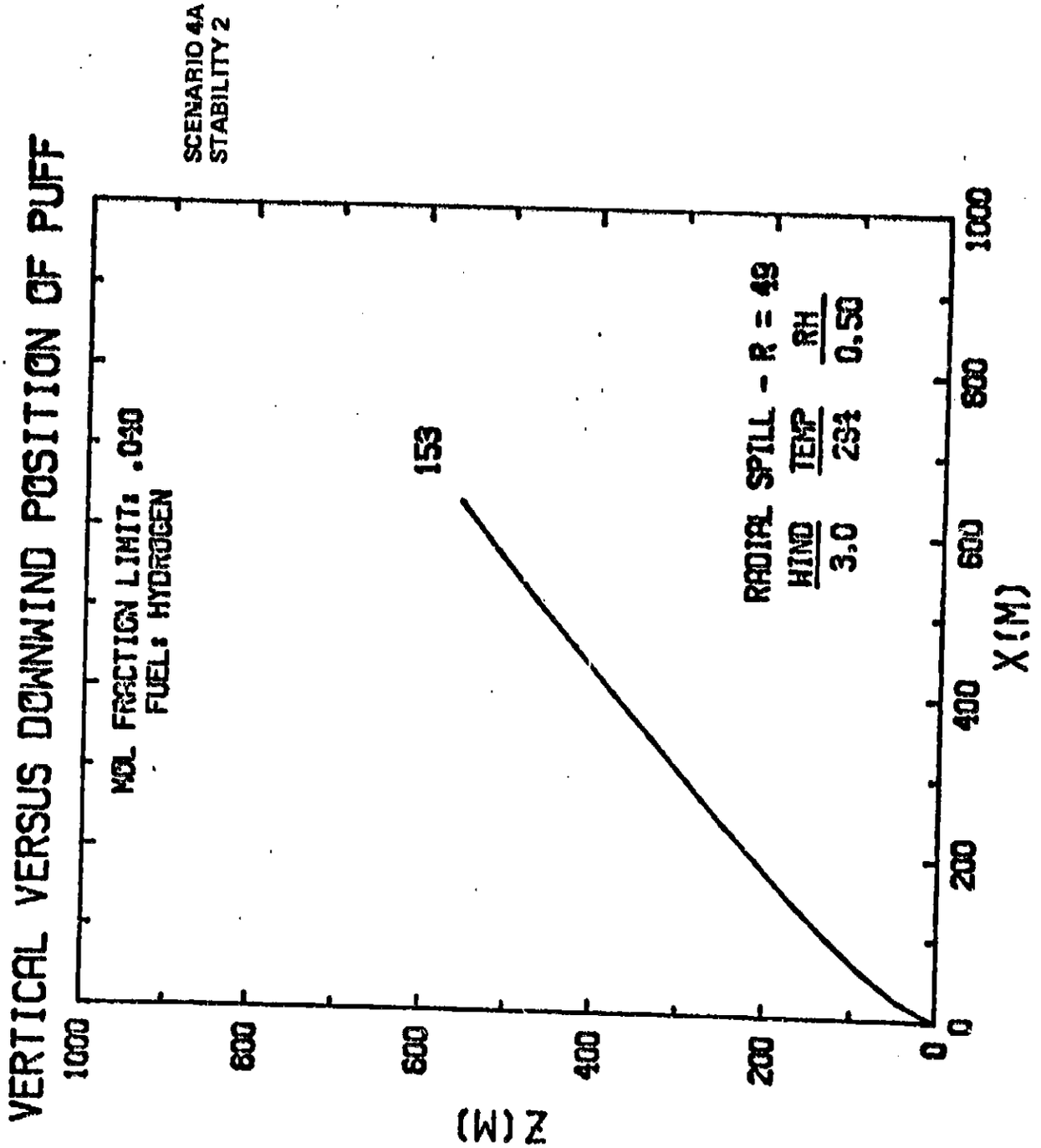

LOOKING AT LARGEST PUFF ONLY

SCENARIO 4A

INITIAL CONDITIONS

RADIAL SPILL - RADIUS: 49.0 FUEL: HYDROGEN SURFACE ELEVATION: 0.

EVAPORATION RATE: 1.940E-3 TEMP: 294 RELATIVE HUMIDITY: .50

STABILITY: 2 WIND: 3.0 M/S FMF LOWER LIMIT: .040

IT	XP M	T K	DELTEM K	A	U M/S	ZP M	ANG DEG	VP CU.M	U1 M/S	U2 M/S	U4 M/S	FMF	VES CU.M	VET CU.M	VEB CU.M	R M	ZTZP M	LL M	LB M
0	0.	20.3	0.0	0.00	0.0	.05	0.	.771E+03	0.000	0.000	0.000	1.000	0.0	0.0	0.0	0.0	.05	0.00	0.00
1	0.	20.5	273.5	-.05	-.0	.05	80.	.867E+03	.130	.102	0.000	.999	7.3	0.0	0.0	49.0	.05	0.00	0.00
10	1.	23.4	270.6	.37	.3	.96	57.	.997E+03	.204	.081	0.000	.992	9.7	2.6	2.6	51.3	.05	0.00	0.00
20	5.	35.5	258.2	1.50	2.1	11.99	66.	.156E+04	.363	.054	0.000	.962	18.4	29.0	29.0	59.5	.06	0.00	0.00
30	24.	85.4	207.3	2.27	4.0	44.48	62.	.442E+04	.521	.020	0.000	.820	46.3	172.8	172.8	93.8	.09	0.00	0.00
40	57.	152.0	139.4	1.41	4.2	85.89	56.	.111E+05	.527	.008	0.000	.585	86.1	343.9	343.9	113.6	.12	0.00	0.00
50	98.	198.2	92.0	.94	4.1	126.95	52.	.210E+05	.512	.004	0.000	.405	128.1	474.3	474.3	140.2	.15	0.00	0.00
60	143.	227.2	61.7	.74	4.0	167.34	49.	.339E+05	.506	.002	0.000	.289	174.8	595.1	595.1	164.2	.17	0.00	0.00
70	191.	246.0	41.9	.65	4.1	207.92	47.	.500E+05	.513	.002	0.000	.213	229.5	724.3	724.3	186.7	.19	0.00	0.00
80	241.	258.6	29.1	.57	4.2	249.37	46.	.696E+05	.524	.001	0.000	.162	292.6	862.7	862.7	209.2	.22	0.00	0.00
90	293.	267.4	20.1	.52	4.3	291.82	45.	.929E+05	.537	.001	0.000	.126	363.7	1008.6	1008.6	229.1	.24	0.00	0.00
100	347.	272.7	14.4	.46	4.4	335.45	44.	.120E+06	.552	.001	0.000	.100	443.0	1163.1	1163.1	249.2	.26	0.00	0.00
110	402.	276.9	9.9	.43	4.5	380.04	43.	.151E+06	.563	.001	0.000	.081	527.6	1316.6	1316.6	269.1	.28	0.00	0.00
120	458.	278.2	8.3	.35	4.5	425.22	43.	.185E+06	.565	.000	0.000	.067	606.6	1448.5	1448.5	287.8	.30	0.00	0.00
130	516.	279.1	7.1	.28	4.4	470.05	42.	.223E+06	.558	.000	0.000	.056	676.5	1551.9	1551.9	305.7	.32	0.00	0.00
140	575.	279.8	6.2	.23	4.3	514.03	42.	.263E+06	.546	.000	0.000	.048	739.5	1635.6	1635.6	322.8	.34	0.00	0.00
150	635.	280.2	5.5	.20	4.2	556.96	41.	.305E+06	.533	.000	0.000	.041	796.8	1705.1	1705.1	339.1	.35	0.00	0.00

VERTICAL VERSUS DOWNWIND POSITION OF PUFF

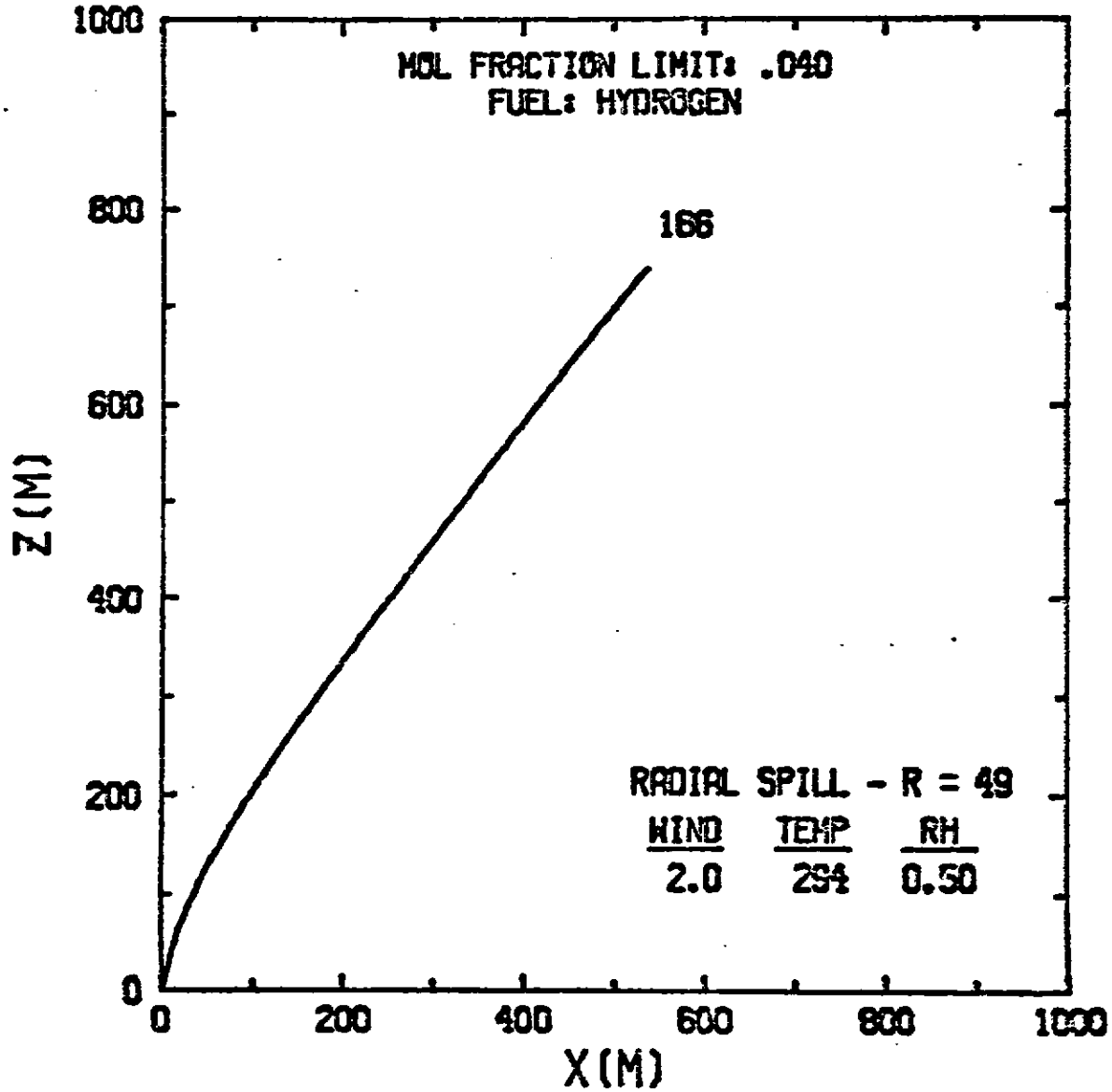

SCENARIO 4A
STABILITY 1

LOOKING AT LARGEST PUFF ONLY

INITIAL CONDITIONS

SCENARIO 4A

RADIAL SPILL - RADIUS: 49.0 FUEL: HYDROGEN SURFACE ELEVATION: 0.

EVAPORATION RATE: 1.940E-3 TEMP: 294 RELATIVE HUMIDITY: .50

STABILITY: 1 WIND: 2.0 M/S FMF LOWER LIMIT: .040

IT	XP M	T K	DELTEM K	A	W M/S	ZP M	ANG DEG	VP CU.M	U1 M/S	U2 M/S	U4 M/S	FMF	VES CU.M	VET CU.M	VEB CU.M	R M	ZTZP M	LL M	LW M
0	0.	20.3	0.0	0.00	0.0	.05	0.	.771E+03	0.000	0.000	0.000	1.000	0.0	0.0	0.0	0.0	.05	0.00	0.00
1	0.	20.5	273.5	-.06	-.0	.05	85.	.865E+03	.086	.102	0.000	1.000	5.9	0.0	0.0	48.9	.05	0.00	0.00
10	0.	22.4	271.5	.24	.2	.58	64.	.953E+03	.125	.084	0.000	.995	6.9	.8	.8	50.5	.05	0.00	0.00
20	2.	27.4	266.3	.83	1.4	7.70	76.	.116E+04	.248	.069	0.000	.982	12.0	6.7	6.7	54.2	.06	0.00	0.00
30	8.	46.2	246.5	2.01	3.6	32.53	76.	.210E+04	.464	.041	0.000	.934	26.9	47.8	47.8	65.6	.07	0.00	0.00
40	25.	98.6	192.3	2.09	4.8	76.75	72.	.543E+04	.606	.016	0.000	.774	61.8	175.8	175.8	89.7	.09	0.00	0.00
50	50.	153.9	135.1	1.34	4.8	125.29	68.	.115E+05	.604	.007	0.000	.571	101.7	291.5	291.5	115.1	.12	0.00	0.00
60	80.	192.6	94.5	.93	4.7	172.77	65.	.199E+05	.585	.004	0.000	.416	142.3	380.1	380.1	137.9	.14	0.00	0.00
70	111.	218.2	67.7	.72	4.6	219.14	63.	.305E+05	.574	.003	0.000	.310	185.3	459.7	459.7	158.5	.17	0.00	0.00
80	145.	235.6	50.0	.59	4.5	264.85	61.	.431E+05	.567	.002	0.000	.238	230.7	534.7	534.7	177.3	.19	0.00	0.00
90	180.	247.9	37.4	.52	4.5	310.25	60.	.579E+05	.565	.001	0.000	.188	280.2	611.1	611.1	195.9	.20	0.00	0.00
100	216.	256.8	28.2	.47	4.6	355.84	59.	.749E+05	.570	.001	0.000	.151	335.3	692.4	692.4	213.3	.22	0.00	0.00
110	253.	263.3	21.4	.44	4.6	401.97	58.	.943E+05	.578	.001	0.000	.124	396.2	778.4	778.4	230.2	.24	0.00	0.00
120	291.	268.2	16.2	.42	4.7	448.86	57.	.116E+06	.588	.001	0.000	.103	463.8	870.2	870.2	246.7	.26	0.00	0.00
130	330.	272.0	12.1	.40	4.8	496.68	56.	.141E+06	.601	.001	0.000	.086	538.5	968.1	968.1	263.0	.27	0.00	0.00
140	370.	274.0	9.8	.35	4.9	545.44	56.	.168E+06	.610	.000	0.000	.073	615.5	1064.1	1064.1	278.8	.29	0.00	0.00
150	410.	274.9	8.6	.30	4.9	594.56	55.	.198E+06	.611	.000	0.000	.063	686.0	1144.5	1144.5	294.0	.31	0.00	0.00
160	452.	275.5	7.6	.25	4.8	643.35	55.	.230E+06	.605	.000	0.000	.055	749.2	1209.4	1209.4	308.8	.32	0.00	0.00
170	493.	276.0	6.8	.21	4.8	691.41	54.	.263E+06	.594	.000	0.000	.048	806.4	1262.7	1262.7	323.0	.34	0.00	0.00
180	536.	276.3	6.2	.18	4.7	738.53	54.	.298E+06	.582	.000	0.000	.043	858.6	1307.0	1307.0	336.7	.35	0.00	0.00

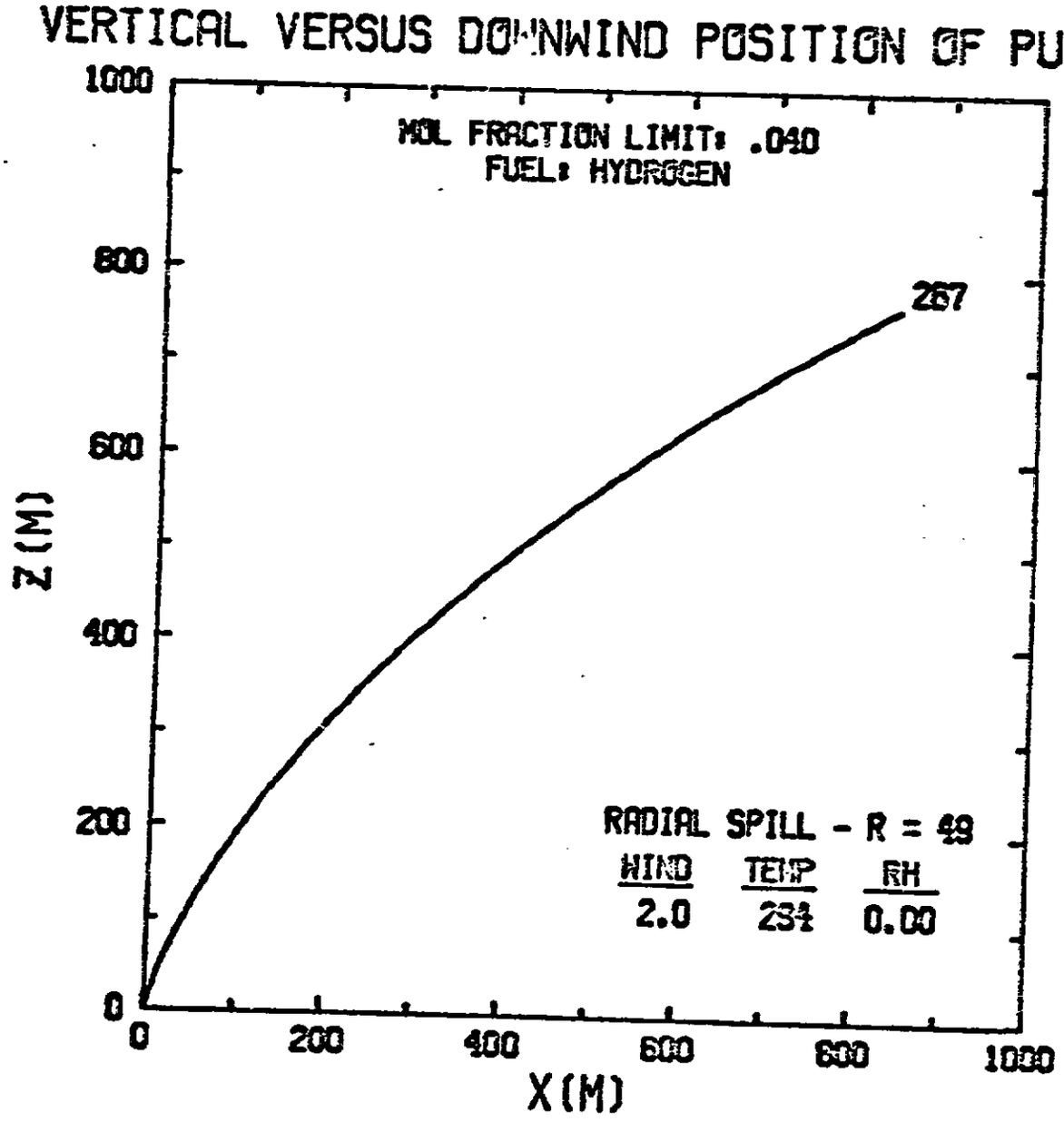
VERTICAL VERSUS DOWNWIND POSITION OF PUFF
MOL FRACTION LIMIT: .040
FUEL: HYDROGEN
SCENARIO 4A
STABILITY 6
267
RADIAL SPILL - R = 49
WIND 2.0
TEMP 294
RH 0.00
Z(M)
X(M)
0
200
400
600
800
1000

.OSTING AT LARGEST PUFF ONLY

SCENARIO 4A

INITIAL CONDITIONS

RADIAL SPILL - RADIUS: 49.0 FUEL: HYDROGEN SURFACE ELEVATION: 0.

EVAPORATION RATE: 1.940E-3 TEMP: 294 RELATIVE HUMIDITY:0.00

STABILITY: 6 WIND: 2.0 M/S FMF LOWER LIMIT: .040

IT	XP M	T K	DELTEM K	A	U M/S	ZP M	ANG DEG	VP CU.M	U1 M/S	U2 M/S	U4 M/S	FMF	VES CU.M	VET CU.M	VEB CU.M	R M	ZTZP M	LL M	LW M
0	0.	20.3	0.0	0.00	0.0	.05	0.	.771E+03	0.000	0.000	0.000	1.000	0.0	0.0	0.0	0.0	.05	0.00	0.00
1	0.	20.5	273.5	-.07	-.0	.05	85.	.864E+03	.086	.102	0.000	1.000	5.9	0.0	0.0	48.9	.05	0.00	0.00
10	0.	22.2	271.8	.16	.1	.35	52.	.944E+03	.112	.085	0.000	.995	6.5	.7	.7	50.4	.05	0.00	0.00
20	2.	26.2	267.9	.57	1.0	5.17	72.	.112E+04	.211	.072	0.000	.984	10.4	4.9	4.9	53.4	.06	0.00	0.00
30	7.	38.2	256.1	1.31	2.6	22.71	74.	.170E+04	.363	.049	0.000	.952	19.4	27.5	27.5	61.2	.06	0.00	0.00
40	20.	73.4	219.1	1.94	4.2	57.55	71.	.380E+04	.522	.023	0.000	.845	42.8	111.7	111.7	79.8	.08	0.00	0.00
50	42.	131.8	163.2	1.52	4.6	102.29	68.	.855E+04	.580	.010	0.000	.659	80.2	231.4	231.4	104.2	.11	0.00	0.00
60	69.	177.5	118.0	.98	4.6	148.61	65.	.156E+05	.574	.005	0.000	.488	118.7	326.1	326.1	127.2	.13	0.00	0.00
70	100.	207.8	88.1	.64	4.4	193.33	63.	.245E+05	.546	.003	0.000	.366	152.9	392.4	392.4	147.6	.15	0.00	0.00
80	132.	227.6	68.2	.45	4.1	235.67	61.	.347E+05	.516	.002	0.000	.284	182.6	439.9	439.9	165.6	.17	0.00	0.00
90	166.	240.9	54.6	.34	3.9	275.75	59.	.461E+05	.490	.002	0.000	.223	209.4	477.2	477.2	181.8	.19	0.00	0.00
100	201.	250.2	45.0	.26	3.7	313.87	57.	.584E+05	.467	.001	0.000	.188	233.6	507.4	507.4	196.5	.21	0.00	0.00
110	237.	257.0	38.0	.21	3.6	350.24	56.	.715E+05	.446	.001	0.000	.158	255.6	532.2	532.2	210.1	.22	0.00	0.00
120	274.	262.1	32.7	.17	3.4	385.05	55.	.852E+05	.428	.001	0.000	.136	275.7	552.9	552.9	222.6	.23	0.00	0.00
130	312.	265.9	28.6	.14	3.3	418.47	53.	.996E+05	.411	.001	0.000	.118	294.1	570.3	570.3	234.4	.24	0.00	0.00
140	350.	269.0	25.4	.12	3.2	450.62	52.	.114E+06	.396	.001	0.000	.105	310.9	584.9	584.9	245.4	.26	0.00	0.00
150	388.	271.4	22.8	.10	3.0	481.60	51.	.130E+06	.383	.001	0.000	.093	326.2	597.1	597.1	255.8	.27	0.00	0.00
160	428.	273.4	20.6	.09	2.9	511.51	50.	.146E+06	.370	.001	0.000	.084	340.2	607.3	607.3	265.6	.28	0.00	0.00
170	468.	275.0	18.8	.08	2.8	540.41	49.	.162E+06	.358	.000	0.000	.077	353.0	615.6	615.6	275.0	.29	0.00	0.00
180	508.	276.3	17.3	.07	2.7	568.36	48.	.178E+06	.347	.000	0.000	.070	364.5	622.2	622.2	283.9	.30	0.00	0.00
190	548.	277.4	16.0	.06	2.7	595.42	47.	.195E+06	.336	.000	0.000	.065	374.8	627.2	627.2	292.4	.31	0.00	0.00
200	589.	278.3	14.9	.05	2.6	621.63	47.	.211E+06	.326	.000	0.000	.060	384.0	630.9	630.9	300.5	.31	0.00	0.00
210	631.	279.1	14.0	.04	2.5	647.02	46.	.228E+06	.316	.000	0.000	.056	392.1	633.2	633.2	308.2	.32	0.00	0.00
220	672.	279.8	13.2	.04	2.4	671.62	45.	.246E+06	.307	.000	0.000	.052	399.2	634.2	634.2	315.7	.33	0.00	0.00
230	714.	280.3	12.4	.03	2.3	695.47	44.	.263E+06	.297	.000	0.000	.049	405.2	634.0	634.0	322.8	.34	0.00	0.00
240	757.	280.8	11.8	.03	2.3	718.58	44.	.280E+06	.289	.000	0.000	.046	410.2	632.6	632.6	329.7	.34	0.00	0.00
250	799.	281.2	11.2	.02	2.2	740.97	43.	.297E+06	.280	.000	0.000	.044	414.1	630.2	630.2	336.3	.35	0.00	0.00
260	842.	281.6	10.7	.02	2.1	762.66	42.	.315E+06	.272	.000	0.000	.041	417.1	626.7	626.7	342.6	.36	0.00	0.00

VERTICAL VERSUS DOWNWIND POSITION OF PUFF

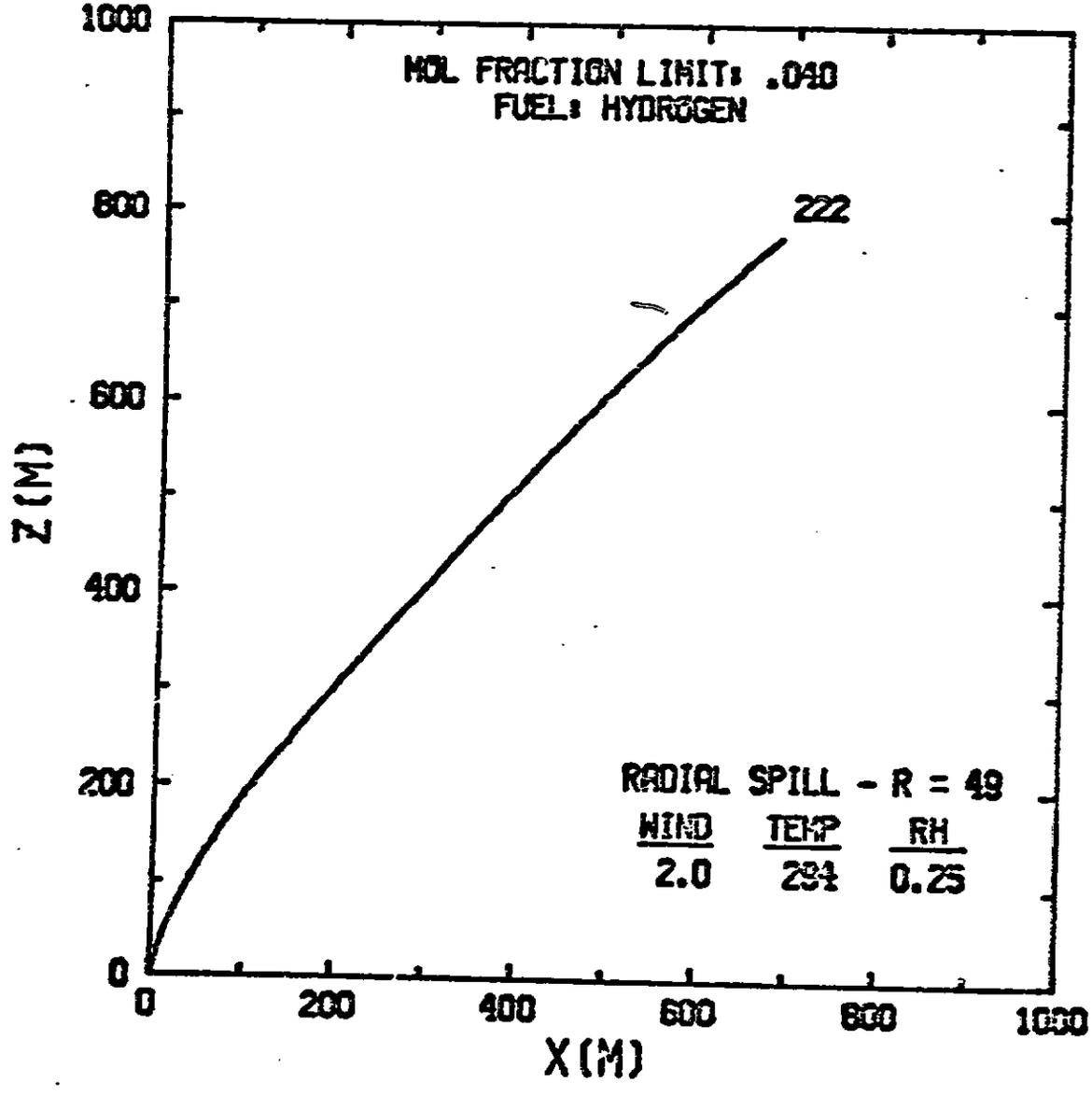

SCENARIO 4A
STABILITY 6

LOOKING AT LARGEST PUFF ONLY

INITIAL CONDITIONS

SCENARIO 4A

RADIAL SPILL - RADIUS: 49.0 FUEL: HYDROGEN SURFACE ELEVATION: 0.

EVAPORATION RATE: 1.940E-3 TEMP: 294 RELATIVE HUMIDITY: .25

STABILITY: 6 WIND: 2.0 M/S FMF LOWER LIMIT: .040

IT	XP	T	DELTEM	A	W	ZP	ANG	VP	U1	U2	U4	FMF	VES	VET	VEB	R	ZTZP	LL	LW
	M	K	K		M/S	M	DEG	CU.M	M/S	M/S	M/S		CU.M	CU.M	CU.M	M	M	M	M
0	0.	20.3	0.0	0.00	0.0	.05	0.	.771E+03	0.000	0.000	0.000	1.000	0.0	0.0	0.0	0.0	.05	0.00	0.00
1	0.	20.5	273.5	-.06	-.0	.05	85.	.865E+03	.086	.102	0.000	1.000	5.9	0.0	0.0	45.9	.05	0.00	0.00
10	0.	22.3	271.7	.20	.2	.46	59.	.948E+03	.119	.084	0.000	.995	6.7	.8	.8	50.4	.05	0.00	0.00
20	2.	26.8	267.3	.69	1.2	6.34	74.	.115E+04	.228	.071	0.000	.983	11.1	5.7	5.7	53.8	.06	0.00	0.00
30	7.	41.6	252.7	1.61	3.1	27.19	75.	.187E+04	.408	.045	0.000	.944	22.6	35.8	35.8	63.1	.07	0.00	0.00
40	22.	85.4	209.3	1.91	4.5	66.51	71.	.447E+04	.560	.019	0.000	.914	50.8	139.4	139.4	84.1	.09	0.00	0.00
50	46.	138.6	156.5	1.21	4.5	111.54	68.	.949E+04	.561	.009	0.000	.625	83.4	242.0	242.0	107.9	.11	0.00	0.00
60	74.	179.0	116.6	.76	4.2	155.00	64.	.164E+05	.531	.005	0.000	.471	113.5	311.8	311.8	129.1	.13	0.00	0.00
70	105.	207.0	89.0	.54	4.0	196.08	62.	.247E+05	.502	.003	0.000	.362	141.6	363.9	363.9	147.9	.15	0.00	0.00
80	137.	226.7	69.0	.44	3.9	235.33	60.	.344E+05	.483	.002	0.000	.286	169.9	410.9	410.9	165.0	.17	0.00	0.00
90	171.	241.1	54.4	.39	3.8	273.63	58.	.454E+05	.476	.002	0.000	.232	201.3	460.6	460.6	180.8	.19	0.00	0.00
100	206.	252.0	43.3	.37	3.8	311.72	57.	.579E+05	.476	.001	0.000	.191	236.8	515.4	515.4	196.0	.20	0.00	0.00
110	242.	260.3	34.7	.35	3.9	350.10	55.	.721E+05	.481	.001	0.000	.159	276.9	575.4	575.4	210.6	.22	0.00	0.00
120	279.	266.8	28.0	.33	3.9	389.07	54.	.880E+05	.490	.001	0.000	.134	321.6	640.3	640.3	225.0	.23	0.00	0.00
130	317.	272.0	22.5	.33	4.0	428.84	54.	.106E+06	.501	.001	0.000	.114	371.7	710.9	710.9	239.2	.25	0.00	0.00
140	355.	274.8	19.4	.27	4.1	469.37	53.	.125E+06	.307	.001	0.000	.098	421.1	776.7	776.7	252.8	.26	0.00	0.00
150	394.	277.0	17.0	.23	4.0	509.98	52.	.146E+06	.505	.001	0.000	.085	465.0	829.0	829.0	266.1	.28	0.00	0.00
160	434.	278.7	15.0	.19	4.0	550.17	52.	.169E+06	.498	.000	0.000	.074	504.4	871.5	871.5	278.9	.29	0.00	0.00
170	475.	280.1	13.4	.16	3.9	589.67	51.	.192E+06	.489	.000	0.000	.066	540.1	906.5	906.5	291.3	.30	0.00	0.00
180	516.	281.1	12.1	.14	3.8	628.35	51.	.217E+06	.479	.000	0.000	.059	572.6	935.5	935.5	303.1	.32	0.00	0.00
190	557.	282.0	11.0	.12	3.7	666.13	50.	.243E+06	.467	.000	0.000	.053	602.2	959.7	959.7	314.5	.33	0.00	0.00
200	599.	282.6	10.1	.11	3.6	702.98	50.	.269E+06	.456	.000	0.000	.048	629.2	979.8	979.8	325.4	.34	0.00	0.00
210	642.	283.1	9.4	.09	3.5	738.91	49.	.296E+06	.445	.000	0.000	.044	653.8	996.4	996.4	335.8	.35	0.00	0.00
220	684.	283.5	8.7	.08	3.5	773.90	49.	.324E+06	.433	.000	0.000	.040	676.1	1009.8	1009.8	345.9	.36	0.00	0.00

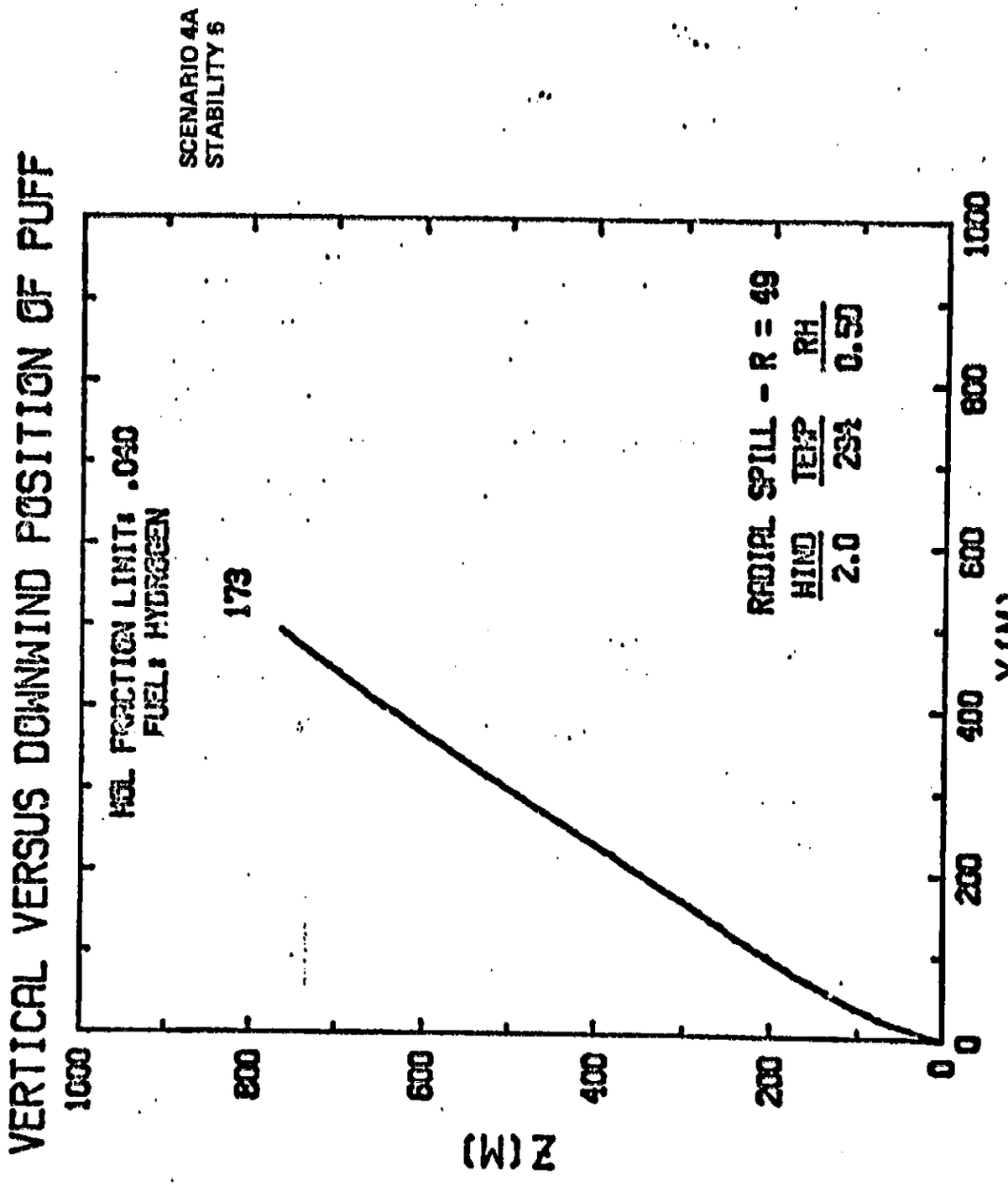

LOOKING AT LARGEST PUFF ONLY

INITIAL CONDITIONS

RADIAL SPILL - RADIUS: 49.0

EVAPORATION RATE: 1.940E-3

STABILITY: 6

SCENARIO 4A

FUEL: HYDROGEN

TEMP: 294

WIND: 2.0 M/S

SURFACE ELEVATION: 0.

RELATIVE HUMIDITY: .50

FMF LOWER LIMIT: .040

IT	XP M	T K	DELTEM K	A1	U M/S	ZP-ZS M	ANG DEG	VP CU.M	U1 M/S	U2 M/S	U4 M/S	FMF	VES CU.M	VET CU.M	VEB CU.M	R M	ZTZP M	LL M	LW M
0	0.	20.3	0.0	0.00	0.0	0.0	0.	0.	0.000	0.000	0.000	1.000	0.0	0.0	0.0	0.0	0.00	0.00	0.00
1	0.	20.4	273.6	0.00	0.0	.1	90.	.861E+03	0.000	.102	0.000	1.000	3.2	0.0	0.0	48.9	.05	0.00	0.00
10	0.	22.3	271.7	.05	.2	.5	66.	.946E+03	.121	.084	0.000	.995	6.8	.7	.7	50.4	.05	0.00	0.00
20	2.	26.9	267.2	.16	1.3	6.9	77.	.115E+04	.240	.070	0.000	.984	11.6	5.6	5.6	53.8	.06	0.00	0.00
30	7.	43.4	250.9	.23	3.5	30.1	77.	.195E+04	.447	.044	0.000	.942	25.1	39.9	39.9	64.0	.07	0.00	0.00
40	23.	93.6	201.2	.04	4.8	73.5	73.	.501E+04	.608	.017	0.000	.795	58.9	161.7	161.7	87.4	.09	0.00	0.00
50	47.	152.2	143.0	-.01	4.9	122.6	69.	.110E+05	.615	.008	0.000	.592	100.4	284.6	284.6	113.4	.12	0.00	0.00
60	76.	195.8	99.9	-.01	4.8	171.4	66.	.196E+05	.604	.004	0.000	.430	144.9	383.7	383.7	137.1	.14	0.00	0.00
70	107.	226.1	69.8	.01	4.8	219.6	64.	.308E+05	.602	.003	0.000	.318	195.1	478.5	478.5	159.0	.17	0.00	0.00
80	140.	247.4	48.1	.02	5.0	268.5	62.	.447E+05	.615	.002	0.000	.241	256.2	584.5	584.5	180.0	.19	0.00	0.00
90	175.	262.5	32.7	.02	5.2	319.1	61.	.620E+05	.640	.001	0.000	.186	331.0	706.5	706.5	200.4	.21	0.00	0.00
100	211.	272.0	22.9	.01	5.4	371.9	60.	.825E+05	.670	.001	0.000	.145	420.5	843.9	843.9	220.3	.23	0.00	0.00
110	249.	280.3	14.3	.02	5.6	426.7	60.	.108E+06	.691	.001	0.000	.116	515.6	978.9	978.9	240.4	.25	0.00	0.00
120	287.	284.3	9.8	.01	5.8	483.6	59.	.136E+06	.717	.001	0.000	.093	626.2	1139.7	1139.7	259.8	.27	0.00	0.00
130	327.	285.5	8.2	-.00	5.8	541.5	59.	.168E+06	.721	.000	0.000	.077	723.0	1247.1	1247.1	278.3	.29	0.00	0.00
140	367.	286.3	7.1	-.01	5.7	599.1	58.	.202E+06	.711	.000	0.000	.064	808.3	1338.1	1338.1	296.0	.31	0.00	0.00
150	408.	286.8	6.2	-.01	5.6	655.5	58.	.239E+06	.696	.000	0.000	.055	884.9	1411.4	1411.4	313.0	.33	0.00	0.00
160	450.	287.1	5.5	-.01	5.4	710.6	58.	.279E+06	.678	.000	0.000	.047	954.6	1471.9	1471.9	329.1	.34	0.00	0.00
170	493.	287.3	5.0	-.01	5.3	764.3	57.	.320E+06	.660	.000	0.000	.041	1018.5	1522.6	1522.6	344.5	.36	0.00	0.00

VERTICAL VERSUS DOWNWIND POSITION OF PUFF

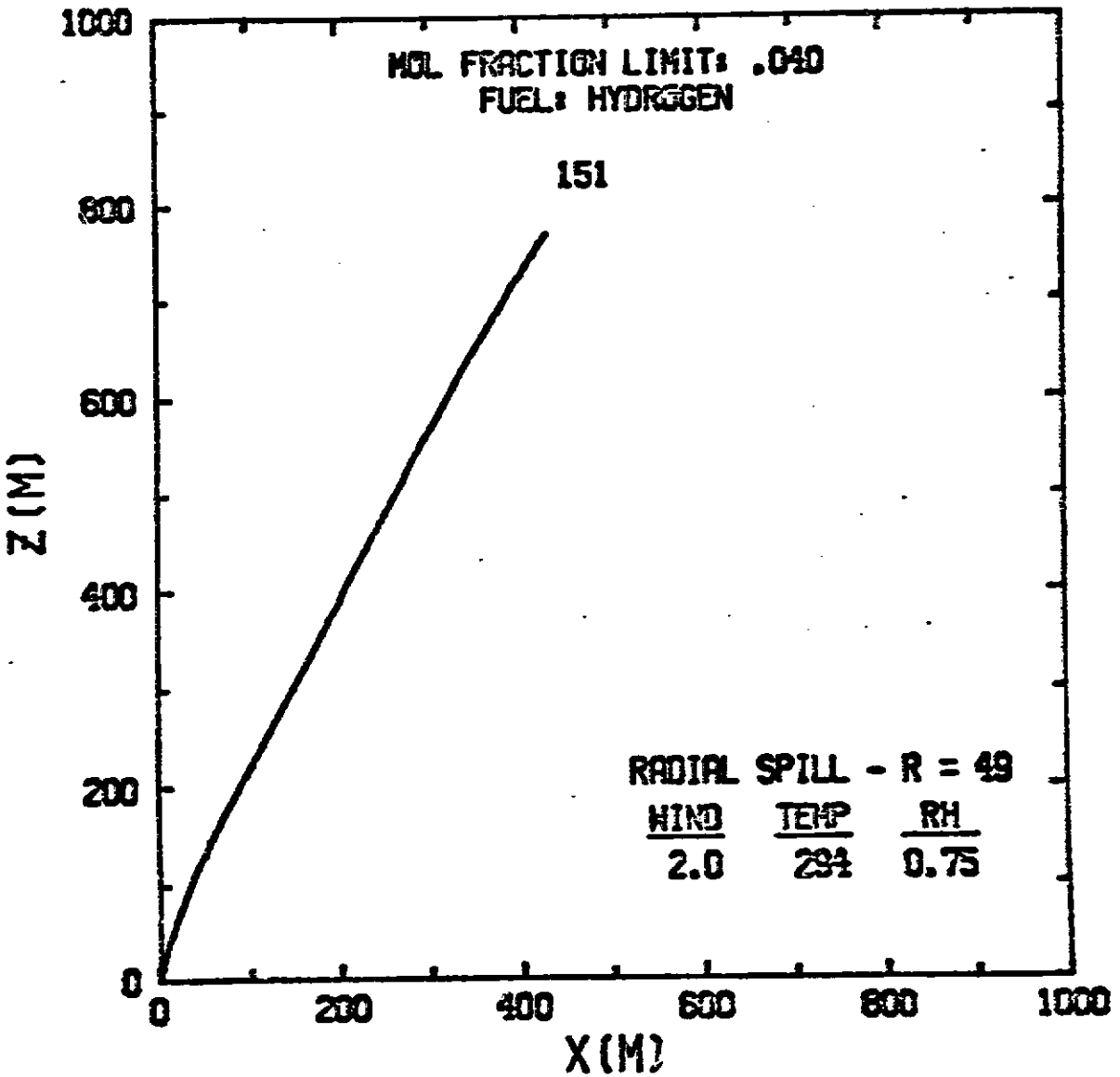

SCENARIO 4A
STABILITY 6

LOOKING AT LARGEST PUFF ONLY

INITIAL CONDITIONS

RADIAL SPILL - RADIUS: 49.0

EVAPORATION RATE: 1.940E-3

STABILITY: 6

SCENARIO 4A

FUEL: HYDROGEN SURFACE ELEVATION: 0.

TEMP: 294 RELATIVE HUMIDITY: .75

WIND: 2.0 M/S FMF LOWER LIMIT: .040

IT	XP M	T K	DELTEM K	A	W M/S	ZP M	ANG DEG	VP CU.M	U1 M/S	U2 M/S	U4 M/S	FMF	VES CU.M	VET CU.M	VEB CU.M	R M	ZTZP M	LL M	LW M
0	0.	20.3	0.0	0.00	0.0	.05	0.	.771E+03	0.000	0.000	0.000	1.000	0.0	0.0	0.0	0.0	.05	0.00	0.00
1	0.	20.5	273.5	-.06	-.0	.05	85.	.865E+03	.086	.102	0.000	1.000	5.9	0.0	0.0	49.0	.05	0.00	0.00
10	0.	22.6	271.4	.28	.3	.73	68.	.959E+03	.132	.084	0.000	.995	7.2	.9	.9	50.6	.05	0.00	0.00
20	2.	28.2	265.9	.98	1.6	9.12	77.	.122E+04	.368	.067	0.000	.981	12.9	7.8	7.8	54.9	.06	0.00	0.00
30	9.	51.7	242.7	2.41	4.1	37.66	76.	.238E+04	.515	.037	0.000	.923	31.6	61.4	61.4	68.3	.07	0.00	0.00
40	28.	113.7	181.1	2.29	5.2	86.08	72.	.657E+04	.650	.013	0.000	.739	74.6	213.8	213.8	95.6	.10	0.00	0.00
50	54.	175.3	120.1	1.60	5.3	138.90	69.	.143E+05	.664	.006	0.000	.526	128.2	356.2	356.2	123.5	.13	0.00	0.00
60	84.	219.1	76.8	1.27	5.5	192.75	66.	.256E+05	.677	.003	0.000	.370	193.1	491.2	491.2	149.7	.16	0.00	0.00
70	117.	249.3	46.4	1.16	5.7	248.56	65.	.410E+05	.709	.002	0.000	.264	276.9	643.9	643.9	174.9	.18	0.00	0.00
80	152.	269.7	25.6	1.10	6.1	307.75	64.	.613E+05	.755	.001	0.000	.193	385.6	825.9	825.9	199.7	.21	0.00	0.00
90	188.	281.7	13.2	1.00	6.4	370.48	63.	.867E+05	.795	.001	0.000	.143	511.4	1017.9	1017.9	223.9	.23	0.00	0.00
100	226.	290.1	4.3	.94	6.8	436.75	63.	.118E+06	.844	.001	0.000	.109	669.3	1243.8	1243.8	248.1	.26	0.00	0.00
110	265.	290.4	3.6	.71	6.9	505.66	62.	.154E+06	.859	.001	0.000	.085	810.5	1425.0	1425.0	270.4	.28	0.00	0.00
120	305.	290.5	3.1	.55	6.8	574.26	62.	.193E+06	.846	.000	0.000	.068	931.5	1557.5	1557.5	291.8	.30	0.00	0.00
130	346.	290.4	2.7	.44	6.6	641.31	62.	.237E+06	.824	.000	0.000	.056	1038.8	1661.0	1661.0	311.9	.33	0.00	0.00
140	388.	290.2	2.5	.36	6.4	706.44	61.	.283E+06	.800	.000	0.000	.047	1136.0	1745.3	1745.3	331.9	.35	0.00	0.00
150	431.	290.0	2.3	.30	6.2	769.55	61.	.333E+06	.775	.000	0.000	.040	1225.0	1815.8	1815.8	348.9	.36	0.00	0.00

VERTICAL VERSUS DOWNWIND POSITION OF PUFF

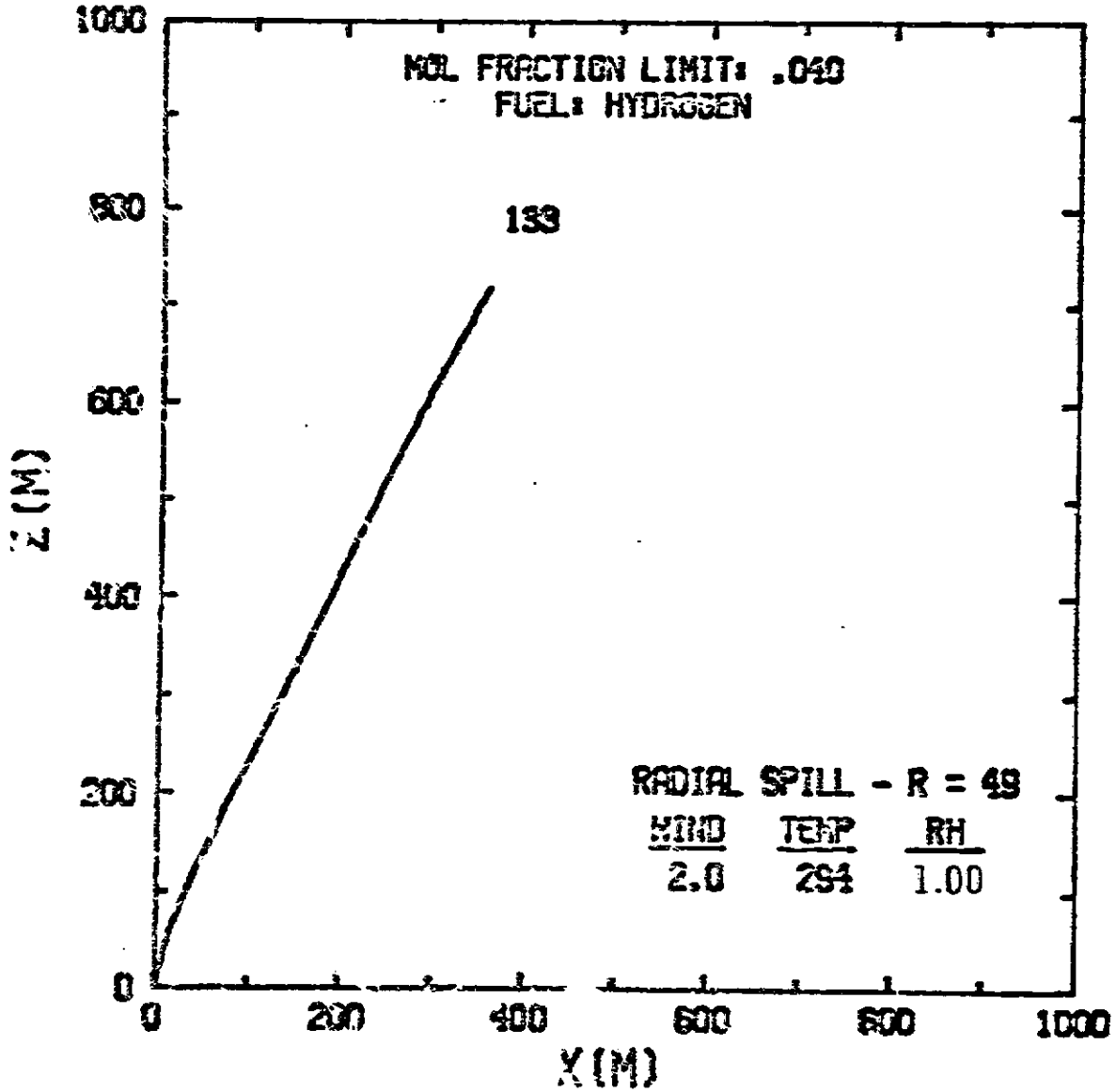

SCENARIO 4A
STABILITY 6

LOOKING AT LARGEST PUFF ONLY

INITIAL CONDITIONS

SCENARIO 4A

RADIAL SPILL - RADIUS: 49.0 FUEL: HYDROGEN SURFACE ELEVATION: 0.

EVAPORATION RATE: 1.949E-3 TEMP: 294 RELATIVE HUMIDITY:1.00

STABILITY: 6 WIND: 2.0 M/S FMF LOWER LIMIT: .040

IT	XP M	T K	DELTEM K	A	U M/S	ZP M	ANG DEG	VP CU.M	U1 M/S	U2 M/S	U4 M/S	FMF	VES CU.M	VET CU.M	VEB CU.M	R M	ZTZP M	LL M	LW M
0	0.	20.3	0.0	0.00	0.0	.05	0.	.771E+03	0.000	0.000	0.000	1.000	0.0	0.0	0.0	0.0	.05	0.00	0.00
1	0.	20.5	273.5	-.05	-.0	.05	85.	.866E+03	.086	.102	0.000	1.000	5.9	0.0	0.0	49.0	.05	0.00	0.00
10	0.	22.7	271.3	.32	.3	.87	71.	.964E+03	.137	.083	0.000	.995	7.4	1.0	1.0	50.7	.05	0.00	0.00
20	2.	29.0	265.1	1.14	1.9	10.58	78.	.125E+04	.290	.066	0.000	.980	13.9	9.1	9.1	55.3	.06	0.00	0.00
30	10.	58.2	236.3	2.84	4.6	43.00	76.	.271E+04	.568	.032	0.000	.910	37.3	78.3	78.3	71.4	.07	0.00	0.00
40	30.	128.6	166.4	2.49	5.6	95.35	72.	.784E+04	.691	.011	0.000	.701	88.8	254.8	254.8	101.3	.11	0.00	0.00
50	58.	193.5	102.1	1.83	5.8	152.21	69.	.173E+05	.720	.005	0.000	.482	157.0	424.3	424.3	131.5	.14	0.00	0.00
60	89.	238.7	57.2	1.37	6.2	211.89	67.	.316E+05	.760	.003	0.000	.327	248.2	606.1	606.1	160.4	.17	0.00	0.00
70	123.	268.8	26.7	1.49	6.7	275.97	66.	.519E+05	.823	.002	0.000	.226	374.6	828.6	828.6	189.0	.20	0.00	0.00
80	158.	285.9	9.2	1.35	7.1	344.83	65.	.787E+05	.877	.001	0.000	.160	527.4	1069.2	1069.2	216.8	.23	0.00	0.00
90	195.	295.5	-1.0	1.22	7.7	418.82	65.	.113E+06	.946	.001	0.000	.116	726.7	1360.7	1360.7	244.5	.26	0.00	0.00
100	234.	294.6	-.5	.88	7.7	495.91	65.	.152E+06	.958	.001	0.000	.087	895.5	1575.8	1575.8	269.4	.28	0.00	0.00
110	274.	293.7	-.2	.66	7.5	572.08	64.	.196E+06	.936	.000	0.000	.068	1038.7	1729.2	1729.2	293.1	.31	0.00	0.00
120	315.	293.8	-.7	.55	7.3	646.08	64.	.245E+06	.909	.000	0.000	.055	1170.8	1854.9	1854.9	315.5	.33	0.00	0.00
130	357.	293.0	-.3	.44	7.1	718.02	64.	.298E+06	.883	.000	0.000	.045	1294.8	1965.1	1965.1	336.3	.35	0.00	0.00

REFERENCES

1. G. D. Brewer, R. E. Morris, R. H. Lange and J. W. Moore, "Study of the Application of Hydrogen Fuel to Long-Range Subsonic Transport Aircraft," NASA CR-132559, Lockheed-California Company and Lockheed-Georgia Company, January, 1975.

2. G. D. Brewer and R. E. Morris, "Study of LH_2 Fueled Subsonic Passenger Transport Aircraft," NASA CR-144935, Lockheed-California Company, January, 1976.

3. G. D. Brewer, R. E. Morris, G. W. Davis, E. F. Versaw, G. R. Cunnington, Jr., J. C. Riple, C. F. Baerst and G. Garmong, "Final Report - Study of Fuel Systems for LH_2-Fueled Subsonic Transport Aircraft," NASA CR-145319, Lockheed-California Company, December 1977.

4. L. K. Carson, G. W. Davis, E. F. Versaw, G. R. Cunnington, Jr., E. J. Daniels, "Study of Methane Fuel for Subsonic Transport Aircraft," NASA CR-159320, Lockheed-California Company, September, 1980.

5. R. D. McCarty, J. Hord, H. M. Roder, "Selected Properties of Hydrogen (Engineering Design Data)", NBS Monograph 168, February 1981.

6. Anon., ASTM D-1655-80a Jet A, "Standard Specification for Aviation Turbine Fuels".

7. Anon., Mil-T-5624L Military Specification, "Turbine Fuel, Aviation, Grades JP-4 and JP-5".

8. H. C. Barnett and R. R. Hibbard, "Properties of Aircraft Fuels", NACA Technical Note 3276, Lewis Flight Propulsion Laboratory, August 1956.

9. Anon., "Data Book for Designers", prepared by EXXON Co., USA, 1973.

10. Joseph M. Kuchta, "Fire and Explosion Manual for Aircraft Accident Investigators, AFAPL-TR-73-74, August 1973.

11. B. R. Rich, "Lockheed CL-400 Liquid Hydrogen Fueled Mach 2.5 Reconnaissance Vehicle," presented at the Working Symposium of LH_2-Fueled Aircraft held at NASA-Langley Research Center, May 15-16, 1973.

12. Anon., "Interim Report on an Investigation of Hazards Associated With Liquid Hydrogen Storage and Use," Arthur D. Little, Inc., January 15, 1959.

13. R. D. Witcofski, "Dispersion of Flammable Vapor Clouds Resulting from Large Spills of Liquid Hydrogen," NASA Technical Memorandum 83131, May 1981.

14. Visit with Mr. William Hogan and group at Lawrence Livermore National Laboratory on 13 January 1981.

15. National Transportation Safety Board "A Study of U.S. Air Carrier Accidents 1964-69, NTSB AAS-72-5, dated May 1972.

16. National Transportation Safety Board, "Annual Reviews of Aircraft Accident Data," NTSB - ARC - 74-1 (1970-72), 74-2 (1973), 76-1 (1974), 77-1 (1975), 78-1 (1976) and 78-2 (1977).

17. Contract NAS1-16083 "Transport Aircraft Crashworthiness," a study performed by Lockheed-California Co. for NASA-Langley Research Center and FAA Technical Center, (report in preparation).

18. V. L. Streeter and E. B. Wylie, Hydraulic Transients, McGraw-Hill Book Co. New York, 1967.

19. M. Jakob, Heat Transfer, John Wiley & Sons, New York, Volume I, 1955.

20. F. M. Henderson, Open Channel Flow, MacMillan Co., New York, 1966.

21. W. T. Chou, Open Channel Hydraulics, McGraw-Hill Book Company, New York, 1959.

22. J. Fay, "Unusual Fire Hazard of LNG Tanker Spills", Combustion Science and Technology, Vol. 7, page 47, 1973.

23. Havens, Jerry A., 1979, a description and assessment of the SIGMET LNG vapor Dispersion Model, Report CG-M-3-79, NTIS, Springfield, VA 22161

24. Hartwig, Syhrius, (ed)., 1980 Heavy Gas and Risk Assessment, D. Rediel Publishing Co., Kluver Boston, Inc., Lincoln Building, 160 Old Derby St. Hingham, MA 02043.

25. Telford, James W., 1966, The Convective Mechanism in Clear Air, Journal of the Atmospheric Sciences 23, 652666, November.

26. Gifford, Frandkin A., Jr. 1968, An outline of theories of diffusion in the lower layers of the atmosphere, Chapter 3 in Meteorology and Atomic Energy, edited by David H. Slade, report TID-24190 available from NTIS, Springfield, VA 22161.

27. O'Laughlin, B. D. and Brewer, G. D., Future Fuels for Aircraft, Jane's 1981-82 Aviation Annual, Micheal J. H. Taylor, editor. Jane's Publishing Co., Ltd., 1981, London.

28. F. M. Anthony, J. Z. Colt, R. G. Helenbrook, Development and Validation of Cryogenic Foam Insulation for LH_2 Subsonic Transports, NASA CR-3404, February 1981.